NASA CONTRACTOR REPORT

NASA CR-2303

NASA CR-2303

ANALYSIS OF THE FEASIBILITY OF AN EXPERIMENT TO MEASURE CARBON MONOXIDE IN THE ATMOSPHERE

by M. H. Bortner, F. N. Alyea, R. N. Grenda, G. R. Liebling, and G. M. Levy

Prepared by
GENERAL ELECTRIC COMPANY
Philadelphia, Pa. 19101
for Langley Research Center

NATIONAL AERONAUTICS AND SPACE ADMINISTRATION • WASHINGTON, D. C. • OCTOBER 1973

1. Report No.	2. Government Accession No.	3. Recipient's Catalog No.
NASA CR-2303		

4. Title and Subtitle	5. Report Date
ANALYSIS OF THE FEASIBILITY OF AN EXPERIMENT TO MEASURE CARBON MONOXIDE IN THE ATMOSPHERE	October 1973
	6. Performing Organization Code

7. Author(s)	8. Performing Organization Report No.
M. H. Bortner, F. N. Alyea, R. N. Grenda, G. R. Liebling and G. M. Levy (Barringer Research Limited)	

9. Performing Organization Name and Address	10. Work Unit No.
General Electric Company **Space Division - Space Sciences Laboratory** **P. O. Box 8555** **Philadelphia, PA 19101**	**630-52-00-01**
	11. Contract or Grant No. **NAS1-10139**
	13. Type of Report and Period Covered **Contractor Report**
12. Sponsoring Agency Name and Address National Aeronautics and Space Administration Washington, D.C. 20546	14. Sponsoring Agency Code

15. Supplementary Notes

This is a topical report.

16. Abstract

An analysis has been carried out to determine the feasibility of measuring atmospheric carbon monoxide from a remote platform using the correlation interferometry technique. The Carbon Monoxide Pollution Experiment (COPE) has been found to be a feasible method for obtaining a global carbon monoxide map and a vertical carbon monoxide profile. It has been determined that CO data can be obtained with an accuracy of 10 percent using this technique on the first overtone band of CO at 2.3μ. That band has been found to be much more suitable than the stronger fundamental band at 4.6μ. Calculations for both wavelengths are presented which illustrate the effects of atmospheric temperature profiles, inversion layers, ground temperature and emissivity, CO profile, reflectivity, and atmospheric pressure. The applicable radiative transfer theory on which these calculations are based is described together with the principles of the technique.

17. Key Words (Suggested by Author(s))	18. Distribution Statement
Carbon monoxide **Atmospheric measurement** **Air pollution** **Atmospheric chemistry** **Interferometer** **Correlation**	**Unclassified - Unlimited**

19. Security Classif. (of this report)	20. Security Classif. (of this page)	21. No. of Pages	22. Price*
Unclassified	**Unclassified**	261	Domestic, $6.25 Foreign, $8.75

* For sale by the National Technical Information Service, Springfield, Virginia 22151

FOREWORD

This report was prepared for NASA as part of contract NAS1-10139 with Langley Research Center under the Advanced Applications Flight Experiments (AAFE) Program. The objective of this contract is the development of the Carbon Monoxide Pollution Experiment ("COPE"). This experiment is designed to obtain data for the investigation of mechanisms by which CO is removed from the earth's atmosphere. The approach uses an orbiting platform to remotely map global CO concentrations and determine vertical CO profiles using a correlation interferometer measurement technique being developed by Barringer Research Ltd. The instrument is to be capable of measuring CO over the range .02 to 20 atm.-cm. and of measuring other trace atmospheric constituents.

The report covers one aspect of the study - the analysis of the feasibility of the experiment. A previous report was concerned with the CO problem and a forthcoming report will be concerned with the breadboard instrument - its design, fabrication and testing. The technique is, of course, suitable for the measurement of other atmospheric trace species, and such applications are currently under study.

The authors would like to express their appreciation to several co-workers who have contributed significantly to the work described herein and to related work - specifically, to S. H. Chandra who did most of the work on scintillation effects described herein; to D. N. Vachon who provided meteorological information such as that on precipitable water and cloud cover; to J. C. Burns who made numerous helpful suggestions and reviewed much of the work; to S. L. Neste who assisted with the calculations; to H. W. Goldstein who reviewed and evaluated much of the work; and R. H. Kummler who contributed many valuable suggestions in his consultation throughout the work.

Page Intentionally Left Blank

TABLE OF CONTENTS

Page

LIST OF FIGURES

LIST OF TABLES

ANALYSIS OF THE FEASIBILITY OF AN EXPERIMENT TO MEASURE CARBON MONOXIDE IN THE ATMOSPHERE

By M. H. Bortner, F. N. Alyea, R. N. Grenda and G. R. Liebling, General Electric Co., Space Sciences Laboratory, and G. M. Levy, Barringer Research Ltd.

1. INTRODUCTION

One of the major problems in the field of remote sensing of atmospheric pollutant concentrations consists of determining what measurements should be made and what information can be obtained from a given measurement. It is, therefore, economically advisable to simulate (to the extent possible) measurements with the computer and utilize the results to determine the most useful instrument measurements. This report describes passive measurement of pollutants via their absorption of sunlight. The simulation consists of defining a representative model atmosphere and subsequently solving the radiative transfer equation to obtain the spectrum falling on the instrument and then calculating the action of the instrument to determine the signal produced. Effects such as reflected sunlight, earthshine, atmospheric absorption and atmospheric emission must be considered in order to yield physically meaningful solutions to the equation. The specific pollutant or chemical species of interest will determine the spectral region for which the atmospheric transmission will be computed. For the case in which the instrument is an interferometer, the Fourier transform of the spectrum is then calculated to produce an interferogram. Treatment of the interferogram produces the measurement of the pollutant.

The various portions of this type of calculation are described herein as applied to the calculation of the measurement of atmospheric carbon monox-

ide by the correlation interferometer. The results of calculations are discussed.

The model has been used to investigate the feasibility of the use of the correlation interferometer to measure CO, to consider the usefulness of the measurement in looking for a CO sink*, and to define the exact spectral band which should be used for most reliable and useful results. The measurements to be made include a mapping of CO concentrations by looking downward toward the earth and a determination of the vertical CO profile by looking at the sun through the earth's limb, as described in Section 4.

The model is the basis for a program which computes the upwelling radiation for both the mapping and the limb modes. It calculates the spectrum incident on the instrument and the resulting interferogram. Another program then is used to invert the results to obtain CO densities. The model has been used to calculate transmission to determine the range of sensitivity, the effect of various atmospheric and source parameters, and the effect of interfering species.

* Bortner, Kummler, and Jaffe (1972) have reviewed the sources, sinks, and concentrations of carbon monoxide in the earth's atmosphere.

2. ATMOSPHERIC MODELS

2.1 Composition Models

The analytical work performed employed several atmospheric models involving several variations of the carbon monoxide, water, and temperature profiles and one carbon dioxide and one methane profile.

Specifically, ten CO profiles were used. These are given in Table 2.1.1 and shown graphically in Figure 2.1.1. Profile 1 is that for a constant mixing ratio of 0.1 ppm; profile 2 is that for 10 ppm up to 2 km and 0.1 ppm above that; profile 3 is that for a constant mixing ratio of 0.01 ppm; profile 4 is that representing a sink in the 20-45 km range with the mixing ratio dropping from 0.1 to 0.01 ppm over this altitude range; profile 5 is that representing a low altitude sink with an effect up to 9 km, having a mixing ratio of 0.01 ppm at 0 km and 0.1 ppm at 9 km; profile 6 represents a low altitude sink with an effect up to 1 km, having a mixing ratio of 0.01 ppm at 0 km increasing to 0.1 ppm at 1 km; profile 7 also represents a low altitude sink with an effect up to 3 km, having a mixing ratio of 0.005 ppm at 0 km and 0.1 ppm at 3 km; profile 8 represents a low altitude sink with an effect up to 1 km as in profile 6, but having a mixing ratio of 0.01 ppm up to 1 km and 0.1 ppm above. It is important for the mapping measurements to show the effects of these differences except for profile 4, the effect of which should be shown in the limb experiment. The total number densities from which the CO number densities were obtained with the above mixing ratios were taken from Bortner and Kummler (1968) in which they were derived mainly from CIRA (1965) representing mean conditions throughout the year for latitude near 30°.

For purposes of making calculations (Section 7.3) to compare with those of the Convair group (Ludwig, 1970) CO models 9 and 10, Table 2.1.1

TABLE 2.1.1 CO PROFILES (cm^{-3})

Altitude (km)	1	2	3	4	5	6	7	8	9	10
0	2.54(12)	2.54(14)	2.54(11)	2.54(12)	2.54(11)	2.54(11)	1.27(11)	2.54(11)	6.35(12)	6.35(11)
0.5					3.64(11)		2.43(11)			
1	2.31(12)	2.31(14)	2.31(11)	2.31(12)	4.62(11)	1.22(12)	4.62(12)	2.31(11)	5.78(12)	5.78(11)
1.5					5.62(11)		9.00(11)			
2	2.09(12)	2.09(14)	2.09(11)	2.09(12)	6.27(11)	2.31(12)	1.21(12)	2.09(12)	5.22(12)	5.22(11)
2.5					7.07(11)		1.60(12)			
3	1.89(12)	1.89(12)	1.89(11)	1.89(12)	7.56(11)	1.89(12)	1.89(12)	1.89(12)	4.72(12)	4.72(11)
3.5					8.10(11)					
4	1.70(12)	1.70(12)	1.70(11)	1.70(12)	8.50(11)	1.70(12)	1.70(12)	1.70(12)	4.25(12)	4.25(11)
4.5					8.80(11)					
5	1.53(12)	1.53(12)	1.53(11)	1.53(12)	9.18(11)	1.53(12)	1.53(12)	1.53(12)	3.82(12)	3.82(11)
6	1.37(12)	1.37(12)	1.37(11)	1.37(12)	9.59(11)	1.37(12)	1.37(12)	1.37(12)	3.42(12)	3.42(11)
7	1.23(12)	1.23(12)	1.23(11)	1.23(12)	9.84(11)	1.23(12)	1.23(12)	1.23(12)	3.08(12)	3.08(11)
8	1.09(12)	1.09(12)	1.09(11)	1.09(12)	9.81(11)	1.09(12)	1.09(12)	1.09(12)	2.72(12)	2.72(12)
9	9.71(11)	9.71(11)	9.71(10	9.71(11)	9.71(11)	9.71(11)	9.71(11)	9.71(11)	2.43(12)	2.43(11)
10	8.60(11)	8.60(11)	8.60(10)	8.60(11)	8.60(11)	8.60(11)	8.60(11)	8.60(11)	2.15(12)	2.15(11)
15	4.05(11)	4.05(11)	4.05(10)	4.05(11)	4.05(11)	4.05(11)	4.05(11)	4.05(11)	1.01(12)	1.01(11)
20	1.85(11)	1.85(11)	1.85(10)	1.85(11)	1.85(11)	1.85(11)	1.85(11)	1.85(11)	4.63(11)	4.63(10)
25	8.33(10)	8.33(10)	8.33(9)	4.16(10)	8.33(10)	8.33(10)	8.33(10)	8.33(10)	2.08(11)	2.08(10)
30	3.83(10)	3.83(10)	3.83(9)	9.58(9)	3.83(10)	3.83(10)	3.83(10)	2.83(10)	9.58(10)	9.58(9)
35	1.76(10)	1.76(10)	1.76(9)	2.93(9)	1.76(10)	1.76(10)	1.76(10)	1.76(10)	4.40(10)	4.40(9)
40	8.31(9)	8.31(9)	8.31(8)	1.04(9)	8.31(9)	8.31(9)	8.31(9)	8.31(9)	2.08(10)	2.08(9)
45	4.09(9)	4.09(9)	4.09(8)	4.09(8)	4.09(9)	4.09(9)	4.09(9)	4.09(9)	1.02(10)	1.02(9)
50	2.14(9)	2.14(9)	2.14(8)	2.14(8)	2.14(9)	2.14(9)	2.14(9)	2.14(9)	5.35(9)	5.35(8)
55	1.17(9)	1.17(9)	1.17(8)	1.17(8)	1.17(9)	1.17(9)	1.17(9)	1.17(9)	2.92(8)	2.92(8)
60	6.36(8)	6.36(8)	6.36(7)	6.36(7)	6.36(8)	6.36(8)	6.36(8)	6.36(8)	1.59(8)	1.59(8)
65	3.47(8)	3.47(8)	3.47(7)	3.47(7)	3.47(8)	3.47(8)	3.47(8)	3.47(8)	8.68(8)	8.68(7)
70	1.82(8)	1.82(8)	1.82(7)	1.82(7)	1.82(8)	1.82(8)	1.82(8)	1.82(8)	4.55(8)	4.55(7)
75	9.01(7)	9.01(7)	9.01(6)	9.01(6)	9.01(7)	9.01(7)	9.01(7)	9.01(7)	2.28(8)	2.28(7)
80	4.16(7)	4.16(7)	4.16(6)	4.16(6)	4.16(7)	4.16(7)	4.16(7)	4.16(7)	1.04(8)	1.04(7)
85	1.65(7)	1.65(7)	1.65(6)	1.65(6)	1.65(7)	1.65(7)	1.65(7)	1.65(7)	4.12(7)	4.12(6)
90	6.59(6)	6.59(6)	6.59(5)	6.59(5)	6.59(6)	6.59(6)	6.59(6)	6.59(6)	1.65(7)	1.65(6)
95	2.52(6)	2.52(6)	2.52(5)	2.52(5)	2.52(6)	2.52(6)	2.52(6)	2.52(6)	6.30(6)	6.30(5)
100	1.04(6)	1.04(6)	1.04(5)	1.04(5)	1.04(6)	1.04(6)	1.04(6)	1.04(6)	2.60(6)	2.60(5)
Total (cm^{-2})	2.13(18)	5.83(19)	2.13(17)	2.12(18)	1.35(18)	2.01(18)	1.84(18)			

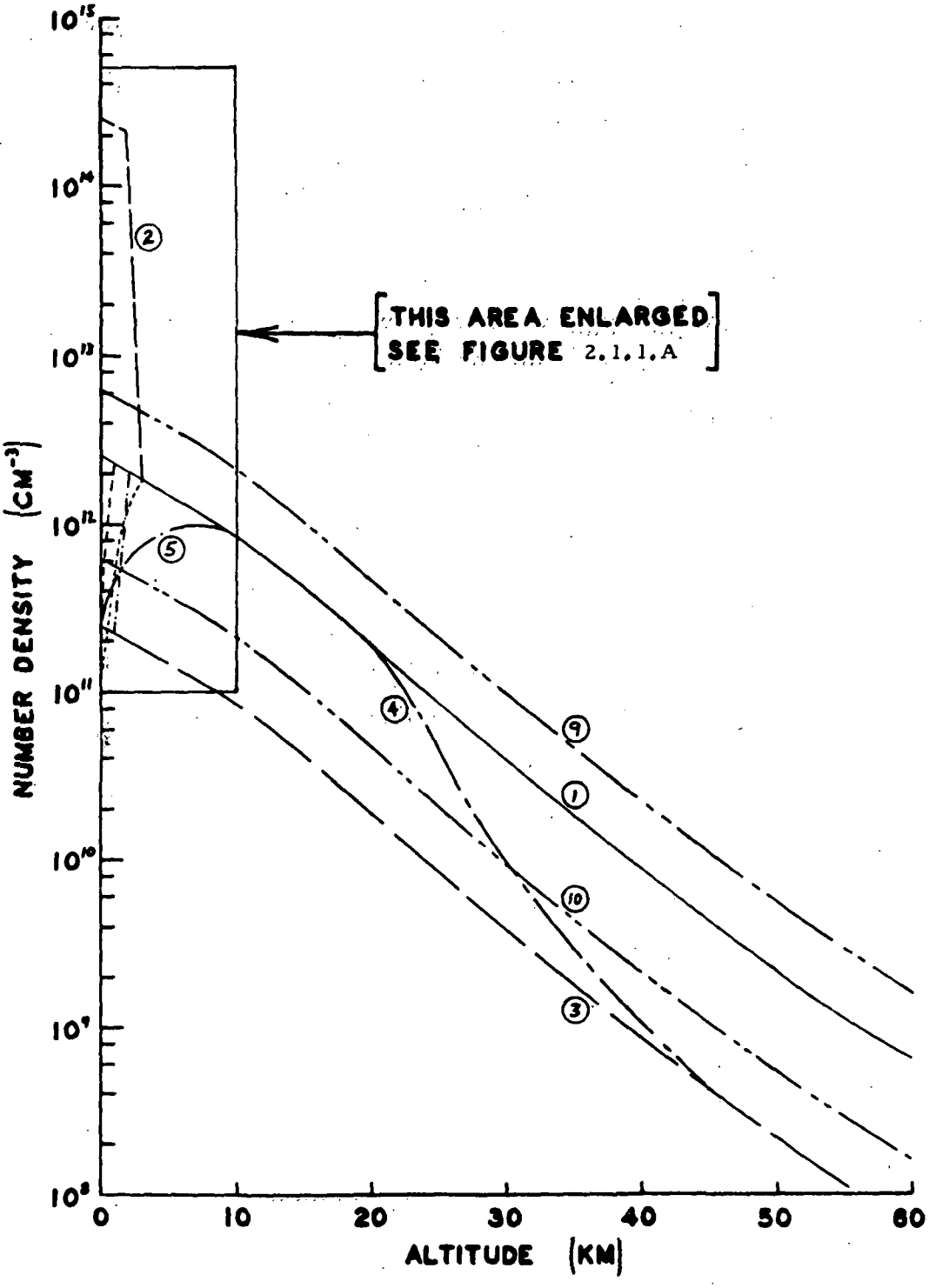

Figure 2.1.1 CO Profiles

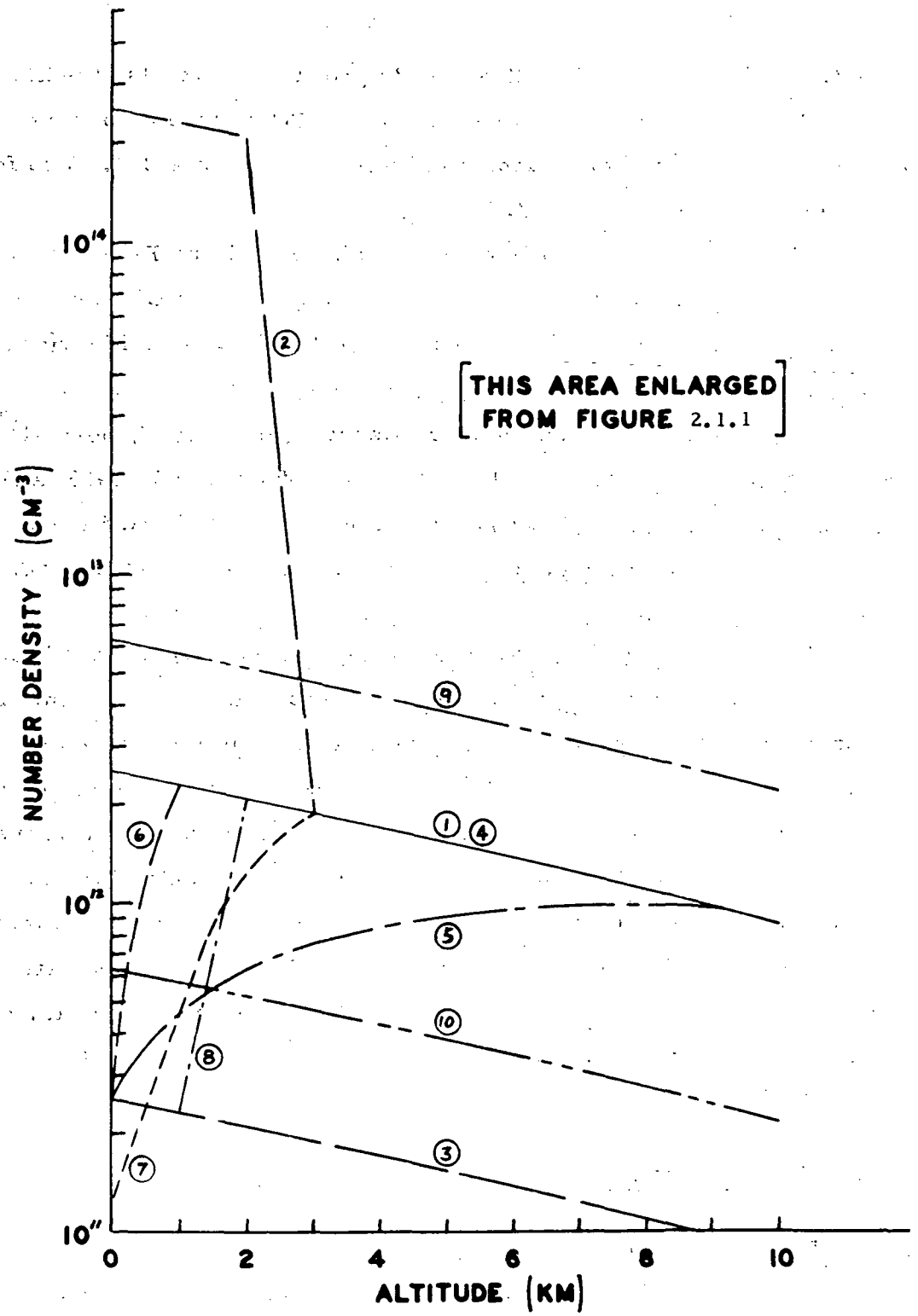

Figure 2.1.1.A CO Profiles

and Figure 2.1.1, representing 0.025 and 0.25 ppm CO, were also treated.

The optical thickness (total number of CO molecules per cm^2 column of sight) is given for the mapping experiment in Figure 2.1.2 and for the limb experiment in Figure 2.1.3.

The CO_2 profile used is given in Table 2.1.2 and Figure 2.1.4. The CO_2 is based on a constant mixing ratio of 320 ppm. The CH_4 profile, taken from Cadle and Powers (1966) is shown in Table 2.1.2 and Figure 2.1.4, and corresponds to a constant mixing ratio of 2 ppm.

The three water profiles, corresponding to a dry[1], normal[2], and a wet[3] atmosphere, were taken from Gutnick, 1962; Oppel, 1963; and Linquist, 1965; respectively. These are given in Table 2.1.2 and Figure 2.1.5. These are equivalent to approximately 0.2, 1.5, and 3 percipitable cm H_2O.

The planned satellite experiment may be best carried out in a polar orbit. Without noting reasons, advantages, and disadvantages, this is excellent for the mapping experiment, but restricts the limb measurements to the polar regions. This is not a problem, however, since above the tropopause, it is to be expected that there is no appreciable latitude effect on the concentrations. Keneshea (1971) has calculated the OH concentration at different latitudes and found little variation. Since the chief CO removal mechanism at these altitudes is, in all probability, CO + OH reaction, the rate of CO removal should be about constant with latitude. The small temperature effect on the rate constant should not cause significant variation of CO with latitude.

2.2 Temperature and Pressure Models

Four specific temperature profiles were used. These are shown in Table 2.1.3 and Figure 2.1.6. Profile 1 corresponds to a cold atmosphere (AFCRL, 1966); profile 2 corresponds to an average atmosphere (AFCRL, 1966); profile 3 corresponds to a hot atmosphere (AFCRL, 1966);

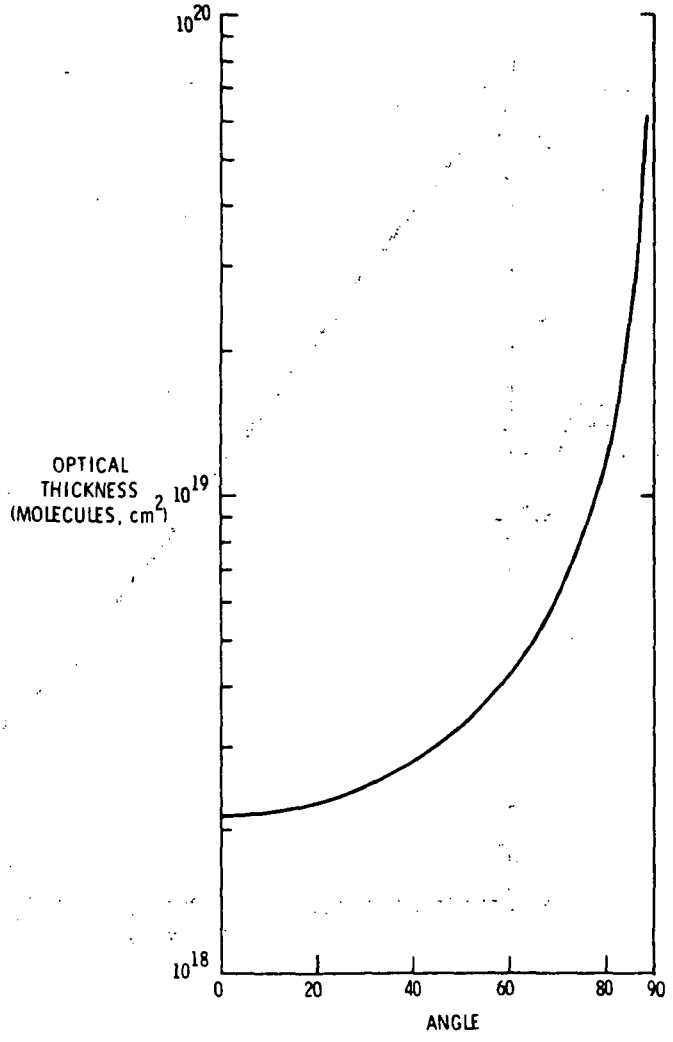

Figure 2.1.2 Optical Thickness as a Function of Angle from Vertical

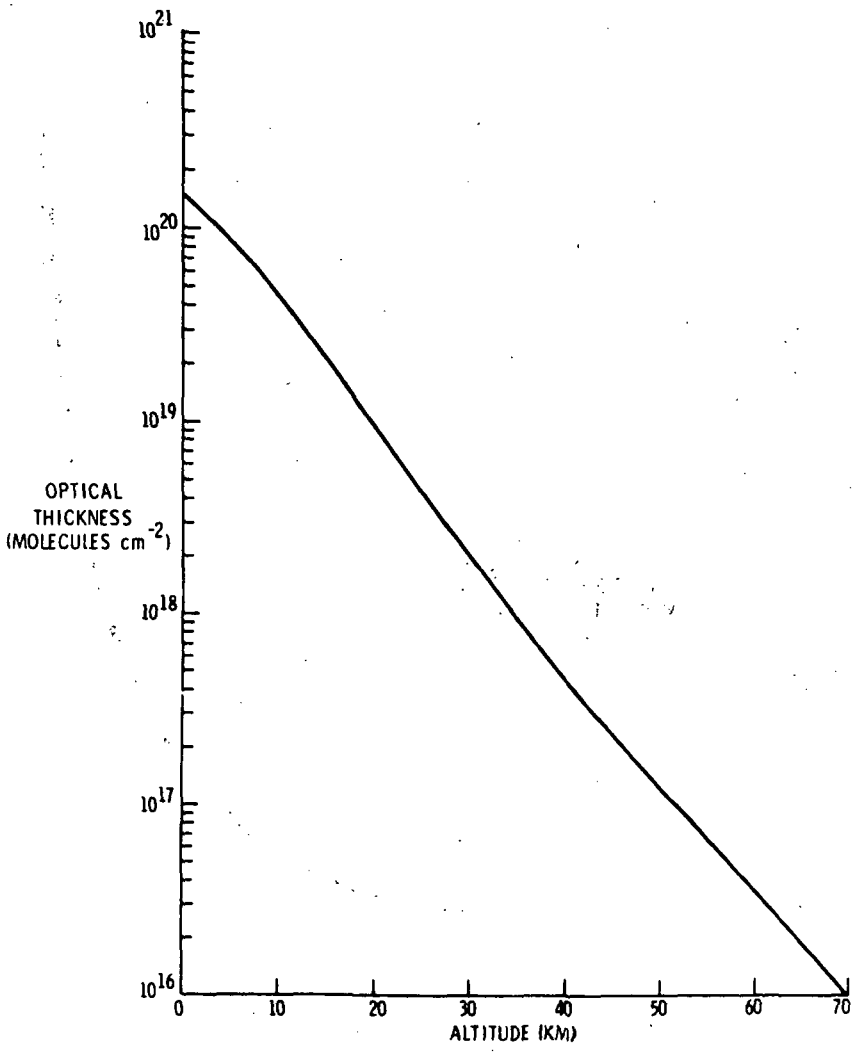

Figure 2.1.3 Optical Thickness for Limb Transmission Experiment as a Function of Grazing Altitude

TABLE 2.1.2 CONCENTRATION PROFILES

Altitude (km)	CO_2	CH_4	H_2O (1)	H_2O (2)	H_2O (3)
0	7.8 (15)	5.0 (13)	3.0 (16)	2.3 (17)	4.6 (17)
1	6.8 (15)	4.1 (13)			
2	5.9 (15)	3.7 (13)	1.2 (16)	9.9 (16)	1.9 (17)
3	5.0 (15)	3.1 (13)			
4	4.3 (15)	2.7 (13)	5.1 (15)	3.8 (16)	7.4 (16)
5	3.9 (15)	2.3 (13)			
6	3.3 (15)	2.1 (13)	1.2 (15)	1.5 (16)	2.7 (16)
7	3.0 (15)	1.8 (13)			
8	2.5 (15)	1.4 (13)	4.1 (14)	3.9 (15)	8.2 (15)
9	2.2 (15)	1.3 (13)			
10	2.0 (15)	1.2 (13)	9.1 (13)	5.1 (14)	1.7 (15)
15	1.0 (15)	5.8 (12)			
20	5.0 (14)	2.9 (12)	1.8 (13)	5.9 (13)	1.5 (13)
25	2.4 (14)	1.3 (12)			
30	1.2 (14)	7.0 (11)	3.4 (12)	8.4 (13)	2.8 (12)
35	6.3 (13)	4.4 (11)			
40	3.2 (13)	1.8 (11)			
45	1.7 (13)	8.5 (10)			
50	8.2 (12)	4.2 (10)			
55	4.1 (12)	2.0 (10)			
60	2.1 (12)	1.0 (10)			
65	1.2 (12)	5.0 (9)			
70	5.2 (11)	2.4 (9)			
75	1.2 (11)	1.0 (9)			
80	1.0 (11)	5.0 (8)			
85	3.7 (10)	2.1 (8)			
90	2.0 (10)	1.0 (8)			
95	7.5 (9)	4.0 (7)			
100	3.1 (9)	1.0 (7)			

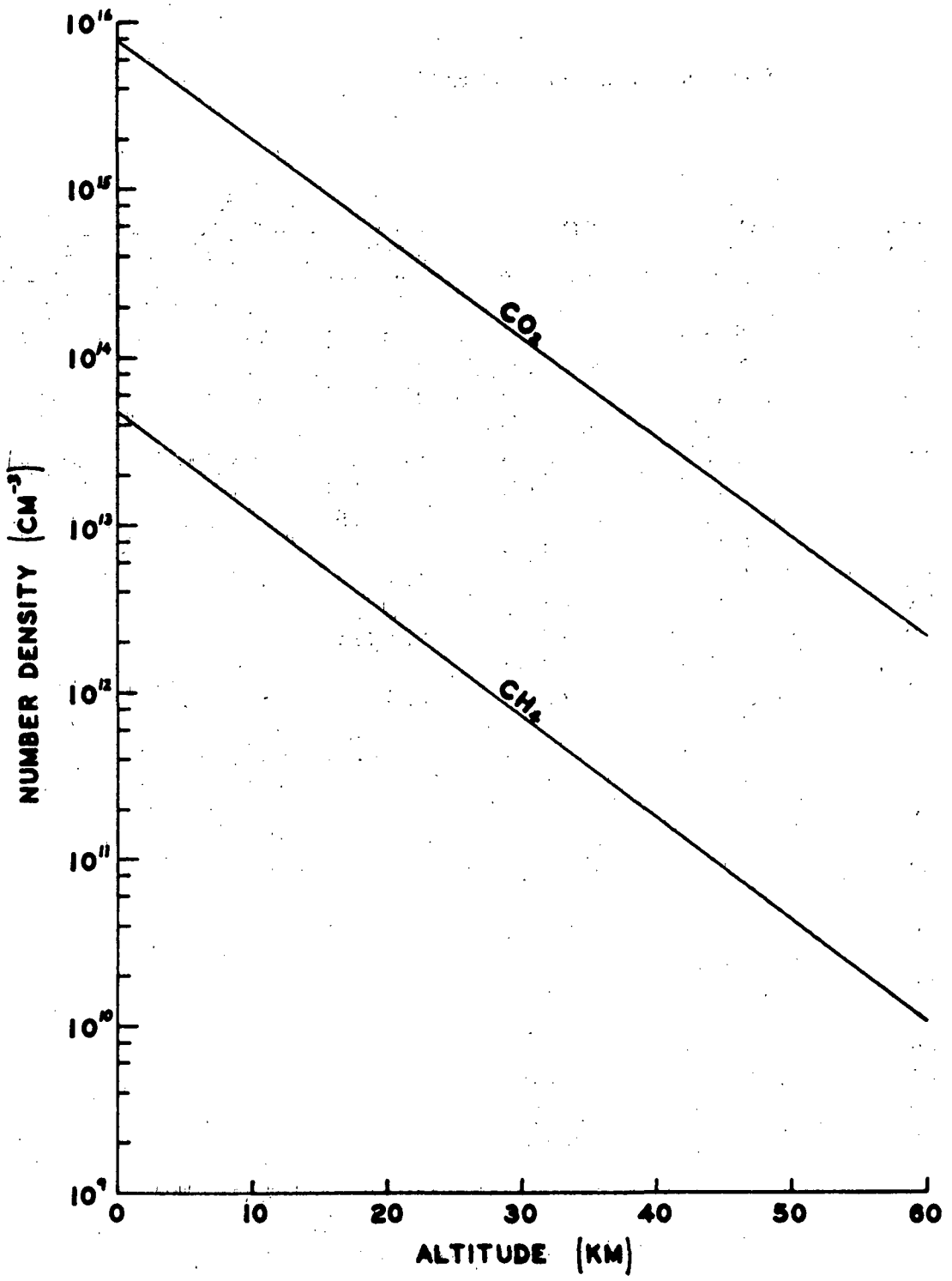

Figure 2.1.4 CO_2 and CH_4 Profiles

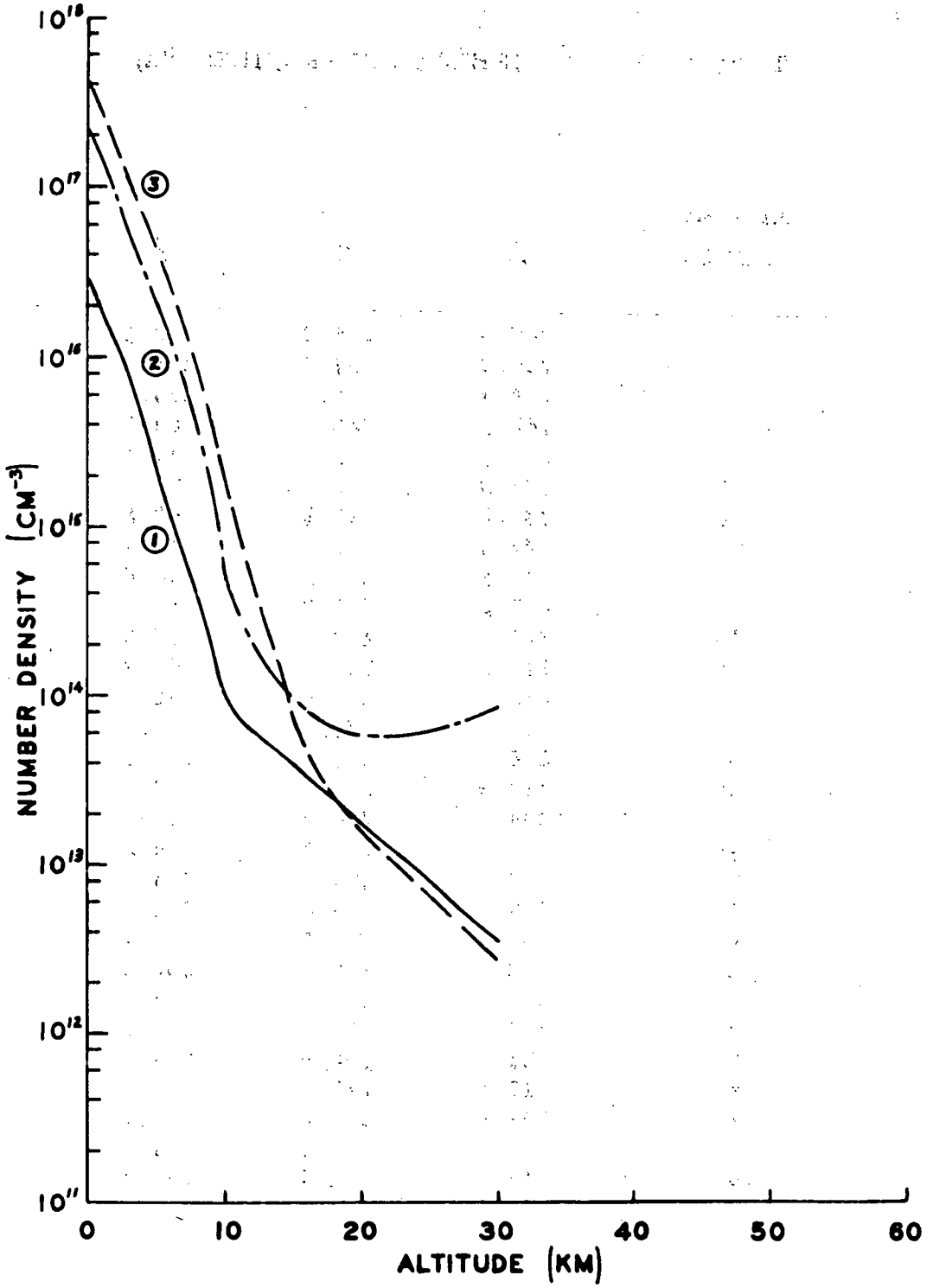

Figure 2.1.5 H_2O Concentrations

TABLE 2.1.3 TEMPERATURE PROFILES (°K)

Altitude (km)	1	2	3
0	257.3	288.2	302.6
1	259.3	281.7	295.9
2	256.1	275.2	289.4
3	252.8	268.6	284.3
4	247.8	262.2	277.4
5	241.0	255.7	270.6
6	234.2	249.2	263.8
7	227.4	242.7	257.1
8	220.6	236.2	250.4
9	217.2	229.7	243.7
10	217.2	223.3	237.0
15	217.2	216.6	203.7
20	214.2	216.6	206.7
25	211.2	221.6	221.4
30	216.0	226.5	232.3
35	222.3	236.5	243.2
40	234.6	250.4	254.0
45	247.0	264.2	264.8
50	259.3	270.6	270.2
55	259.1	265.6	263.4
60	250.9	255.8	253.1
65	248.4	239.3	236.0
70	245.4	219.7	218.9
75	234.7	200.2	201.8
80	223.9	180.6	184.8
85	213.1	180.6	177.1
90	202.3	180.6	177.0
95	211.0	195.5	184.3
100	218.5	210.0	190.7

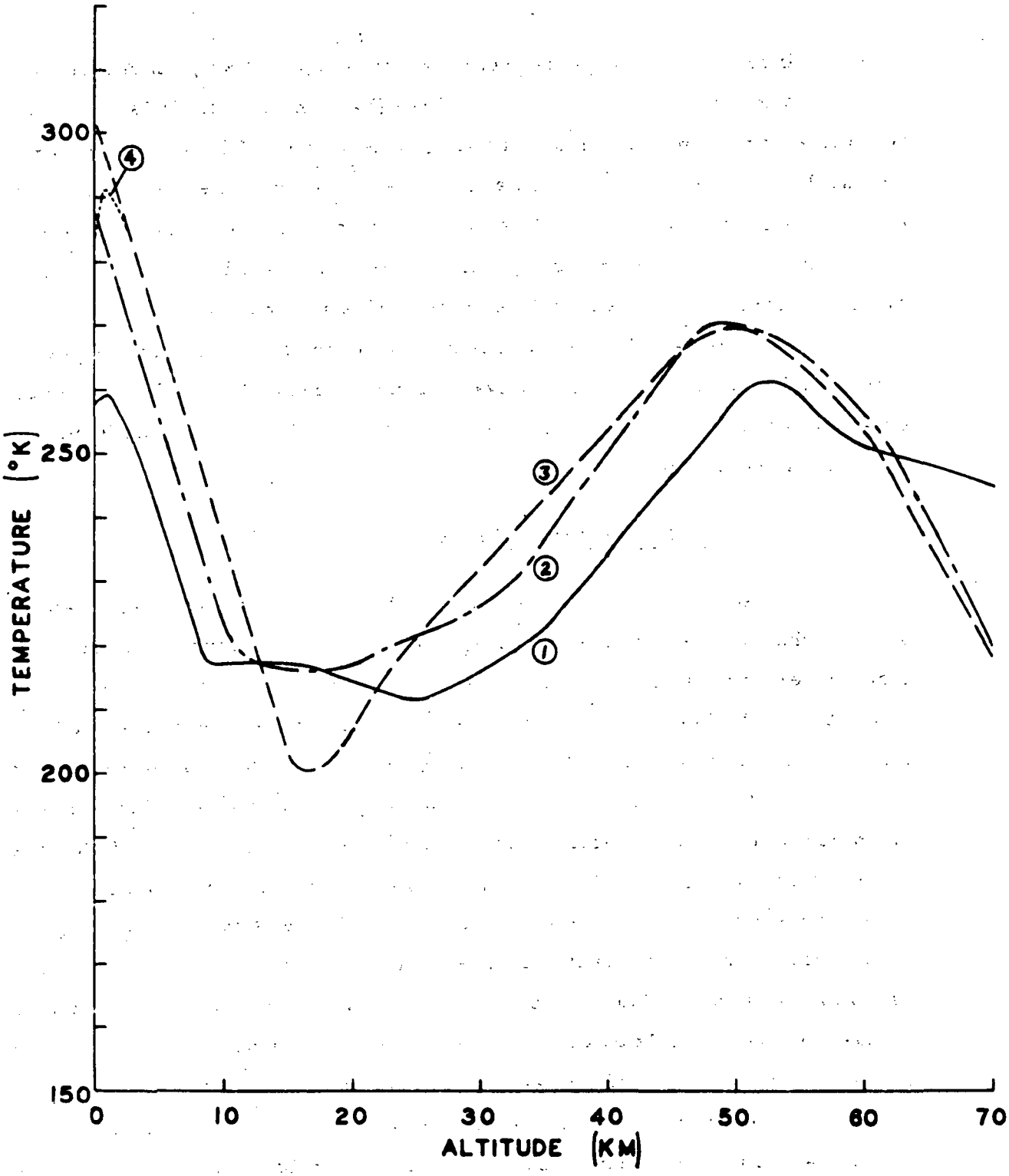

Figure 2.1.6 Temperature Profiles

profile 4 involves a low altitude inversion layer (up to 2 km), based on average values for Vandenberg AFB, June 1970 (Vachon, 1971). It is important that these variations should have no large effect on the CO measurements. Any such effects require detailed accurate supplemental measurements and make the interpretation of the data much more complex and, for practical purposes, means that many fewer data can be interpreted. Analysis of such effects is covered in subsequent sections of this report.

For calculations, described later, made to compare results of these studies with those of the Convair group (Ludwig, 1970), four other temperature models were used. These are given in Tables 2.1.4 and Figure 2.1.7 as models 5 through 11.

2.3 Other Atmospheric Characteristics

In the development of the COPE experiment a number of atmospheric characteristics must be considered. Those of greatest interest are cloud cover, precipitable water, pressure, temperature, and inversion layers. A report (Vachon, 1971) was prepared which presented a base of detailed information on these characteristics which can be extended or refined.

Significant cloud cover denies the possibility of making the desired observation since radiation (of either the 2.3 or 4.6 μ band of CO) does not penetrate the clouds. The amount of cloud cover has been found to vary mainly between 0.3 and 0.8 around the world. There is no part of the globe where there is not an appreciable time when the atmosphere is cloud free. An empirical formulation was developed to relate the probability of having a cloud-free line-of-sight at various look angles as a function of the frequency of occurrence of scattered, broken, and overcast cloud cover.

Data on precipitable water in the atmosphere shows variation between about 0.5 and 5 cm. Although there is considerable variation there are predictable trends for any region and season. The knowledge of these

TABLE 2.1.4 TEMPERATURE MODELS FOR COMPARATIVE CALCULATIONS

Altitude (km)	5	6	7	8	9	10	11
Ground	288.16	288.16	288.16	288.16	288	275	275
0.0	288.16	288.16	288.16	288.16	288	288	275'
0.15		294.6					
1	278.2	278.2	281.3	281.3	281.3	281.3	279.2
1.2							280
2	264.2	264.2	274.6	274.6	274.6	274.6	274.6
2.68				270.0	270.0	270.0	270.0
3	254.8	254.8	267.8	254.8	254.8	254.8	254.8
4	247.8	247.8	261.1	247.8	247.8	247.8	247.8
5	242.2	242.2	254.4	242.2	242.2	242.2	242.2
6	237.6	237.6	247.6	237.6	237.6	237.6	237.6
7	233.6	233.6	240.9	233.6	233.6	233.6	233.6
8	229.4	229.4	234.2	229.4	229.4	229.4	229.4
9	225.8	225.8	227.4	225.8	225.8	225.8	225.8
10	222.2	222.2	222.0	222.2	222.2	222.2	222.2
12	216.0	216.0	216.6	216.0	216.0	216.0	216.0
15	216.0	216.0	216.6	216.0	216.0	216.0	216.0
20	216.0	216.0	216.6	216.0	216.0	216.0	216.0
25	218.0	218.0	221.6	218.0	218.0	218.0	218.0
30	228.0	228.0	226.5	228.0	228.0	228.0	228.0
35	239.0	239.0	236.5	239.0	239.0	239.0	239.0
40	252.0	252.0	250.4	252.0	252.0	252.0	252.0
45	266.0	266.0	264.2	266.0	266.0	266.0	266.0
50	270.0	270.0	270.6	270.0	270.0	270.0	270.0

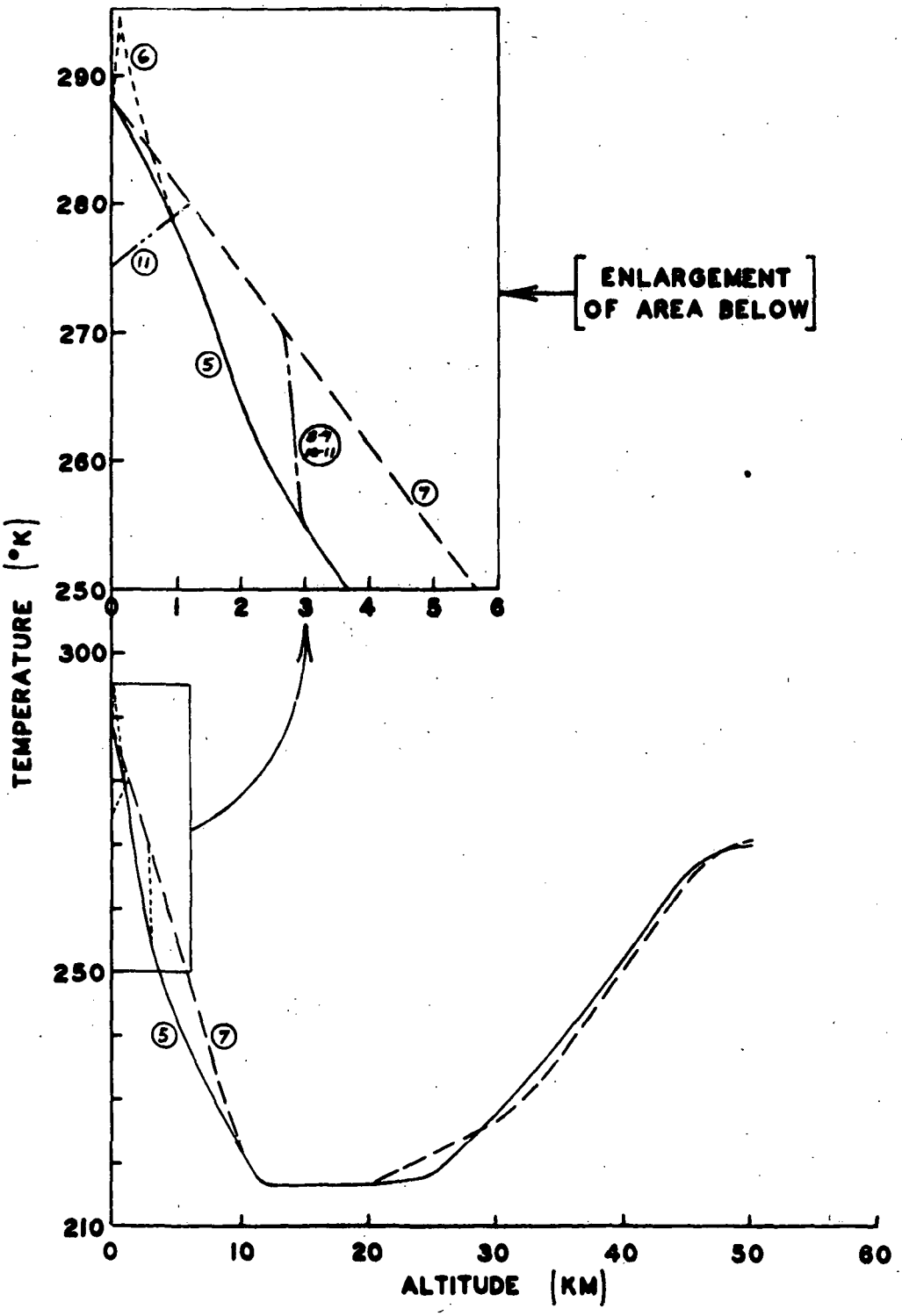

Figure 2.1.7 Temperature Profiles for Comparative Calculations

trends now appears to be unnecessary as can be seen in later discussions (Section 7.4).

One effect which must be considered in remote sensing from a fast moving vehicle is the possibility of a Doppler shift. If there is a large velocity component in the direction of the observed radiation, there is a Doppler shift which is determined by $\Delta\nu = \nu\frac{v_s}{c}$ where v_s is the velocity component in the line-of-sight, or $\Delta\nu = \nu\frac{v}{c}\cos\theta$ where θ is the angle between the line-of-sight and the vehicle movement. In the limb experiment, the satellite may be traveling very nearly direct toward or away from the sun so that $\cos\theta \approx 1$, and v_s is of the order of 7×10^5 cm sec^{-1}. Thus $\frac{v_s}{c} = \frac{\Delta\nu}{\nu}$ is of the order of 2.3×10^5. Thus at 2.3 μ, $\Delta\nu = 0.1$ cm^{-1}, and at 4.6 μ, $\Delta\nu = 0.05$ cm^{-1}. These shifts are of the order of a Doppler line-width, which is the width of the line at the upper altitudes, i.e. those of interest in the limb experiment. If the technique is spectral and employs a reference cell of any sort on board this is extremely important and probably means that the technique is not suitable for the limb measurement. For the correlation interferometric technique a Doppler shift essentially appears as a phase shift which can be readily taken into account.

2.4 The Effect of Scintillations

2.4.1 Introduction: - Scintillations in the light intensity of a beam are introduced by atmospheric turbulence. When the light from a small light source of constant intensity passes through a long path in the atmosphere, the energy collected through a small aperture at the other end is not constant; rather it fluctuates with time. The effects of such fluctuations (usually called scintillations) on the performance of a ground-looking scanning Michelson interferometer are discussed here. The output of a scanning Michelson interferometer is normally a time varying signal. Therefore, any scintillations in the light beam, before it is collected by the Michelson inter-

ferometer, can introduce spurious fluctuations in the wave form of the interferometer output. However, the effects of scintillations will be negligible if the amplitude of these scintillations turns out to be smaller than the error of digitalization in the interferometer output wave form. First, we shall qualitatively explain why the scintillation effects will not be significant with the earth-looking interferometer. Next, we shall quantitatively determine the extent of the effect of scintillation on the interferometer data.

2.4.2 Qualitative Explanation: - It is generally said that to the eye, stars, which have an angular subtense of a hundredth arc sec or less, appear to twinkle. On the other hand, objects of larger angular subtense - such as planets, which have angular subtense from several arc secs to 30-40 arc sec - do not. Consider Figure 2.4.1 and suppose that with a receiver (a telescope or the pupil of the eye) of diameter, d, on the ground we observe an object outside the earth's atmosphere, subtending an angle θ. For the purpose of scintillations, we take the height of the "top" of the atmosphere as 100 km. (The exact value of the height of the "top" is not important for the present discussion.) For an eye-pupil, AD = d $\simeq$ 6 mm so that, if the object is a star ($\theta \simeq 0.01$ arc sec), BC $\simeq$ 10 mm. On the other hand, if the object is a planet ($\theta \simeq 20$ arc sec), BC $\simeq$ 10,000 mm (10 meter). Thus, in the case of the planet, it is the increased number of atmospheric turbulence eddies perpendicular to the line-of-sight and within the light cone ABCD that are responsible for reducing the scintillations and stabilizing the intensity.

If we view a star ($\theta = 0.01$ arc sec) with a 100 cm aperture telescope, then AD $\simeq$ 100 cm and BC $\simeq$ 100 cm, and again the number of turbulence eddies perpendicular to the line-of-sight will have increased and, consequently, scintillation will be decreased. This is, of course, an observed fact: scintillations become negligible when photo-electric measurements of the brightness of a star are made with a large aperture telescope.

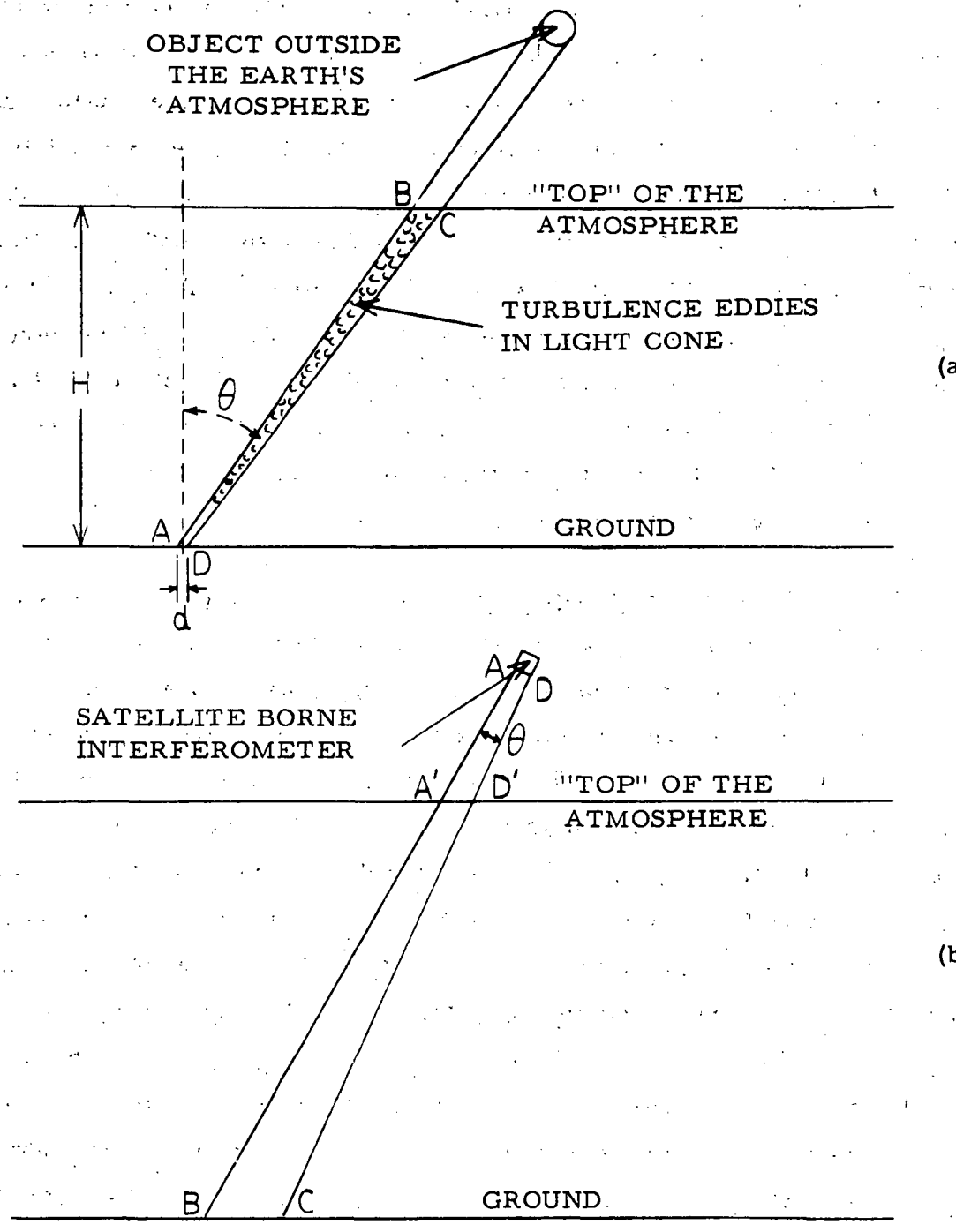

Figure 2.4.1 Geometry for Consideration of Scintillations

The situation of an earth-looking scanning Michelson interferometer is shown in Figure 2.4.1 b. Consider an interferometer receiver of diameter, AD, 3-inches. Then for a wavelength of 2 μ and resolution, $\Delta\nu$, of 0.5 cm^{-1}, the throughput is 0.006 (cm^2 ster), which gives $\theta \simeq 6 \times 10^{-3}$ radians (= 1200 arc sec) and therefore $A'D' = 600$ meters and BC = 1200 meters. Even if the height of the satellite or that of the "top" of the atmosphere is different from the above values, it is quite evident that, due to the large value of θ, dimensions $A'D'$ and BC of Figure 2.4.1 b will be very much larger than the corresponding dimensions for the case of a planet or a large aperture telescope considered above. Consequently there will be a very large number of turbulent eddies in the direction perpendicular to the line-of-sight and the effects of the scintillation will be negligible.

2.4.3 Criterion for "Significant" Amount of Scintillations: - The instrument used for this purpose will be a Michelson interferometer in which the beam of light falling on the instrument is split with a beam splitter into two mutually coherent beams which are then made to interfere with each other to produce Haidinger fringes. Light from the central region of this fringe pattern is collected by a photo detector and the output of the instrument is an electrical signal. The spectral nature of the radiations is analyzed by varying the optical phase difference between the two beams and recording the fluctuating electrical output; that is, the interferogram. The fluctuations in this recorded signal contain the information on the spectral properties of the radiations. However, the light beam falling on the instrument fluctuates in intensity. The observed interferogram will have spurious fluctuations resulting from the modulation of the interferogram by light intensity fluctuations. In Section 2.4.5, therefore, we shall investigate the influence of incident light beam intensity fluctuations upon the energy spectrum obtained with the interferometer.

2.4.4 Additive and Multiplicative Noise: - Before we make quantitative calculations of scintillations, we must point out the distinction between multiplicative and additive noise.

2.4.4.1 Additive Noise: - Let the amplitude of the noise be independent of the signal. This will be the case with digitization noise. For a six-bit word, the digitization noise amplitude will be: $1/2^6 = .016 \simeq 1.6\%$. Under such a situation, the greater the bandwidth -- (i.e. the greater the phase difference for scanning) -- the spikier the reconstructed spectrum. Therefore, to reduce digitization noise the path difference for scanning should not be greater than that dictated by the needs of spectral resolution. Conversely, even a small additive error can produce large errors in the reconstructed spectrum if the bandwidth of the scan is large. Of course the greater the amplitude of the additive noise (e.g. digitization noise) the greater will be the amplitude of the spurious spikes in the reconstructed spectrum.

2.4.4.2 Multiplicative Noise: - The noise is multiplicative when it is dependent upon the signal level, i.e. when the amplitude of the noise is a certain fraction of the instantaneous signal. For example, let the true interferogram be $F_o(\omega)$ giving a true spectrum, $f_o(\lambda)$.

Then,

$$f(\lambda) = \mathcal{F}\left[F(\omega)\right]$$

where $\mathcal{F}$ represents the usual linear operation of Fourier transform of a real signal. Let the multiplicative noise be a fraction, $\epsilon(\omega)$, of the signal, $F(\omega)$, where the value of fraction $\epsilon(\omega)$ is a random variable. Therefore the observed interferogram can be represented as

$$F_{obs}(\omega) = F_o(\omega) + \epsilon(\omega) F_o(\omega) = \left[1 + \epsilon(\omega)\right] F_o(\omega)$$

Therefore the observed reconstructed spectrum will be

$$f_{obs}(\lambda) = \mathcal{F}\left[F_{obs}(\omega)\right] = \mathcal{F}\left[F_o(\omega)\right] + \mathcal{F}\left[\epsilon(\omega)\right] F_o(\omega)\Big]$$

$$= f_o(\lambda) + \mathcal{F}\left[\epsilon(\omega)\, F_o(\omega)\right].$$

The error in the reconstructed spectrum therefore will be

$$\Delta f(\lambda) \equiv f_{obs}(\lambda) - f_o(\lambda) = \mathcal{F}\left[\epsilon(\omega)\, F_o(\omega)\right].$$

But, since $\epsilon(\omega)$ is a random variable,

$$\mathcal{F}\left[\epsilon(\omega)\, F_o(\omega)\right] \leq |\epsilon_{max}|\, \mathcal{F}\left[F_o(\omega)\right] = |\epsilon_{max}| \cdot f_o(\lambda).$$

where ϵ_{max} is the maximum likely fractional error in the interferogram. Consequently, the maximum likely error in the reconstruction spectrum will be

$$\frac{\Delta f(\lambda)}{f_o(\lambda)} \leq |\epsilon_{max}|.$$

The effect of light intensity scintillations will be a multiplicative error on the observed interferogram and the reconstructed spectrum. Therefore, for example, if the scintillation amplitude is 1%, the error in the observed intensities in the reconstructed spectrum will not be more than 1%.

2.4.5 Calculation of the Scintillation Effect: - The effect of an atmospheric refractive index inhomogenity on the light propagating through turbulent atmosphere and the consequent scintillation effects have been investigated by various authors, as noted in the following discussion. We shall make use of these investigations in calculating the magnitude of the scintillation expected from an earth-looking satellite.

An exact mathematical description of atmospheric turbulence is not possible. However, with some reasonable assumptions, the problem becomes tractable. In the work of earlier investigators the atmospheric turbulence is assumed to be homogeneous and isotropic and the spectral energy distribution in the turbulence is assumed to be given by the Kolmogoroff theory. Let $C_\ell(\rho)$ be the convariance of the log-amplitude between two measurement points separated by a distance, ρ. Then, scintillations in a laser beam traveling through a uniform atmosphere have been calculated by Fried and Seidman (1967) showing that for $\rho = o$, $C_\ell(O)$ can be written as a product of two factors:

$$C_\ell(O) = C_\ell^S(O) \cdot f_o(\Omega) \qquad \text{Eq. 2.1}$$

where the first factor, $C_\ell^S(O)$, the value of $C_\ell(O)$ associated with a point source, is given by:

$$C_\ell^S(O) = \text{constant} \cdot k^{7/6} z^{11/6} C_N^2 \qquad \text{Eq. 2.2}$$

($k = \frac{2\pi}{\lambda}$, λ = wavelength of light, z = path length, and C_N^2 is the refractive index structure constant). The second factor is a function of the parameter Ω (where $\Omega = k\alpha_o^2/z$, and α is the linear source size). The value of $f(\Omega)$ is given by Fried and Seidman (1967, Equation 4.12).

For the case of an earth-looking satellite, the atmosphere in the line-of-sight is not uniform and therefore C_N^2 is not a constant. Based on the data presented by Hufnagel (1964), it has been shown (Fried and Cloud, 1966) that the value of C_N^2 at an altitude, h, is given by:

$$C_N^2 = 4.2 \times 10^{-14} h^{-1/3} \exp(-h/h_o)_3 \qquad \text{Eq. 2.3}$$

where the scale height, h_o, is 3.2×10^3 meters. Fried (1967b) has made an evaluation of $C_\ell(O)$ and $f_n(\Omega)$ for the case of altitude dependent C_N^2 given by Eq. 2.3. Following him we can derive:

$$C_\ell^S(O) = 0.122 \sec^{11/16}\theta\left[\frac{2.3}{\lambda}\right]^{7/6}$$

where the wavelength, λ, is in microns. For $\lambda = 2.3$ microns and $\theta = O$; $C_\ell^S(O) = 0.122$, i.e. for a point source on the ground $C_\ell(O) = 0.122$.

To calculate the magnitude of scintillations we first calculate the fractional intensity variance $C_I(O)$ from the relation (Fried, 1967a).

$$C_I(O) = \exp\left[4C_\ell(O)\right] - 1 \qquad \text{Eq. 2.4}$$

thus for $C_\ell(O) = 0.122$ we get:

$$C_I(O) = 0.629.$$

Noting that the above value is for fractional intensity and comparing Eq. 4 of Fried (1957a) with Eq. 13-13 of Tartskii (1961), we obtain the RMS deviation of the scintillation $= \sqrt{0.629 - .79} \simeq 80\%$.

The above RMS value of scintillation has been obtained for a point source on the ground. However, the Michelson interferometer on the satellite will have a field-of-view of, say, four degrees (which gives 3.8×10^{-3} steradians for a circular field-of-view). This increase in the field-of-view will decrease the magnitude of scintillations.

Fried has evaluated the function $f_n(\Omega)\ 1 = C_\ell(O)/C_\ell^S(O)$ that gives the reduction in $C_\ell(O)$ with increasing value of the source size parameter, Ω. This dependence of $C_\ell(O)/C_\ell^S(O)$ on Ω is shown in Figure 2.4.2. For our case of an earth-viewing instrument in a satellite we put Ω in a more useful form:

$$\Omega = \frac{\omega h^2 \sec\theta}{\lambda h_o}$$

where

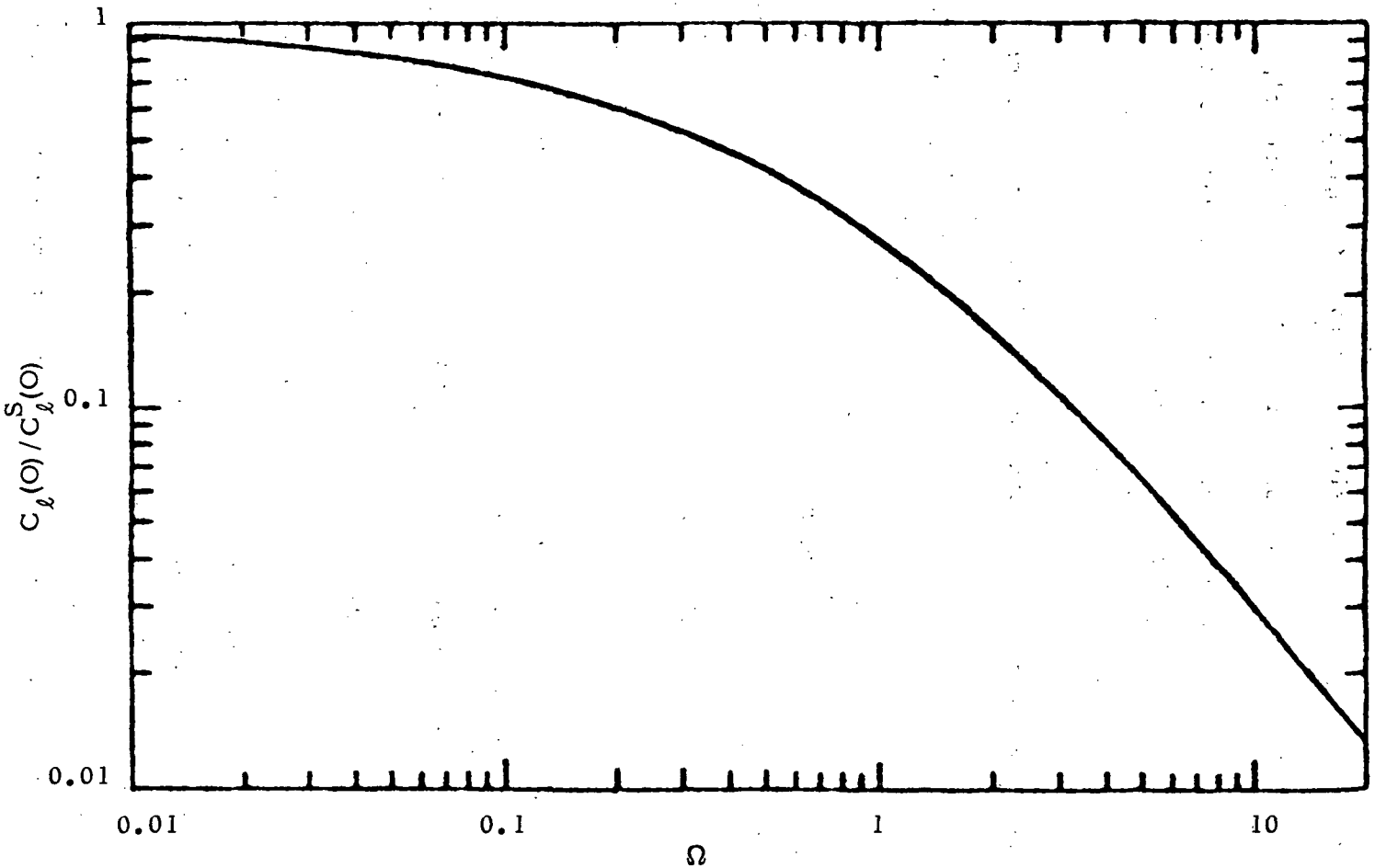

Figure 2.4.2 Dependence of the Normalized Log-Amplitude Variance $C_1(O)/C_1(O)$ Upon the Normalized Source Size Ω for Observations from Space of a Ground-Based Source (Fried, 1967b).

ω = solid angle of the field-of-view in steradians,

h = height of the satellite orbit about the ground,

h_o = scale height of turbulence (3.2×10^3 meters),

θ = zenith angle of the instrument with respect to the source point on the ground, and

λ = wavelength.

To calculate the upper bound on the magnitude of scintillation we take:

ω = 10^{-6} steradians (for two arc minute field-of-view)

h = 10^5 meters

h_o = 3.2×10^3 meters

θ = 0

λ = 2.3×10^{-6} meters

Thus, $\Omega \simeq 10^6$.

This is a very large value for Ω and from Figure 2.4.2 it is quite clear that the value of $C_\ell(O)/C_\ell^S(O)$ for $\Omega \simeq 10^6$ is essentially zero (less than 10^{-6}). Since $C_\ell^S(O) = 0.122$ as calculated above, $C_\ell(O) < 0.122 \times 10^{-6}$ therefore

$$C_I(O) = \exp\left[4C_\ell(O)\right] - 1 < 0.5 \times 10^{-6},$$

and the RMS value of scintillation amplitude will be less than 0.07%. Therefore, we conclude that, for the above described technique of measuring carbon monoxide with a Michelson interferometer on an orbiting satellite, the effects of atmospheric scintillations will be less than 0.1% in the reconstructed spectrum.

It should be noted that for calculating the upper bound for scintillation, we have already chosen the greatly exaggerated values for the

parameters. For example, we have taken $\omega = 10^{-6}$ radians while the actual value will be 4×10^{-3} radians or greater. Similarly the height of the satellite will be much greater than 10^{5} meters chosen here. For the situation in question, therefore, the conclusion is that the effect of scintillation will be negligible.

3. SPECTRAL CONSIDERATIONS

3.1 The CO Infrared Spectrum

The infrared spectrum has been discussed in detail elsewhere (Bortner and Kummler, 1971). The two bands under consideration herein are the first overtone band centered about 2.35 μ and the fundamental band centered about 4.67 μ. The positions and the energies of the various rotational lines of these bands is given in Table 3.1.1 for the first overtone band and in Table 3.1.2 for the fundamental band. The line strengths of the lines of each band are given in Table 3.1.3. It can be seen that the fundamental band is stronger than the overtone by a factor of the order of 100. The fundamental is less interfered with by absorption due to other atmospheric constituents. The overtone band is capable of much simpler interpretation, being much less affected by atmospheric temperatures, ground temperatures, and ground emissivity. As seen in Figure 3.2.1 the radiation seen in this experiment in the overtone band region would consist almost exclusively of reflected sunlight while that radiation for the fundamental band region would be mainly earthshine with some effect of reflected sunlight and serious atmospheric emission effects. These factors will be discussed later.

3.2 Intensity of Reflected Solar Radiation and Earthshine

3.2.1 Solar Reflection: - The solar radiation reaching the earth and being reflected can be calculated for any wavelength as follows. From blackbody radiation tables (Bowen, 1963) the radiant intensity, J, for a 5900 K blackbody is calculated to be 9.3×10^{1} watt cm^{-2} sr^{-1} μ^{-1} at 2.3 μ and 8.0×10^{0} at 4.6 μ. The average irradiance, H, incident on the earth's atmosphere (and incident on the earth's surface in the absence of any atmospheric atten-

TABLE 3.1.1 ENERGY & WAVELENGTH OF VIBRATION-ROTATION LINES OF CO (2-0)

2 - 0

R BRANCH			P BRANCH		
$J' - J''$	CM^{-1}	$\lambda(\mu)$	$J' - J''$	CM^{-1}	$\lambda(\mu)$
1- 0	4263.831	2.34531	0- 1	4256.211	2.34951
2- 1	4267.536	2.34327	1- 2	4252.296	2.35167
3- 2	4271.170	2.34128	2- 3	4248.311	2.35388
4- 3	4274.734	2.33933	3- 4	4244.257	2.35612
5- 4	4278.227	2.33742	4- 5	4240.133	2.35842
6- 5	4281.649	2.33555	5- 6	4235.940	2.36075
7- 6	4285.000	2.33372	6- 7	4231.678	2.36313
8- 7	4288.280	2.33194	7- 8	4227.347	2.36555
9- 8	4291.488	2.33019	8- 9	4222.947	2.36801
10- 9	4294.625	2.32849	9-10	4218.479	2.37052
11-10	4297.690	2.32683	10-11	4213.942	2.37307
12-11	4300.684	2.32521	11-12	4209.337	2.37567
13-12	4303.605	2.32363	12-13	4204.664	2.37831
14-13	4306.454	2.32210	13-14	4199.923	2.38100
15-14	4309.231	2.32060	14-15	4195.114	2.38373
16-15	4311.935	2.31914	15-16	4190.237	2.38650
17-16	4314.567	2.31773	16-17	4185.293	2.38932
18-17	4317.125	2.31636	17-18	4180.282	2.39218
19-18	4319.611	2.31502	18-19	4175.203	2.39509
20-19	4322.024	2.31373	19-20	4170.058	2.39805
21-20	4324.363	2.31248	20-21	4164.845	2.40105
22-21	4326.628	2.31127	21-22	4159.567	2.40410
23-22	4328.821	2.31010	22-23	4154.221	2.40719
24-23	4330.939	2.30897	23-24	4148.810	2.41033
25-24	4332.983	2.30788	24-25	4143.332	2.41352
26-25	4334.953	2.30683	25-26	4137.788	2.41675
27-26	4336.849	2.30582	26-27	4132.179	2.42003
28-27	4338.670	2.30485	27-28	4126.504	2.42336
29-28	4340.417	2.30393	28-29	4120.763	2.42674
30-29	4342.089	2.30304	29-30	4114.957	2.43016
31-30	4343.686	2.30219	30-31	4109.086	2.43363
32-31	4345.208	2.30139	31-32	4103.150	2.43715
33-32	4346.654	2.30062	32-33	4097.149	2.44072
34-33	4348.026	2.29989	33-34	4091.083	2.44434
35-34	4349.321	2.29921	34-35	4084.953	2.44801
36-35	4350.541	2.29856	35-36	4078.759	2.45173
37-36	4351.685	2.29796	36-37	4072.501	2.45549
38-37	4352.753	2.29740	37-38	4066.178	2.45931
39-38	4353.745	2.29687	38-39	4059.792	2.46318
40-39	4354.660	2.29639	39-40	4053.342	2.46710

TABLE 3.1.2 ENERGY & WAVELENGTH OF VIBRATION-ROTATION LINES OF CO (1-0)

1 - 0

R BRANCH			P BRANCH		
J' - J''	CM^{-1}	λ(μ)	J' - J''	CM^{-1}	λ(μ)
1- 0	2147.083	4.65748	0- 1	2139.428	4.67415
2- 1	2150.858	4.64931	1- 2	2135.548	4.68264
3- 2	2154.598	4.64124	2- 3	2131.634	4.69124
4- 3	2158.301	4.63327	3- 4	2127.684	4.69994
5- 4	2161.970	4.62541	4- 5	2123.701	4.70876
6- 5	2165.602	4.61765	5- 6	2119.683	4.71769
7- 6	2169.198	4.61000	6- 7	2115.631	4.72672
8- 7	2172.759	4.60244	7- 8	2111.545	4.73587
9- 8	2176.282	4.59499	8- 9	2107.426	4.74513
10- 9	2179.770	4.58764	9-10	2103.273	4.75449
11-10	2183.220	4.58039	10-11	2099.086	4.76398
12-11	2186.634	4.57324	11-12	2094.867	4.77357
13-12	2190.011	4.56619	12-13	2090.614	4.78328
14-13	2193.351	4.55923	13-14	2086.328	4.79311
15-14	2196.653	4.55238	14-15	2082.010	4.80305
16-15	2199.918	4.54562	15-16	2077.659	4.81311
17-16	2203.145	4.53897	16-17	2073.275	4.82329
18-17	2206.334	4.53240	17-18	2068.860	4.83358
19-18	2209.486	4.52594	18-19	2064.412	4.84399
20-19	2212.599	4.51957	19-20	2059.932	4.85453
21-20	2215.674	4.51330	20-21	2055.421	4.86518
22-21	2218.710	4.50712	21-22	2050.878	4.87596
23-22	2221.708	4.50104	22-23	2046.303	4.88686
24-23	2224.667	4.49505	23-24	2041.697	4.89789
25-24	2227.587	4.48916	24-25	2037.060	4.90903
26-25	2230.469	4.48336	25-26	2032.393	4.92031
27-26	2233.310	4.47766	26-27	2027.694	4.93171
28-27	2236.113	4.47205	27-28	2022.965	4.94324
29-28	2238.875	4.46653	28-29	2018.205	4.95490
30-29	2241.598	4.46110	29-30	2013.415	4.96669
31-30	2244.281	4.45577	30-31	2008.595	4.97860
32-31	2246.924	4.45053	31-32	2003.745	4.99065
33-32	2249.527	4.44538	32-33	1998.865	5.00284
34-33	2252.089	4.44032	33-34	1993.956	5.01516
35-34	2254.611	4.43536	34-35	1989.017	5.02761
36-35	2257.092	4.43048	35-36	1984.049	5.04020
37-36	2259.532	4.42570	36-37	1979.051	5.05293
38-37	2261.931	4.42100	37-38	1974.025	5.06579
39-38	2264.289	4.41640	38-39	1968.970	5.07880
40-39	2266.605	4.41188	39-40	1963.886	5.09194

TABLE 3.1.3 CO LINE STRENGTHS (cm^{-2} atm^{-1})

	FUNDAMENTAL (Benedict, 1962)		OVERTONE (Kostkowski, 1961)	
	R	P	R	P
0	1.970		.0163	
1	3.878	1.927	.0321	.0158
2	5.643	3.707	.0467	.0303
3	7.100	5.251	.0592	.0428
4	8.261	6.491	.0691	.0527
5	9.059	7.386	.0760	.0598
6	9.482	7.920	.0797	.0638
7	9.544	8.105	.0805	.0651
8	9.286	7.980	.0785	.0638
9	8.760	7.591	.0742	.0604
10	8.032	7.002	.0682	.0555
11	7.170	6.278	.0610	.0495
12	6.240	5.480	.0532	.0430
13	5.301	4.665	.0453	.0365
14	4.400	3.876	.0376	.0301
15	3.568	3.145	.0306	.0243
16	2.830	2.494	.0243	.0192
17	2.196	1.934	.0189	.0148
18	1.668	1.486	.0144	.0112
19	1.241	1.091	.0107	.00828
20	0.904	0.793	.00779	.00597
21	0.645	0.566	.00557	.00423
22	0.451	0.395	.00390	.00294
23	0.309	0.290	.00268	.00200
24	0.208	0.181	.00180	.00133
25	0.137	0.119	.00119	.000872
26	0.0884	0.0766	.000765	.000556
27	0.0589	0.0483	.000486	.000350
28	0.0349	0.0300	.000302	.000215
29	0.0212	0.0182	.000184	.000130
30	0.0127	0.0108	.000110	.0000770
31	0.00743	0.00634	.0000642	.0000446
32	0.00427	0.00364	.0000371	.0000254
33	0.00241	0.00205	.0000209	.0000142
34	0.00134	0.00113	.0000116	.0000078

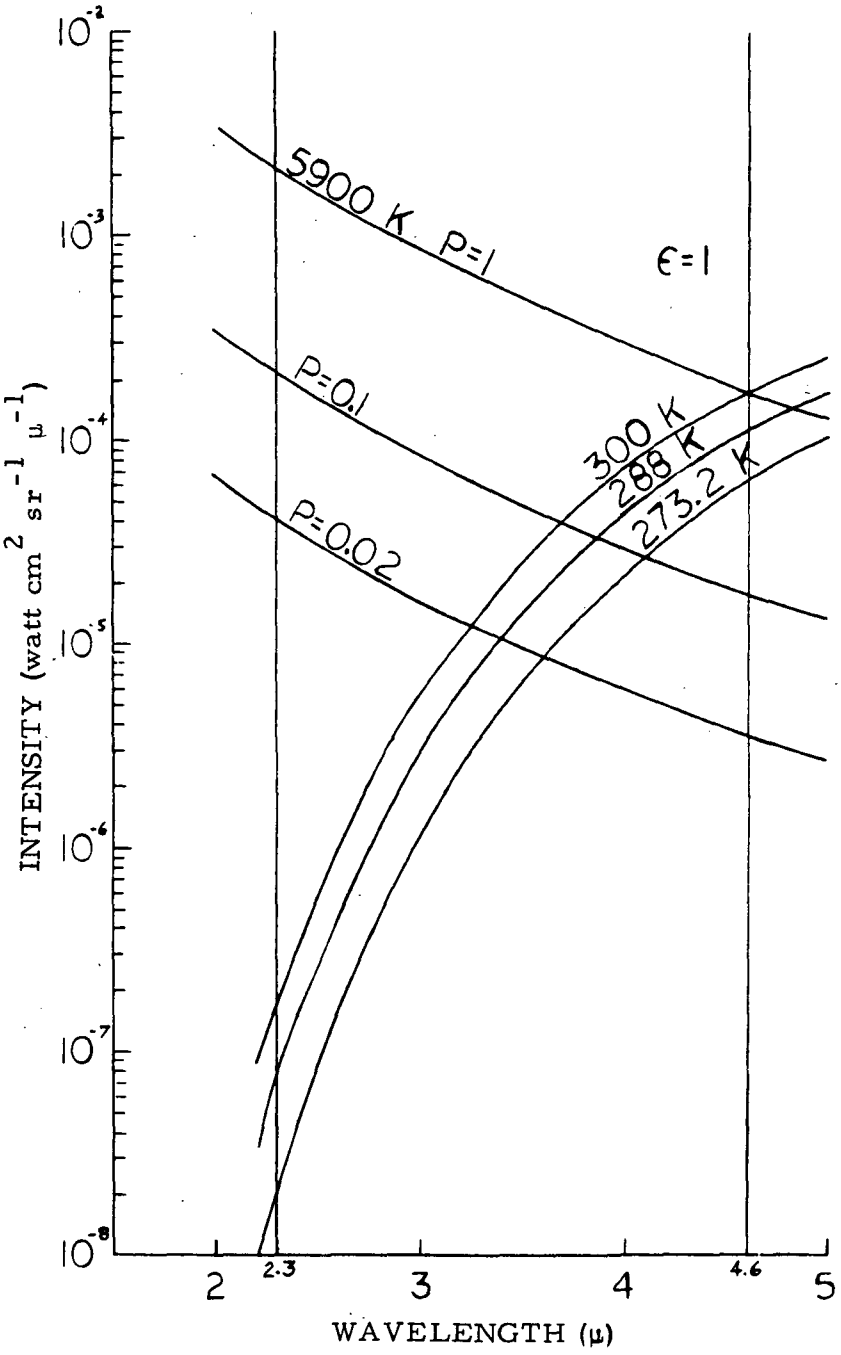

Figure 3.2.1 Reflected Sola~ Radiation and Earthshine

uation is (Thekaekara, 1971) 6.8×10^{-3} watts cm^{-2} μ^{-1} at 2.3 μ and 5.5×10^{-4} watts cm^{-2} μ^{-1} at 4.6 μ.

The reflected solar radiation, N, from the earth's surface is the

$$N \text{ (watts cm}^{-2} \text{ ster}^{-1} \mu^{-1}) = \frac{\rho H}{\pi}$$

The values of N are thus 2.16×10^{-3} ρ watt cm^{-2} $ster^{-1}$ μ^{-1} at 2.3 μ and 1.68×10^{-4} ρ watt cm^{-2} $ster^{-1}$ μ^{-1} at 4.6 μ. The intensities (in watt cm^{-1} sr^{-1} μ^{-1}) are shown in Figure 3.2.1 for various reflectivities.

3.2.2 Earthshine: - From blackbody radiation tables (Bowen, 1963) the radiant intensity is given for a 300 °K blackbody and by the ratio

$$\frac{R_T}{R_{300}} = \frac{e^{1.439 \times 10^4 \lambda \times 300}{}^{-1}}{e^{1.439 \times 10^4 \lambda T}{}^{-1}}$$

the intensities (watts cm^{-2} sr^{-1} μ^{-1}) for 273.2 and 288 K blackbodies were calculated giving the following, as shown in Figure 3.2.1.

T_g	2.3 μ	4.6 μ
273.2	2.0×10^{-8}	6.15×10^{5}
288	7.54×10^{-8}	1.11×10^{-4}
300	1.60×10^{-7}	1.71×10^{-4}

3.2.3 Ratio of Reflected Solar Radiation and Earthshine Intensities: - The ratios of reflected sunlight to earthshine at 2.3 μ are thus

ρ	T_g:	273.2 K	288 K	300 K
0.02		2×10^3	5.4×10^2	2.5×10^2
0.1		1×10^4	2.7×10^3	1.2×10^3
1.0		1×10^5	2.7×10^4	1.2×10^4

and the ratios of earthshine to reflected sunlight at 4.6 μ are

ρ	T_g:	273.2 K	288 K	300 K
0.02		1.78×10^1	3.20×10^1	4.95×10^1
0.1		3.56×10^0	6.40×10^0	9.90×10^0
1.0		3.56×10^{-1}	6.40×10^{-1}	9.90×10^{-1}

Page Intentionally Left Blank

4. RADIATIVE THEORY

4.1 Theory

To study the feasibility of the CO density measurements and the effect of various atmospheric parameters on such measurements, calculations have been made using the radiative transfer theory described in this section. First, the physical model and solution thereof are presented and then the physical parameters and their scaling relationship with altitude are defined.

The model includes absorption and emission of photons along a ray from the source to the detector. The two geometries considered are direct solar observation - limb experiment, and absorption of the earth's albedo - mapping experiment. Provisions are made for adding earthshine to reflection of sunlight from the earth's surface. However, phenomena such as scattering resonance fluorescence and radiation trapping have been neglected. Boltzmann populations as described by the local atmospheric temperature have been assumed for the upper and lower states of all transitions and the line profiles are given by the Voigt function at all altitudes. Doppler shifts as caused by atmospheric winds and by relative motion between the atmosphere and the satellite have been neglected.

The monochromatic radiative transfer equation is given (Chandrasekhar, 1960) by:

$$\frac{dI_\nu}{dS} = \epsilon_\nu - I_\nu \alpha_\nu \qquad \text{Eq. 4.1}$$

Where:

I_ν = spectral intensity (watts/cm^3-ster-cm^{-1})

S = distance along ray (cm)

ϵ_ν = spectral emission coefficient (watts/cm^2-ster-cm^{-1}), a function of S

α_ν = spectral absorption coefficient (cm^{-1}), a function of S

Formally,

$$I_\nu = C \exp(-\int \alpha_\nu dS') + \exp(-\int \alpha_\nu dS') \int \epsilon_\nu \exp\left[\int \alpha_\nu dS''\right] dS' \quad \text{Eq. 4.2}$$

For the limb boundary condition:

$$I_\nu(z) = I_{o,\nu} \exp(-\int_o^z \alpha_\nu dS'') + \exp(-\int_o^z \alpha_\nu dS'') \int_o^z \epsilon_\nu \exp(\int_o^{S'} \alpha_\nu dS'') dS' \quad \text{Eq. 4.3}$$

or

$$I_\nu(z) = I_{o,\nu} \exp(-\int_o^z \alpha_\nu dS'') + \int_o^z \epsilon_\nu \exp(-\int_{S'}^z \alpha_\nu dS'') dS' \quad \text{Eq. 4.4}$$

The geometry for this situation is shown in Figure 4.1.1.

For the mapping experiment, two conditions are required. The solar energy is attenuated as it penetrates to the earth's surface. At this point, it is reflected and the total intensity increased by earthshine. The resulting flux is then further attenuated by the atmosphere until the satellite is reached. It is pointed out that atmospheric emission which is reflected by the earth into the field-of-view of the detector is negligible and therefore not included in the model. The geometry of the mapping experiment is given in Figure 4.1.2 and is described mathematically by Equation 4.5.

$$I_\nu = \rho_\nu \left[I_{o,\nu} \exp(-\int_o^{z_1} \alpha dS'') + \int_o^{z_1} \epsilon_\nu \exp(\int_{S'}^{z_1} \alpha_\nu dS'') dS'\right] \quad \text{Eq. 4.5}$$

$$+ I_e \exp(-\int_o^z \alpha_\nu dx'') + \int_o^z \epsilon_\nu \exp(-\int_{x'}^z \alpha_\nu dx'') dx'$$

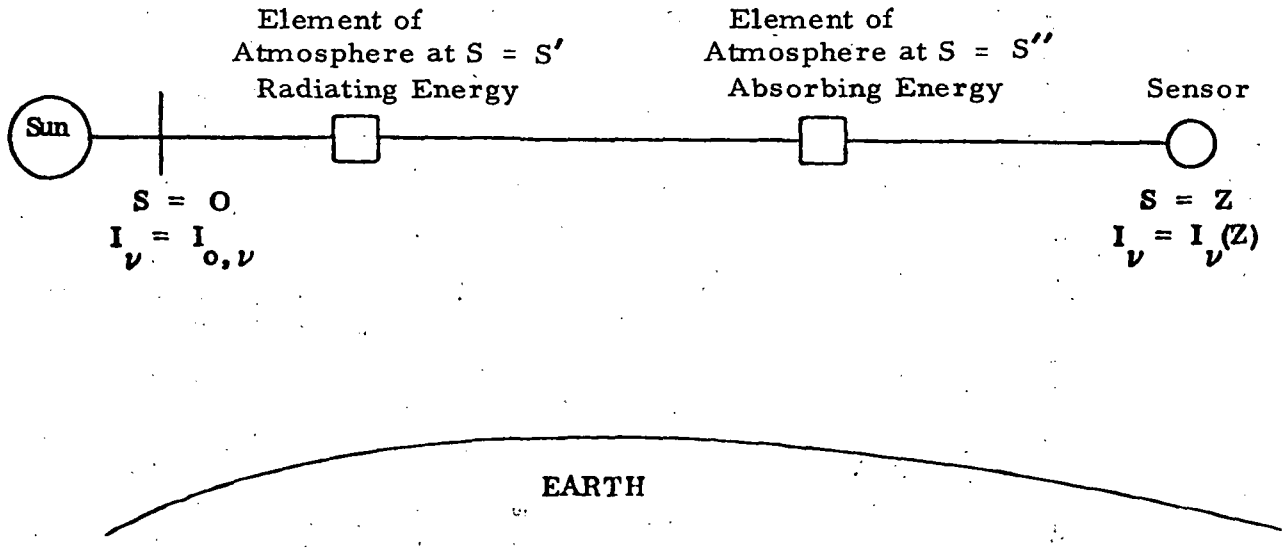

Figure 4.1.1 Geometry for Limb Conditions

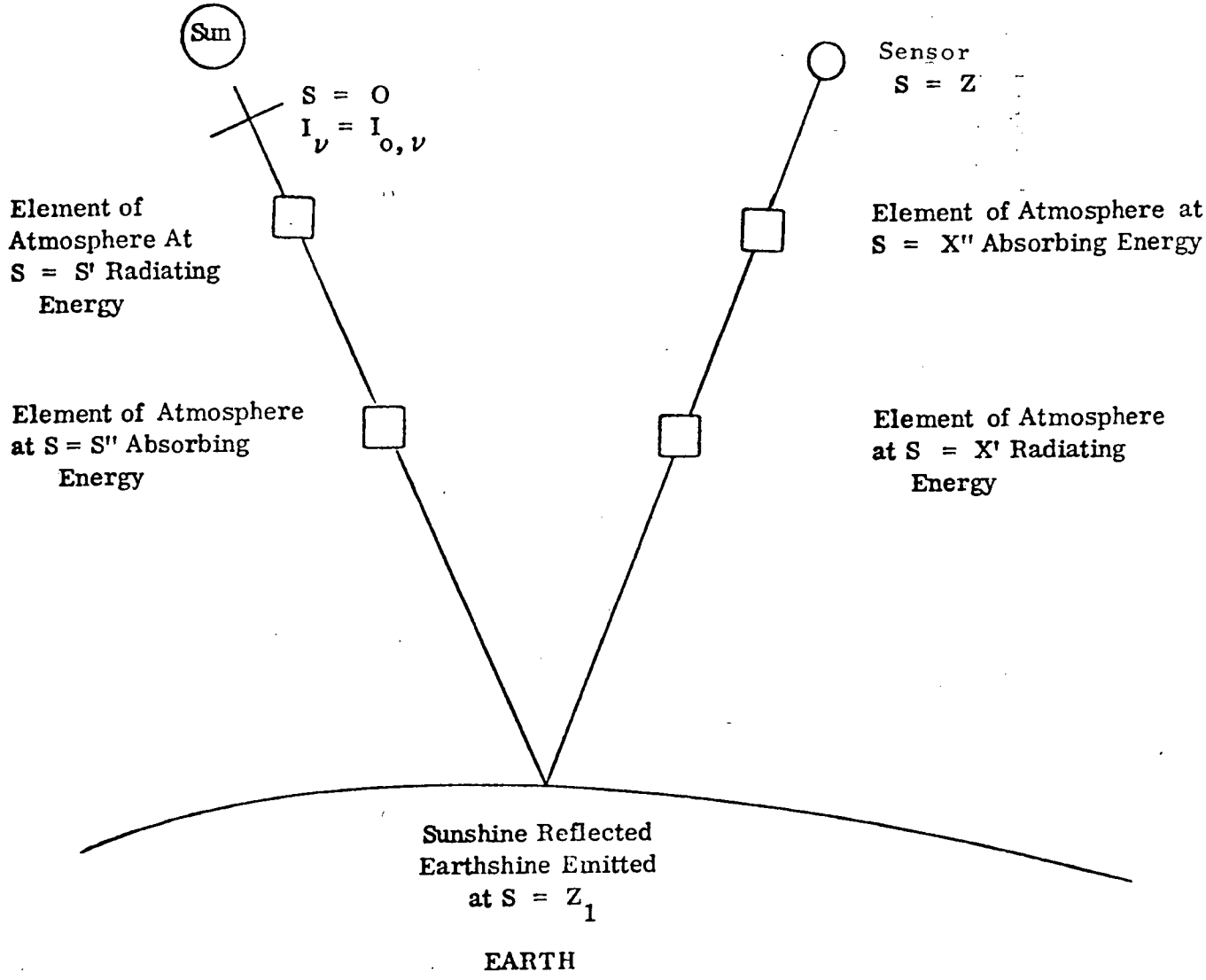

Figure 4.1.2 Geometry for Mapping Conditions

Where

I_e = earthshine (watts/cm^2-ster-cm^{-1})

ρ_ν = earth reflection coefficient

Equations 4.4 and 4.5 have been numerically integrated along the rays indicated in Figures 4.1.1 and 4.1.2 using Simpson's rule. The properties ϵ_ν and α_ν are functions of altitude which must be evaluated prior to integration. This is considered below.

On a microscopic basis, for a single rotational line (Kulander, 1964),

$$\epsilon_\nu = \epsilon\varphi_\nu = \frac{n_u h c\nu}{4\pi} A_{u\ell} \varphi_\nu \qquad \text{Eq. 4.6}$$

$$\alpha_\nu = (\alpha_A - \alpha_S)\, \varphi_\nu = (n_\ell B_{\ell u} - n_u B_{u\ell}) \frac{h c\nu}{4\pi} \varphi_\nu \qquad \text{Eq. 4.7}$$

where

φ_ν = Voigt profile (1/cm^{-1})

n_u, n_ℓ = upper and lower state number densities (particles/cm^3)

$hc\nu$ = energy per transition (watt sec/transition)

α_A = absorption coefficient (cm^{-1}/cm)

α_S = stimulated emission coefficient (cm^{-1}/cm)

$A_{u\ell}$ = Einstein coefficient for spontaneous emission

$$\left(\frac{\text{Transitions}}{\text{Sec. Particle}} \right)$$

$B_{\ell u}$ = Einstein coefficient for absorption

$$\left(\frac{\text{Transitions}}{\text{Particle}} \cdot \frac{\text{Cm-Ster}}{\text{Watt Sec.}} \right)$$

$B_{u\ell}$ = Einstein coefficient for stimulated emission

$$\left(\frac{\text{Transitions}}{\text{Particle}} \cdot \frac{\text{Cm-Ster}}{\text{Watt Sec.}} \right)$$

It is noted that the definition of the Einstein coefficients is arbitrary but that they are related by Kirchoff's Law for equilibrium at temperature, T.

$$\epsilon_\nu = B_\nu(T)\, \alpha_\nu \qquad \text{Eq. 4.8}$$

$$B_\nu(T) = \frac{2hc^2\nu^3}{e^{hc\nu/kT}-1} \left(\text{watts/cm}^2\text{-ster-cm}^{-1}\right)$$

Thus,

$$n_u A_{u\ell} = (n_\ell B_{\ell u} - n_u B_{u\ell})\, B_\nu(T) \qquad \text{Eq. 4.9}$$

or

$$\frac{A_{u\ell}/B_{u\ell}}{(n_\ell B_{\ell u}/n_u B_{u\ell})} = \frac{2hc^2\nu^3}{\exp(hc\nu/kT)-1} \qquad \text{Eq. 4.10}$$

But, at equilibrium the Boltzmann distribution is:

$$\frac{n_\ell}{n_u} = \frac{g_\ell}{g_u} \exp(hc\nu/kT) \qquad \text{Eq. 4.11}$$

and by comparison

$$g_\ell B_{\ell u} = g_u B_{u\ell} \qquad \text{Eq. 4.12}$$

$$A_{u\ell} = B_{u\ell} \cdot 2hc^2\nu^3 \qquad \text{Eq. 4.13}$$

The Voigt profile, φ_ν, is defined in terms of the Doppler and Lorentz half widths, i.e. half the line width at half the peak intensity (Armstrong, 1967).

$$\varphi_\nu = \frac{1}{\alpha_D}\left(\frac{\ln 2}{\pi}\right)^{1/2} K(x, y) \qquad \text{Eq. 4.14}$$

$$K(x, y) = \frac{y}{\pi}\int_{-\infty}^{\infty} \frac{\exp(-t^2)}{y^2 + (x - t)^2}\, dt \qquad \text{Eq. 4.15}$$

$$y = \frac{\alpha_L}{\alpha_D}(\ln 2)^{1/2} \qquad \text{Eq. 4.16}$$

$$x = \frac{(\nu - \nu_o)}{\alpha_D}(\ln 2)^{1/2} \qquad \text{Eq. 4.17}$$

α_D = Doppler half width (cm^{-1}) Eq. 4.18

$$= \frac{\nu_o}{c}\left[\frac{2R(\ln 2)\, T}{M}\right]^{1/2} = 3.58 \times 10^{-7}\, \nu_o \left[\frac{T}{M}\right]^{1/2} cm^{-1}$$

α_L = Lorentz half width (cm^{-1}) Eq. 4.19

$$= \Gamma/2\pi c$$

$$= \frac{1.4\, p\, \sigma_{12}^2 N_o \left[\frac{8\pi}{\overline{M} R T}\right]^{1/2}}{2\pi^2 c}$$

Where

Γ = gas collision frequency (sec^{-1})

p = pressure ($dynes/cm^2$)

σ_{12}^2 = optical collision cross-section (cm^2)

$\overline{M}$ = reduced mass of the colliding species (gm/gm mol)

R = gas constant (erg/gm mol ^oK)

T = temperature (^oK)

N_o = Avagadro's number (particles/gm mol)

c = velocity of light (cm/sec)

The Doppler and Lorentz widths are functions of temperature and pressure and thus are easily obtained at any point along the ray from the atmospheric properties. The integral, $K(x, y)$, is then calculated using a subroutine developed by Armstrong (1967). It should be noted that

$$\int_{-\infty}^{\infty} K(x, y)\, dx = \pi^{1/2}$$

The emission coefficient number density product necessary for Equations 4.6 and 4.7 is most easily obtained by scaling experimentally derived line strengths which are defined as (Penner, 1959, p.20):

$$S_{\ell u} = \frac{1}{8\pi c \nu^2} \frac{\bar{N}_\ell}{\bar{P}} A_{u\ell} \frac{g_u}{g_\ell} \left[1 - \exp\left(-\frac{hc\nu}{k\bar{T}}\right)\right] \qquad \text{Eq. 4.20}$$

Where

$S_{\ell u}$ = line strength (cm^{-2}-atm^{-1})

ν = wavenumber (cm^{-1})

$\bar{P}$ = pressure (atm)

$\bar{N}_\ell$ = lower state population for conditions where $S_{\ell u}$ is measured (particles/cm^3)

g_u, g_ℓ = statistical weights $(2J + 1)$

$A_{u\ell}$ = Einstein coefficient

$$\left(\frac{\text{Transitions}}{\text{Sec. Particle}}\right)$$

Using equation 4.11 and rearranging

$$n_u A_{u\ell} = \frac{8\pi c\nu^2 \bar{P}}{\left[\exp(hc\nu/k\bar{T}) - 1\right]} S_{\ell u} \qquad \text{Eq. 4.21}$$

Where

n_u = upper state population for conditions where $S_{\ell u}$ is measured. (particle/cm^3)

But

$$\frac{n_u}{\bar{n}_u} = \frac{n_t}{\bar{n}_t} \cdot \frac{\bar{Q}}{Q} \cdot \frac{\exp(-hc\nu/kT)}{\exp(-hc\nu/k\bar{T})} \qquad \text{Eq. 4.22}$$

Where

n_t = total number density

Q = partition function

E = upper state energy

Thus, combining Equations 4.19 and 4.20

$$n_u A_{u\ell} = 8\pi c\nu^2 \bar{P} S_{\ell u} \frac{\exp\left(-\frac{hc\nu}{k}\left[\frac{1}{T} - \frac{1}{\bar{T}}\right]\right)}{\left[\exp\left(-\frac{hc\nu}{k\bar{T}}\right) - 1\right]} \frac{\bar{Q}}{Q} \frac{n_t}{\bar{n}_t} \qquad \text{Eq. 4.23}$$

If several lines contribute to the absorption at a specific wavenumber, the total absorption coefficient is obtained by summation. The computational algorithm then uses $S_{\ell u}$ as a basis. $n_u A_{u\ell}$ from Equation 4.21 gives $(n_\ell B_{\ell u} - n_u B_{u\ell})$ from Equation 4.9. This, in conjunction with φ_ν, leads to α_ν via Equation 4.7. Equation 4.5 can then be integrated over altitude.

4.2 Synthetic Spectrum - Fourier Transform Program

4.2.1 Introduction: - Early in the development of this program it became necessary to devise a means for simulating the types of measurements to be performed. Because of the complexity of the atmospheric spectra, a digital computer simulation appeared most suitable.

A computer program was required which would compute the transmission spectrum of the atmosphere over some predetermined infrared region for multiple gas species with overlapping spectra, taking into account that for certain strong transitions the atmosphere is not optically thin. The program must be able to include the effects of a bandpass filter to simulate the bandpass of the measurement instrument. Since the instrument is an interferometer, rather than a spectrometer, the Fourier transform of the spectrum must be obtained to simulate the instrument output.

A computer program was written for use on the Langley Research Center - CDC computer system which computes theoretical absorption-emission spectra of the earth's atmosphere as would be observed by an exo-atmospheric detector, and the Fourier transform of the spectrum. The program permits computation of a spectrum for three possible geometric configurations. Case 2 is for use when the instrument looks directly at the sun through the earth's atmosphere. It calculates transmission, including absorption and emission of solar radiation through the atmospheric limb. Cases 1 and 3 are for use when the instrument looks downward. Case 3 calculates absorption of solar radiation reflected off the surface of the earth; while case 1 calculates transmission, including absorption and emission, of blackbody radiation emitted by the surface of the earth. Geometry of the cases considered are shown in Figure 4.2.1. Geometry case 1 is used when blackbody radiation of the earth's surface dominates solar radiation. This occurs at wavelengths greater than about 4 μ. Since temperatures in the at-

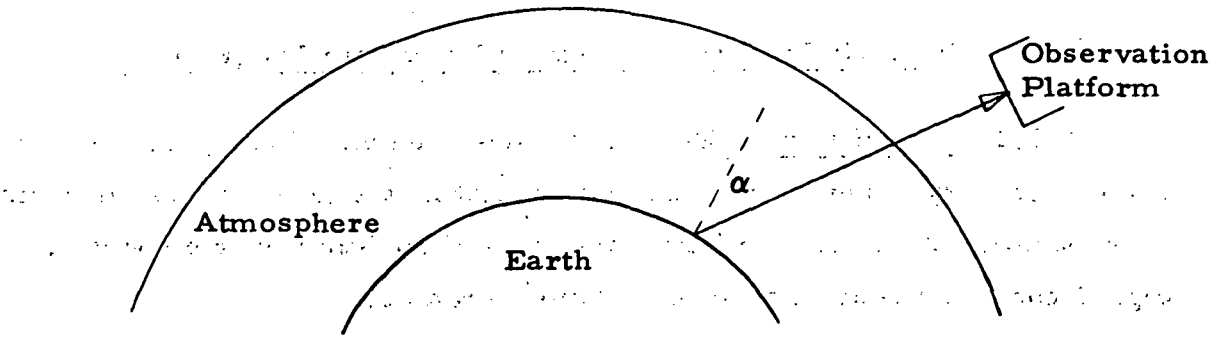

Case 1. Blackbody Emission from Earth's Surface.
Includes Absorption and Emission in Intervening Atmosphere.

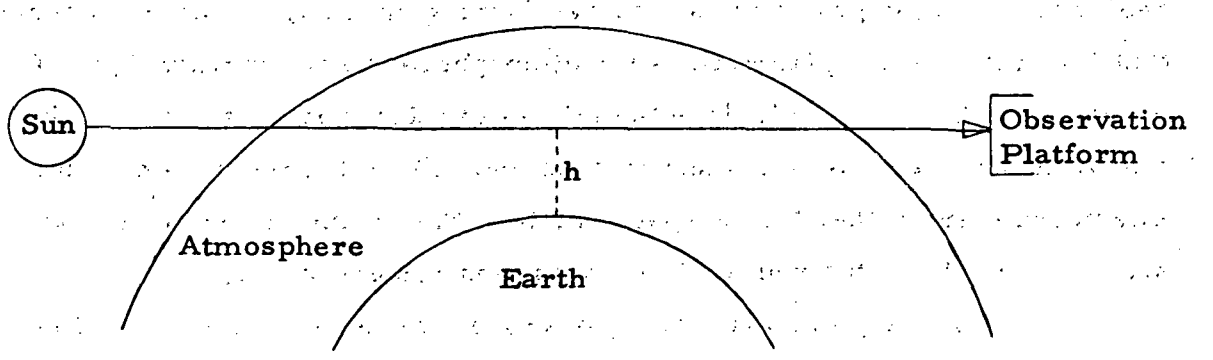

Case 2. Limb Transmission of Solar Radiation.
Includes Absorption and Emission in Intervening Atmosphere.

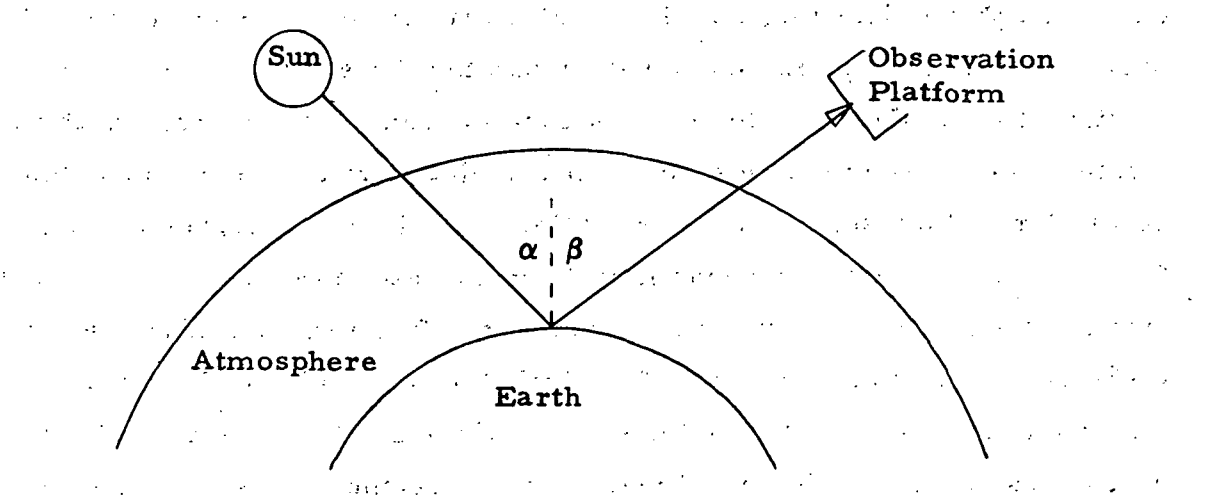

Case 3. Solar Radiation Reflected from Surface of Earth.
Includes Only Atmospheric Absorption.

Figure 4.2.1 Geometries of Atmospheric Transmission Calculations

mosphere are comparable to the surface temperature, the effects of emission within the atmosphere itself must be included in the computation of the spectrum in addition to absorption. Conversely, geometry case 3 is used when solar radiation dominates blackbody radiation from the earth's surface, which occurs below about 4 μ. In this case, the source temperature is far greater than the atmospheric temperature and hence only absorption in the atmosphere need be considered.

Spectra are computed for atmospheres comprised of up to three gaseous components, having a total of 150 discrete absorption lines. Inputs to the program consist of a list of molecular absorption lines to be included in the synthetic spectrum, some thermodynamic properties of the constituent gases, the physical properties of the model atmosphere to be employed, and the limits of the spectrum to be synthesized. Since the object is to simulate the spectrum arriving at an exo-atmospheric instrument, it is also possible to superimpose a bandpass filter on the spectrum. Outputs from the program are tabulated spectra, plotted spectra and Fourier transforms, and the Fourier transform punched on cards for additional processing.

4.2.2 Theoretical Problem Formulation: - A detailed formulation of the problem is given in Section 4.1. The problem consists basically of computing infrared atmospheric transmission spectra as determined by absorption and emission from molecular rotational-vibrational transitions of the atmospheric constituents.

As shown in Section 4.1, the basic equation which is to be solved (Chandrasekhar, 1960) is Equation 4.4. The first term of this expression gives the absorption of incident radiation between the source and the top of the atmosphere. The second term gives the additional radiation contributed by emission in the atmosphere, as diminished by absorption by the part of atmosphere lying between the emitting part and the top of the atmosphere. This expression gives the net intensity at the top of the atmos-

phere at a single frequency. The program described herein solves this expression for enough frequency values to define a spectrum over some desired frequency range.

4.2.3 Program Structure: - The program solves the radiative transfer equations set forth in Section 4.1 for an input set of molecular transitions and an input model atmosphere.

Theoretical spectra may be calculated which cover frequency ranges of several hundred wavenumbers. Since at each frequency point the entire set of radiative transfer equations must be solved and integrated through the atmosphere, the problem program is clearly CPU bound. In order to keep processor time within reasonable limits, use is made of data tables, calculated initially and then combined in proper sequence to produce absorption and emission coefficients. Although this approach conserves execution time, it does so at the expense of core storage. To conserve core storage, an overlay structure is used, resulting in the following storage requirements (numbers given are thousands of words, octal):

Main segment, including I/O buffers	10
Overlayed segments	4
Common block	44
System, including plot routines	15
Total	75

This is equivalent to about 32,000 decimal locations. To further conserve storage, extensive use is made of the EQUIVALENCE statement to reuse storage locations of data tables. Some arrays are used for storage of four different tables at different points in the program.

The program is written entirely in FORTRAN IV. An overall

view of general program flow is given below, followed by a detailed description of individual components. A listing is given in Appendix A.

4.2.3.1 Program Flow: - As noted above, the overall construction of the program involves the generation of data tables which are combined to produce the desired absorption and emission coefficients, which are then used to compute the overall transmission. The following is a general outline of the sequence of operations in the program. These steps follow to a great extent the development of the theoretical model given in Section 4.1.

Step 1. - Calculate Voigt Profiles - tables of constants are calculated which are used in determining the Voigt function. Tables are calculated for varying values of the Voigt function parameters: X, the displacement between frequency of interest and the line center frequency; and Y, the ratio of Lorentz to Doppler broadening.

Step 2. - Calculate Atmospheric Tables - model atmosphere parameters are read in, including atmospheric temperature, pressure and species concentrations as a function of altitude. Data are read in defining the desired geometry case, and atmospheric properties are computed for points along the radiation path. Tables of constants are calculated which will be used in computing the Lorentz and Doppler widths as functions of altitude and species type.

Step 3. - Calculate Line Tables - line information for all molecular lines to be included in the spectrum is read in and sorted by frequency. For each line a frequency band is defined which is the frequency region in which each particular line must be considered.

Step 4. - Calculate Absorption and Emission Coefficient Factors - for each line at each altitude an absorption and (if re-

quired for the desired geometry case) an emission coefficient is calculated. The coefficients are calculated for the line center frequency.

Step 5. - Calculate Spectrum - for each frequency within the desired spectral region the frequency bands defined in Step 3 are searched to determine which lines must be considered at that particular frequency. For each line at each altitude a Voigt profile is calculated from the tables of Step 1, and multiplied by the absorption and emission coefficients of Step 4. Coefficients for overlapping lines are added, and the integration of equation (4.4) is performed. After completion of one frequency point the frequency is incremented by a variable amount based on the proximity of line centers. If a line center is close, then the transmission will be varying rapidly and small frequency increments are taken. Tabulations of the spectrum are printed.

Step 6. - Apply Filter and Take Transform - the spectrum calculated in Step 5 is multiplied by an input bandpass filter function. The resultant spectrum is then Fourier transformed to give the interferogram.

Step 7. - Plot - the spectrum and interferogram are plotted on a Calcomp drum plotter.

4.2.3.2 Program Routines: -

Main Segment. - Resident in core at all times is a short main program. This program, designated segment zero in the CDC segmentation scheme, performs no calculations, but simply calls the subroutines that perform the calculations in the proper sequence. The main segment also reserves space in blank common for the extensive arrays which will be used.

A flow chart for the main segment is given in Figure 4.2.2.

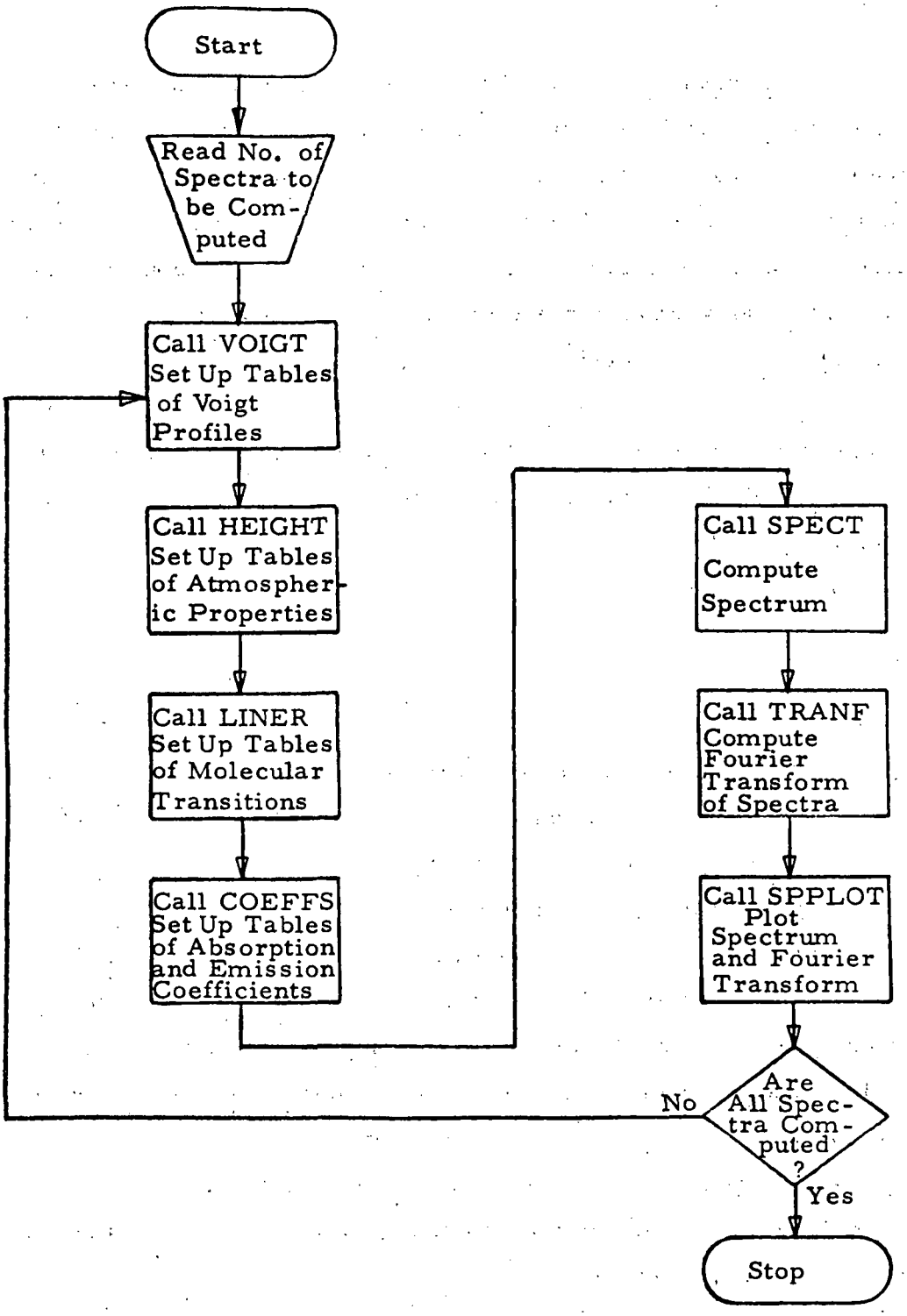

Figure 4.2.2 Program SPECTRA Main Segment

Subroutine VOIGT. - The Voigt profile is a molecular line shape function which results from a superposition of independent Lorentz and Doppler line broadening (Armstrong, 1967). Lorentz broadening in the atmosphere is a function of atmospheric pressure and is dominant at sea level, while Doppler broadening is temperature dependent and is dominant at high altitudes. At altitudes between these two extremes there is a continuous degree of superposition of the two effects.

The Voigt profile at a frequency, ν, for a line centered at ν_o is a function of two variables, X and Y, given by Equations 4.16 and 4.17. For the lines which will be included in the computation of atmospheric spectra, the range of values for X and Y which can reasonably be expected to be encountered are

$$0 \leq X \leq 10^4$$

$$0 \leq Y \leq 24.$$

As noted above, the general approach in this program is to compute data tables which will be combined to produce the desired spectra. Since it is known that Voigt functions will be required later with X and Y values falling in the ranges defined above, tables of these functions are derived as indicated in Figure 4.2.3. Tables of 27 values of X and 25 values of Y are defined in a DATA statement. The Voigt function, $\Phi(X, Y)$ is computed for all 675 combinations of X and Y using a subroutine developed by Armstrong (1967). It is also known that interpolation of Voigt functions will be required. For this reason, the actual values of Voigt function are not stored. Instead, for a constant value of Y and three consecutive values of X, a quadratic function is fitted through the three corresponding values of Φ, the Voigt function. The resulting quadratic equation is

$$\Phi(X_i, Y_i) = A_{ij}(X_i)^2 + B_{ij}(X_i) + C_{ij} \qquad \text{Eq. 4.24}$$

The tables stored for later use are the 25 x 25 tables of A, B, and C.

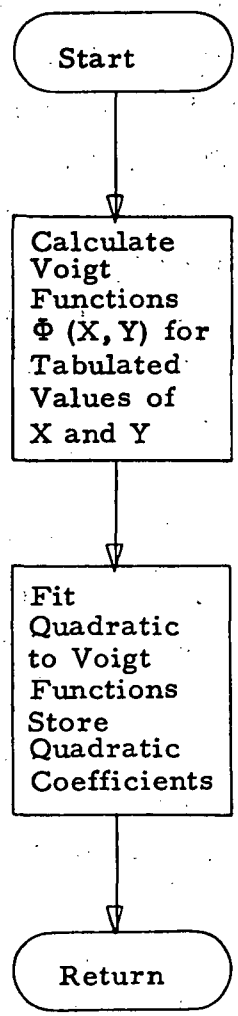

Figure 4.2.3 Program SPECTRA First Segment (Subroutine VOIGT)

Subroutine HEIGHT. - The primary function of subroutine HEIGHT is to set up tables of atmospheric properties along the radiation path. The routine reads data which defines the molecular species to be included in the computation of the spectrum. The program will accept from one to three species. For each species a data card is required which includes the symbol of the species, e.g., CO, H_2O, N_2O, etc., the molecular weight of the species, the number of molecular lines which will be furnished for each species, and the partition function of the species. The partition function will be required in the program as a function of temperature. To facilitate this, the partition function, Q, is calculated for several temperatures from data in the JANAF Tables. It is found that over the temperature range of interest to this program, Q can be represented as a quadratic, i.e.

$$Q(T) = AT^2 + BT + C \qquad \text{Eq. 4.25}$$

The coefficients A, B, and C are evaluated manually and used as inputs to the program in place of the actual partition function.

The next set of input data defines the geometric case to be considered, as shown in Figure 4.2.4. If limb transmission (case 2) is indicated, then the grazing altitude, h (KM), is defined. In case 1 the zenith angle of the observer α (degrees) is specified, while in case 3 the zenith angles of the source, α, and observer, β, are specified. The routine assigns a case number 4 to the special case of geometry case 3 where $\alpha = \beta$. This results in a shortening of computation time by a factor of two.

Data is then read which defines the model atmosphere to be employed. These data consist of a table of altitudes (KM) and tables which specify the following parameters at corresponding altitudes: temperature (degree K), pressure (millibar), and concentrations of species specified earlier (particles/cc). The set of altitudes for which these properties are specified is arbitrary, but should cover the range 0 - 100 KM and must be

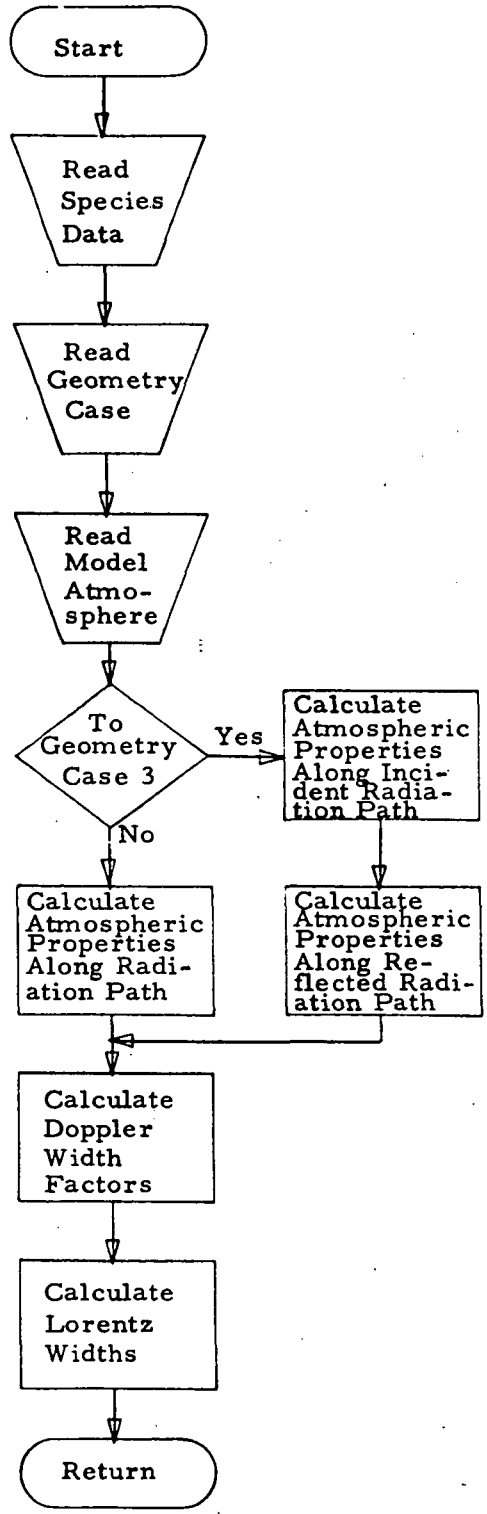

Figure 4.2.4 Program SPECTRA Second Segment (Subroutines HEIGHT, INTERP)

monotonic. These data are then combined with the geometric case data to compute tables of atmospheric properties along the actual line of observation. This procedure is similar for cases 1 and 3, but different for case 2, and will therefore be described separately.

For the limb transmission case, case 2, the top of the atmosphere is defined to be 100 KM. Using this condition, and the grazing altitude, h, the total path length through the atmosphere is calculated. This path is then divided into 48 equal segments, and the altitude at the end of each segment is calculated. An interpolation is performed on the input atmospheric model tables for this altitude to obtain the atmospheric properties at this altitude. A linear interpolation is performed for the temperature parameter, while a logarithmic interpolation is performed for pressure and species concentrations. Counting the end points, this results in tables of atmospheric properties for 49 points uniformly distributed along the radiation path.

For geometry case 1, a similar approach is taken in that tables of parameters are computed for points along the radiation path. In these cases the top of the atmosphere is defined to be 96 KM. The atmosphere is divided into 48 altitude steps as follows; starting at 0 KM the first 16 steps are incremented by 1 KM each, the next 16 are incremented by 2 KM each and the third 16 by 3 KM each. The total radiation path length is computed, using the zenith angle, and the path lengths corresponding to the predefined altitude steps are calculated. Using the same interpolations as for case 2, the atmospheric properties at these altitude steps are computed. Again counting the end points, a table of atmospheric properties at 49 points along the radiation path is generated. For geometry case 3, this calculation is performed twice, for the entering and reflected radiation, using the two different zenith angles. If the zenith angles are equal, then only one table is computed, but in effect it will later be used twice.

The Doppler halfwidth is given by Equation 4.18. Since α_D will be repeatedly calculated later, considerable time can be saved if as much as

possible of this expression can be precalculated. Therefore, a table of Doppler width factors is computed for each path position, which determines T, and each species, which determines M. Hence,

$$\mathrm{DOPP}(I,J) = \frac{1}{C}\left(\frac{2RT_j \ln 2}{M_i}\right)^{1/2} \qquad \text{Eq. 4.26}$$

It is now only necessary to multiply the approximate DOPP value by ν_o, the line frequency to obtain α_D for an transition at any point in the atmosphere.

Similarly, the Lorentz halfwidth, α_L, for any line is assumed to be 0.06 cm^{-1} at STP. Tables of α_L are therefore calculated for all points, j, along the radiation path by

$$\alpha_L(j) = 0.06 \times \frac{P_j}{P_s} \times \left(\frac{T_s}{T_j}\right)^{1/2} \qquad \text{Eq. 4.27}$$

where

P_s = standard pressure = 1000 mbar

T_s = standard temperature = 273 ^{o}K

Subroutine LINER. - Subroutine LINER reads data concerning the individual lines to be included in the computed spectrum, sorts the lines by wavenumber, and computes the frequency band over which each line contributes to the spectrum.

In Subroutine HEIGHT, up to three chemical species were defined as contributing to the spectrum. Subroutine LINER reads the set of transition lines to be considered for each species. Up to 150 lines are permitted, distributed in any way among the three species. For each line it is necessary to specify the center frequency (cm^{-1}), the line strength (cm^{-2} atm^{-1}) and the lower state energy (cm^{-1}).

After reading this line data, LINER sorts the lines and corresponding line data in order of ascending center frequency. A search is performed to determine the minimum line strength. For each line a frequency band is determined over which the line must be considered in computing the spectrum. The line inclusion band is determined by fitting a Gaussian line shape over each line with a nominal 0.06 cm^{-1} halfwidth. The line inclusion band is the frequency band over which the line has a strength which exceeds a previously defined minimum. This minimum is presently taken as 1% of the strength of the weakest line. If the line inclusion band is computed to be greater than ± 5 cm^{-1}, it is truncated to ± 5 cm^{-1}.

Subroutine COEFFS. - Subroutine COEFFS computes, for each line at its center frequency and for each altitude in the model atmosphere, the absorption coefficients and, if required by the geometry case being considered, the emission coefficients. Using the definitions of Einstein coefficients, the absorption and emission coefficients for line ℓ of species i at altitude h can be shown to be:

$$\alpha_{\ell,h} = \frac{\left[C_{i_h}\right]}{A_N} \cdot e^{E_\ell \cdot C_2 \cdot \left(\frac{1}{T_o} - \frac{1}{T_h}\right)} \cdot \frac{\left(1-e^{\frac{-C_2\nu_\ell}{T_h}}\right)}{\left(1-e^{\frac{-C_2\nu_\ell}{T_o}}\right)} \cdot S_\ell \cdot \frac{Q_{i_{300}}}{Q_{i_{T_h}}} \quad \text{Eq. 4.28}$$

$$\epsilon_{\ell,h} = \frac{\left[C_{i_h}\right]}{A_N} \cdot e^{E_\ell \cdot C_2 \cdot \left(\frac{1}{T_o} - \frac{1}{T_h}\right)} \cdot \frac{e^{\frac{-C_2\nu_\ell}{T}}}{\left(1-e^{\frac{-C_2\nu_\ell}{T_o}}\right)} \cdot 2C^2 h \cdot S_\ell \cdot \nu_\ell^{\,3} \cdot \frac{Q_{i_{300}}}{Q_{i_{T_h}}}$$

Eq. 4.29

where

$\left[C_{i_h}\right]$ = concentration of species i at altitude h $\left(\frac{\text{particle}}{\text{cm}^{-3}}\right)$

A_N = schematic/number

E_ℓ = lower state energy of line ℓ (cm^{-1})

C_2 = second Planck constant

T_o = standard temperature = 300^oK

T_h = temperature at altitude h (^oK)

ν_ℓ = center frequency of line ℓ (cm^{-1})

S_ℓ = strength of line ℓ (cm^{-2} atm^{-1})

$Q_{i_{T_h}}$ = partition coefficient of species i at the temperature at altitude h

These factors do not represent the complete absorption and emission coefficients since they are lacking the Voight line profile function. This last term will be included in the next subroutine.

Subroutine SPECT.- Subroutine SPECT performs the actual spectrum evaluation. For each frequency point in the spectrum, the precalculated data tables are accessed, and equation 1 is evaluated, giving the observed intensity.

In order to keep the computer running time within reasonable limits, it is necessary to restrict the total number of frequency points at which the spectrum is computed. On the other hand, it is necessary to include a number of points sufficient to maintain adequate spectral resolution, particularly in the rapidly varying regions of line centers. To satisfy these requirements, a frequency increment system was devised whereby large increments, up to 0.512 cm^{-1} are used in those parts of the spectrum distant

from line centers, while small increments, as small as 0.001 cm^{-1} are used in the vincinity of line centers. The frequency increment scheme operates as follows.

The first frequency point is defined by input data. After the intensity is computed, for this frequency value, as will be described below, a search is made of the table of line center frequencies to determine the closest line center, at either higher or lower frequency. The absolute value of the frequency difference between the nearest line center and the current frequency point is used in an algorithm to compute the next frequency increment. If this difference is zero, an increment of 0.001 cm^{-1} is used. At every second point from the line center the increment is doubled until a maximum of 0.512 cm^{-1} is reached at 1.0 cm^{-1} from the line center. The computed increment is added to the current frequency value, the spectral intensity is computed for the new frequency, and the process is repeated until a final frequency, defined by input data, is reached.

Each group of 100 spectral points is printed and also written on a magnetic scratch tape. This permits the computation of spectra with large numbers of points without extensive storage requirements.

At each frequency value, the spectral intensity is computed as follows. The table of line inclusion bands, determined by subroutine LINER, is searched to determine which lines must be included in the computation of the spectral intensity at this frequency. A table is made of lines to be included. For a given altitude step in the model atmosphere, the Lorentz and Doppler line widths are obtained for each line in the line inclusion table. The Lorentz width was computed in subroutine HEIGHT. The Doppler width is computed by multiplying the appropriate entry in the DOPP table, also computed in subroutine HEIGHT, by the corresponding line center frequency. The Doppler and Lorentz line widths are used to compute the X and Y parameters of the Voight function, as given in Equations 4.16 and 4.17.

These X and Y values are used in a table lookup of the Voigt function tables generated in Subroutine VOIGT, and, using a three point Lagrange interpolation, the Voigt function is evaluated for a given line at a particular frequency and position in the model atmosphere. The Voigt function is multiplied by the appropriate absorption, and if required, by the geometry case in use, the emission coefficient factors generated in Subroutine COEFFS, giving the final absorption and emission coefficients for a given line at a specified frequency and altitude. If the search of line inclusion bands indicated that more than one line must be included at this frequency, i.e., the lines overlap, this process of determining absorption and emission coefficients is repeated for each overlapping line. The absorption and emission coefficients are summed for all contributing lines to give a single net absorption or emission coefficient.

This process of computing absorption and, if required, emission coefficients is repeated for all altitude steps in the input model atmosphere, as defined in Subroutine HEIGHT. A table of absorption and emission coefficients is generated for a single frequency covering all altitude steps and including the effects of overlapping lines. The radiative transfer equation (equation 4.10) is evaluated using the tabulated coefficients, employing Simpson's rule integrations. The incident radiation for geometry case 1 is blackbody radiation from the ground. The ground temperature is taken as 288.2 ^{o}K, with an albedo of 1.0; however, both parameters can be varied by input data. For geometry cases 2, 3, 4, the incident radiation is solar radiation based on a solar temperature of 5800 ^{o}K, with an emissivity of 1.0. For geometry case 3, where incident solar radiation is reflected from the ground at an angle different from the incident angle, the intensity computed in the manner described above gives the attenuated solar radiation at ground level. The entire process is repeated for the reflected beam to give the radiation at an exoatmospheric observing platform. For geometry case 4, where solar radiation is reflected from the ground at the same angle as the incident angle,

the computed absorption is simply doubled to give the total absorption from the double pass. In both geometry cases 3 and 4, a ground reflectivity may be specified by input data. The intensity at ground level is further reduced by a factor of π to account for lambertion diffusion by the ground.

By this method the spectral intensity at a single frequency is computed. The subroutine then computes the next frequency point by the line center proximity method described above, and the entire process is repeated for the new frequency point. This procedure is continued until a stopping frequency, specified by input data, is reached.

Segment Six. - The sixth segment of this program contains three subroutines. Subroutine TRANF prepares the spectrum computed above for the Fourier transform, applies a bandpass filter function as defined in Subroutine FLTRS, and calls Subroutine FRXFM to perform the Fourier transform. Subroutine TRANF then prepares both the spectrum and interferogram for plotting.

In the description of Subroutine SPECT it was noted that the spacing between points on the frequency scale of the computed spectrum is variable rather than uniform. In order to perform the Fourier transform, however, it is necessary that the frequency spacing between points be uniform. The first task of Subroutine TRANF, therefore is to perform conversion of the spectrum to a uniform scale. The interval between the spectral limits is divided into a number of uniform divisions. The number of divisions must be a power of two, and is taken as 2^{12} unless otherwise specified by input data. The spectrum is read from the intermediate scratch tape in blocks of 100 points, as written by Subroutine SPECT. The conversion to the uniform scale between the limits of each uniform interval, i.e.:

$$S_{\nu_u} = \int_{\nu_1}^{\nu_2} S_{\nu'_n} \, d\nu'$$

where

S_{ν_u} = Spectral intensity of point in spectrum on uniform frequency scale

$S_{\nu'_u}$ = spectral intensity on non-uniform scale

$\nu_2 - \nu_1$ = one frequency interval of uniform scale

Following conversion of the spectrum to a uniform frequency scale, a filter function is applied to simulate the bandpass of a measurement instrument. Several types of filter functions are available, the choice being specified by input data. A Lorentz or Gaussian shaped filter function may be specified, in which case the input data consists of the center frequency, the peak transmittance and the half height - half width. A problem has been noted, however, in using these two functions in conjunction with the Fourier transform. Because the Lorentz and Gaussian functions asymptotically approach zero, but do not become zero in the defined spectral range, there is introduced into the Fourier transform high frequency components. These components can be eliminated by forcing the filter function to zero while still within the spectral range. This is accomplished by using a third filter function, referred to as a power function, having the form:

$$\tau_\nu = \tau_{max} \cdot \left[1 - \left(\frac{\nu - \nu_o}{w}\right)^2\right]^n \qquad \nu - \nu_o < w$$

$$\tau_\nu = 0 \qquad \nu - \nu_o \geq w$$

where the center frequency, ν_o, the width, w, and the exponent, n, are all specified by input data. This function has the property of becoming zero within the frequency range of the computed spectrum and thereby preventing high frequency components in the Fourier transform.

In the event that a filter bandpass is required which does not fit any of these three analytic forms, it is also possible to provide input filter data in the form of the calibration curve, i.e., a table of frequencies and corresponding transmittances may be specified. Up to fifty calibration points may be specified.

It is also possible to superimpose any number of filters, using any mixture of the above filter types.

Following the application of the filters to the computed spectrum, the spectrum is written on magnetic tape for subsequent plotting. The Fourier transform of the spectrum is then computed. The Fourier transform subroutine, FRXFM, is a standard library routine based on the Cooley-Tukey algorithm, and returns the real and imaginary components of the Fourier transform. These are converted to amplitude and phase components of an interferogram by the expressions

$$A_i = \left(R_i^2 + I_i^2 \right)^{1/2} \cdot S$$

$$\Phi_i = \frac{1}{2\pi} \tan^{-1} \left(\frac{I_i}{R_i} \right)$$

where

R, I = real, imaginary components of Fourier transform

S = plotting scale factor.

The computed interferogram looks much like an amplitude modulated radio signal in that it consists of a carrier wave modulated by the relatively lower frequency envelope. In the interferogram the carrier contains information concerning the spectral region for which the interferogram is computed. Since this information is already known, it is advantageous to eliminate the carrier and retain only the envelope, since this relaxes the required accuracy of the sampling point.

The elimination of the carrier is performed by "synchronously detecting" it with an input reference frequency which lies approximately in the middle of the spectrum being computed.

The delay scale for the interferogram is based on the frequency range of the initial spectrum. The delay for the first interferogram point is zero, and the delay increment for each subsequent point is

$$\Delta d = \frac{1}{\nu_f - \nu_i}$$

where

ν_i, ν_f = initial, final frequencies of the computed spectrum.

The amplitude, phase and delay tables of the interferogram are written on magnetic tape for subsequent plotting. In addition, the real and imaginary Fourier transform components are punched on output data cards for subsequent use in deriving interferogram correlation functions.

Subroutine SPPLOT. - Subroutine SPPLOT reads the spectrum and interferogram from the magnetic tape written by previous subroutines, and generates plots of them. Plots are made on the twelve inch CALCOMP drum plotter at Langey Research Center, using the standard system library of plotting routines.

Following generation of the plotted output, program control is returned to the main segment where the entire spectrum computation process is repeated if desired.

5. CORRELATION INTERFEROMETRY

5.1 Principles of Interferometry

The use of spectral techniques for the remote measurement of concentrations of trace atmospheric species is dependent on separating out the effects of the species being measured from those of all other species present in the optical path. In techniques where a part of the spectrum is measured, the separation must be obtained by spectral resolution. Thus, some separable part of the spectrum must show an appreciable effect of the species being measured and any significant effects of other species must be such that they can be eliminated. If a different technique is used effects must still be separable but the separation criteria is no longer spectral resolution but a type of resolution peculiar to that technique. Such a technique is interferometry. In this technique the separation is accomplished by a resolution of path differences.

The instrument being developed for this program is a correlation interferometer. The following discussion will describe the basic theory of its operation. More detail on this and on the specific instrument itself will be given elsewhere (Bortner, et. al., 1973).

An interferometer is a fairly simple device (Figure 5.1.1). The essential elements are a beam splitter and two mirrors, plus a detector to measure the radiation output. Light from the source is incident on the beam splitter, B. At the beam splitter it is divided into two paths; one portion of the light goes to one mirror, M_1; the other portion of the light goes to the other mirror, M_2. The two portions recombine at the beam splitter and the intensity of the light once they recombine is registered by the detector, D. The intensity of the radiation received by the detector will depend on the difference between the lengths of the paths traveled by the beams in the two arms. The length of the path F-B-M_1-B-D can be different from that of the

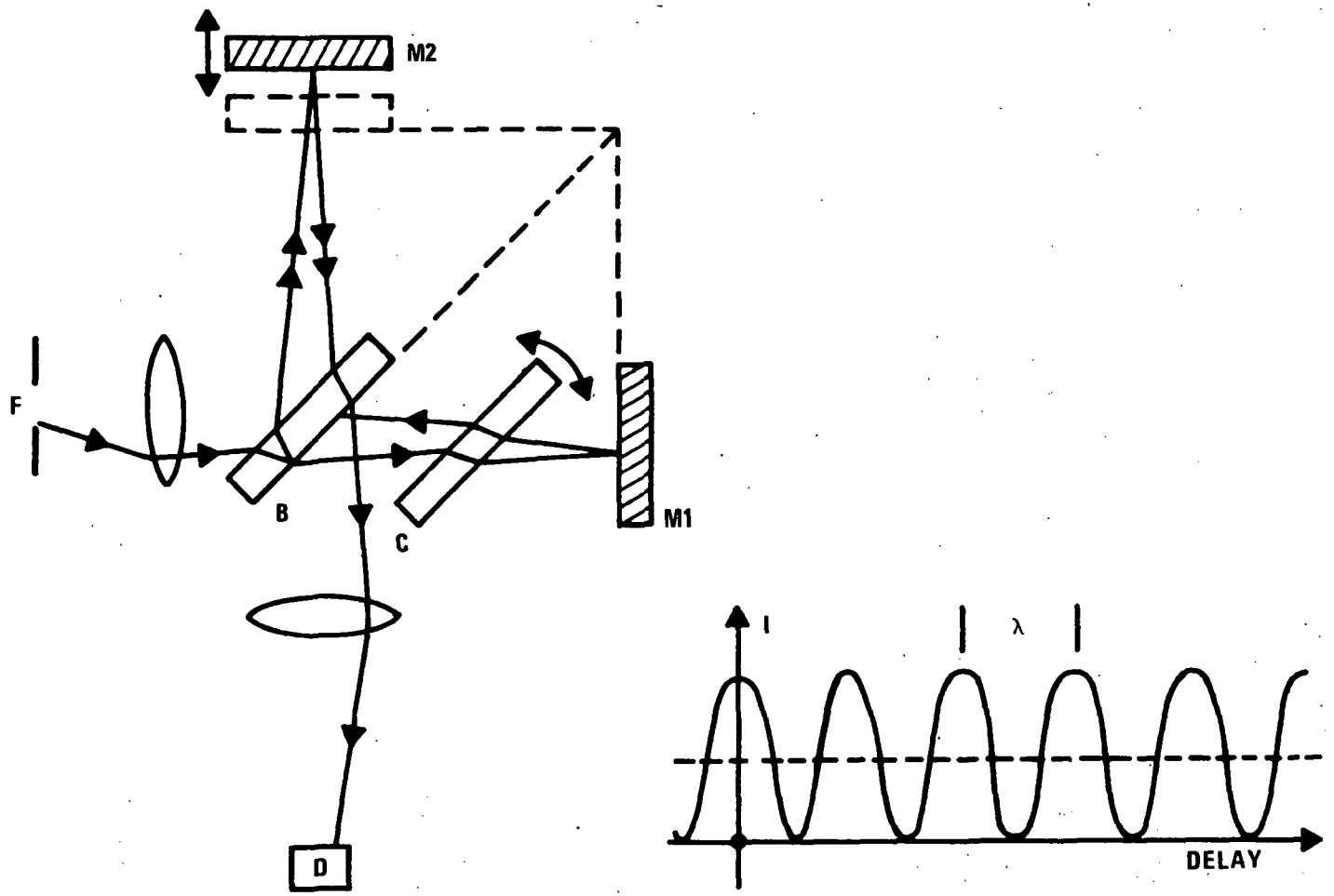

Figure 5.1.1 Interferometer and Interferometer Output

path F-B-M_2-B-D. If the two optical paths are exactly the same, the path difference (delay*) is zero, and there is a peak in intensity. If monochromatic radiation enters the instrument, and if the path difference is increased by one-half the wavelength, the intensity reaching the detector goes down essentially to zero. Then as it increases again towards one wavelength path difference, another peak occurs. This sinusoidal oscillation about a mean level repeats at intervals of one wavelength if the light is monochromatic. The instrument actually does a Fourier transformation of the spectrum of the radiation entering. The way in which the delay is scanned, the way in which the path difference is changed is in most instruments a matter of shifting one of the mirrors. This certainly does the job, but it causes some unnecessary alignment problems. One of the features of the COPE instrument is that the problem of having to scan and maintain the position of the mirror accurately is avoided by not scanning the end mirror, but, instead, scanning a plate of refractive material in one arm of the interferometer. Many interferometers have such a refractive plate, but generally it is left in a constant position. If this plate is rotated, the path length in that arm of the interferometer will vary. This will accomplish the same effect as moving one of the mirrors back and forth without the alignment problems. This is a specific advantage of the technique of this instrument. Other advantages, some of which are advantages of interferometry in general, include a large light throughput, multiplexing of spectral elements, a compact yet flexible instrument, and a handy output.

5.2 Relationship Between Spectra and Interferograms

In Figure 5.2.1 a few particular cases of the relationship between spectra and interferograms are shown. As shown on the previous figure, monochromatic spectrum produces an interferogram which is essentially a

* The term "delay" refers to the temporal variation of the interferometer signal. This is related to the variation of the path difference by the scan velocity.

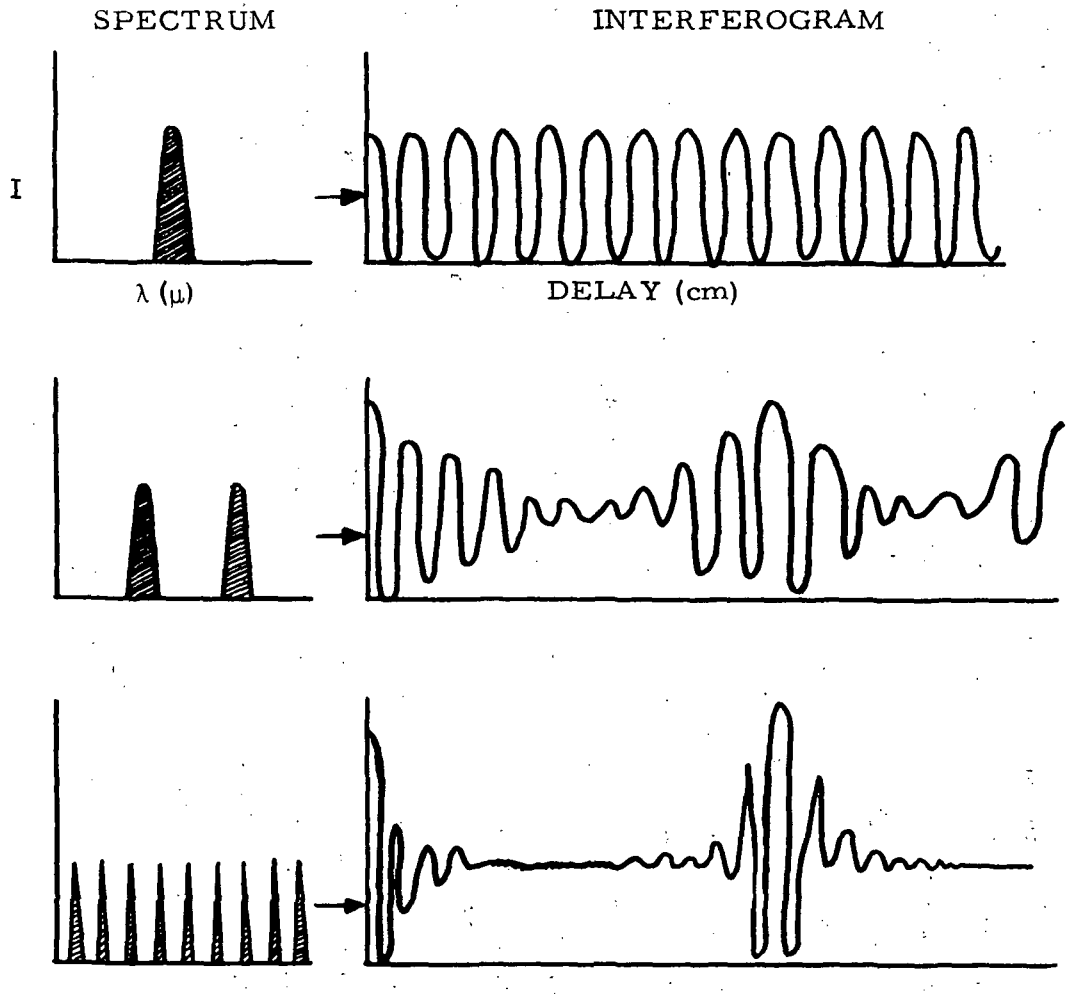

Figure 5.2.1 Relation of Interferogram and Spectrum

sinusoidal variation as the delay is scanned. If instead of a single monochromatic line there is a pair of monochromatic lines, then the two sinusoidals due to lines will beat together. Again a characteristic maximum is obtained at zero delay. As the oscillations beat together, they get out of phase and go through a minimum, then maximize again at a point characteristic of the line separation. If there are a number of regularly spaced lines, the beat patterns will all reinforce at zero delay again, but they very rapidly get out of step with each other and decay to very small values. Then there appears a point where they all reinforce again at a delay which is inversely proportional to the spacing between the lines. This is almost exactly the effect seen in the case of carbon monoxide as shown in Figure 5.2.2, which gives the actual spectrum* and interferogram. The spectrum displays fairly regularly spaced lines. There is certainly a noticeable change in the spacing from one end to the other, but it is certainly not a random spacing. As seen in the previous figure, there is reinforcement for zero delay which dies out rather rapidly, and then, at a delay which is characteristic of the spacing between the lines (about 3 cm^{-1}), the interferogram amplitude peaks up again. In general the relationship between the spectrum of the radiation and the interferogram of the radiation is given by a Fourier transformation, the cosine Fourier transformation. That is, the interferogram, apart from the constant term, is the cosine Fourier transform of the spectrum (Figure 5.2.3). The interferogram signal, as a function of path difference is given by:

$$I(\chi) = 2 \int_0^\infty \Pi_i \left(S_i(\sigma) \right) \cos (2 \pi \sigma \chi) \, d\sigma$$

where

σ = frequency (cm^{-1})

$S_i(\sigma)$ = spectral input at σ ($ergs\text{-}cm^{2}\text{-}ster^{-1}(cm^{-1})^{-1}\text{-}sec^{-1}$)

χ = path difference (cm)

*This spectrum is that given by Plyler (1952) with the mercury emission lines omitted.

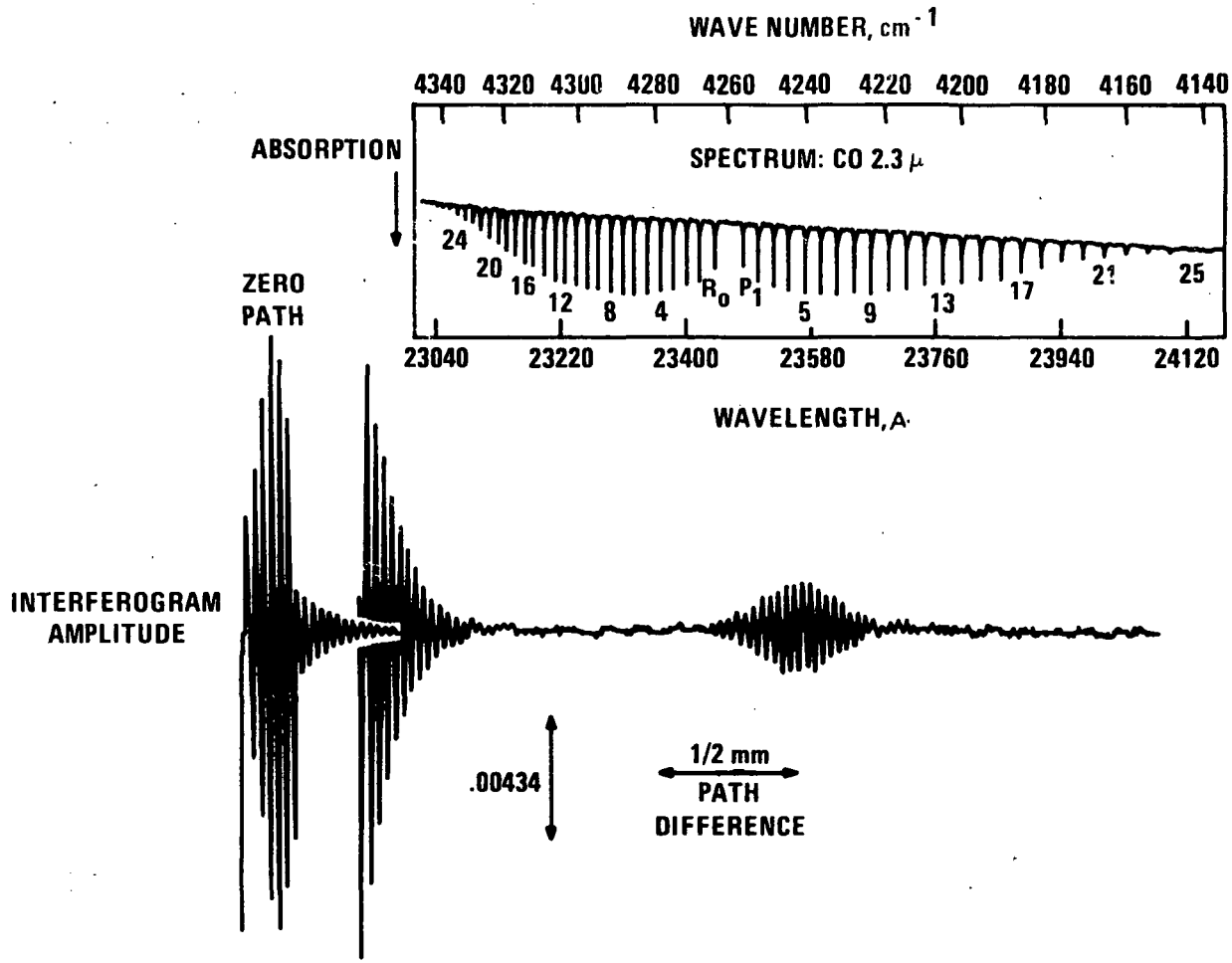

Figure 5.2.2 Interferogram and Spectrum of CO

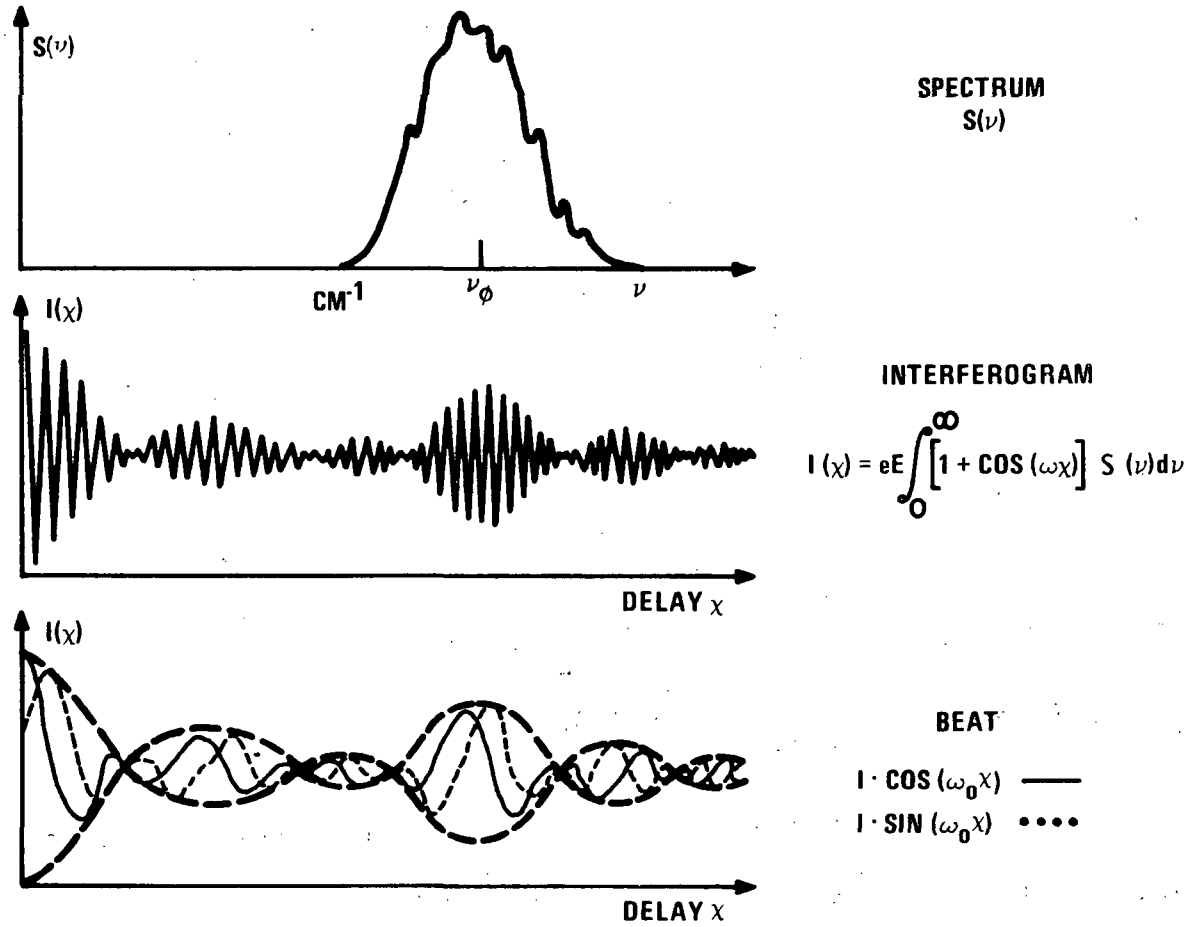

Figure 5.2.3 Heterodyning of Interferogram

Several relationships exist between the interferogram and the spectrum from which it is produced. The interferogram has a carrier frequency directly related to the mean frequency of the spectrum producing it. It will be amplitude and phase modulated, the amplitude and phase modulation being described by the band envelope shown. From an interferogram up to a given delay, the spectrum could be reconstructed with a resolution given inversely by the delay out to which the interferogram is obtained. So, from an interferogram from zero to 1 centimeter, inverse Fourier transformation reproduces a spectrum to resolution of one wave number (cm^{-1}). Conversely, if the information characteristic of one wave number resolution is not needed, if the information need only be characterized by a 3 cm^{-1} resolution, then it is only necessary to scan the interferogram out to 1/3 cm (3 millimeters) to obtain information equivalent to a resolution of three wave numbers. It is very important to do this. Significant improvements in signal to noise ratio are obtained by limiting ourselves to scanning only the portion of the interferogram which gives the best signal to noise ratio. If essentially all the information on any given species (all the effect of that species on the interferogram) occurs over a small part of the interferogram, only that range of path difference need be scanned. The operation of the correlation interferometer involves the treatment of the interferogram data directly to obtain data on species densities rather than the use of the spectrum obtained by the Fourier transform of the interferogram. With such an operation the concept of spectral resolution loses meaning. Although the spectrum which can be obtained from an interferogram has a resolution which is the reciprocal of the path difference scanned, the ability to obtain data on one species in the presence of others by direct examination of the interferogram, is not dependent on the length of path-difference scan. For example, if a scan of 0 to 2 cm were used to produce an interferogram but a given species of interest has an effect only between 1.0 and 1.2 cm, as much information on that species can be obtained by scanning from 1.0 to 1.2 cm as from 0.0 to 2.0 cm even though the

longer scan could produce a spectrum of 0.5 cm^{-1} resolution whereas the shorter scan could not. Rather than spectral resolution, the separation of effects of various species is accomplished by a spatial resolution of path difference which is dependent on such factors as smoothness of path-difference scan.

Another relationship between the spectrum and the interferogram is that the spectrum of the incoming radiation can be severely band-limited by optical filters. If it is band-limited, and if an interferogram that would reproduce the spectrum only to a limited resolution is taken, then the spectrum could be characterized by a fairly small number of points. On the other hand, to characterize the interferogram in this form with its very rapid oscillations (the oscillations are essentially proportional to the mean frequency and not to the width) with any degree of accuracy, relatively large number of points on the order of at least one per cycle of oscillation would be needed. This would be many more points than are necessary to characterize the spectrum to a corresponding resolution. There is a lot of redundancy in the information because of the band limitation. The method used in the correlation interferometer to eliminate the redundancy is simply to take the amplitude and phase modulated sinusoid and heterodyne it down with a local oscillator, where the local oscillator is the interferogram of radiation somewhere around the mean frequency of the spectrum. By heterodyning the interferogram down with a cosine or a sinusoidal variation, the interferogram is reduced to its essential variations. This is illustrated in the bottom part of Figure 5.2.3. All the information necessary to characterize the interferogram can be retrieved by sampling a relatively small number of points, a few points for each of the much longer cycles shown in the bottom figure. There is a slight difference whether the interferogram is beat with a sinusoid at a given wavelength or a cosine; slightly different beat-down interferograms are obtained. Actually both of them are used but, through most of the remaining discussion this fact will be ignored. In generating the local oscillator for carrying out the heterodyning, radiation which passes through the same interferometer as does the

signal radiation is used. This insures that the local oscillator always has the correct phase relationship with the signal interferogram. It also relaxes some of the accuracy needed in the knowledge of the plate drive (the scan drive). If this were not done, the scan drive would have to be known accurately to within a very small fraction of the wavelength. By having the local oscillator going through the same interferometer, this problem is alleviated. Probably the main objection to interferometers is that most people think in terms of using a spectrum and in order to obtain a spectrum from the interferometer, the interferogram must be transformed. This problem is avoided completely by not looking at the spectrum at all. It is not really necessary to use the spectrum. The measurement can be made quite adequately on the interferogram itself. This is a major advantage of the correlation interferometer.

5.3 The Measurement in the Presence of Interferents

Figure 5.3.1 outlines very briefly the basic principles by which the measurement on the interferogram is made. There are essentially two problems involved in a measurement of this type. We are trying to measure the CO burden on the basis of the radiation received from a satellite. The problems in making the measurement are: (1) can the measurement be made with sufficient accuracy in view of the noise limitations, and (2) can the measurement be made under conditions where the radiation received is affected not only by the gas that we are trying to measure, in this case carbon monoxide, but is also severely affected by other gases. In fact, the radiation is much more affected by such things as water vapor and methane. Ignoring for the moment this problem of the interference species, consider how a measurement would be made. Consider an interferogram due to a target signal, say CO, such as shown. There are different ways by which one could measure the CO burden which produced this signal level. One might sit at a constant delay and measure the signal level at that point. If the CO burden were

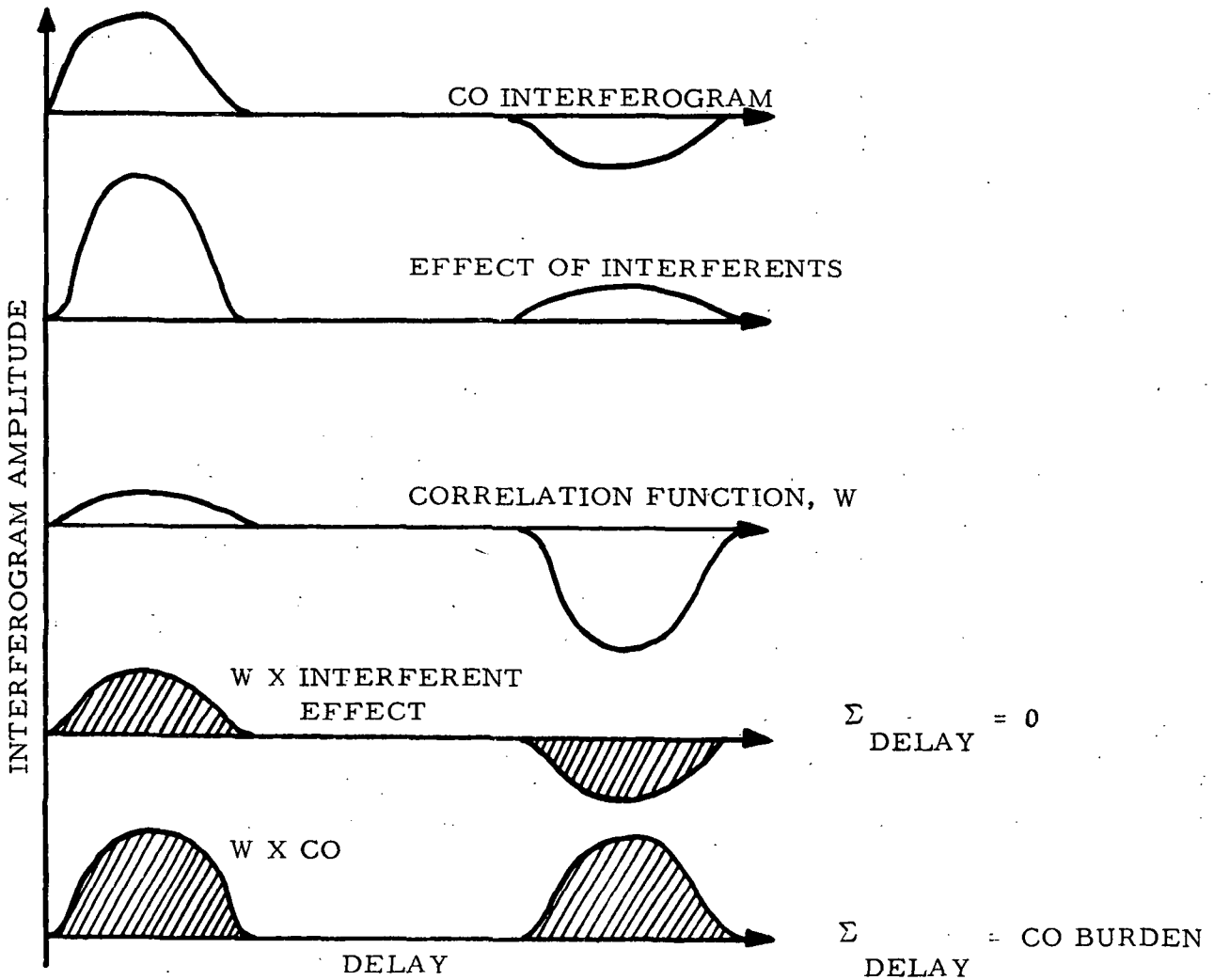

Figure 5.3.1 Application of Correlation Function

doubled, the effect of CO on the intensity we would measure would be doubled (for the moment assuming variations are linear with the gas burden); the intensity would essentially be a measure of the carbon monoxide burden. If there were a constant noise level associated with the measurement of any point then the best point to make a measurement would be at the point where the signal level is maximum. If a finite range of delay were scanned, then the measurements made at all points would be combined to get some sort of average measurement of the carbon monoxide burden. In general, the optimum measurement that can be made in such circumstances is given by combining all the measurements, all the intensities of the various points, in a manner related directly to the intensity of the signal shape. That is a weighting function or correlation function is generated and this is multiplied together with the signal. The measurement made is the integral of the correlation function times the signal, the integral over the delay range which is scanned. It is integrated and the measurement obtained is directly proportional to, in this case, the carbon monoxide burden. The signal-to-noise ratio in such a measurement can be shown to be optimum when the correlation function looks exactly in shape like the target signal. That result holds when there are no interferents. Now consider another gas species which is affecting the signal received, for example water vapor. If a point measurement of the intensity were used, the signal received would not be simply the signal due to carbon monoxide but the sum of the signals due to the carbon monoxide and to the water vapor. Even if the carbon monoxide level were to remain the same, drastically varying measurements due to variations in water vapor might be obtained so that a very poor measurement of CO would be obtained by sitting at that point. A region where a signal is unaffected by all interferents may not be available or if it is, the signal-to-noise ratio achievable at the point might not be adequate for the measurement. This problem is handled as follows. The correlation function used is not matched exactly to the target gas signal shape. The correlation function (W) is adjusted so that when it is

cross-correlated with the interferents and the result is integrated over the range scanned, all the positive correlation regions are balanced exactly by the negative correlation regions, so that the total area under the curve, the total result of the measurement, comes out to zero as illustrated, still maintaining the correlation function as close as possible to that constraint to the signal interferogram (target interferogram) in order to still get as large a positive correlation between the correlation function and the target gas as possible. The result of the measurement is still proportional to the carbon monoxide burden. In principle, if there are a number of interferents of this sort, rejection of these interferents can still be achieved so long as we have at least as many points to describe our correlation function as we have gases which are affecting the radiation. The measurement of the target gas can be made in real time. The first gas, in this case CO, and any other gases which significantly affect the interferogram can be measured.

5.4 An Example of the Use of Interferograms

As an example of the interferograms resulting from overlapping spectra (using three imaginary species), Figure 5.4.1 shows spectra (drawn with relative frequency scale in cm^{-1}) and the major features of a portion of the interferogram envelopes for species A, B, and C, and for all combinations of them. Thus, from the spectrum of A, the lines at relative positions of 1 and 3 cm^{-1} give a peak in the interferogram envelope at 0.5 cm; those at 1 and 6 cm^{-1} give one at 0.2 cm^{-1}; those at 3 and 6 cm^{-1} give one at 0.33 cm^{-1}. Similarly, B gives peaks at 0.28 cm and 0.55 cm. However, in the interferograms of AB an additional effect occurs between .25 and .36 cm. This is due to the combination of the line at the relative frequency of 1 cm^{-1} in the A spectrum and of that at 4.8 cm^{-1} in the B spectrum. Other effects are also present in the AB interferogram due to other combinations of lines. If it is desired to determine the concentration of species C in the presence of

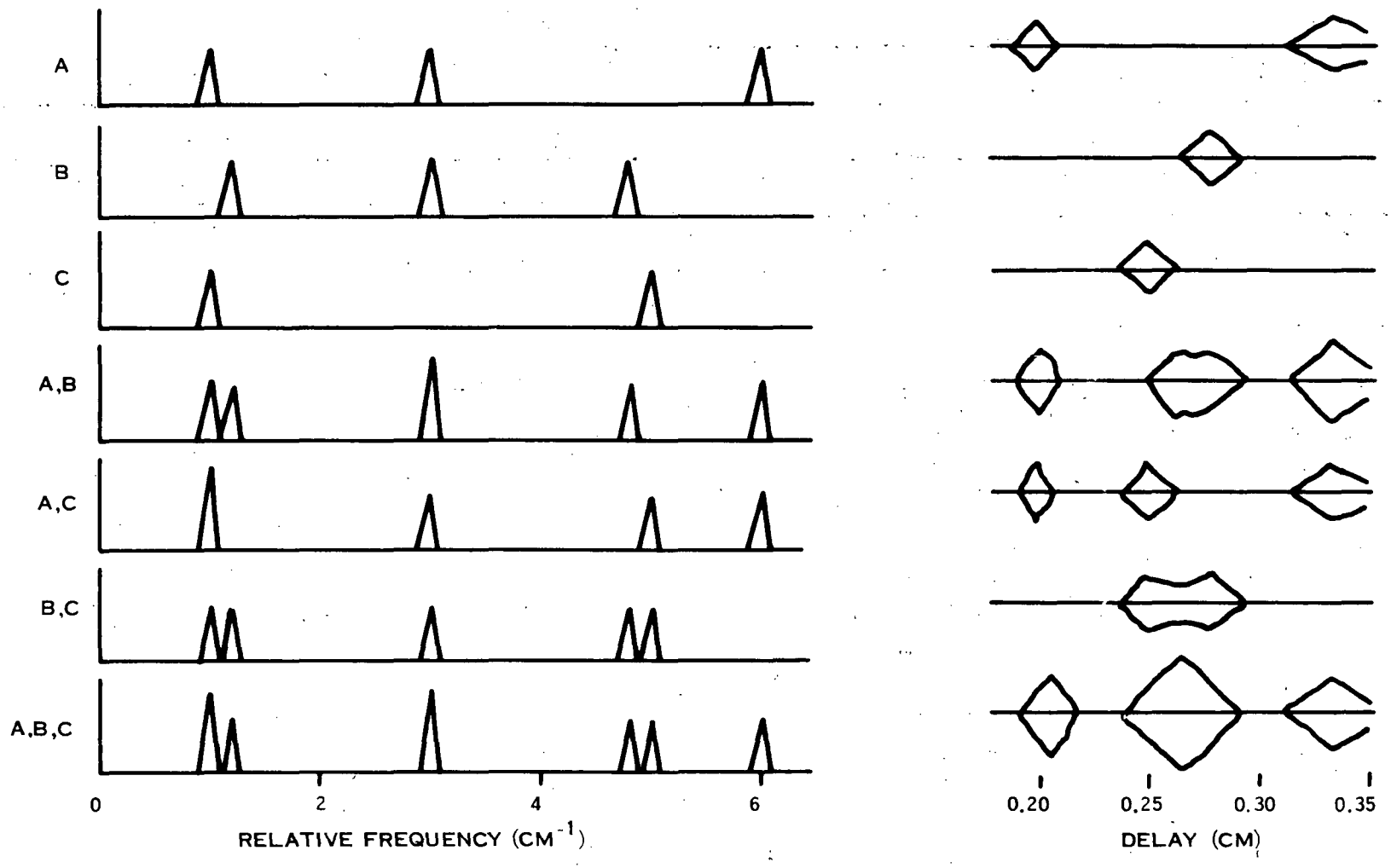

Figure 5.4.1 Spectra and Interferogram Envelopes for Three Species with Overlapping Spectra and Their Combinations

A and B, the spectrum or the interferogram of the A-B-C mixture must be different from that of the A-B mixture. The spectra show an appreciable difference only around $\nu'_{rel} = 5\ cm^{-1}$ where A-B-C extends about $0.2\ cm^{-1}$ past A-B. Thus, a $.2\ cm^{-1}$ spectral resolution would be required to make the measurement. In the interferograms, the region around .25 cm path difference shows a variance. The region from .24 to .26 could be used to make a measurement C. Actually a larger region would be used and the effects of A and B separated out.

The spectra of A, B, and C are related to each other somewhat as those of H_2O, CH_4, and CO in a real case, except that the latter are more complex. In that case a spectral region much affected by CO is chosen and separated out by an optical filter.

In the correlation interferometer, the path difference scan is limited principally to that portion of the interferogram which is most affected by the gas whose density is being measured (excluding that portion near zero path difference). In the case of CO that portion of the interferogram obtained with path differences between 2.70 and 3.95 mm has been selected. Since the lines in the first overtone band of CO are separated by about $3\ cm^{-1}$ on the average this shows up in that part of the interferogram centered at about $1/3\ cm^{-1} = .33\ cm = 3.3\ mm$. Thus, the CO spectrum is as shown in Figure 5.2.2 and the interferogram (using a spectral filter centered at $4278\ cm^{-1}$) is also shown in Figure 5.2.2. In this the major effect of the CO is seen to be in the region of 0.3 cm. Taking this portion of the interferogram between 0.27 and 0.395 cm gives essentially all of the information on CO that can be obtained from the interferogram. The determination of CO is not, however, the simple measurement of this peak in the interferogram since other gases, particularly CH_4 and H_2O also have some effect in this region. Thus, this peak is divided up into a number of sections, 32 in the case of our instrument. The effect of each gas on each of these 32 sections is determined in effect,

by calibration.*

Thus, in the simplest case, a portion of the interferogram affected only by H_2O is chosen to determine the amount of H_2O** and the remainder of the interferogram is, in effect, corrected using these data and calibration information. CH_4 is dealt with similarly. Thirty-two different effects could be dealt with this way. Since in a real case portions of the interferogram affected by a single gas are not always available, the set of 32 simultaneous equations is solved to determine the amounts of individual gases causing the combined effects.

The output of the interferometer will be voltages, each related to the concentration (column density) of one species. The calibrations can be thought in terms of these voltages. Thus, to be able to separate out the effects of individual species it is necessary to resolve parts of the interferogram which show the effects of these species. In the A-B-C example this resolution must be of the order of 0.2 mm which is readily attainable. The spectral resolution required for a similar separation of effects would be 0.2 cm^{-1} which is not attainable with the spectrum which would be produced from the interferogram obtained with this instrument. Thus, by directly using the interferogram the effects of specific species and hence its density is measureable whereas it would not be if the interferogram were converted to a spectrum and that used for the measurement. This comparatively simple measurement can be made very much faster than can a measurement of the same

---

*Actually, the effects of specific gases, other than that being measured (such as CO), need not be specifically known by calibration. The calibration can consist of 31 different atmospheric conditions with one amount of CO and a different amount of CO with one of these conditions. The measurement of CO is then made by determining the effect on each section of the interferogram of other gases of the atmosphere ad determined by a best fit of the 32 points.

**Since the H_2O spectrum and hence its interferogram is affected by temperature, two or more portions of the interferogram must be used to take this effect into account.

species by a high-resolution spectromatic technique, whether by a spectrometer technique or by an interferometric technique which employs the Fourier transform of a interferogram obtained over a large range of path difference.

Page Intentionally Left Blank

6. CORRELATION TREATMENT

6.1 Basic Principles

6.1.1 Instrument Output: - The interferometer receives radiation, the spectral characteristics of which are affected by a number of parameters. We wish to measure one of these parameters (CO burden), with as high accuracy as possible and as little interference as possible from variation in the other parameters. Within the instrument, optical filters limit the range of the radiation to a fairly narrow spectral region where CO absorption has the greatest relative effect on the radiation.

The correlation interferometer operates by varying the delay between the two beams of a Michelson interferometer over a defined range. As the delay is swept, a sinusoidal type signal is generated at the detector output. This signal is both amplitude and phase modulated. The band center and width are directly related to the center and width of the optical spectral filter, while the modulations are characteristic of the more detailed spectral information.

6.1.2 Preprocessing: - An important function of the interferometer electronics hardware is to reduce the high sampling rate implied by the relatively high center frequency of the interferogram signal, by synchronously detecting the signal with a reference signal, (similar to the local oscillator in a homodyne system). This reference is generated from the interferogram of radiation having stable spectral characteristics. The reference radiation passes through the same interferometer system as the signal radiation, so that to a very large extent the reference derived from its interferogram is fixed in phase relative to the interferogram of any given signal radiation, regardless of any irregularities in scan, or variations in the interferometer arm lengths.

When this synchronous detection is carried out, the result is a signal containing only the information of the sidebands of the original signal, beat down to zero frequency mean. (Actually two such signals are produced, from references both in phase and in quadrature phase with the reference interferogram.) The signal's information is still band limited, by virtue of the original spectral band limitations. The signal is therefore integrated and digitized at an interval sufficient to retrieve this information, producing a preprocessed, digitized, interferogram.

6.1.3 Final Processing: - Final processing consists of applying a linear digital filter ("weighting function" or "weights") to the preprocessed interferogram. The filtering operation consists of taking the weights, one for each point of the interferogram, multiplying them together with the corresponding interferogram points, and summing the results. The weights are chosen, in a manner to be described below, so as to give a final result which is insensitive to variations in all parameters except the desired one. (The weights are also chosen to give a result which is optimized against a mixture of noises.) The result may be directly converted using a defined zero point and scale factor, to units of target gas burden (atm-cm, ppm-m), etc.

6.2 Determination of Weights

6.2.1 Basic Philosophy and Theory: - The determination of the weights is based on the possibility of representing any observed interferogram as a linear combination of component interferograms. The number of such component interferograms required to represent a range of actual observed interferograms to some accuracy, will depend on a number of factors depending on the range of conditions under which the interferograms are observed. The number will depend mainly on the number of parameters which vary significantly over the range of conditions, and to a lesser extent on the

degree of non-linearity in the variations of the interferograms with these parameters. (Parameters will characteristically represent factors such as water vapour burden, methane burden, and temperature profile, as well as the target CO burden).

Consider then any interferogram I within the defined range. It may be written as a linear combination of N constituent interferograms. Using the index K to define the point on the interferogram, and J to define the particular constituent interferogram we may write

$$I(k) = \sum_{j=1}^{N} q_J \, I_J(k)$$

The q_J's are the strengths of the constituent interferograms in the particular interferogram observed. Let us assume one of these, q_{J1}, is the target gas burden.

Now the final processing consists of the application of a weighting function, H(k), to the interferogram. The resulting measurement is

$$M = \sum_{k} H(k) \, I(k)$$

$$= \sum_{J} q_j \sum H(k) \, I_J(k)$$

From this, it can be seen that if we can find weights H(k) that give

$$\sum_{k=1}^{Nk} H(k) \, I_J(k) = \begin{cases} 1 & J = J1 \\ \emptyset & J \neq J1 \end{cases}$$

then the measurement will be $M = q_{J1}$, the target burden. If J varies from 1 to N, then this is a set of N equations in as many unknowns H(k) as there

are interferogram points (NK). In order for these equations to be satisfiable, there must be at least as many interferogram points as there are constituents ($Nk \geq N$). In the case that $Nk = N$, there are N linear equations in N unknowns, and the solution for the H(k) is straightforward.

In the case that there are more interferogram points than there are constituent interferograms, there are many possible weighting functions which will satisfy the N equations. It is however possible to choose a unique set of weights by considering the noises in making the measurement, and minimizing their effect on the measurement.

6.2.2 Noises in Measurement: - The noises operate in the following manner. The total integration time for measurement of a given point may be written D(k) (its duration, assumed unity up till now). The contribution to the final measurement for that point is actually $\Delta M(k)$.

$$\Delta M(k) = \Big[H(k)\ D(k) \Big]\ I(k)$$

The noise contribution for that point is significant in how it can vary this from its "correct" value. The noises may or may not decrease with integration time: that is, they may be either random or synchronous with the scan. They may or may not depend on the expected level of the interferogram itself $\langle I \rangle_k$, (an RMS value for the constituent interferograms at a given point): that is, they may be either additive or multiplicative.

A discussion of various physical origins for these noises will be presented elsewhere (Section 6.2.4). However, it is sufficient at this point to be able to characterize them by four numbers, $a_1 \ldots a_4$, which represent the severities of the four possible combinations of noise type:

a_1	-	Random Additive	(RA)
a_2	-	Random Multiplicative	(RM)
a_3	-	Synchronous Additive	(SA)
a_4	-	Synchronous Multiplicative	(SM)

The noises will combine in an RMS manner to give the mean square noise contribution $\Delta N^2(k)$ to the measurement at a particular interferogram point, and we may write

$$\Delta N^2(k) = \left[H(k)\, D(k)\right]^2 \times \left[(a_1 + a_2 \langle I\rangle_k^2)/D(k) + (a_3 + a_4 \langle I\rangle_k^2)\right]$$

$$= \left[H(k)\, D(k)\right]^2 G(k) .$$

G(k) is an effective mean square interferogram error for point k (although it may originate through error in either H, D, or I).

6.2.3 Derivation of Weights: -

The total measurement is thus

$$M = \sum_k \Delta M(k) = \sum_k \left[HD\right] I$$

and the total squared noise is

$$N^2 = \sum_k \Delta N^2(k) = \sum_k \left[HD\right]^2 G.$$

It is possible to choose, given the various $I_J(k)$ and the duration D(k), those values for $\left[HD\right]_k$ which minimize the above noise term; subject to the con-

straint that $M = q_{J1}$, the target quantity, regardless of what values the other quantities may have (to the extent that the assumed linear representation is valid). The solution, derived elsewhere (Grenda, et al, 1971), is

$$\left[HD\right]_k = \sum_J A^{-1}_{J,J1}\, I_J(k)/G(k),$$

where A^{-1} is the inverse of the matrix

$$A_{J,L} = \sum_k I_J(k)\, I_L(k)/G(k).$$

(Knowing D(k), $H(k) = HD_k/D(k)$.

A couple of points should be noted. First, the weights produced in this manner may be multiplied by an arbitrary scale factor, to give a new set of weights; however, the signal to noise ratio will remain unchanged. Secondly, if G(k), (the squared noise at a given point) is multiplied by a scale factor; (i.e. if all noise terms a_i are increased by the same factor), then there is no change to the weights produced. In fact, G(k) may be written as:

$$G(k) = \text{const} \times \left[1 + R\,\langle I\rangle^2\right]_k$$

where $$R = \left[a_2/D(k) + a_4\right] \Big/ \left[a_1/D(k) + a_3\right]$$

represents the relative importance of the multiplicative terms with respect to the additive terms. If we assume D(k) is constant, then this one parameter will determine the weights produced; whether they optimize against multiplicative noises ($R >> 1$), additive noises ($R << 1$), or some intermediate mixture. Analysis of the way R varies with the a's for reasonable values of the noises should indicate which terms will have most affect on the shape of the weights produced when varied.

Similarly, it is possible to examine the relative importance of the two multiplicative terms (in the numerator). In fact, the ratio of their contribution to the total final noise is given by $a_4 \times D/a_2$. The same is true for the two additive terms. On the other hand, to examine the total contribution of both multiplicative terms in comparison to the contribution of the additive terms, it is necessary to first calculate the weights. Once this has been done the absolute importance of the four noises may then be calculated, in the same units as those in which the target burden is measured:

$$N_1^2 = a_1 \Sigma (HD)^2 / D$$

$$N_2^2 = a_2 \Sigma (HD)^2$$

$$N_3^2 = a_3 \Sigma (HD <I>^2 / D$$

$$N_4^2 = a_4 \Sigma (HD <I>)^2$$

6.2.4 Physical Origins for the Noise Terms: - The various noise terms may each arise due to one or more sources. Some possible sources are listed below:

RA: - Detector noise.
- Photon noise.
- Other electrical noises.
- Digitization of integrated outputs.

RM: - Scintillation or rapid variations in target, albedo or illumination.
- Random errors in derivation of reference signal.
- Random variations in scan waveform.

SA: - Presence of spectral signatures which were not represented in sample used to derive weights.

- Crosstalk from reference into signal channel.

SM: - Inaccuracies in carrying out multiplications (truncation of weights).

- Change in scan waveform from the shape when the weights were derived.

6.3 Software

6.3.1 Description: - As described in detail above, processing of interferograms, either theoretical or experimental, consists of applying a linear digital filter ("correlation function" or "weights") to the interferogram. These weights are chosen so as to give a final result which is indicative of the quality of one of the atmospheric components contributing to the interferogram, and which is insensitive to variations in all other parameters. The filtering operation consists of taking the weights, one for each point of the interferogram, multiplying them together with the corresponding interferogram points, and summing the results. (The weights are also chosen to give a result which is optimized against a mixture of noises.) The results are also directly converted using a defined zero point and scale factor, to units of target gas burden (atm-cm, ppm-m), etc.

A software package has been developed for use with a large computer system to input interferograms deriving the weights for a given noise mixture, evaluate the noise severities, and to simulate measurement on interferograms using the weights.

The procedure for the determination of the weights is to accept a set of interferograms and define the delay region over which the weights are to be applied. One interferogram is designated as "nominal", and another designated as "target". Weights are derived, based on the assumption that

all interferograms except "target" represent a single value of the desired parameter (CO burden), while other parameters are varied. The interferogram designated as "nominal" is assumed to represent the same values for the other parameters as does "target"; i.e. "nominal" and "target" are assumed to differ only in the size of the target parameter.

The weights determined will then give measurements which have a zero for the target parameter value used in "nominal", and a scale of 1 for the target parameter variation between "nominal" and "target".

(In order to reduce the sizes of numbers to be handled, the nominal interferogram is subtracted from all others, so that difference interferograms are actually used. Because of assumptions of linearity, this makes no difference to the algorithm for determining the weights.)

(It may also be noted that the program actually deals with interferograms containing both inphase and quadrature phase components. They are just handled as if there were twice as many data points I(k); although an extra index is needed to reference the two components.)

Values are input to the program representing the noise levels (RA, RM, SA, SM), and the total time, T, available for measurement. (The measurement time should include any duty cycle factor which may make it shorter than elapsed time. Values for RA, etc. will be discussed later.) Based on these, the a_i are calculated.

The interferograms and noise parameters are then input to a subprogram which carries out the weight generating algorithm, returning the weights.

Provision is included in the program for putting out the noise components for given a_i and T, and to also put out the expression relating to the size of the noises to the parameters.

An AGC function is also carried out by the program. In the case of computer generated theoretical interferograms, the normalization is done on the basis of the interferogram value at the first point, (assumed to

be the zero delay point, proportional to the total radiation received). For interferograms generated by the actual instrument, a good deal of the AGC function is carried out by the hardware. However, a term proportional to the duration of the measurement remains (number of scans). This factor is removed for tapes generated by the NOVA by dividing all interferogram points by the total number of fringes duration of the measurement at each point, as the values are put into core. A flow chart of the program is given in Figure 6.3.1. A listing is given in Appendix B.

6.3.2 Values for Noise Inputs: - Values for the noise terms may be determined by either knowledge or estimation of system parameters, or else empirically by the examination of instrument generated interferograms. Conversions from the values input to the a_i, also depend on whether the interferogram set was computer or instrument generated. Certain terms depend on whether the program is running with instrument generated (INS) or computer generated (COM) interferograms.

The inputs are RMS noise levels for the following conditions:

RA - Noise for $\left\{\begin{array}{l}\text{unit (1 fringe) integration time (INS)}\\ \text{unit bandwidth (COM)}\end{array}\right\}$, interferogram units

RM - Noise for unit integration time, fractional interferogram units

SA - Noise in limit of long integration normalized to 1 fringe integration units (INS)

as a fraction of DC level x 10 (COM)

SM - Noise in limit of long integration, fractional units

6.3.3 Noise Values Based on Instrument Measurements: - If empirical observations are available from the instrument the appropriate variations, ΔV, of measured values, V, taken under conditions of N fringes inte-

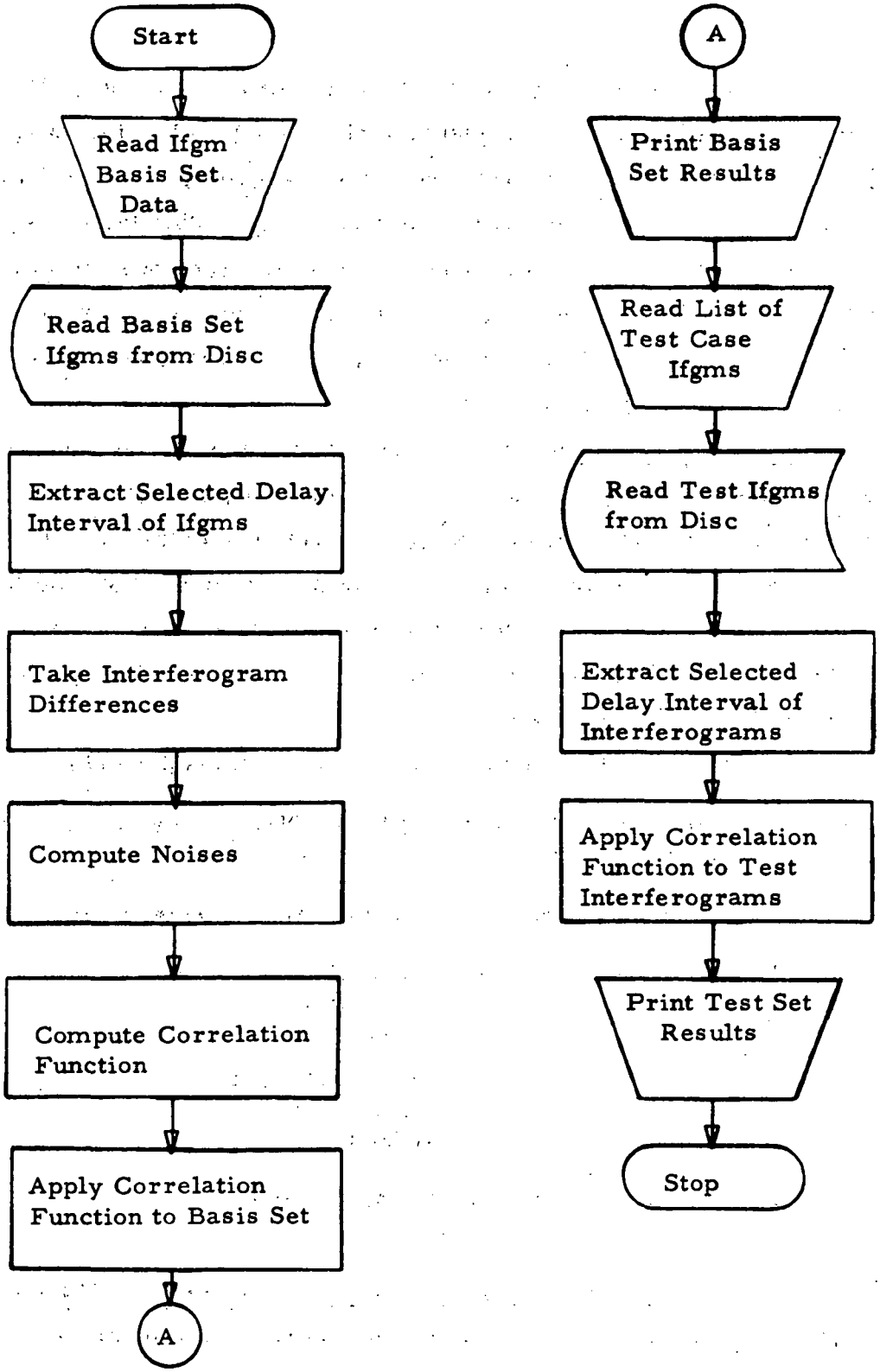

Figure 6.3.1 Correlation Function Program Flowchart

gration per point, the necessary conversions are listed below: (Time, T, used with these inputs should be the total duration of the measurement to be optimized for, in fringes.)

$$RA = \langle \Delta V \rangle / \sqrt{N}$$

$$RM = \langle \Delta V / V \rangle \times \sqrt{N}$$

$$SA = \langle \Delta V / V \rangle$$

6.3.4 RA and SA for Computer Interferograms: - In the case of computer generated interferograms, for the RA term, a system NEP for 1 Hz bandwidth may be known, along with the system throughput, T (cm^2 sterad), including instrument inefficiencies). The conversion to RA will depend on the the interferogram units used. These may be either watts/cm^2 sterad, or equivalent width of the instrument plus atmosphere transfer function. (These correspond to units in the original spectrum of watts/cm^2 sterad cm^{-1}, and fractional transmission, respectively.) The conversions are:

Units for Original Spectrum	Detector Limited	Photon Limited
W/cm^2 sterad cm^{-1}	NEP/(T x DNU)	$\sqrt{2\pi N_\nu h\nu/T}$/DNU
Fractional Transmission	NEP/(T x N_ν x DNU)	$\sqrt{2\pi h\nu/N_\nu T}$/DNU

N_ν is the background radiance, in W/cm^2 sterad cm^{-1}, and DNU is the spectral interval at which the original spectrum was sampled when the Fourier transform was taken. (Provision is included in the program for transferring DNU along with the interferograms. If this has been done, it may be set to 1 in the above conversion.)

A rough estimate for the SA term may be made for use with the computer interferograms as follows. The mean optical depth, x, may be estimated for those absorbing constituents which have not been included in the computer modelling, those constituents which might not be represented in the range of observation used to define the weights). Assuming that the spectrum of their absorption is random, then the value to be used for SA would be SA = X (giving a_3 = X times the interferogram DC level). In practice, the spectrum is never completely white. If we assume a 1/f type of variation, then RA should be decreased according to the distance of the interferogram working region from zero, a factor of 10 (implying a distance of 10^2 fringes from the origin) has been built into the program. Thus, for a system working N fringes from zero delay,

$$SA \sim X/(N/100)^{1/2}$$

This procedure does not work for non-random interfering spectra. If a direct estimate can be made of the interferogram amplitude due to an unaccounted interferent, as a fraction X of the DC level, then the number to use is

$$SA \sim 10\ X.$$

(It may be recalled that it is possible to decide on the basis of a_1 and a_3 whether or not the SA noise is significant in comparision to RA noise.)
In terms of the inputs, the quantities to consider are listed below.

	Interferogram	
	Instrument	Computer
QA	RA/SA $\sqrt{DT}$	4 RA/SA x WO x DNU x $\sqrt{DT}$
QM	RM/SM $\sqrt{DT}$	RM/SM $\sqrt{DT}$

For the computer QA term, WØ is the interferogram DC level, DNU the spectrum step if transferred with the interferogram. DT is the duration for the measurement of a single point, (fringes for the instrument, seconds for the computer interferograms).

When a Q is much greater than 1, the associated random term dominates the synchronous term, and vice versa.

6.3.5 Data Output: - The output of this program is a list of the target species burden in both test units of target gas burden. One test unit is the difference in species burden between the target and nominal interferograms. Since the actual burden is stored along with the interferogram, usually in atm-cm, it is possible for the program to convert the test units into burden units.

In addition to applying the correlation function and listing the target species burden for the test interferograms, as a check the correlation function is also applied to the basic set of interferograms from which the correlation function was generated.

7. RESULTS

Calculations have been made with several programs. Initial calculations were made with a single-line model. For each of several lines of the overtone and fundamental bands, calculations were made of absorption across the line, the line shape as a function of altitude, net absorption as a function of altitude for various CO density profiles (including sinks and various temperature profiles, integrated net absorption as a function of ground temperature and emissivity, and of other factors which influence the net intensity. With a second program, calculations were made, for the limb mode, of the effect of instrument error on the inversion of measured total CO densities in the path to obtain a CO profile. With a multi-line program which computes the spectrum incident on the instrument, generates the corresponding interferogram, and, with another program, inverts this to CO densities in the path, calculations were made to determine the sensitivity of the technique and the effects of various atmospheric parameters.

7.1 Atmospheric Transmission

7.1.1 Calculation Model: - Absorption by the CO overtone (2.3 μ) and fundamental (4.6 μ) bands has been studied using the computational technique described above. The geometry selected for the calculation considers a satellite observing the earth from the zenith. Consequently, lines of the fundamental band are strongly absorbed whereas those of the overtone band are relatively weak. The results then are based on a comparison between these two cases with emphasis placed on the effect of assumed atmospheric profiles on the observed signal.

Two programs for the calculation of atmospheric spectral transmission were written. One is a single line model used to calculate atmo-

spheric transmission for a variety of conditions appropriate to the CO problem. Specifically, it was used to compare the first overtone and fundamental bands, to determine the effect of ground temperature variations, to determine the effect of variation and uncertainty ground emissivities (at specific wavelengths), to test the effect of different Lorentz half-widths, and to test the effect of low-altitude CO sinks on the transmitted signal.

The second program is a multi-line model which computes atmospheric transmission for multiple overlapping spectral lines. It has been used to calculate the spectrum incident on the instrument, and the output interferogram. A separate program establishes weighting functions and uses them to compute CO density.

The program can handle a total of 150 different lines, distributed in any way between three chemical species (CO plus any two others). Three different cases (Figures 4.1.1, 4.1.2) are incorporated in the program:

1. Ground blackbody radiation (4.6 μ)
2. Limb transmission (2.3 or 4.6 μ)
3. Reflected sunlight (2.3 μ)

Parameters which can be varied by means of input data include the temperature and species concentration profiles of the atmosphere, ground temperature and emissivity, reflectivity, viewing angles, incident radiation angle, and grazing height.

The line overlap system operates basically as follows. For each spectral line, a "line inclusion band" is computed. This is the frequency band over which each line must be considered. The limits of each band are the distance one must go from each line center to reach a threshold intensity. This threshold intensity is defined as a preselected percentage (usually 1%) of the weakest line. For the purposes of determining these bands, a Lorentz line shape of nominal width 0.06 cm^{-1} is assumed.

The spectrum is not computed at uniformly spaced points. The spacing varies from as low as 0.001 cm^{-1} near the line centers to as much as 0.5 cm^{-1} between lines. The actual computation of the net transmission is done by solving the basic radiative transfer equation in much the same way as previously described for the single-line calculations. The overlap of lines is represented by addition of their absorption and emission coefficients.

The complexity of the computation has resulted in a program too large to fit a 32 K word computer memory. It was therefore necessary to use an overlay system, whereby each section of the program is stored on a disc and brought into memory as needed. Using this system, the program occupies a maximum of about 24 K words. Preliminary runs using geometry case 1 and 13 CO lines had a running time of about two minutes.

7.1.2 Single- and Multi-line Models and Line Shapes: - The net change in intensity for the R7 line of the fundamental is given in Figure 7.1.1. This shows by the solid curve the results obtained by the single-line model and by the x's the results obtained by the multi-line model. These agree within 1% and it can be concluded that the comparison of the fundamental and overtone bands can be carried out using the single-line model.

A variety of atmospheric models were used for the computations (AFCRL, 1966). The pressure was taken from the 1966 U. S. Standard Atmosphere. Temperature and CO concentration profiles were varied as shown in Section 2. For all calculations discussed in the following pages, the conditions used, if not otherwise stated, are:

CO Profile 1
Temperature Model 2
Ground Temperature = 0 km Atmospheric Temperature
Emissivity = 1.0

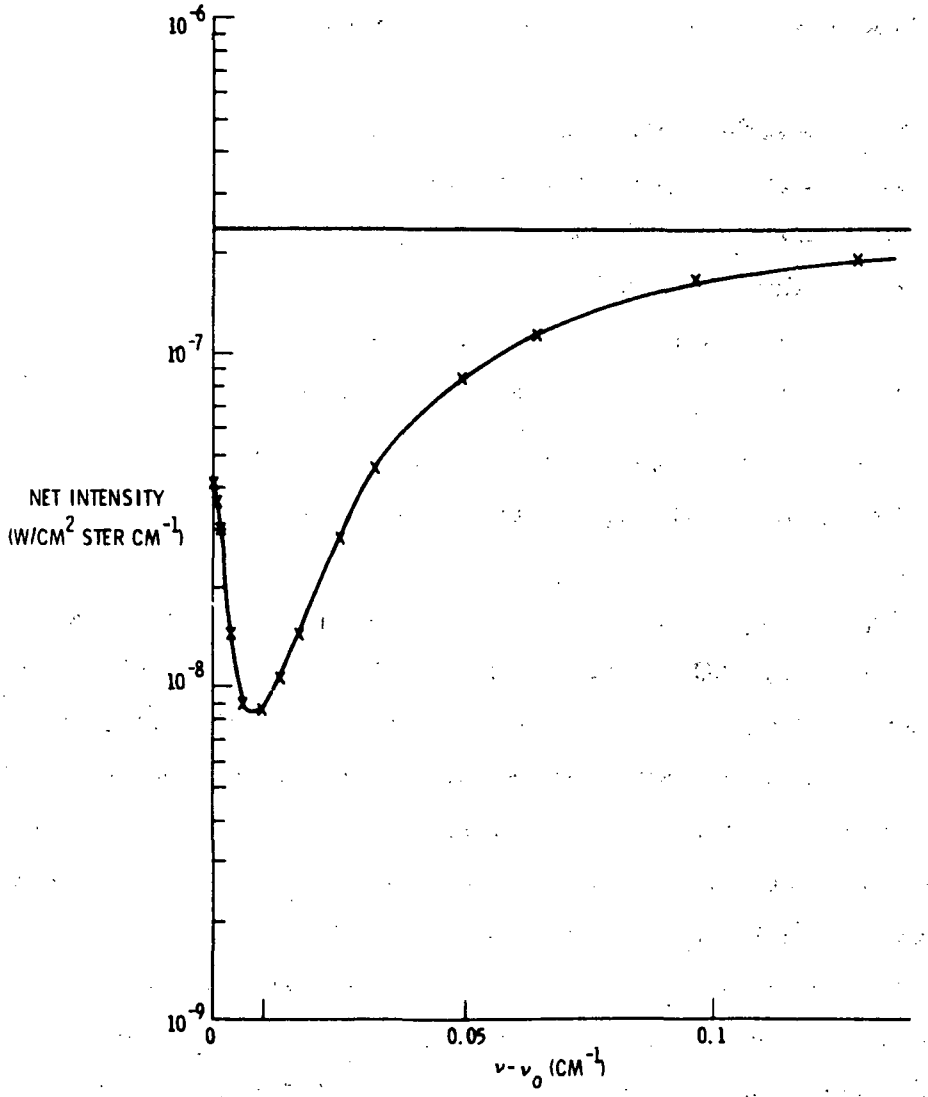

Figure 7.1.1 Comparison of Single and Overlapping Line Absorption Spectra through Standard Atmosphere

Reflectivity = 0.1

Bandpass = 20 cm^{-1}

Lorentz Half-width (R7) = 0.06 cm^{-1}

Calculations have been made for six CO profile models (Table 2.1.1, Figure 2.1.1)

1. Standard (0.1 ppm)
2. Low Altitude Urban Source
3. Low CO (0.01 ppm)
4. High Altitude Sink
5. Low Altitude Sink (Effect to 9 km)
6. Low Altitude Sink (Effect to 3 km)

These models were used to evaluate the emission and absorption coefficient and compute the CO absorption spectrum which would be observed at an altitude of 80 km.

The absorption and emission coefficients are functions of pressure, temperature, and CO number density. This is illustrated by Figure 7.1.2 which shows the spectral absorption coefficient of the 4.6 μ P8 line as a function of altitude for the standard temperature and CO models. At low altitudes the lines are Lorentz broadened and then as altitude increases, Doppler broadening dominates. When these absorption coefficients are integrated over the atmosphere, the line profile variation with altitude is manifested by an emission peak at the center of the absorption line. This behavior is illustrated in Figure 7.1.3. Physically, earthshine is absorbed up to an altitude of about 30 km. At this point, the atmospheric temperature rises and the light flux is increased by emission. However, because the line profiles are very sharp at this altitude, the emission is observed only near the line center.

A second example of the importance of atmospheric emission is illustrated in Figure 7.1.4. Here the net change in absorbed intensity

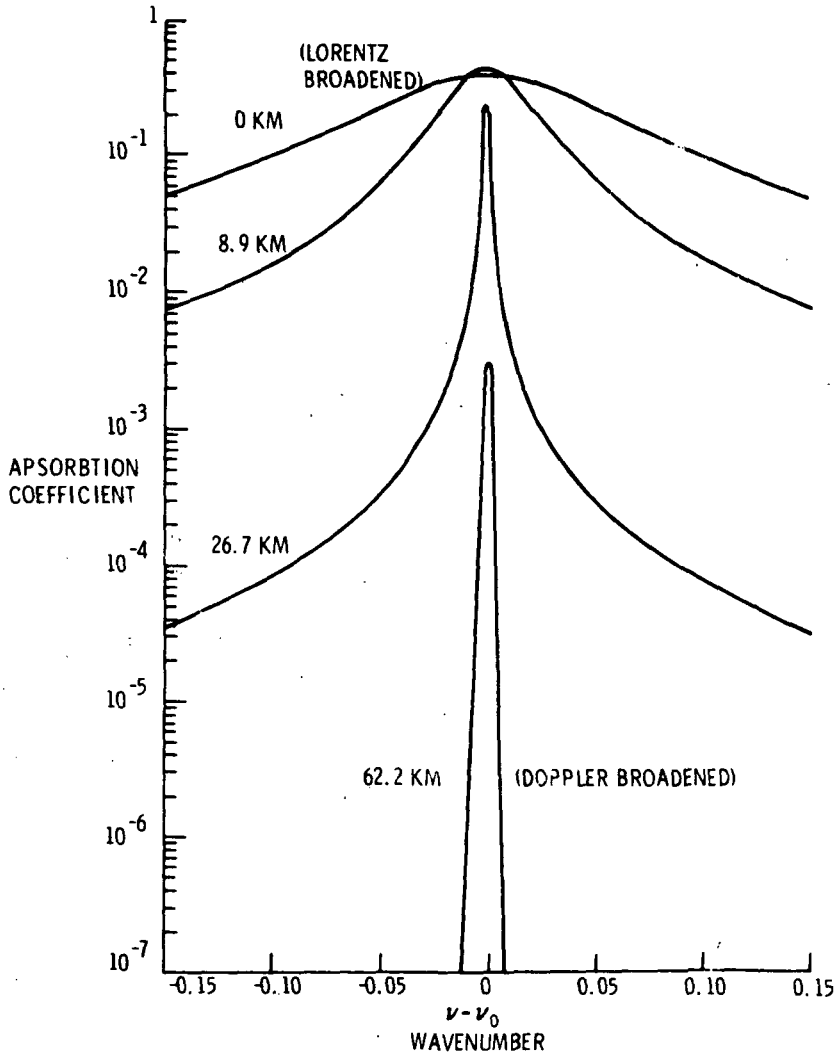

Figure 7.1.2 Absorption Line Profiles (P8)

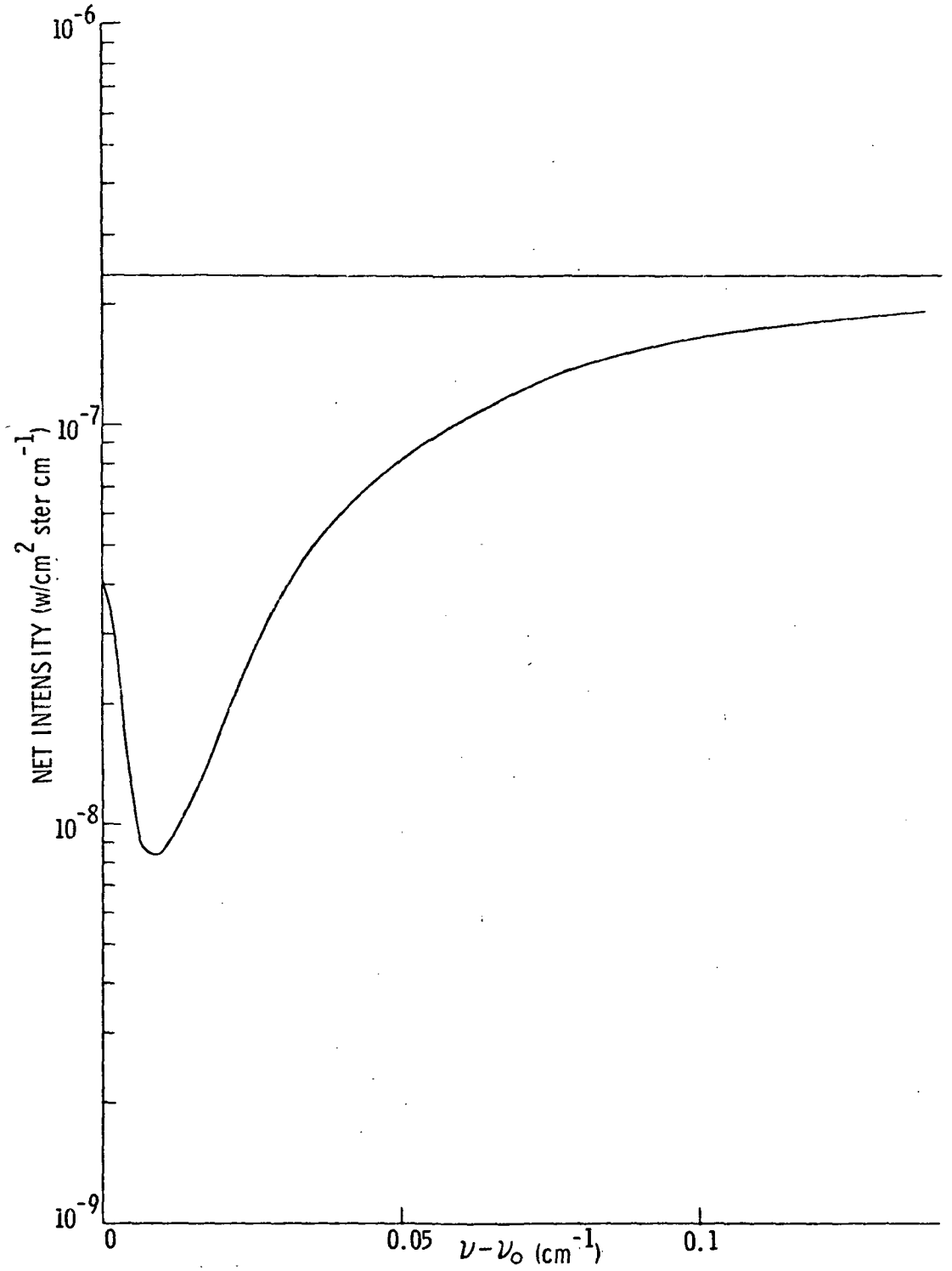

Figure 7.1.3 Line Profile Showing Emission Peak at Center

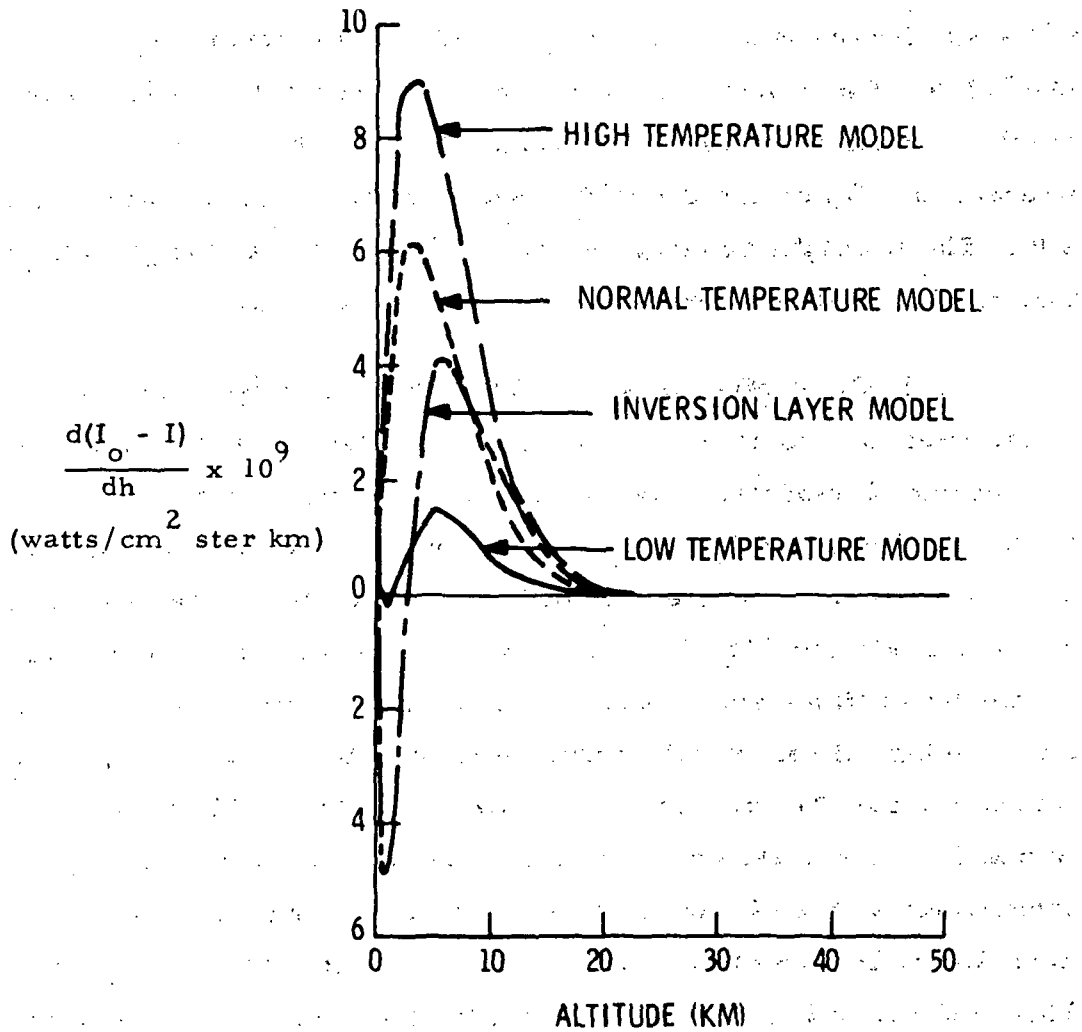

Figure 7.1.4 Variation of Rate Change in Absorbed Intensity Fundaments (4.6 μ) (R7 Line)

with altitude as integrated over the P8 line of the fundamental is shown as a function of altitude for the four temperature models and the standard CO model. Two temperature profiles have inversion layers which cause a net increase in the light flux (negative absorption). When the temperature drops there is less photon emission and the net absorption increases. For the case of the P8 line of the overtone, this behavior is not observed as shown in Figure 7.1.5. The reason for this is source temperature. In the case of the overtone, reflected sunshine dominates the intensity at the earth's surface, whereas at 4.6 μ earthshine is the dominant contributor to the ground intensity. The atmospheric temperature can be higher than the ground temperature and hence atmospheric emission becomes important.

7.1.3 CO Profile Effects: - The effect of CO number density profile on the intensity has been examined using the standard temperature profile and the six CO models. The results for the change of intensity with altitude for the P8 line of the fundamental are shown as a function of altitude in Figure 7.1.6. In all cases, except the urban atmosphere, the change in intensity peaks between 6 to 10 km whereas it should peak at ground level except for the low-altitude sink models. This peak is caused by a balance between the changing CO concentration and the emission. In the case of the urban atmosphere, the CO concentration profile dominates. This balance should be emphasized in that the change in absorption at 4.6 microns is not directly proportional to the CO concentration. On the other hand, similar calculations for the P8 line at 2.3 μ are a direct measure of the CO number density. This is shown in Figure 7.1.7. The difference between the two wavelengths is again caused by the effective source temperature.

These data show that absorption spectra as observed from 80 km depend on the atmospheric profiles of the absorbing species and on temperature. The temperature dependence of the spectra is controlled by the temperature of the absorbed source. For the case where earthshine is im-

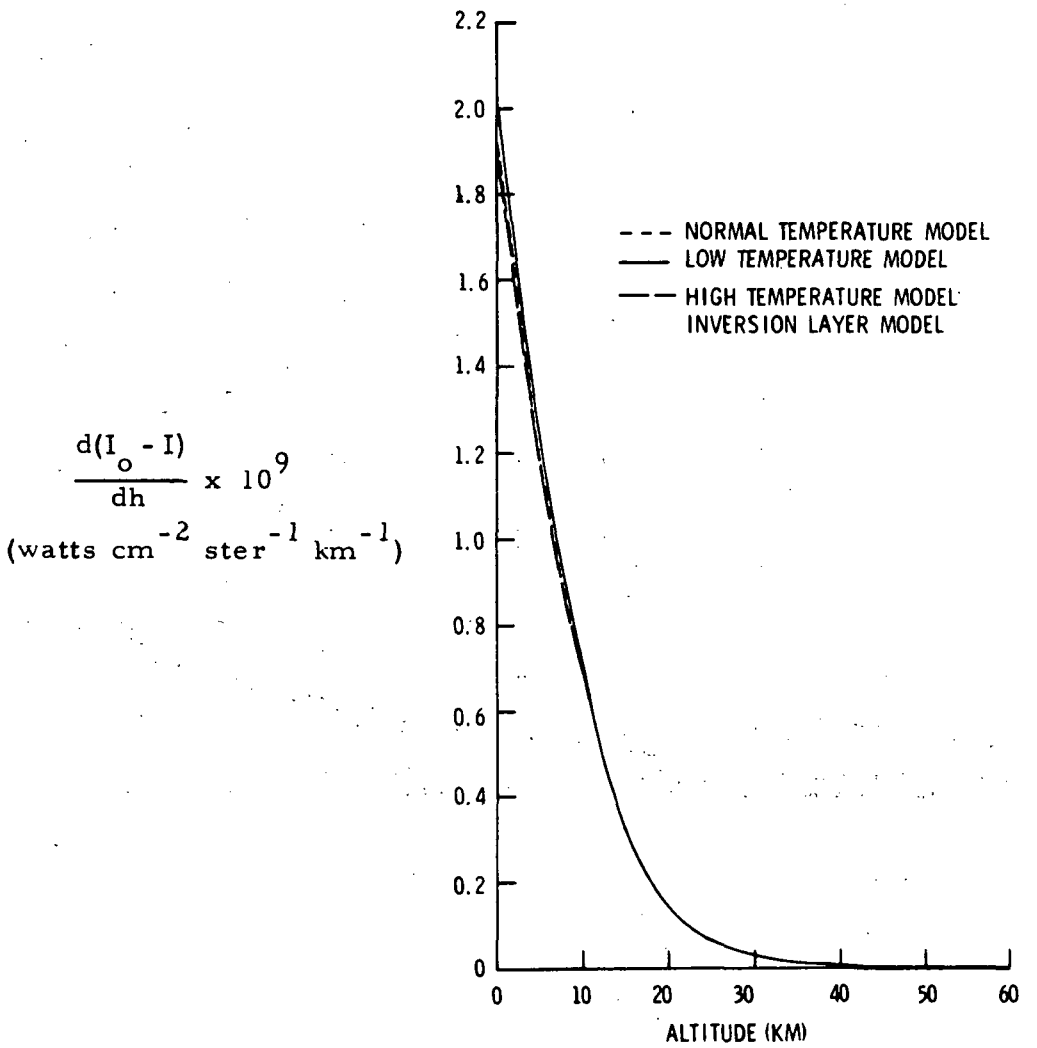

Figure 7.1.5 Variation of Rate of Change in Absorbed Intensity Overtone (2.3 μ) (R7 Line)

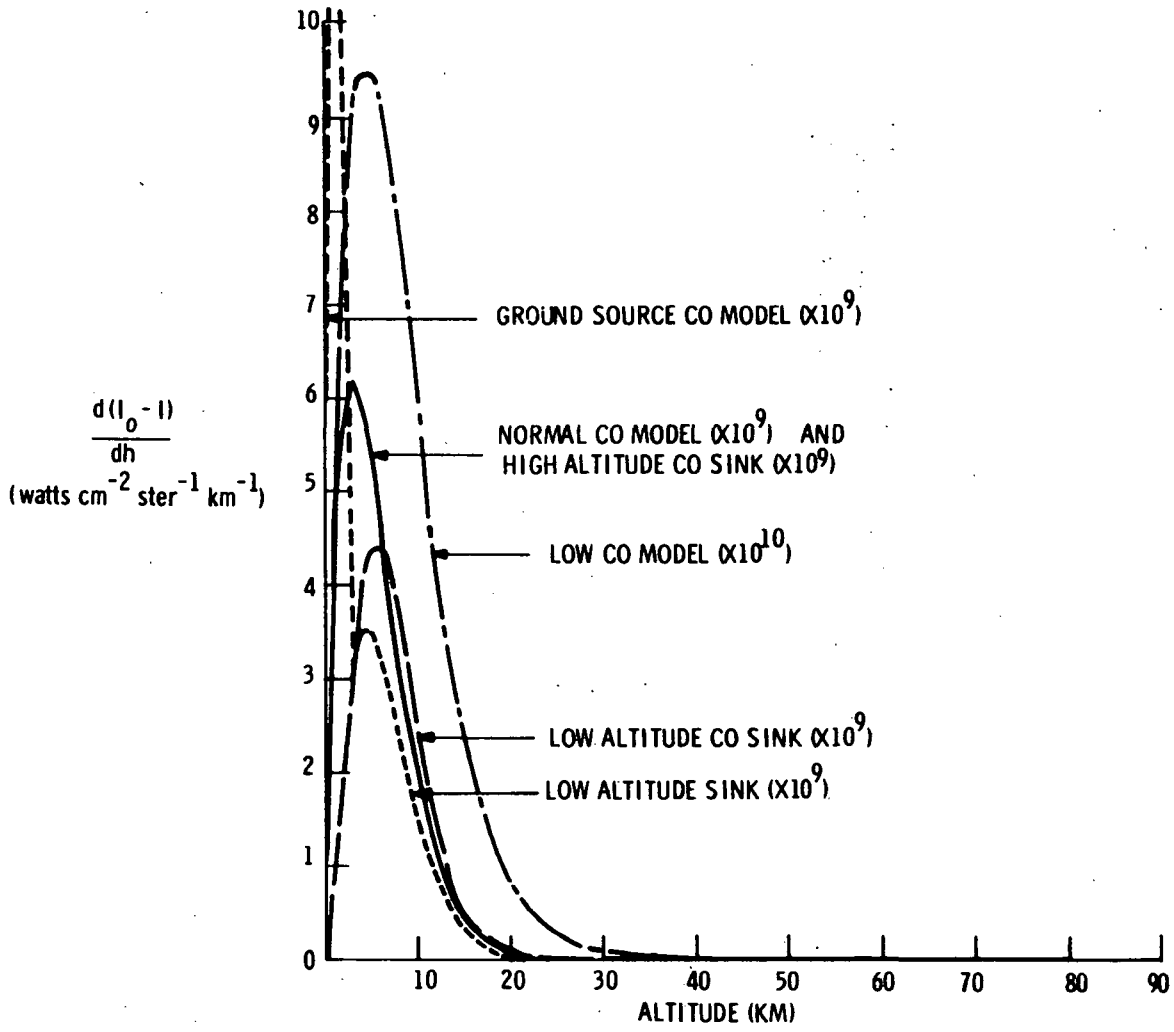

Figure 7.1.6 Variation of Rate Change in Absorbed Intensity Fundamental (4.6 μ)

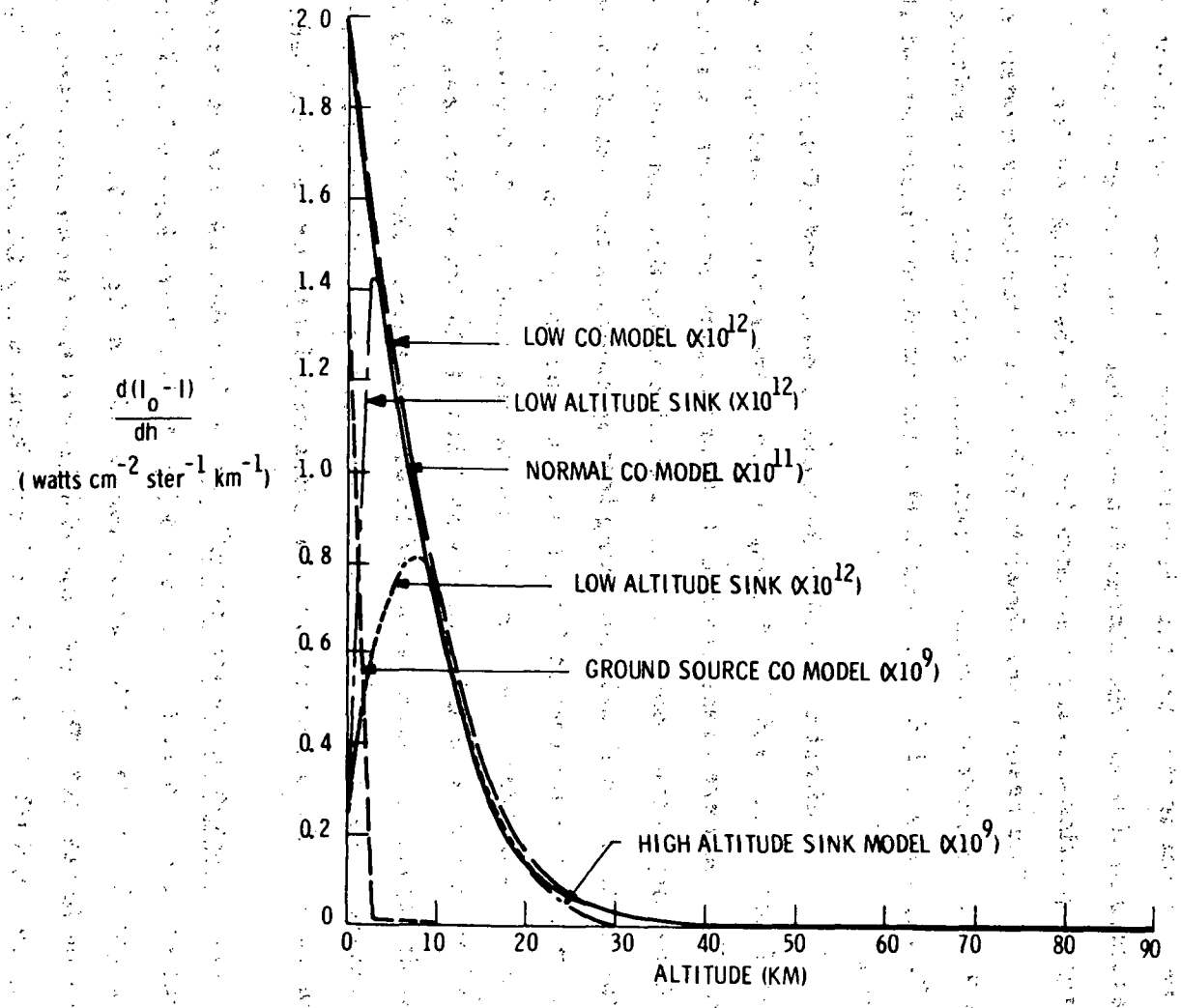

Figure 7.1.7 Variation of Rate of Change in Absorbed Intensity Overtone (2.3 μ)

portant the absorption profiles are strongly effected by the atmospheric temperature profile. Also in this case, the change in absorption with altitude is not a direct measure of the absorbing species. On the other hand, when the absorbed source is the sun, the absorbed signal is almost independent of the temperature profile and the change in absorption with respect to altitude is directly proportional to the concentration of the absorbing species.

The results are shown in Table 7.1.1 for the six models and in Table 7.1.2 for models in which concentrations of the CO were multiples (.1, .2, .4, .8, 1., 1.6, 3.2, and 6.4) of the standard atmosphere at all altitudes.

The effect of low altitude sinks on measured CO densities is seen in Tables 7.1.3 and 7.1.4 using temperature models 2 and 4, respectively. The numbers presented are those of the percent difference of the actual CO density in the model and that calculated using the computed net absorption for that model and converting that by means of the data of Table 7.1.2. It can be seen that at 4.6 μ the errors are larger than the differences in the amounts of CO in the standard and the sink models. To improve these results, an atmospheric CO profile would have to be known for measured CO densities; this cannot be assumed to be obtainable. The errors for the temperature model 2 are less drastic than those of model 4 which has an inversion layer. The latter errors are extremely large for the 4.6 μ band.

7.1.4 Temperature Profile Effects: - Calculations have been made for temperature models 1, 2, 3, and 4 (Table 7.1.3 and Figure 7.1.6) using the 0.1 ppm CO model. The calculations shown in Figures 7.1.4 and 7.1.5 were made for the R7, P1, P8, and P26 lines of the fundamental band and the R7, P1, P8, and P26 lines of the overtone band, using CO model 1. The results for this are shown in Table 7.1.5. The tabulated results show a great dependence on the atmospheric temperature model for the 4.6 μ band and little dependency for the 2.3 μ band. The graphical data of Figures 7.1.4 and 7.1.5

TABLE 7.1.1 EFFECT OF CO PROFILE ON ABSORPTION

FUNDAMENTAL (4.6 μ)

CO MODEL	$n_{CO}(cm^{-2})$	R7	P1	P8	P26
STANDARD	2.15 (18)	.2002	.0810	.1700	.00104
LOW ALTITUDE SOURCE	5.21 (19)	.6620	.2974	.5695	.0167
LOW CO	2.15 (17)	.0439	.0119	.0350	.000107
HIGH ALTITUDE SINK	2.09 (18)	.2006	.0807	.1703	.00102
LOW ALTITUDE SINK (9 km)	1.37 (18)	.1580	.0642	.1335	.000614
LOW ALTITUDE SINK (3 km)	1.93 (18)	.1963	.0795	.1666	.000965

OVERTONE (2.3 μ)

CO MODEL	$n_{CO}(cm^{-2})$	R7	P1	P8	P26
STANDARD	2.15 (18)	.00647	.00144	.00462	.0000098
LOW ALTITUDE SOURCE	5.21 (19)	.1226	.0299	.0953	.000431
LOW CO	2.15 (17)	.000662	.000146	.000471	.0000011
HIGH ALTITUDE SINK	2.09 (18)	.00631	.00140	.00451	.0000097
LOW ALTITUDE SINK (9 km)	1.37 (18)	.00418	.00095	.00292	.0000037
LOW ALTITUDE SINK (3 km)	1.93 (18)	.00582	.00130	.00413	.0000068

TABLE 7.1.2 EFFECT OF CO COLUMN DENSITY ON FRACTIONAL NET ABSORPTION

FUNDAMENTAL (4.6 μ)

$n_{CO}(cm^{-2})$	R7	P1	P8	P26
2.15 (17)	.0439	.0119	.0350	.000107
4.3 (17)	.0741	.0223	.0604	.00020
8.6 (17)	.1174	.0405	.0978	.000410
1.72 (18)	.1769	.0692	.1496	.000820
2.15 (18)	.2002	.0810	.1710	.00104
3.44 (18)	.2585	.1108	.2205	.00163
6.88 (18)	.3714	.1683	.3183	.00322
1.37 (19)	.5292	.2470	.4545	.00629

OVERTONE (2.3 μ)

$n_{CO}(cm^{-2})$	R7	P1	P8	P26
2.15 (17)	.000662	.000146	.000471	.0000011
4.3 (17)	.00131	.000286	.000926	.0000015
8.6 (17)	.00260	.000569	.00185	.0000032
1.72 (18)	.00518	.00115	.00369	.0000071
2.15 (18)	.00647	.00144	.00462	.0000099
3.44 (18)	.0102	.00228	.00729	.000014
6.88 (18)	.0197	.00455	.0142	.000030
1.37 (19)	.0370	.00895	.0272	.000059

TABLE 7.1.3 EFFECT OF CO PROFILES ON DERIVED CO CONCENTRATIONS (% DEVIATION)

FUNDAMENTAL (4.6 μ)

CO MODEL	$n_{CO}(cm^{-2})$	R7	P1	P8	P26
HIGH ALTITUDE SINK	2.09 (18)	0.2	0.0	8.3	2.5
LOW ALTITUDE SINK (9 km)	1.37 (18)	14.6	10.5	18.0	4.9
LOW ALTITUDE SINK (3 km)	1.93 (18)	8.1	2.7	12.7	1.0

OVERTONE (2.3 μ)

CO MODEL	$n_{CO}(cm^{-2})$	R7	P1	P8
HIGH ALTITUDE SINK	2.09 (18)	3.5	4.5	3.5
LOW ALTITUDE SINK (9 km)	1.37 (18)	6.1	6.1	6.1
LOW ALTITUDE SINK (3 km)	1.93 (18)	2.7	2.7	2.7

TABLE 7.1.4 EFFECT OF PROFILES ON DERIVED CO CONCENTRATIONS - TEMPERATURE INVERSION (% DEVIATION)

FUNDAMENTAL (4.6 μ)

CO MODEL	$n_{CO}(cm^{-2})$	R7	P1	P8	P26
LOW ALTITUDE SINK (9 km)	1.37 (18)	13.3	10.4	17.0	0.04
LOW ALTITUDE SINK (3 km)	1.93 (18)	0.9	29.5	32.6	35.2

OVERTONE (2.3 μ)

CO MODEL	$n_{CO}(cm^{-2})$	R7	P1	P8
LOW ALTITUDE SINK (9 km)	1.37 (18)	7.4	7.4	7.4
LOW ALTITUDE SINK (3 km)	1.93 (18)	3.6	4.7	2.6

TABLE 7.1.5 EFFECT OF TEMPERATURE PROFILE ON ABSORPTION

4.6 μ	R7	P1	P8	P26
LOW TEMPERATURE	.1613	.0677	.1328	.000489
NORMAL TEMPERATURE	.2002	.0810	.1700	.00104
HIGH TEMPERATURE	.1942	.0772	.1662	.00134
INVERSION LAYER	.1270	.0521	.1063	.000433
2.3 μ				
LOW TEMPERATURE	.00660	.00152	.00462	.0000062
NORMAL TEMPERATURE	.00647	.00144	.00462	.0000098
HIGH TEMPERATURE	.00637	.00140	.00461	.000014
INVERSION LAYER	.00639	.00140	.00461	.000013

show the contribution of various altitudes to the net absorption. The 2.3 μ band shows absorption as a function of altitude to be as would be expected whereas the 4.6 μ band shows much less absorption below about 5 km (and, in fact, a significant net emission in some regions) which is an important region for CO sink studies.

7.1.5 Ground Temperature Effects: - The calculations described above included a ground temperature of each model at 0 km. Calculations have also been made for a different ground temperature. The following cases were carried out.

T_{Ground}	Atm. T. Model	$T_{Model\ Atm.}$
288.2	2	288.2
288.2	1	257.3
288.2	3	302.6
288.2	4	283.2
273.2	2	288.2
284.2	2	288.2
287.2	2	288.2
289.2	2	288.2
291.2	2	288.2
308.2	2	288.2

The results of these calculations are shown in Tables 7.1.6 and 7.1.7 and in Figure 7.1.8. Drastic effects are seen for the fundamental band (4.6 μ) and negligible effects are seen for 2.3 μ. From Figure 7.1.8 for the R7 line of the fundamental band it can be seen that an underestimate of the ground emission by 14% (as would be caused by an underestimate of the ground temperature by 4^{o}) causes a 12% overestimate in the CO density while a 12% over-

TABLE 7.1.6 EFFECT OF GROUND TEMPERATURE ON ABSORPTION

FUNDAMENTAL (4.6 μ)

		R7	P1	P8	P26
LOW TEMPERATURE	257.3	.1613	.0677	.1328	.000489
	288.2	.2500	.1030	.2117	.00104
HIGH TEMPERATURE	302.6	.1942	.0772	.1662	.00134
	288.2	.1342	.0550	.1128	.00415
INVERSION LAYER	283.2	.1270	.0521	.1063	.000433
	288.2	.1540	.0622	.1302	.000793

OVERTONE (2.3 μ)

		R7	P1	P8	P26
LOW TEMPERATURE	257.3	.00660	.00152	.00462	.0000061
	288.2	.00657	.00150	.00459	.0000053
HIGH TEMPERATURE	302.6	.00637	.00140	.00461	.0000137
	288.2	.00634	.00138	.00457	.0000122
INVERSION LAYER	283.2	.00639	.00140	.00461	.0000128
	288.2	.00635	.00139	.00458	.0000144

TABLE 7.1.7 EFFECT OF GROUND TEMPERATURE ON APPARENT ABSORPTION OF SOURCE RADIATION

FUNDAMENTAL (4.6 μ)

Tg	R7
273.2	.1337
284.2	.1866
287.2	.1971
288.2	.2002
289.2	.2033
291.2	.2091
308.2	.2428

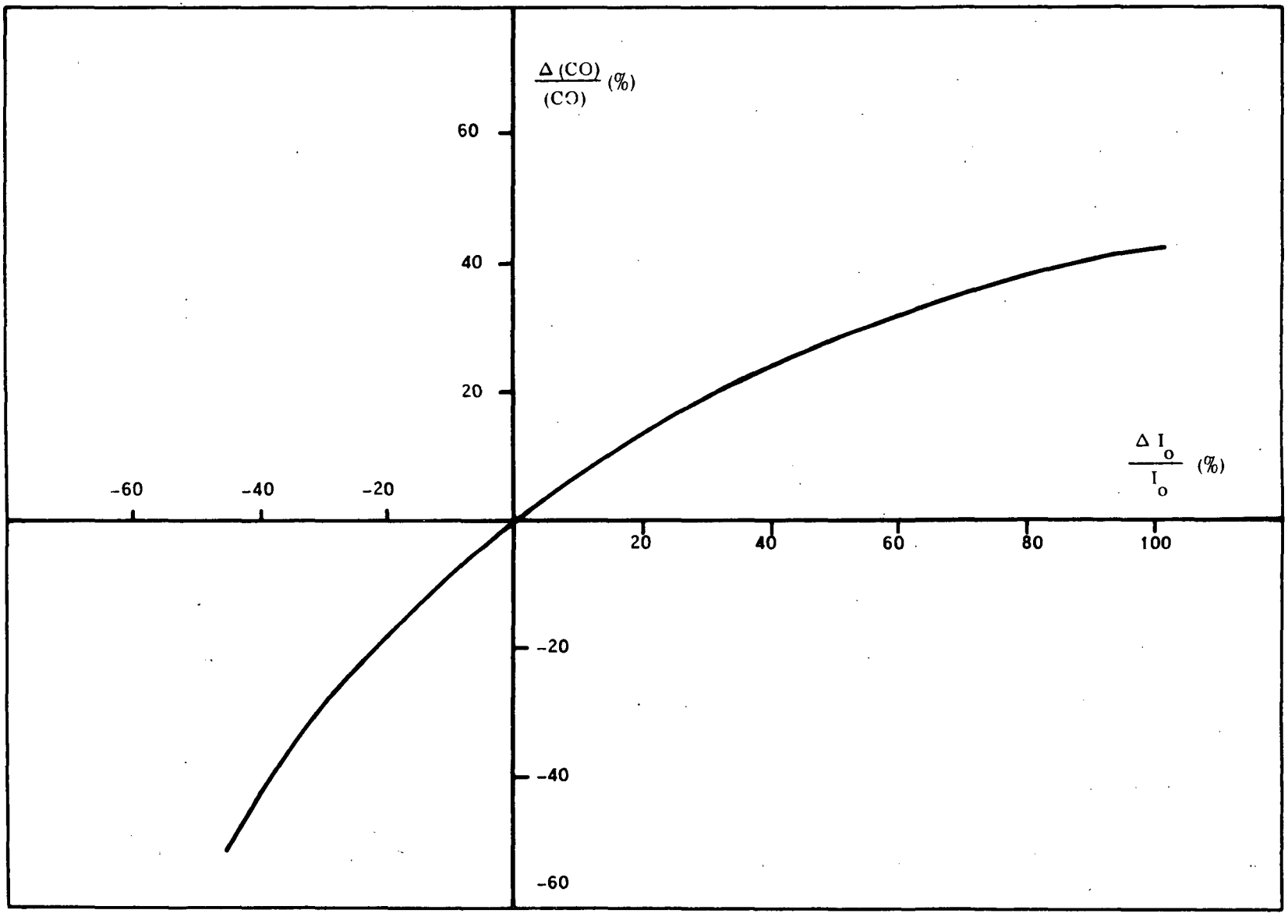

Figure 7.1.8 Effect of Change in Earth Emission Intensity on Predicted CO Density (4.6 μ - R7 Line)

estimate of the earth emission (a three degree overestimate of the ground temperature) would cause about an 8% underestimate in CO density. These calculations all used the same temperature profile (2) and the same CO profile (1), varying the earth emission. When searching for sinks which cause changes in CO density of the order of 10% such errors are larger than can be tolerated. Other lines of the fundamental show similar effects. The curve for the R7 and other lines of the overtone would lie on the abscissa showing that there is no ground intensity effect on this band.

7.1.6 Emissivity Effects: - In calculations described above, an emissivity of 1 was used. Since certain ground areas have appreciably different emissivities, calculations have been made using emissivity values of 0.95, 0.9, 0.8, and 0.7 for the 4.6 μ band and a value of 0.7 for the 2.3 μ band, with each of the four temperature models.

Drastic effects in the fractional net apparent absorption are seen by the data in Table 7.1.8 at 4.6 μ while those at 2.3 μ are negligible. Figure 7.1.8 shows that a change (ΔI_ν) in ground emissivity from 1 to .9 to .8 gives changes in measured CO density of 8% and 18%, respectively. CO density is obtained from intensity changes by use of data in Table 7.1.2.

It can be seen that atmosphere and ground temperatures and ground emissivities would have to be very accurately measured to be able to interpret any CO data obtained by remote measurements at 4.6 μ. It appears that the best expected temperature data will have an accuracy of $\pm$ 2 K (Houghton and Smith, 1970; Abel, et al, 1970a; Abel, et al, 1970b). These data would not be expected to be this accurate if an inversion layer exists. Even $\pm$ 2 K would present substantial effects at 4.6 μ. Further, the ground temperature and emissivity would have to be measured accurately and would have to be known to be that of 4.6 μ, since the emissivity may vary with wavelength.

TABLE 7.1.8 EFFECTS OF EMISSIVITY ON FRACTIONAL NET ABSORPTION FOR R7 LINES

TEMPERATURE MODEL	ϵ	4.6 μ	2.3 μ
LOW TEMPERATURE	1	.161	.00660
	0.95	.155	
	0.9	.149	
	0.8	.133	
	0.7	.113	.00657
NORMAL TEMPERATURE	1	.200	.00647
	0.95	.196	
	0.9	.191	
	0.8	.180	
	0.7	.165	.00644
NORMAL TEMPERATURE Tg = 288.2	1	.200	
	0.9	.191	
	0.7	.165	
HIGH TEMPERATURE	1	.194	.00637
	0.95	.190	
	0.9	.184	
	0.8	.172	
	0.7	.156	.00634
INVERSION LAYER	1	.127	.00639
	0.95	.119	
	0.9	.110	
	0.8	.0886	
	0.7	.0710	.00635

7.1.7 Effects of Other Parameters: - Calculations made to test the effect of reflectivity show this effect to be small for the 4.6 μ band and negligible for the 2.3 μ band. These data are given in Table 7.1.9. The effect is due to a change in source intensity with no accompanying change in atmospheric emission.

Calculations made to show the effect of Lorentz half-width on absorption. Significant effects were found for some conditions for the 4.6 μ band while the effects on the 2.3 μ band were small. Results are shown in Tables 7.1.10 and 7.1.11. This shows that the value of σ_{12}^2 in Equation 4.21 must be known to accuracies of the order of 10% for the fundamental, while for the overtone an accuracy of 50% is sufficient.

Calculations to test the effect of bandpass (the distance from the center of the line over which the absorption is integrated) were made. As expected this has an appreciable effect if too small a bandpass is taken. Data for four lines of the 4.6 and 2.3 μ bands are given in Tables 7.1.12 and 7.1.13 for bandpasses ($\nu = \nu_o$) of 20, 2, and 0.1 cm^{-1}.

7.2. Expansion of Overtone and Fundamental Bands

Using the data given in the preceeding tables, a summary may be made of the two general wavelength regions, the 2.3 μ band of the first overtone of CO and the 4.6 μ band of the fundamental of CO. All other CO bands have been found to be impractical (Bortner and Kummler, 1971).

The absorption of the 2.3 μ radiation has been found to be sufficient to produce the required sensitivities and ranges using the correlation interferometer technique for optical thicknesses appropriate to both the mapping and the limb experiments, considering nominal ambient atmospheric concentrations and reasonable fractions thereof.

The absorption of the 4.6 μ radiation is, of course, sufficient for the experiments. One difficulty arises at the higher optical thicknesses ap-

TABLE 7.1.9 EFFECT OF REFLECTIVITY ON FRACTIONAL NET APPARENT ABSORPTION

	ρ	R7
FUNDAMENTAL (4.6 μ)	0.4	.2058
	0.1	.2002
	0.02	.1986
OVERTONE (2.3 μ)	0.4	.00651
	0.1	.00647
	0.02	.00655

TABLE 7.1.10 EFFECT OF LORENTZ HALF-WIDTH ON APPARENT ABSORPTION OF FUNDAMENTAL (4.6 μ)

		R7	P1	P8	P26
STANDARD CO	.06	.2002	.0810	.1700	.0010
	.09	.2387	.0905	.2012	.0010
LOW ALTITUDE SOURCE	.06	.6620	.2974	.5695	.0167
	.09	.8052	.3555	.6921	.0178
LOW CO	.06	.0439	.0119	.0350	.0001
	.09	.0470	.0121	.0370	.0001
HIGH ALTITUDE SINK	.06	.2006	.0807	.1703	.0010
	.09	.2390	.0898	.2014	.0010

TABLE 7.1.11 EFFECT OF LORENTZ HALF-WIDTH ON ABSORPTION OVERTONE (2.3 μ)

		R7	P1	P8	P26
STANDARD CO	.06	.00647	.00144	.00462	.0000098
	.09	.00647	.00142	.00461	.0000085
LOW ALTITUDE SOURCE	.06	.1226	.0299	.0953	.000431
	.09	.1312	.0303	.1005	.000420
LOW CO	.06	.000662	.000146	.000471	.0000011
	.09	.000649	.000140	.000457	.0000006
HIGH ALTITUDE SINK	.06	.00631	.00140	.00451	.0000097
	.09	.00631	.00139	.00450	.0000083

TABLE 7.1.12 EFFECT OF BANDPASS ON FRACTIONAL NET APPARENT ABSORPTION

FUNDAMENTAL (4.6 μ)

		R7	P1	P8	P26
LOW TEMPERATURE	20	.1613	.0677	.1328	.00049
	2	.1593	.0670	.1314	.00047
	0.1	.1086	.0142	.0951	.00042
NORMAL TEMPERATURE	20	.2002	.0810	.1700	.00104
	2	.1979	.0804	.1682	.00102
	0.1	.1286	.0635	.1155	.00093
HIGH TEMPERATURE	20	.1942	.0772	.1662	.00134
	2	.1921	.0766	.1646	.00133
	0.1	.1264	.0610	.1138	.00120
INVERSION LAYER	20	.1270	.0521	.1063	.00043
	2	.1260	.0518	.1056	.00041
	0.1	.0977	.0450	.0852	.00040

TABLE 7.1.13 EFFECT OF BANDPASS ON FRACTIONAL NET APPARENT ABSORPTION

OVERTONE (2.3 μ)

		R7	P1	P8	P26
LOW TEMPERATURE	20	.00660	.00152	.00462	.0000062
	2	.00656	.00150	.00459	.0000053
	0.1	.00544	.00125	.00383	.0000053
NORMAL TEMPERATURE	20	.00647	.00144	.00462	.0000098
	2	.00643	.00143	.00459	.0000089
	0.1	.00531	.00118	.00381	.0000087
HIGH TEMPERATURE	20	.00637	.00140	.00461	.000014
	2	.00633	.00138	.00457	.000012
	0.1	.00521	.00114	.00378	.000012
INVERSION LAYER	20	.00639	.00140	.00461	.000013
	2	.00635	.00139	.00458	.000012
	0.1	.00523	.00115	.00378	.000011

propriate to the lower altitude limb measurements. Under such conditions the absorption is so strong that it is well off the linear portion of the curve-of-growth with ambient atmospheric CO concentrations resulting in a loss of sensitivity in the CO measurements.

The data show that there is considerably more error in measurement at 4.6 μ of the CO column density in the important case of a low altitude sink than for the same measurement at 2.3 μ. Since a major objective of the experiment is to search for a potential low altitude sink, this indicates a definite advantage for 2.3 μ. In the case of a temperature inversion drastic errors are found in the case of a low altitude sink. Since temperature inversions are common the 2.3 μ has another distinct advantage. In general it can be said that the 4.6 μ is greatly affected by the temperature profile. This is as expected due to contribution of atmospheric emission. The 2.3 μ radiation is essentially unaffected, as is desired. Similarly the ground temperature and the ground emissivity, have larger effects (not desired) on the CO absorption signal at 4.6μ but not at 2.3 μ.

The calculations show that, assuming measurement of CO absorption can be made on the 2.3 μ band, that band is much to be preferred over the 4.6 μ band for data interpretation. The advantages are:

1. Measurements of temperature of the atmosphere, ground temperature, and emissivity are not needed for 2.3 μ but accurate values are required for 4.6 μ.

2. The signal at 2.3 μ is affected significantly, as desired by the CO concentration in the lowest few kilometers in the atmosphere, but not significantly at 4.6 μ and in a manner very difficult to interpret.

3. The measurements at 2.3 μ are readily interpreted directly in terms of CO densities whereas those at 4.6 μ must be interpreted by use of an atmospheric model calculation at each point, assuming the required atmospheric data are available for the latter.

7.3 Comparative Calculations

Calculations given above of predicted 4.6 μ CO band transmission showed large effects caused by inversion layers, ground temperatures and emissivities, and little effect of low-altitude sinks. It was suggested to us that other calculations (Ludwig, 1970) did not show effects of such magnitude. Further calculations were made to make a reasonably direct comparison of the computational methods. Two specific comparisons were carried out. One calculation was that of the transmission of a single line, the P19 line. The second was for several lines to be compared with the results of a band model calculation.

The single-line calculation was carried out for four temperature models, shown in Table 2.1.4 as models 5, 6, 7, and 8, and a 0.2 ppm CO model. It is not known what exact temperature model was used in the calculation to which the present ones are being compared, but it is believed that it is in the range covered by these models; the authors reporting (Ludwig, 1970, p22) those calculations merely state that they used a "representative temperature model". The results of the calculations are shown in Figure 7.3.1, which plots the transmission over the line profile (The circles showing the results of Ludwig (1970), the remaining symbols being our results for the four models.). It can be seen that there is excellent agreement between the two calculations. The only visible difference is at the line

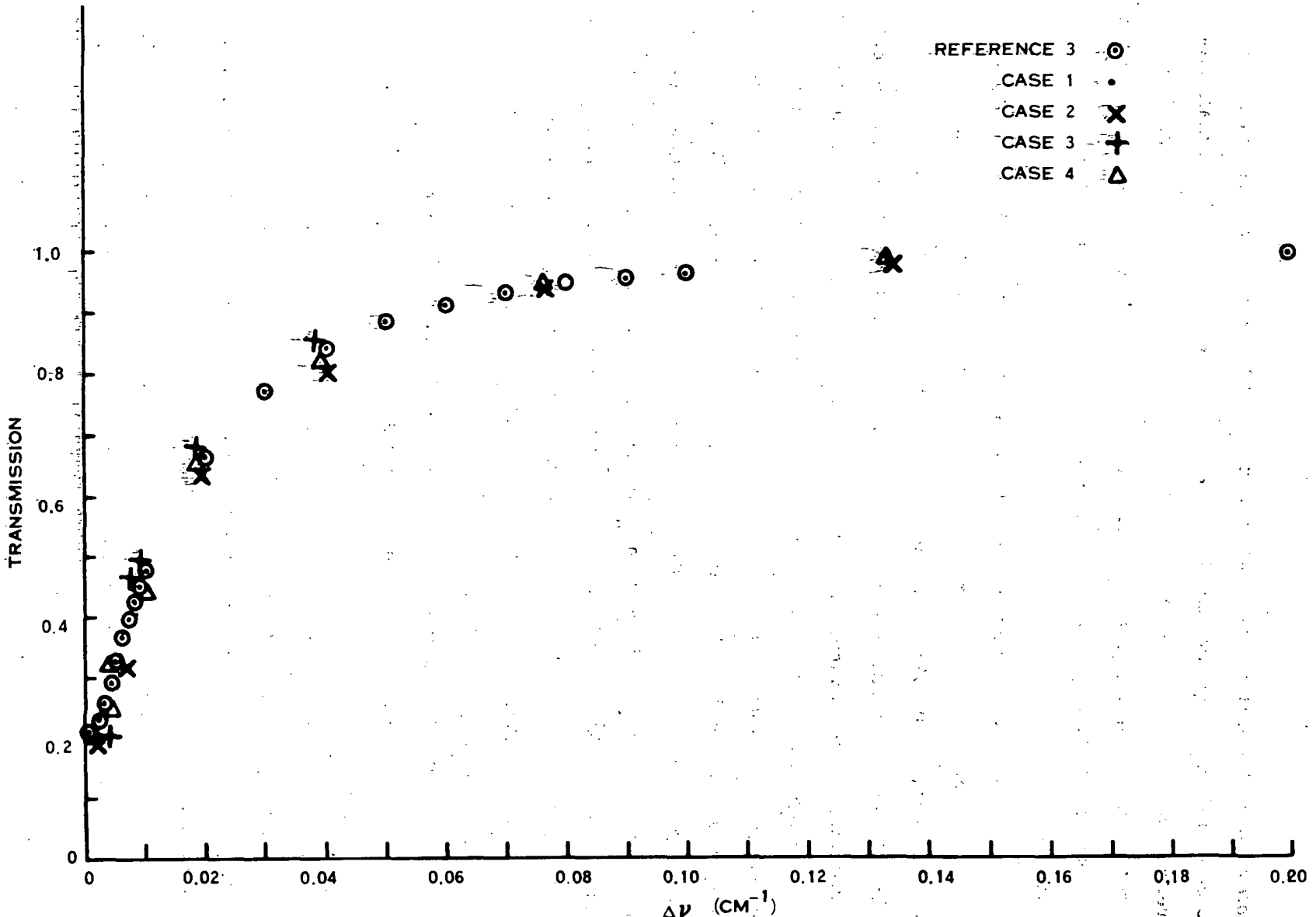

Figure 7.3.1 P19 Transmission Calculations

center where the present calculations yield a 19 to 20% transmission while the calculations being compared show a 21% transmission. This small difference may be due to differences in temperature models. From .002 cm^{-1} from the center outward, the two calculations show no appreciable difference. The integrated absorption over the line would certainly show no meaningful variation.

The other comparison which is informative is one showing the effects of a temperature inversion and of ground temperature variation. Data (Ludwig, 1970, p9) are given as models 9, 10, and 11 in Table 7.3.1. Model 10 shows the effect of a ground temperature different from the lowest atmospheric temperature, the results (Ludwig, 1970) showing a calculated signal change variation over the band of 50 and 68% for .25 and .025 ppm CO atmospheres, respectively. These can be compared with previously presented results, Table 7.1.7, of our calculations which show a 33% decrease in absorption for a single line (R7) of the same band. Model 11 shows the effect of a temperature inversion layer giving variations of signal change over the band of 42 and 55% for the .25 and .025 ppm CO atmospheres, respectively (Ludwig, 1970). These may be compared with our results, Table 7.1.5, showing changes of 37, 36, 37, and 76% for the R7, P1, P8, and P26 lines of that band, respectively.

For one case of interest, a low altitude sink model, Table 7.1.4., no data were given on the other calculations (Ludwig, 1970) to compare with ours.

It can also be noted that a graphical representation of the effect of ground temperature differences on CO calculations, Table 7.1.8., can be roughly compared to those of Ludwig (1970, p16) and seen to give reasonable agreement.

It can be concluded that the two programs give the same results, at least as nearly as we can determine with available information.

TABLE 7.3.1 TEMPERATURE MODELS AND RESULTS FOR COMPARISON BAND CALCULATIONS

Model	9	10	11	Reference
Signal Change				
.25 ppm CO	7.14	3.59	4.16	a
.025 ppm CO	1.35	0.43	0.61	a
Relative Signal Change				
.25 ppm CO	1	0.50	0.58	a
.1 ppm CO	1	0.33	0.46	b
.025 ppm CO	1	0.32	0.45	a

a) Ludwig (1970)

b) This work (Tables 7.1.7 and 7.1.8)

7.4 Limb Inversion Analysis

The limb experiment has been analyzed for the effects of instrumental error on the inversion of the instrument values of total CO in the path to yield CO concentration vs altitude. The calculations have been performed for the three CO sink models to which the limb experiment is relevant. These are the constant mixing ratio model with 0.1 ppm at ground level, the upper atmosphere sink, and the low-level sink with maximum concentration at 9 km. The error sources, which have been introduced, include a random error with standard deviation of 2%, 5%, or 10% and systematic errors of ± 2%, ± 5%, or ± 10%.

For these calculations the atmosphere below an altitude, h_1, was divided into n spherical shells (j = 1, 2, ---n), a distance, Δh, apart (Figure 7.4.1). The atmospheric properties within a shell are assumed to be constant. The altitude of the first shell is given by

$$h_1 = n \Delta h,$$

and the altitude of the jth shell is

$$h_j = h_1 - (j-1) \Delta h$$

The ith ray from the sun to the instrument passes horizontally through the lower edge of the ith shell (j = i). The height of this ray is

$$h_{ii} = h_i - \Delta h$$

The rays passing through the shells can be divided into lengths, a_{ij}, over which the atmospheric properties are assumed to be constant. The lengths a_{ij} are given by:

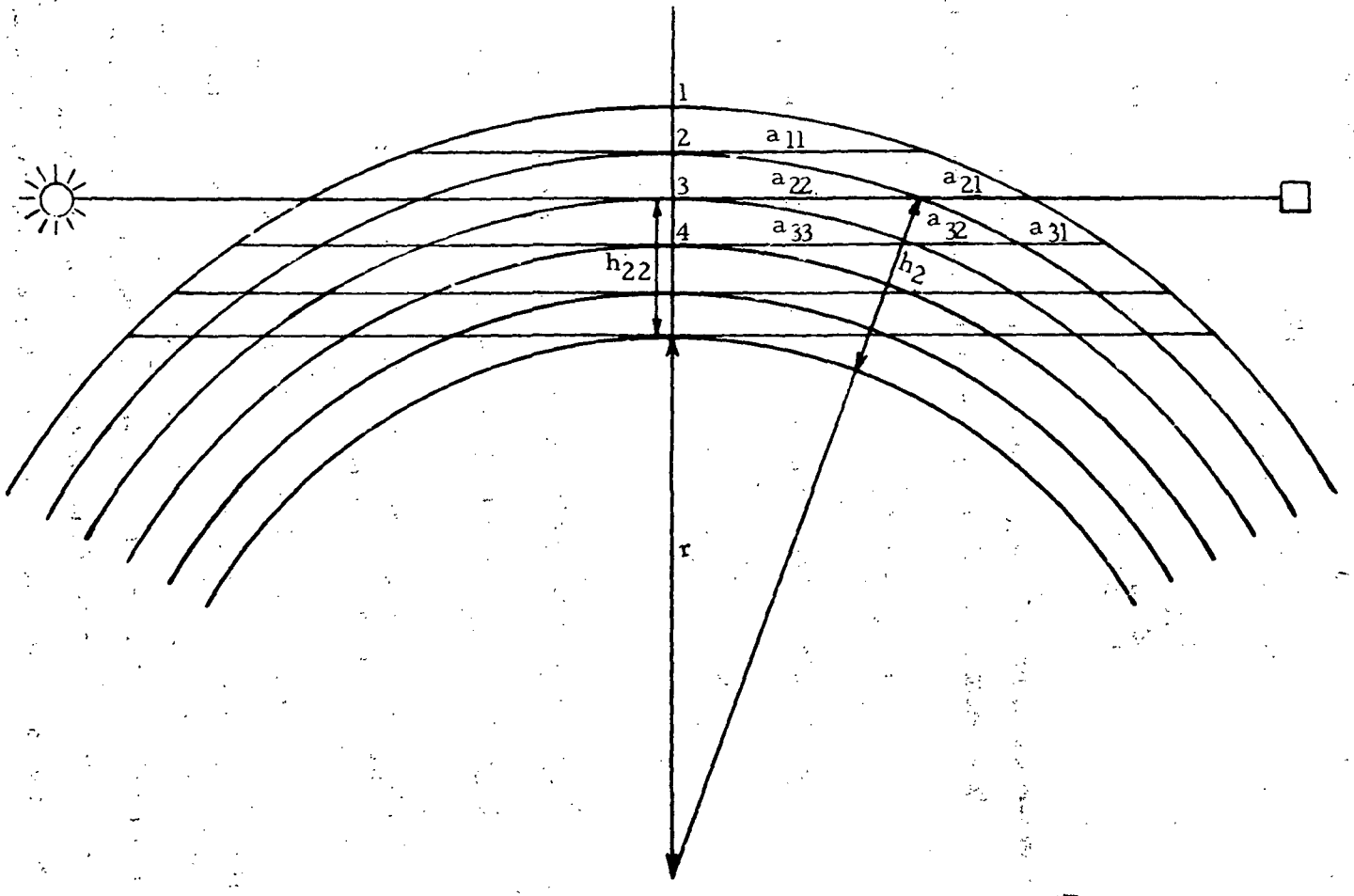

Figure 7.4.1 Shell Model for Limb Inversion Analysis

$$a_{ij} = \left\{(r + h_j)^2 - (r + h_{ii})^2\right\}^{1/2} \qquad \text{if } i = j$$

$$a_{ij} = \left\{(r + h_j)^2 - (r + h_{ii})^2\right\}^{1/2} - \sum_{k=j+1}^{k=i} a_{ik} \qquad \text{if } i \pm j$$

A square matrix (n x n) of the elements a_{ij} can be formed.

In a shell j, the average concentration of CO is given by:

$$c_j = c(h_j - 1/2\,\Delta h)$$

The integrated amount of gas in a horizontal path is given by:

$$\{u_i\} = 2\{c_j\}\,[a_{ij}]$$

where

$\{u_i\}$ ≡ column matrix of integrated amount of CO

$\{c_j\}$ = column matrix of the average concentration of CO

$[a_{ij}]$ = square matrix of path length elements within the shells.

The calculations were carried out with a 40 shell atmospheric model with a 2 km distance between shells. The matrix elements u_i were calculated for the three CO models in Figure 7.4.2 (Models 1, 4, and 5 of Figure 2.1.1 and Table 2.1.1). The correlation interferometer gives an instrument output which is proportional to the total CO in the path, or u_i. In this case the known parameters will be u as a function of altitude, and the

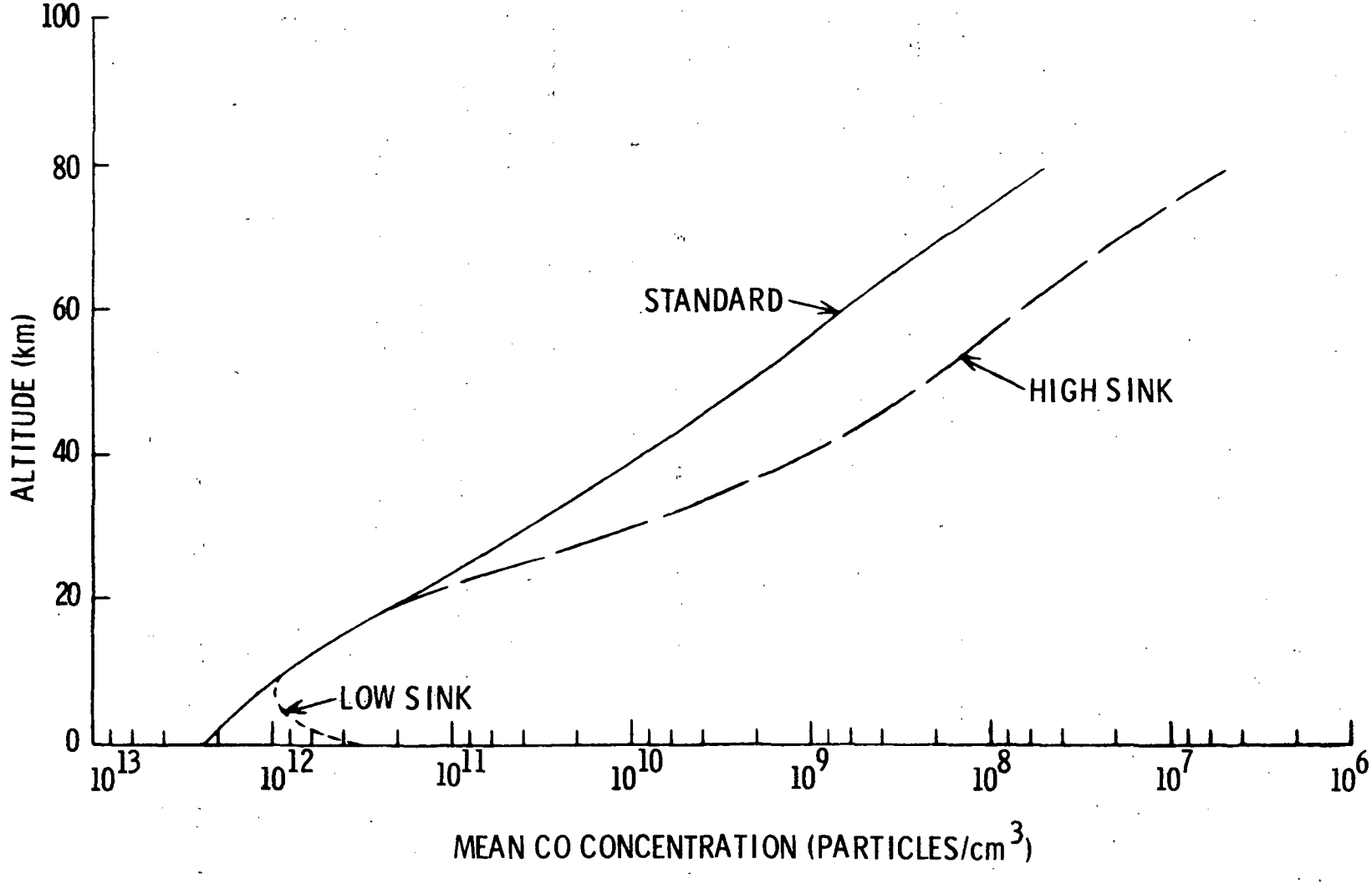

Figure 7.4.2 CO Concentration Models

a_{ij} elements will be known. A set of equations can then be set up to solve for the concentrations c_i.

$$\{c_i\} = 1/2\{u_j\}\left[a_{ij}\right]^{-1}$$

where $\left[a_{ij}\right]^{-1}$ is the inverted matrix $\left[a_{ij}\right]$.

To test for the effects of random or systematic instrument errors, the values of u were computed for each of the three concentration models from the relation $\{u_i\} = 2\{c_j\}\left[a_{ij}\right]$. These values are shown in Figure 7.4.3. The computed values were then changed by fixed amounts

a) random error with 2%, 5%, or 10% standard deviation.

b) systematic error of ± 2%, ± 5%, or ± 10%.

For each of these types of errors, the concentration profile was calculated and compared with the exact profile used as the original input. The results of the calculations are shown in Figures 7.4.4 and 7.4.5 and in Tables 7.4.1, 7.4.2, and 7.4.3.

Figure 7.4.4 shows the result of imposing random errors with standard deviations of 5% and 10% on the measurements of u. With measurement errors of this magnitude the computations show that it is possible to distinguish the carbon monoxide constant mixing ratio concentration profile from the concentration profile which assumes a high altitude sink. The computations with a 2% random error show the same result with a much smaller error. These data were not plotted to avoid cluttering the graph with too many points. The data are tabulated in Tables 7.4.1, 7.4.2, and 7.4.3 for the 2% random error calculations.

Figure 7.4.5 shows the result of performing the data inversion to obtain the concentration profile, when the instrument measurement of the

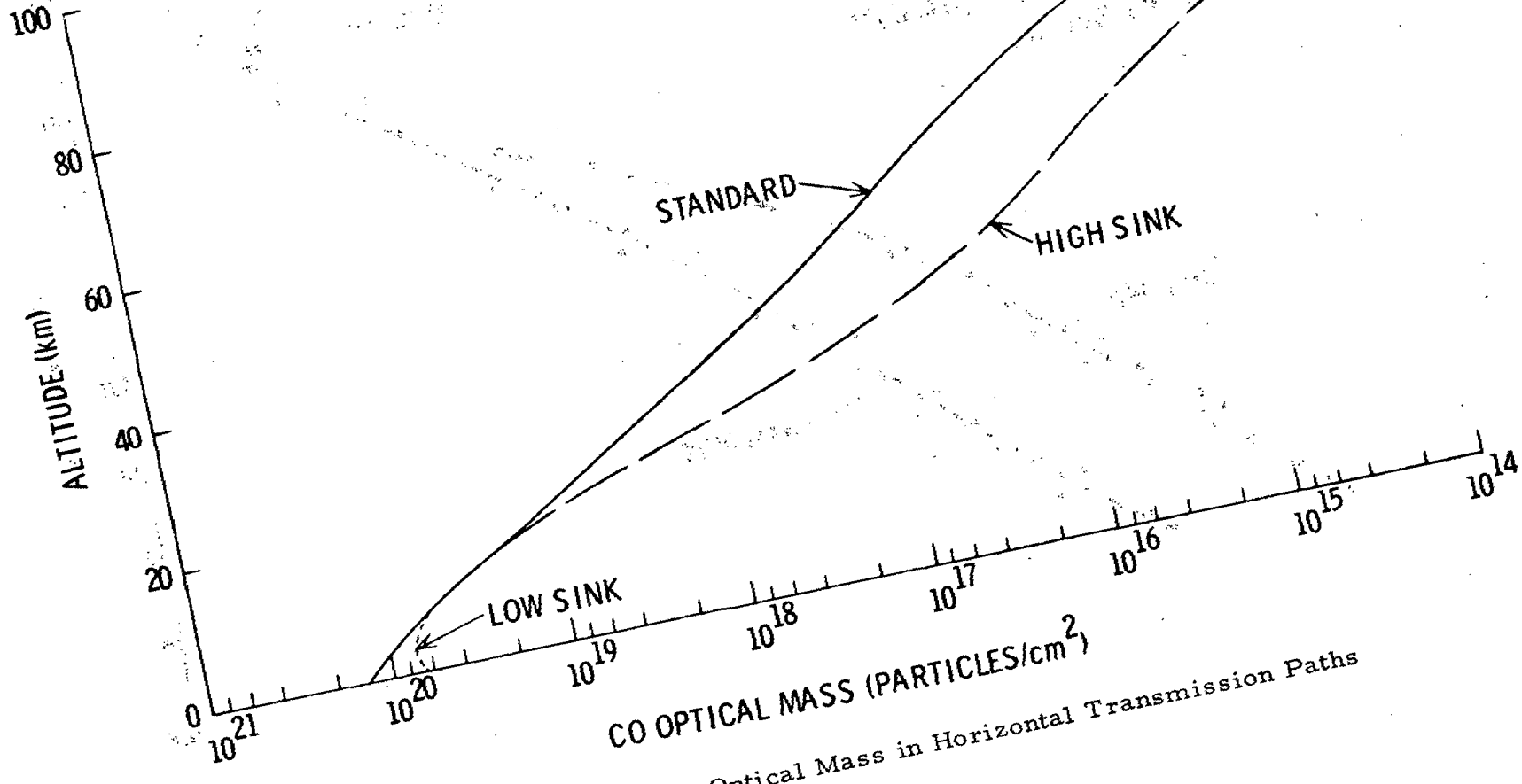

Figure 7.4.3 CO Optical Mass in Horizontal Transmission Paths

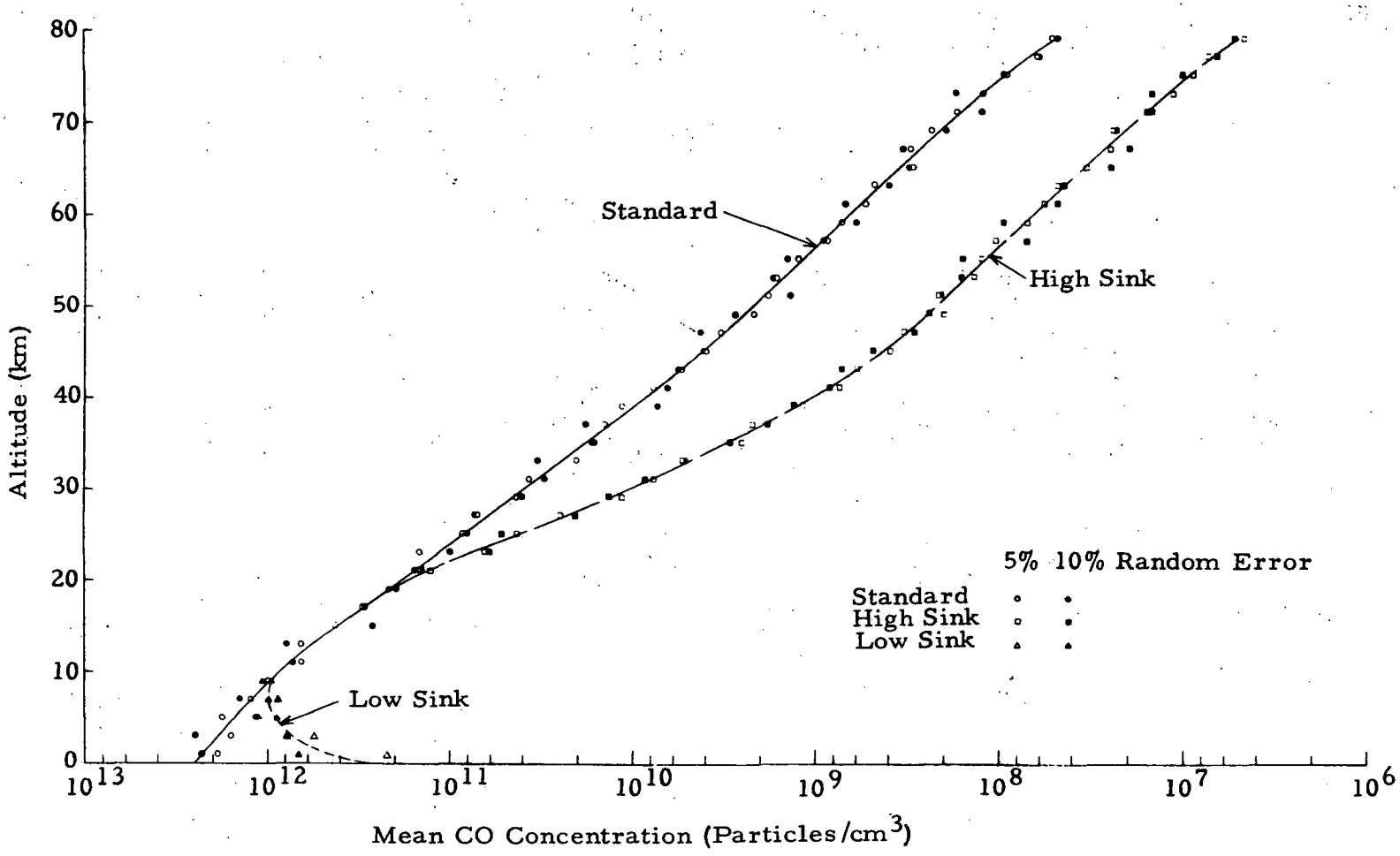

Figure 7.4.4 Computed Atmospheric CO Concentrations with Simulated Instrument Error

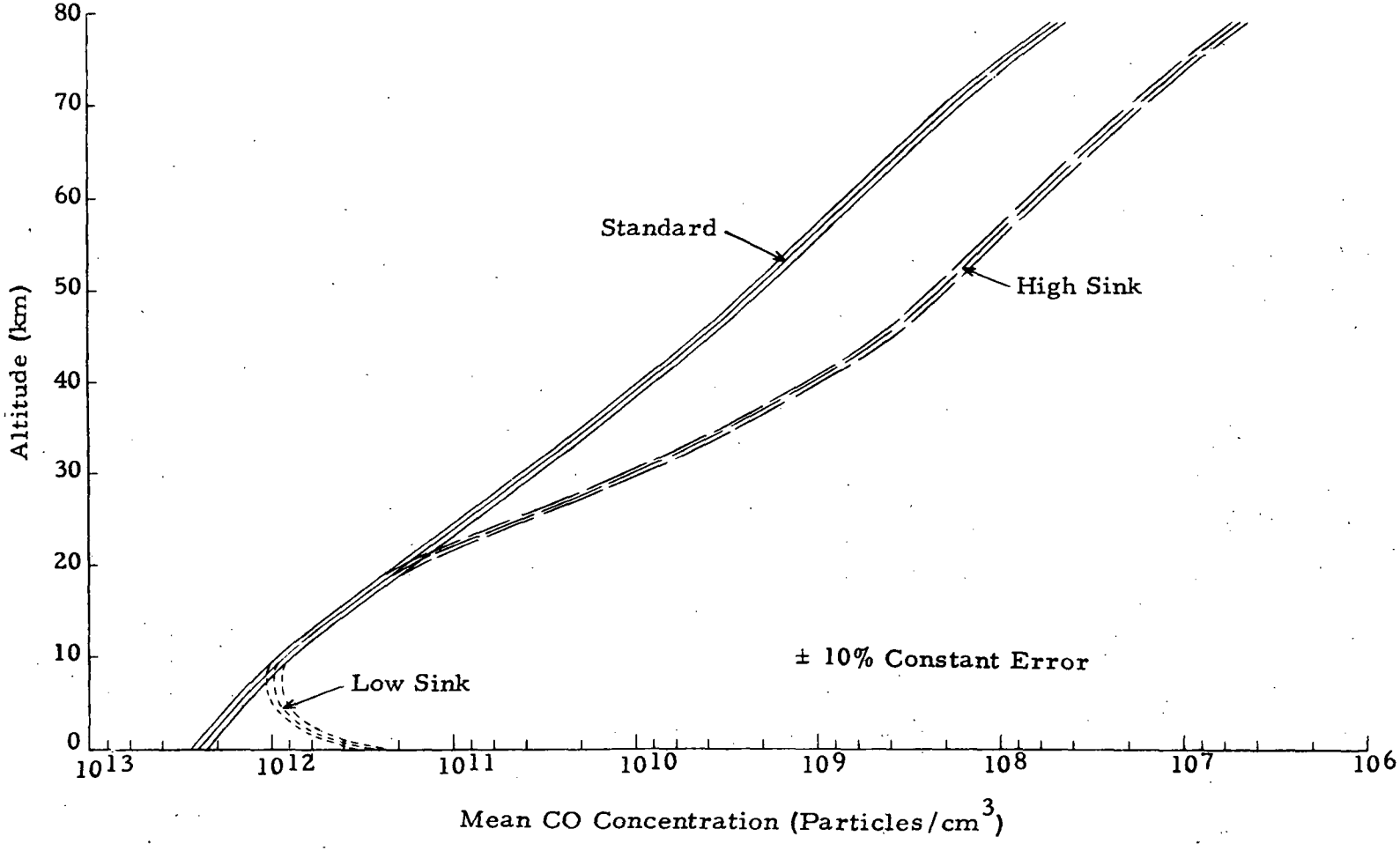

Figure 7.4.5 Computed Atmospheric CO Concentrations with Simulated Instrument Error

TABLE 7.4.1 LIMB TRANSMISSION ANALYSIS FOR STANDARD CO CONCENTRATION MODEL

Altitude (km)	Shell No.	No Error Mean CO Conc. (Part./cm^3)	2% Random Mean CO Conc. (Part./cm^3)	+5% Constant Mean CO Conc. (Part./cm^3)
78.0	40.0	4.885E+07	4.886E+07	5.129E+07
76.0	39.0	6.673E+07	6.606E+07	7.007E+07
74.0	38.0	9.014E+07	9.878E+07	9.465E+07
72.0	37.0	1.203E+08	1.195E+08	1.263E+08
70.0	36.0	1.590E+08	1.626E+08	1.670E+08
68.0	35.0	2.079E+08	2.017E+08	2.133E+08
66.0	34.0	2.695E+08	2.655E+08	2.830E+08
64.0	33.0	3.465E+08	3.423E+08	3.638E+08
62.0	32.0	4.420E+08	4.250E+08	4.641E+08
60.0	31.0	5.620E+08	6.040E+08	5.901E+08
58.0	30.0	7.195E+08	7.108E+08	7.554E+08
56.0	29.0	9.172E+08	9.382E+08	9.631E+08
54.0	28.0	1.166E+09	1.146E+09	1.224E+09
52.0	27.0	1.477E+09	1.536E+09	1.551E+09
50.0	26.0	1.887E+09	1.796E+09	1.982E+09
48.0	25.0	2.417E+09	2.383E+09	2.538E+09
46.0	24.0	3.111E+09	3.051E+09	3.266E+09
44.0	23.0	4.089E+09	4.031E+09	4.293E+09
42.0	22.0	5.402E+09	5.176E+09	5.673E+09
40.0	21.0	7.189E+09	7.765E+09	7.548E+09
38.0	20.0	9.620E+09	1.012E+10	1.010E+10
36.0	19.0	1.296E+10	1.294E+10	1.361E+10
34.0	18.0	1.760E+10	1.809E+10	1.848E+10
32.0	17.0	2.405E+10	2.266E+10	2.525E+10
30.0	16.0	3.283E+10	3.317E+10	3.447E+10
28.0	15.0	4.466E+10	4.292E+10	4.690E+10
26.0	14.0	6.094E+10	6.080E+10	6.399E+10
24.0	13.0	8.335E+10	8.282E+10	8.752E+10
22.0	12.0	1.144E+11	1.142E+11	1.201E+11
20.0	11.0	1.574E+11	1.579E+11	1.653E+11
18.0	10.0	2.163E+11	2.334E+11	2.271E+11
16.0	9.0	2.958E+11	2.874E+11	3.106E+11
14.0	8.0	4.050E+11	4.192E+11	4.252E+11
12.0	7.0	5.542E+11	5.706E+11	5.819E+11
10.0	6.0	7.586E+11	7.687E+11	7.965E+11
8.0	5.0	9.711E+11	9.867E+11	1.020E+12
6.0	4.0	1.227E+12	1.205E+12	1.288E+12
4.0	3.0	1.531E+12	1.522E+12	1.608E+12
2.0	2.0	1.891E+12	1.902E+12	1.986E+12
0.	1.0	2.312E+12	2.414E+12	2.428E+12

TABLE 7.4.2 LIMB TRANSMISSION ANALYSIS FOR UPPER ATMOSPHERE SINK CO CONCENTRATION MODEL

Altitude (km)	Shell No.	No Error Mean CO Conc. (Part./cm^3)	2% Random Mean CO Conc. (Part./cm^3)	+5% Constant Mean CO Conc. (Part./cm^3)
78.0	40.0	4.885E+06	4.951E+06	5.129E+06
76.0	39.0	6.673E+06	6.449E+06	7.007E+06
74.0	38.0	9.014E+06	9.025E+06	9.465E+06
72.0	37.0	1.203E+07	1.254E+07	1.263E+07
70.0	36.0	1.590E+07	1.591E+07	1.670E+07
68.0	35.0	2.079E+07	2.125E+07	2.183E+07
66.0	34.0	2.695E+07	2.803E+07	2.830E+07
64.0	33.0	3.465E+07	3.254E+07	3.638E+07
62.0	32.0	4.420E+07	4.623E+07	4.641E+07
60.0	31.0	5.620E+07	5.591E+07	5.901E+07
58.0	30.0	7.195E+07	6.857E+07	7.554E+07
56.0	29.0	9.172E+07	8.751E+07	9.631E+07
54.0	28.0	1.166E+08	1.225E+08	1.224E+08
52.0	27.0	1.477E+08	1.496E+08	1.551E+08
50.0	26.0	1.887E+08	1.968E+08	1.982E+08
48.0	25.0	2.417E+08	2.387E+08	2.538E+08
46.0	24.0	3.111E+08	3.098E+08	3.266E+08
44.0	23.0	4.089E+08	3.993E+08	4.293E+08
42.0	22.0	5.799E+08	5.751E+08	6.089E+08
40.0	21.0	8.401E+08	8.016E+08	8.821E+08
38.0	20.0	1.240E+09	1.208E+09	1.302E+09
36.0	19.0	1.881E+09	1.878E+09	1.975E+09
34.0	18.0	2.930E+09	2.931E+09	3.076E+09
32.0	17.0	4.651E+09	4.734E+09	4.884E+09
30.0	16.0	7.598E+09	7.715E+09	7.978E+09
28.0	15.0	1.290E+10	1.203E+10	1.354E+10
26.0	14.0	2.319E+10	2.263E+10	2.435E+10
24.0	13.0	4.162E+10	4.227E+10	4.370E+10
22.0	12.0	7.450E+10	7.220E+10	7.822E+10
20.0	11.0	1.320E+11	1.308E+11	1.386E+11
18.0	10.0	2.163E+11	2.163E+11	2.271E+11
16.0	9.0	2.958E+11	2.871E+11	3.106E+11
14.0	8.0	4.049E+11	4.173E+11	4.252E+11
12.0	7.0	5.543E+11	5.271E+11	5.820E+11
10.0	6.0	7.586E+11	7.982E+11	7.965E+11
8.0	5.0	9.710E+11	9.347E+11	1.020E+12
6.0	4.0	1.227E+12	1.172E+12	1.288E+12
4.0	3.0	1.531E+12	1.521E+12	1.608E+12
2.0	2.0	1.889E+12	1.891E+12	1.984E+12
0.	1.0	2.313E+12	2.212E+12	2.426E+12

TABLE 7.4.3 LIMB TRANSMISSION ANALYSIS FOR LOW LEVEL SINK CO CONCENTRATION MODEL

Altitude (km)	Shell No.	No Error Mean CO Conc. (Part./cm^3)	2% Random Mean CO Conc. (Part./cm^3)	+5% Constant Mean CO Conc. (Part./cm^3)
78.0	40.0	4.885E+07	4.886E+07	5.129E+07
76.0	39.0	6.673E+07	6.606E+07	7.007E+07
74.0	38.0	9.014E+07	9.878E+07	9.465E+07
72.0	37.0	1.203E+08	1.105E+08	1.263E+08
70.0	36.0	1.590E+08	1.626E+08	1.670E+08
68.0	35.0	2.079E+08	2.017E+08	2.183E+08
66.0	34.0	2.695E+08	2.655E+08	2.830E+08
64.0	33.0	3.465E+08	3.423E+08	3.638E+08
62.0	32.0	4.420E+08	4.250E+08	4.641E+08
60.0	31.0	5.620E+08	6.040E+08	5.901E+08
58.0	30.0	7.195E+08	7.108E+08	7.554E+08
56.0	29.0	9.172E+08	9.382E+08	9.631E+08
54.0	28.0	1.166E+09	1.146E+09	1.224E+09
52.0	27.0	1.477E+09	1.536E+09	1.551E+09
50.0	26.0	1.887E+09	1.796E+09	1.982E+09
48.0	25.0	2.417E+09	2.383E+09	2.538E+09
46.0	24.0	3.111E+09	3.051E+09	3.266E+09
44.0	23.0	4.089E+09	4.031E+09	4.293E+09
42.0	22.0	5.402E+09	5.176E+09	5.673E+09
40.0	21.0	7.189E+09	7.765E+09	7.548E+09
38.0	20.0	9.620E+09	1.012E+10	1.010E+10
36.0	19.0	1.296E+10	1.294E+10	1.361E+10
34.0	18.0	1.760E+10	1.809E+10	1.848E+10
32.0	17.0	2.405E+10	2.266E+10	2.525E+10
30.0	16.0	3.283E+10	3.317E+10	3.447E+10
28.0	15.0	4.466E+10	4.292E+10	4.690E+10
26.0	14.0	6.094E+10	6.080E+10	6.399E+10
24.0	13.0	8.335E+10	8.282E+10	8.752E+10
22.0	12.0	1.144E+11	1.142E+11	1.201E+11
20.0	11.0	1.574E+11	1.579E+11	1.653E+11
18.0	10.0	2.163E+11	2.334E+11	2.271E+11
16.0	9.0	2.958E+11	2.874E+11	3.106E+11
14.0	8.0	4.050E+11	4.192E+11	4.252E+11
12.0	7.0	5.542E+11	5.706E+11	5.819E+11
10.0	6.0	7.586E+11	7.687E+11	7.965E+11
8.0	5.0	9.711E+11	9.867E+11	1.020E+12
6.0	4.0	9.839E+11	9.620E+11	1.033E+12
4.0	3.0	9.180E+11	9.094E+11	9.639E+11
2.0	2.0	7.559E+11	7.611E+11	7.937E+11
0.	1.0	4.621E+11	5.051E+11	4.852E+11

total CO in the path is high or low by a fixed percentage. The effects of a systematic error of ± 10% are shown in Figure 7.4.5. The computed concentration profile deviates from that computed with no systematic error by the same ± 10% as is present in the instrument measurement of the total CO. Similarly, the computations with systematic errors of ± 2% and ± 5% yield calculated concentration profiles which are in error by ± 2% and ± 5%, respectively.

The computations indicate that instrumental errors of the order of 10% in the measurement of the total CO in the horizontal sight path through the atmosphere do not result in significantly larger errors in the computed CO concentration profile at high altitudes. While the measurement errors are more significant in the case where an inversion in the CO concentration profile occurs (i.e. the low-level sink), they do not invalidate the limb transmission experiment at the higher altitudes. The limb experiment was primarily intended for searching for an upper atmosphere sink, and in this case the effects of reasonable measurement errors are not of sufficient magnitude to permit the upper atmosphere sink profile to be mistaken for the standard constant mixing ratio CO profile.

7.5 Multi-line Model Calculations

7.5.1 The Program: - The first step in the theoretical determination of the feasability of using the correlation interferometric technique for the measurement of CO levels in the atmosphere is the computation of theoretical transmission spectra of the atmosphere in the wavelength regions of interest. Theoretical spectra were calculated by a fairly elaborate computer program, developed by GE. This program has been described in greater detail by Alyea and Liebling elsewhere (Bortner, Grenda, et al, 1971) and will be described only very briefly here. The computer program has the capability of calculating atmospheric transmission spectra for up to three atmospheric constitu-

ents, with a total of up to 150 absorption lines, for three different viewing geometries:

1. Ground black-body radiation including atmospheric absorption and emission.
2. Solar radiation reflected from the ground including atmospheric absorption only.
3. Limb transmission of solar radiation including absorption and emission.

Based on input molecular and atmospheric properties, the Voight profile function, absorption and emission coefficients are computed as a function of altitude for all lines which contribute at a given frequency value. Effects of overlapping lines are considered up to ± 5 cm^{-1}. These coefficients are then integrated in accordance with the basic radiative transfer equation described in Section 4 to produce observed spectra.

Additional subroutines, patterned after Cooley (1965) and Gentleman (1966) then computes the Fourier transforms of the resultant spectra. These Fourier transforms which are closely related to interferograms form the data base for the theoretical feasibility study.

This computer program was used to generate a large number of theoretical spectra and transforms of CO in the presence of H_2O. Spectra were generated in the 2.3 μ spectral region (using geometry case 2) and in the 4.6 μ region (using geometry case 1). The regions covered were 4230 - 4330 cm^{-1} and 2100 - 2200 cm^{-1}, respectively. Spectra included combinations of CO models 1, 2, 3, and 6; H_2O models 1, 2, and 3; temperature models 1, 2, 3, and 4, as described in Section 2. Ground emissivity was varied in the 4.6 μ spectra, and albedo was varied in the 2.3 μ spectra. In all, 53 theoretical spectra and transforms were computed at 2.3 μ, and 19 at 4.6 μ. Although there are many additional combinations which would have

been desirable, extremely long running time of the program (about 10 - 15 minutes on a GE 635 or IBM 360) makes a full gamut of combinations prohibitively costly.

Following generation of these theoretical Fourier transforms, analyses were performed by use of a weighting function computer program. This program, patterned after a program furnished by Barringer Research‡ is an implementation of the weighting function concept described in detail in Section 6.

The weighting function can be considered a correlation function which, when multiplied by the Fourier transform of a spectrum gives a measurement of the CO level. Inputs to the weighting function program consist of a basic set of several Fourier transforms of spectra generated from a constant amount of CO and various combinations of other variables, e.g. temperature profile, H_2O level, etc. One of these transforms is designated as the nominal case. One additional transform is input, designated the target case, which is identical to the nominal case with the exception of a variation in the CO level. The weighting function generated from these cases is then applied to other transforms which were not included in the basic set. It is this operation of generating weighting functions from one set of data and applying them to another set which determines the feasibility of the correlation operation.

The theoretical spectra Fourier transforms described above were used in various combinations as basic sets for the weighting function program. Two groups of studies were made, at 2.3 μ and 4.6 μ. The results of these studies are described below.

Calculations were made using the principles outlined in Sections 5 and 6. The intent of these calculations is to determine the sensitivity of the method in the determination of CO densities, the accuracy to be expected in

‡ The program was written by G. Levy of BRL.

the measurements, the effects of various atmospheric parameters, the optimum wavelength region to be used, and in general, to establish the feasibility of the technique in obtaining the data needed to determine the CO sink.

While the theoretical feasibility studies will be necessary, the establishment of the feasibility will only be accomplished after the instrument is shown to be capable of measuring CO in the atmosphere. Thus, tests of the breadboard will be made on CO and atmospheric gases to see if CO can be measured in amounts similar to those in the atmosphere together with amounts of some interferents which, where possible, are similar to those of the atmosphere. This is not an attempt at simulation but an attempt to see if CO can be measured with the breadboard and to investigate the signal-to-noise ratio, under these conditions. Tests in urban polluted atmosphere will also be used to compare breadboard measurements with those of other methods.

7.5.2 Calculations: -

7.5.2.1 Explanation of Calculations: - The results are presented in tables later. It must be remembered in examining the results that the object of this work is to find the CO sink. Thus, it is important to be able to see an effect produced by a rather small variation from normal CO column density, since, although at ground level the concentration may drop off by a large factor, the total column density may only have small drops, as little as about 10%. Further non-sink areas should not appear as sinks and the accuracy for very low CO column density may be poor, as long as it is good enough to show it to be less than the normal atmospheric amount. It must be emphasized that the most accurate measurements are needed at densities near those of a normal CO profile.

Further the results should not be affected significantly by variations in atmospheric or ground properties, e.g. atmospheric temperature profile, temperature inversion layer, ground temperature, ground emissivity, reflectivity, and the shape of the CO profile.

One of the objectives of this work is to establish the types of conditions of the runs to be used in determining the weighting functions. Thus we are looking for the case giving the best results in terms of the considerations noted above.

The calculated accuracy of the calculations are dependent on the conditions which were used for determining the weighting functions. The results which are presented in the following tables will show this. Each table, noted by a letter designating the case, gives the results for all interferograms, using a specified set of interferograms to determine the weighting functions and then using these weighting functions to determine the CO density in all the interferograms. The band (wavelength) is given together with the conditions for each run.

Tables 7.5.1 through 7.5.21 give the results. Each table gives the percentage difference of the calculated value from the actual amount of CO in the model. The three-right hand columns give data on this model, and are for all cases between the heavy lines. The eight CO model numbers are those of Tables 2.1.1 and Figure 2.1.1. The number in the far right column is the number by which the concentrations of the models (over the entire altitude range) are multiplied. The resulting total optical thickness in atmosphere-centimeters is noted. Five water models were used. Models W1, W2, and W3 correspond to water models 1, 2, and 3 of Table 2.1.2 and Figure 2.1.5; that noted as 4W1 is that where water concentrations are four times those of water model 1 at all altitudes; that noted as 1.5W2 is that where water concentrations are 1.5 times those of water model 2. The column headings note the four corresponding temperature models of Table 2.1.3 and Figure 2.1.6.

Each sheet presents the results using a specific set of runs to obtain the weighting functions and gives the accuracy of the calculated CO for each interferogram of either the 2.3 or 4.6 μ band as noted. The sets

TABLE 7.5.1 CASE A

$\lambda = 2.3\ \mu$		T_1	T_2	T_3	T_4		CO ATM - CM	CO MODEL	MULTI-PLIER	RELATIVE CO
	W3	164.3		295.1						
1.5	W2			205.3			0.0162	3		0.1
	W2	69.8		177.6						
4	W1	-157.8	83.8	170.2						
	W1	[2.8]		69.1						
	W3			132.9						
1.5	W2						0.0324	3	2	0.2
	W2	31.5		80.7						
4	W1									
	W1	1.9		32.1						
	W3	42.7								
1.5	W2						0.0486	3	3	0.3
	W2									
4	W1	-53.6	22.8	48.8						
	W1			52.4*						
	W3			4.2						
1.5	W2						0.1468	6		0.9
	W2	1.5		3.3						
4	W1									
	W1	0.9		1.9						
	W3	[0.0]		[0.0]						
1.5	W2			-3.6			0.1618	1		1
	W2	[0.0]	5.7	[0.0]	0.3					
4	W1	-18.5	0.5	5.4						
	W1	[0.0]		[0.0]						
	W3			-11.8						
1.5	W2						0.2426	1	1.5	1.5
	W2	-4.0		-7.7						
4	W1									
	W1	-1.5		-3.8						
	W3			-55.1						
1.5	W2						4.3376	2		27
	W2	-39.6		-48.0						
4	W1									
	W1	-34.4		-40.6						
	W3			-56.2						
1.5	W2						4.7696	2	1.1	30
	W2	-41.6		-49.3						
4	W1									
	W1	-36.0		-42.1						

*1.5 W 1

TABLE 7.5.2 CASE B

λ = 2.3 μ		T_1	T_2	T_3	T_4		CO ATM - CM	CO MODEL	MULTI-PLIER
	W3	-100.9		2.7					
1.5	W2			-100.4			0.0162	3	
	W2	-178.8		-93.4					
4	W1	-453.6	-142.6	-36.0					
	W1	-221.7		-148.8					
	W3			3.6					
1.5	W2						0.0324	3	2
	W2	-78.7		-39.0					
4	W1								
	W1	-97.6		-64.3					
	W3	-25.6							
1.5	W2						0.0486	3	3
	W2								
4	W1	-134.3	-34.3	-1.4					
	W1			-27.7*					
	W3			1.3					
1.5	W2						0.1488	6	
	W2	-1.0		0.7					
4	W1								
	W1	-1.4		-0.3					
	W3	0.0		0.0					
1.5	W2			-5.8			0.1618	1	
	W2	-0.0	8.0	0.0	0.8				
4	W1	-24.5	2.0	9.4					
	W1	-0.0		0.0					
	W3			-1.5					
1.5	W2						0.2426	1	1.5
	W2	4.8		1.8					
4	W1								
	W1	6.4		3.9					
	W3			-37.1					
1.5	W2						4.3376	2	
	W2	-23.3		-31.2					
4	W1								
	W1	-19.3		-26.6					
	W3			-38.7					
1.5	W2						4.7696	2	1.1
	W2	-25.2		-32.9					
4	W1								
	W1	-21.2		-28.3					

*1.5 W 1

TABLE 7.5.3 CASE C

$\lambda = 2.3\ \mu$		T_1	T_2	T_3	T_4		CO ATM - CM	CO MODEL	MULTI-PLIER
	W3	151.2		263.5					
1.5	W2			229.9			0.0162	3	
	W2	64.2		151.2					
4	W1	-149.8	0.4	50.9					
	W1	2.8		64.1					
	W3			119.3					
1.5	W2						0.0324	3	2
	W2	29.1		69.7					
4	W1								
	W1	1.9		29.9					
	W3	39.4							
1.5	W2						0.0486	3	3
	W2								
4	W1	-50.8	-4.4	10.2					
	W1			62.8*					
	W3			4.0					
1.5	W2						0.1488	6	
	W2	1.4		3.1					
4	W1								
	W1	0.9		1.8					
	W3	0.0		0.0					
1.5	W2			1.8			0.1618	1	
	W2	0.0	0.0	0.0	0.0				
4	W1	-17.6	-6.9	-5.0					
	W1	0.0		0.0					
	W3			-10.7					
1.5	W2						0.2426	1	1.5
	W2	-3.9		-6.8					
4	W1								
	W1	-1.5		-3.7					
	W3			-55.3					
1.5	W2						4.3376	2	
	W2	-40.5		-49.2					
4	W1								
	W1	-35.0		-41.1					
	W3			-56.6					
1.5	W2						4.7696	2	1.1
	W2	-42.2		-49.6					
4	W1								
	W1	-36.6		-42.6					

*1.5 W 1

TABLE 7.5.4 CASE D

$\lambda = 2.3\ \mu$		T_1	T_2	T_3	T_4		CO ATM - CM	CO MODEL	MULTI-PLIER
	W3	-207.1		-11.4					
1.5	W2			-24.4			0.0162	3	
	W2	-40.0		[2.7]					
4	W1	109.2	-45.3	46.0					
	W1	581.1		292.9					
	W3			-3.3					
1.5	W2						0.0324	3	2
	W2	-16.1		2.9					
4	W1								
	W1	292.8		146.2					
	W3	-63.2							
1.5	W2						0.0486	3	3
	W2								
4	W1	40.3	17.0	15.9					
	W1			-5.7*					
	W3			1.1					
1.5	W2						0.1488	6	
	W2	0.5		1.2					
4	W1								
	W1	66.0		30.0					
	W3	-15.4		[0.0]					
1.5	W2			-1.9			0.1618	1	
	W2	[0.0]	[0.0]	[0.0]	0.5				
4	W1	13.7	4.8	3.0					
	W1	59.2		25.8					
	W3			-1.5					
1.5	W2						0.2426	1	1.5
	W2	-0.5		-2.0					
4	W1								
	W1	38.0		14.2					
	W3			-40.0					
1.5	W2						4.3376	2	
	W2	-36.6		-40.7					
4	W1								
	W1	-35.9		-41.3					
	W3			-41.8					
1.5	W2						4.7696	2	1.1
	W2	-38.5		-42.4					
4	W1								
	W1	-38.0		-43.1					

*1.5 W 1

TABLE 7.5.5 CASE E

$\lambda = 2.3\ \mu$		T_1	T_2	T_3	T_4		CO ATM - CM	CO MODEL	MULTI-PLIER
	W3	[0.0]		[0.0]					
1.5	W2			-22.5			0.0162	3	
	W2	[0.0]		[0.0]					
4	W1	-22.5	31.1	34.1					
	W1	[0.0]		[0.0]					
	W3			2.1					
1.5	W2						0.0324	3	2
	W2	3.8		1.0					
4	W1								
	W1	1.9		-0.6					
	W3	5.6							
1.5	W2						0.0486	3	3
	W2								
4	W1	-4.0	11.9	11.5					
	W1			-5.5*					
	W3			1.8					
1.5	W2						0.1488	6	
	W2	4.3		0.2					
4	W1								
	W1	1.1		-3.0					
	W3	4.8		0.6					
1.5	W2			-2.4			0.1618	1	
	W2	3.4	4.7	-1.0	1.3				
4	W1	-0.1	2.7	1.1					
	W1	[0.3]		-4.2					
	W3			-1.4					
1.5	W2						0.2426	1	1.5
	W2	1.5		3.0					
4	W1								
	W1	-1.7		-6.3					
	W3			-40.7					
1.5	W2						4.3376	2	
	W2	-37.5		-41.6					
4	W1								
	W1	-39.4		-43.5					
	W3			-42.5					
1.5	W2						4.7696	2	1.1
	W2	-39.4		-43.4					
4	W1								
	W1	-41.3		-45.2					

*1.5 W 1

TABLE 7.5.6 CASE F

λ = 2.3 μ		T_1	T_2	T_3	T_4		CO ATM - CM	CO MODEL	MULTI-PLIER
	W3	-762.1		[0.0]					
1.5	W2			-18.0			0.0162	3	
	W2	-350.6		[0.0]					
4	W1	-143.3	-48.0	37.5					
	W1	1.1		[0.0]					
	W3			5.7					
1.5	W2						0.0324	3	2
	W2	-168.9		4.4					
4	W1								
	W1	4.8		2.0					
	W3	-244.6							
1.5	W2						0.0486	3	3
	W2								
4	W1	-40.8	-10.8	16.4					
	W1			0.6*					
	W3			8.0					
1.5	W2						0.1488	6	
	W2	-29.7		5.7					
4	W1								
	W1	5.4		1.4					
	W3	-56.4		6.9					
1.5	W2			4.0			0.1618	1	
	W2	-26.9	-10.0	4.6	-2.2				
4	W1	-7.7	-0.4	6.5					
	W1	4.6		[0.3]					
	W3			5.0					
1.5	W2						0.2426	1	1.5
	W2	-17.0		-2.6					
4	W1								
	W1	2.7		-1.7					
	W3			-36.2					
1.5	W2						4.3376	2	
	W2	-35.3		-37.7					
4	W1								
	W1	-36.4		-40.4					
	W3			-38.2					
1.5	W2						4.7696	2	1.1
	W2	-37.2		-39.6					
4	W1								
	W1	-38.3		-42.2					

*1.5 W 1

TABLE 7.5.7 CASE G

$\lambda = 2.3\ \mu$		T_1	T_2	T_3	T_4		CO ATM - CM	CO MODEL	MULTI-PLIER
	W3	0.0		-152.1					
1.5	W2			-228.1			0.0162	3	
	W2	0.0		-285.8					
4	W1	-46.4	-245.2	-350.8					
	W1	0.0		-322.0					
	W3			-75.3					
1.5	W2						0.0324	3	2
	W2	3.1		-142.4					
4	W1								
	W1	1.8		-161.7					
	W3	4.3							
1.5	W2						0.0486	3	3
	W2								
4	W1	-12.3	-80.7	-117.4					
	W1			-75.4*					
	W3			-17.3					
1.5	W2						0.1488	6	
	W2	3.5		-32.5					
4	W1								
	W1	1.1		-38.6					
	W3	3.3		-16.9					
1.5	W2			-24.7			0.1618	1	
	W2	2.6	-18.4	-30.8	-25.3				
4	W1	-2.9	-25.5	-38.0					
	W1	0.3		-36.4					
	W3			-13.8					
1.5	W2						0.2426	1	1.5
	W2	0.8		-23.3					
4	W1								
	W1	-1.6		-27.7					
	W3			-42.4					
1.5	W2						4.3376	2	
	W2	-37.4		-43.1					
4	W1								
	W1	-38.6		-44.1					
	W3			-44.1					
1.5	W2						4.7696	2	1.1
	W2	-39.3		-44.7					
4	W1								
	W1	-40.4		-45.7					

*1.5 W 1

TABLE 5.7.8 CASE H

$\lambda = 2.3\ \mu$		T_1	T_2	T_3	T_4		CO ATM - CM	CO MODEL	MULTI-PLIER
	W3	-1075.0		46.6					
1.5	W2			223.4			0.0162	3	
	W2	-815.4		393.8					
4	W1	-696.6	-3.4	422.8					
	W1	-29.8		314.6					
	W3			22.7					
1.5	W2						0.0324	3	2
	W2	-404.5		197.5					
4	W1								
	W1	-11.9		157.6					
	W3	-355.8							
1.5	W2						0.0486	3	3
	W2								
4	W1	-227.8	[0.6]	140.9					
	W1			74.0*					
	W3			1.8					
1.5	W2						0.1488	6	
	W2	-85.8		42.6					
4	W1								
	W1	0.6		33.4					
	W3	-106.2		[0.0]					
1.5	W2			18.9			0.1618	1	
	W2	-78.3	[0.0]	37.1	21.9				
4	W1	-66.2	[0.0]	40.4					
	W1	[0.0]		28.9					
	W3			-3.4					
1.5	W2						0.2426	1	1.5
	W2	52.9		22.2					
4	W1								
	W1	-0.7		16.7					
	W3			-42.5					
1.5	W2						4.3376	2	
	W2	-38.7		-39.5					
4	W1								
	W1	-35.4		-39.4					
	W3			-44.2					
1.5	W2						4.7696	2	1.1
	W2	-40.3		-41.3					
4	W1								
	W1	-37.2		-41.1					

*1.5 W 1

TABLE 7.5.9 CASE I

$\lambda = 2.3\ \mu$		T_1	T_2	T_3	T_4		CO ATM - CM	CO MODEL	MULTI-PLIER
	W3	[0.0]		[0.0]					
1.5	W2			-21.7			0.0162	3	
	W2	[0.0]		[0.0]					
4	W1	-21.7	30.0	32.9					
	W1	[0.0]		[0.0]					
	W3			0.3					
1.5	W2						0.0324	3	2
	W2	1.8		-0.8					
4	W1								
	W1	[0.0]		-2.4					
	W3	3.0							
1.5	W2						0.0486	3	3
	W2								
4	W1	-6.2	9.1	8.7					
	W1			-7.7*					
	W3			-1.4					
1.5	W2						0.1488	6	
	W2	1.0		-3.0					
4	W1								
	W1	-2.1		-6.1					
	W3	1.4		-2.6					
1.5	W2			-5.5			0.1618	1	
	W2	0.1	1.3	-4.2	-1.9				
4	W1	-3.3	-0.6	-2.2					
	W1	-2.9		-7.3					
	W3			-4.7					
1.5	W2						0.2426	1	1.5
	W2	-1.8		-6.3					
4	W1								
	W1	-5.0		-9.4					
	W3			-42.8					
1.5	W2						4.3376	2	
	W2	-39.7		-43.7					
4	W1								
	W1	-41.6		-45.5					
	W3			-44.6					
1.5	W2						4.7696	2	1.1
	W2	-41.6		-45.4					
4	W1								
	W1	-43.4		-47.2					

*1.5 W 1

TABLE 7.5.10 CASE J

$\lambda = 2.3\ \mu$		T_1	T_2	T_3	T_4		CO ATM - CM	CO MODEL	MULTI-PLIER
	W3	-80.0		[0.0]					
1.5	W2			-18.3			0.0162	3	
	W2	-360.5		[0.0]					
4	W1	-138.4	-48.7	37.1					
	W1	14.0		[0.0]					
	W3			[9.6]					
1.5	W2						0.0324	3	2
	W2	170.1		8.0					
4	W1								
	W1	14.7		5.2					
	W3	-252.1							
1.5	W2						0.0486	3	3
	W2								
4	W1	-34.5	-6.4	20.9					
	W1			5.5*					
	W3			14.7					
1.5	W2						0.1488	6	
	W2	-24.4		12.0					
4	W1								
	W1	12.8		7.1					
	W3	-63.5		13.6					
1.5	W2			10.6			0.1618	1	
	W2	-21.5	-4.4	10.9	3.8				
4	W1	-1.0	5.6	12.5					
	W1	11.8		6.0					
	W3			11.8					
1.5	W2						0.2426	1	1.5
	W2	-11.2		9.0					
4	W1								
	W1	9.6		4.1					
	W3			-31.9					
1.5	W2						4.3376	2	
	W2	-31.1		-33.6					
4	W1								
	W1	-32.4		-36.7					
	W3			-34.6					
1.5	W2						4.7696	2	1.1
	W2	-33.1		-35.6					
4	W1								
	W1	-34.5		-38.6					

*1.5 W 1

TABLE 7.5.11 CASE K

$\lambda = 2.3\ \mu$		T_1	T_2	T_3	T_4		CO ATM - CM	CO MODEL	MULTI-PLIER
	W3	[0.0]		-115.2					
1.5	W2			-192.4			0.0162	3	
	W2	[0.0]		-252.3					
4	W1	-44.3	-226.7	-322.0					
	W1	[0.0]		-302.6					
	W3			-58.5					
1.5	W2						0.0324	3	2
	W2	1.3		-127.6					
4	W1								
	W1	[0.0]		-153.7					
	W3	1.9							
1.5	W2						0.0486	3	3
	W2								
4	W1	-14.0	-76.8	-110.0					
	W1			-65.7*					
	W3			-16.1					
1.5	W2						0.1488	6	
	W2	0.4		-31.8					
4	W1								
	W1	-2.0		-39.4					
	W3	0.2		-16.1					
1.5	W2			-24.1			0.1618	1	
	W2	-0.5	-19.5	-30.4	-25.6				
4	W1	-5.8	-26.6	-38.1					
	W1	-2.8		-37.4					
	W3			-14.3					
1.5	W2						0.2426	1	1.5
	W2	-2.4		-24.0					
4	W1								
	W1	-4.7		-29.3					
	W3			-44.2					
1.5	W2						4.3376	2	
	W2	-39.5		-44.9					
4	W1								
	W1	-40.7		-46.0					
	W3			-45.8					
1.5	W2						4.7696	2	1.1
	W2	-41.4		-46.5					
4	W1								
	W1	-42.5		-47.5					

*1.5 W 1

TABLE 7.5.12 CASE L

$\lambda = 2.3\mu$		T_1	T_2	T_3	T_4		CO ATM - CM	CO MODEL	MULTI-PLIER
	W3	-677.4		-456.5					
1.5	W2			-316.9			0.0162	3	
	W2	-166.3		-117.9					
4	W1	138.6	105.2	144.2					
	W1	623.0		405.0					
	W3			-218.9					
1.5	W2						0.0324	3	2
	W2	-72.0		-56.4					
4	W1								
	W1	320.8		209.1					
	W3	-210.4							
1.5	W2						0.0486	3	3
	W2								
4	W1	59.7	46.3	47.8					
	W1			-93.9*					
	W3			-35.9					
1.5	W2						0.1488	6	
	W2	-0.9		0.0					
4	W1								
	W1	82.9		54.2					
	W3	-49.9		-32.4					
1.5	W2			-19.1			0.1618	1	
	W2	0.0	0.0	0.0	-0.2				
4	W1	29.2	23.0	21.8					
	W1	75.7		48.9					
	W3			-19.0					
1.5	W2						0.2426	1	1.5
	W2	3.9		2.2					
4	W1								
	W1	53.3		33.6					
	W3			-33.6					
1.5	W2						4.3376	2	
	W2	-28.6		-33.2					
4	W1								
	W1	-27.5		-33.1					
	W3			-35.5					
1.5	W2						4.7696	2	1.1
	W2	-30.7		-35.1					
4	W1								
	W1	-29.8		-35.2					

*1.5 W 1

TABLE 7.5.13 CASE M

$\lambda = 2.3\mu$		T_1	T_2	T_3	T_4		CO ATM - CM	CO MODEL	MULTI-PLIER
	W3	-281.3		-72.5					
1.5	W2			-86.4			0.0162	3	
	W2	-103.1		-57.5					
4	W1	55.9	-12.2	-11.4					
	W1	559.5		251.8					
	W3			-30.4					
1.5	W2						0.0324	3	2
	W2	-44.0		-23.7					
4	W1								
	W1	288.5		129.0					
	W3	-83.0							
1.5	W2						0.0486	3	3
	W2								
4	W1	27.3	2.4	1.2					
	W1			-21.7*					
	W3			0.5					
1.5	W2						0.1488	6	
	W2	-0.2		0.6					
4	W1								
	W1	69.7		31.3					
	W3	-16.5		[0.0]					
1.5	W2			-2.0			0.1618	1	
	W2	[0.0]	[0.0]	[0.0]	0.5				
4	W1	14.6	5.1	3.2					
	W1	63.1		27.5					
	W3			0.6					
1.5	W2						0.2426	1	1.5
	W2	1.7		[0.1]					
4	W1								
	W1	42.7		17.3					
	W3			-36.2					
1.5	W2						4.3376	2	
	W2	-32.6		-37.0					
4	W1								
	W1	-31.9		-37.6					
	W3			-38.1					
1.5	W2						4.7696	2	1.1
	W2	-34.6		-38.8					
4	W1								
	W1	-34.0		-39.5					

*1.5 W 1

TABLE 7.5.14 CASE N

$\lambda \approx 2.3\,\mu$		T_1	T_2	T_3	T_4		CO ATM - CM	CO MODEL	MULTI-PLIER
	W3	-1131.9		-771.8					
1.5	W2			-795.9			0.0162	3	
	W2	-825.0		-746.3					
4	W1	-552.0	-668.9	-667.3					
	W1	313.7		-215.7					
	W3			-339.8					
1.5	W2						0.0324	3	2
	W2	-363.5		-328.5					
4	W1								
	W1	202.7		-66.6					
	W3	-310.8							
1.5	W2						0.0486	3	3
	W2								
4	W1	-121.0	-163.6	-165.7					
	W1			-205.0*					
	W3			-6.5					
1.5	W2						0.1488	6	
	W2	-7.7		-6.3					
4	W1								
	W1	-112.4		-46.4					
	W3	-28.4		[0.0]					
1.5	W2			-3.5			0.1618	1	
	W2	[0.0]	[0.0]	[0.0]	0.8				
4	W1	25.0	8.7	5.5					
	W1	108.5		47.2					
	W3			25.0					
1.5	W2						0.2426	1	1.5
	W2	26.9		24.1					
4	W1								
	W1	97.4		53.7					
	W3			7.1					
1.5	W2						4.3376	2	
	W2	13.3		[5.8]					
4	W1								
	W1	14.6		4.6					
	W3			4.1					
1.5	W2						4.7696	2	1.1
	W2	10.1		2.8					
4	W1								
	W1	11.1		1.6					

*1.5 W 1

TABLE 7.1.15 EFFECT OF SURFACE REFLECTIVITY - 2.3μ BAND

CASE	ρ 0.1	ρ 1.0
A	5.74	5.72
B	7.99	7.96
C	0.03	- 0.01
D	- 0.02	0.00
E	4.68	4.69
F	- 10.03	- 10.04
G	- 18.44	- 18.42
H	0.02	0.00
I	1.31	1.31
J	- 4.38	- 4.39
K	- 19.48	- 19.46
L	0.00	0.00
M	- 0.02	0.00
N	- 0.04	0.00

TABLE 7.5.16 CASE P

$\lambda = 4.6\ \mu$		T_1	T_2	T_3	T_4		CO ATM - CM	CO MODEL	MULTI-PLIER
	W3								
1.5	W2						0.0162	3	
	W2		[28.3]		470.0				
4	W1								
	W1								
	W3								
1.5	W2						0.0324	3	2
	W2								
4	W1								
	W1								
	W3								
1.5	W2						0.0486	3	3
	W2								
4	W1								
	W1								
	W3		3.7						
1.5	W2						0.1488	6	
	W2	-2.8	3.8	7.7	26.4				
4	W1								
	W1								
	W3		[0.0]						
1.5	W2						0.1618	1	
	W2	[0.0]	[0.0]	[0.0]	22.3				
4	W1								
	W1								
	W3								
1.5	W2						0.2426	1	1.5
	W2		-14.1						
4	W1								
	W1								
	W3								
1.5	W2						4.3376	2	
	W2		-102.4		-110.7				
4	W1								
	W1								
	W3								
1.5	W2						4.7696	2	1.1
	W2								
4	W1								
	W1								

TABLE 7.5.17 CASE Q

$\lambda = 4.6\,\mu$		T_1	T_2	T_3	T_4		CO ATM - CM	CO MODEL	MULTI-PLIER
	W3								
1.5	W2						0.0162	3	
	W2		-430.0		[20.9]				
4	W1								
	W1								
	W3								
1.5	W2						0.0324	3	2
	W2								
4	W1								
	W1								
	W3								
1.5	W2						0.0486	3	3
	W2								
4	W1								
	W1								
	W3		1.1						
1.5	W2						0.1488	6	
	W2	-6.6	-4.2	6.7	-1.6				
4	W1								
	W1								
	W3		[0.0]						
1.5	W2						0.1618	1	
	W2	[0.0]	-5.1	[0.0]	[0.0]				
4	W1								
	W1								
	W3								
1.5	W2						0.2426	1	1.5
	W2		-3.9						
4	W1								
	W1								
	W3								
1.5	W2						4.3376	2	
	W2		-108.3		-125.4				
4	W1								
	W1								
	W3								
1.5	W2						4.7696	2	1.1
	W2								
4	W1								
	W1								

TABLE 7.5.18 CASE R

$\lambda = 4.6\ \mu$		T_1	T_2	T_3	T_4		CO ATM - CM	CO MODEL	MULTI-PLIER
	W3								
1.5	W2						0.0162	3	
	W2		1729.3		-369.3				
4	W1								
	W1								
	W3								
1.5	W2						0.0324	3	2
	W2								
4	W1								
	W1								
	W3								
1.5	W2						0.0486	3	3
	W2								
4	W1								
	W1								
	W3		0.2						
1.5	W2						0.1488	6	
	W2	-27.0	-9.2	[0.0]	71.0				
4	W1								
	W1								
	W3			7.9					
1.5	W2						0.1618	1	
	W2	[0.0]	[0.0]	[0.0]	77.0				
4	W1								
	W1								
	W3								
1.5	W2						0.2426	1	1.5
	W2		24.8						
4	W1								
	W1								
	W3								
1.5	W2						4.3376	2	
	W2		-116.4		-139.7				
4	W1								
	W1								
	W3								
1.5	W2						4.7696	2	1.1
	W2								
4	W1								
	W1								

TABLE 7.5.19 CASE S

λ = 4.6 μ		T_1	T_2	T_3	T_4		CO ATM - CM	CO MODEL	MULTI-PLIER
	W3								
1.5	W2						0.0162	3	
	W2		-619.8		147.1				
4	W1								
	W1								
	W3								
1.5	W2						0.0324	3	2
	W2								
4	W1								
	W1								
	W3								
1.5	W2						0.0486	3	3
	W2								
4	W1								
	W1								
	W3		-1.1						
1.5	W2						0.1488	6	
	W2	-12.4	-0.9	5.8	38.1				
4	W1								
	W1								
	W3		[0.0]						
1.5	W2						0.1618	1	
	W2	[0.0]	[0.0]	[0.0]	38.6				
4	W1								
	W1								
	W3								
1.5	W2						0.2426	1	1.5
	W2		[0.4]						
4	W1								
	W1								
	W3								
1.5	W2						4.3376	2	
	W2		-107.1		-122.0				
4	W1								
	W1								
	W3								
1.5	W2						4.7696	2	1.1
	W2								
4	W1								
	W1								

TABLE 7.5.20 CASE T

$\lambda = 4.6\,\mu$		T_1	T_2	T_3	T_4		CO ATM - CM	CO MODEL	MULTI-PLIER
	W3								
1.5	W2						0.0162	3	
	W2		3381.2		7103.4				
4	W1								
	W1								
	W3								
1.5	W2						0.0324	3	2
	W2								
4	W1								
	W1								
	W3								
1.5	W2						0.0486	3	3
	W2								
4	W1								
	W1								
	W3		103.2						
1.5	W2								
	W2	195.4	102.0	48.2	-217.6				
4	W1								
	W1								
	W3		[0.0]						
1.5	W2						0.1618	1	
	W2	[0.0]	[0.0]	[0.0]	-315.3				
4	W1								
	W1								
	W3								
1.5	W2						0.2426	1	1.5
	W2		-310.9						
4	W1								
	W1								
	W3								
1.5	W2						4.3376	2	
	W2		[-5.9]		116.4				
4	W1								
	W1								
	W3								
1.5	W2						4.7696	2	1.1
	W2								
4	W1								
	W1								

TABLE 7.5.21 EFFECTS OF ATMOSPHERIC AND SURFACE PARAMETER VARIATIONS - 4.6μ BAND

PARAMETER		CASE 285.2	CASE 288.2
Ground Temperature	P	1.9	0.0
	Q	-5.1	-5.1
	R	5.2	0.0
	S	3.2	0.0
	T	-25.2	0.0
		0.7	1.0
Emissivity	P	6.9	0.0
	Q	-5.4	-5.1
	R	19.6	0.0
	S	11.7	0.0
	T	-93.8	0.0
		T_2 -2	T_2
Gas Temperature	P	0.0	0.0
	Q	-4.1	-5.1
	R	0.0	0.0
	S	0.0	0.0
	T	-0.2	0.0
		0.95	1.0
Relative Atmospheric Pressure	P	-1.4	0.0
	Q	-2.4	-5.1
	R	-5.2	0.0
	S	-2.3	0.0
	T	18.3	0.0

used in obtaining the weighting functions are indicated by the rectangles around the accuracy result. It is not to be expected that the results for either band will be good in all cases and is not a matter for concern that they are not. It should be noted that the major concern is to identify a sink and to identify a source as a source. It is then possible to use weighting functions derived from more appropriate conditions to more accurately determine the CO density. This is especially true for a source region where the use of a high CO condition for the target condition in establishing weighting functions gives the high CO concentrations much more accurately. This can be seen in Case N.

7.5.2.2 The Overtone Band: - The results for the analysis are presented in Tables 7.5.1 through 7.5.15 (cases A through N) for the overtone (2.3 μ) band. Some of the results show accuracy which will fit the accuracy requirements detailed above while some show inaccuracies which are too large to be acceptable. This is as expected.

Cases A, B, C, and D use the same CO models for the base and target cases used for determining the weighting functions. In cases A, B, and C, all runs give accuracy suitable for use with one possible exception (water model 4W1, T1). Except for this one set of conditions, the model 1 cases (standard CO profile), none of the runs show any significant indication of a sink or source. Note that the model with a temperature inversion is quite accurate. For the important situation of the low altitude sink, all runs show good accuracy, all sufficient to show a lower total CO column density than the standard model, that is, a sink. The models with low CO densities show large errors but not so large that sinks are not shown. The model with 1.5 times the standard CO model gives accuracies which all show significant increases over the standard CO. For the models with high CO densities the results are inaccurate, up to about 50%, but such still indicate high CO densities and thus fulfill the purpose. For case D the results are not nearly so

good. The conditions used to determine weighting functions do not include any of the low water density models. One test run with such a model shows, for the standard CO model, a doubling of what it should be. This would indicate a source and so is unacceptable. In general, the errors are too large to be acceptable.

Case E shows the effect of using the very low CO density cases as the base runs and one standard CO model as the target run to obtain the weighting functions. The results are much the same as cases A and C. In this case all results are suitable. Cases F and G show results for similar CO models being used in determining weighting functions but with more restricted temperature conditions. The results are poor. Sinks are indicated where there are no sinks.

Case H is another case where the conditions of temperature and of water content did not cover a sufficient range. Thus large sinks are indicated where there is no sink.

Now consider cases I, J, and K, where all runs used in determining weighting functions were with models having low CO densities (.1, .2, and .3 of standard). For the case, I, where the ranges of temperature and water density employed were wide, the results are good, showing sinks and sources where they occur. With more restricted ranges, Cases J and K, the results are not good, indicating sinks where they do not exist.

For Case L, the weighting functions were obtained using the standard and the low-altitude sink models, but only one water model. Results for other water models are not accurate enough to be used.

For case M, similar results are obtained to case L. No runs with low water densities were used for weighting function obtention and results for such models were inaccurate.

For Case N, where a high CO density model was used in the set for obtaining weighting functions, just about all test runs were inaccurate.

Such results are to be expected since the CO absorption curve is non-linear in part of the region used to determine weighting functions.

In Table 7.5.15 it is seen that a change in the earth's reflectivity has no significant effect on the calculated CO density. It would also be small for the 4.6 μ band.

Some general conclusions can be drawn from these results. They mainly concern the conditions used in obtaining weighting functions. If such, for CO are within the range of CO where absorption is about linear, that is within the range from very low CO densities to slightly above our standard model, the results will be good within the range of water density and temperature covered in the weighting function runs and probably not good outside such range. That is, if water density models 1 and 3 are used, those for in-between water densities have the desirable accuracy, but if models 2 and 3 are used, the results for water model 1 are inaccurate. That is, interpolation gives reasonable results but extrapolation does not.

It is important to note that the variation in total water content does not vary over one area by a factor of more than about four during the year as seen in Figures 7.5.1 through 7.5.4. Thus the extremes used here are wider than those for any one region. Hence, in treating the data for any one area, weighting functions based on the range of conditions for that area can be used rather than those which bracket the range of conditions for all areas.

Conclusions about sinks and sources can also be made. These results show that sinks (even those at low altitude having only a 9% lower CO optical thickness than the standard model) are detected readily and regions of high CO concentration are also readily seen. It is also to be noted that the presence of a temperature inversion layer does not interfere with the results for this (2.3 μ) band.

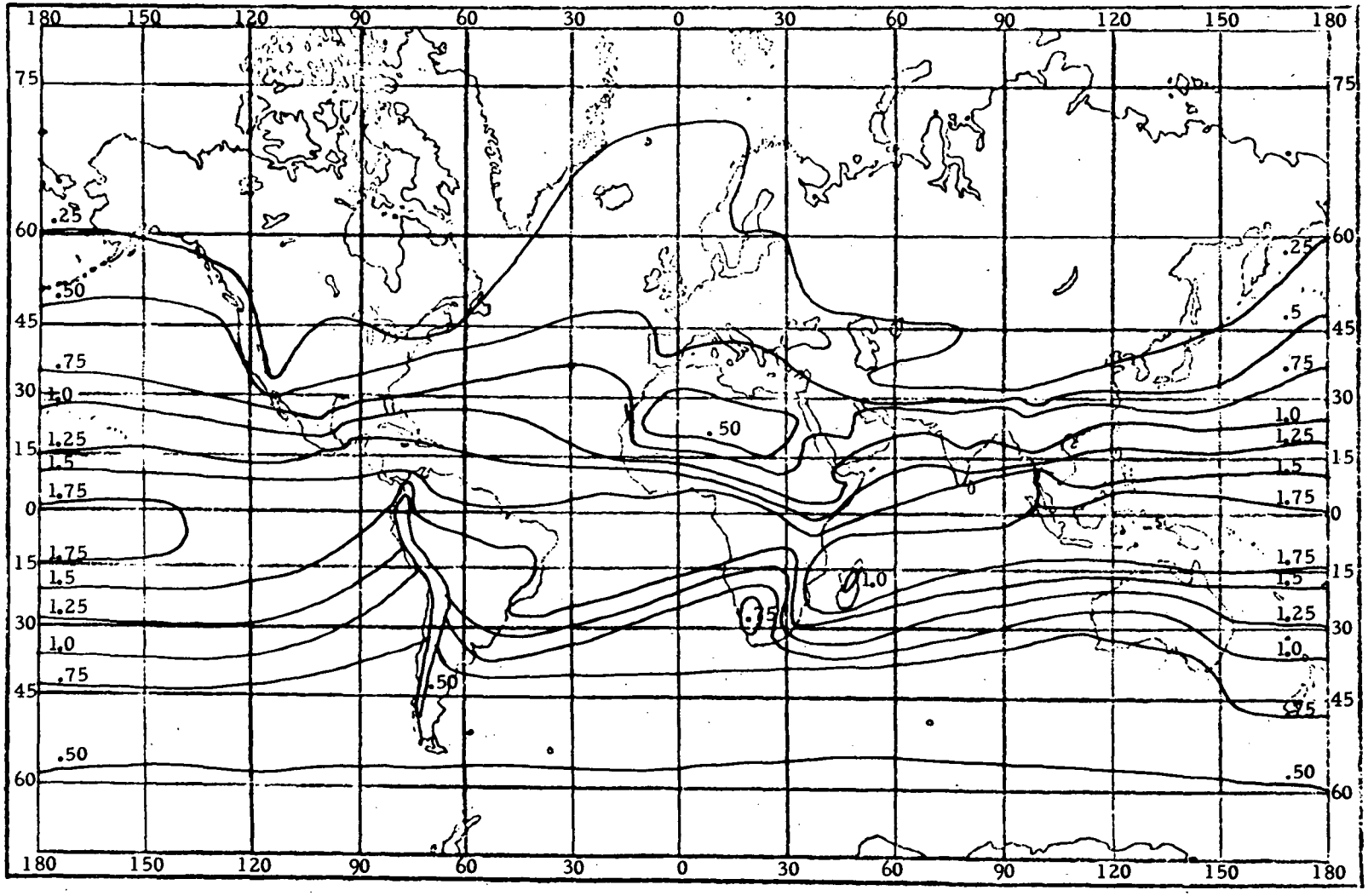

Figure 7.5.1 January Mean Precipitable Water (in inches) from Tuller - 1968

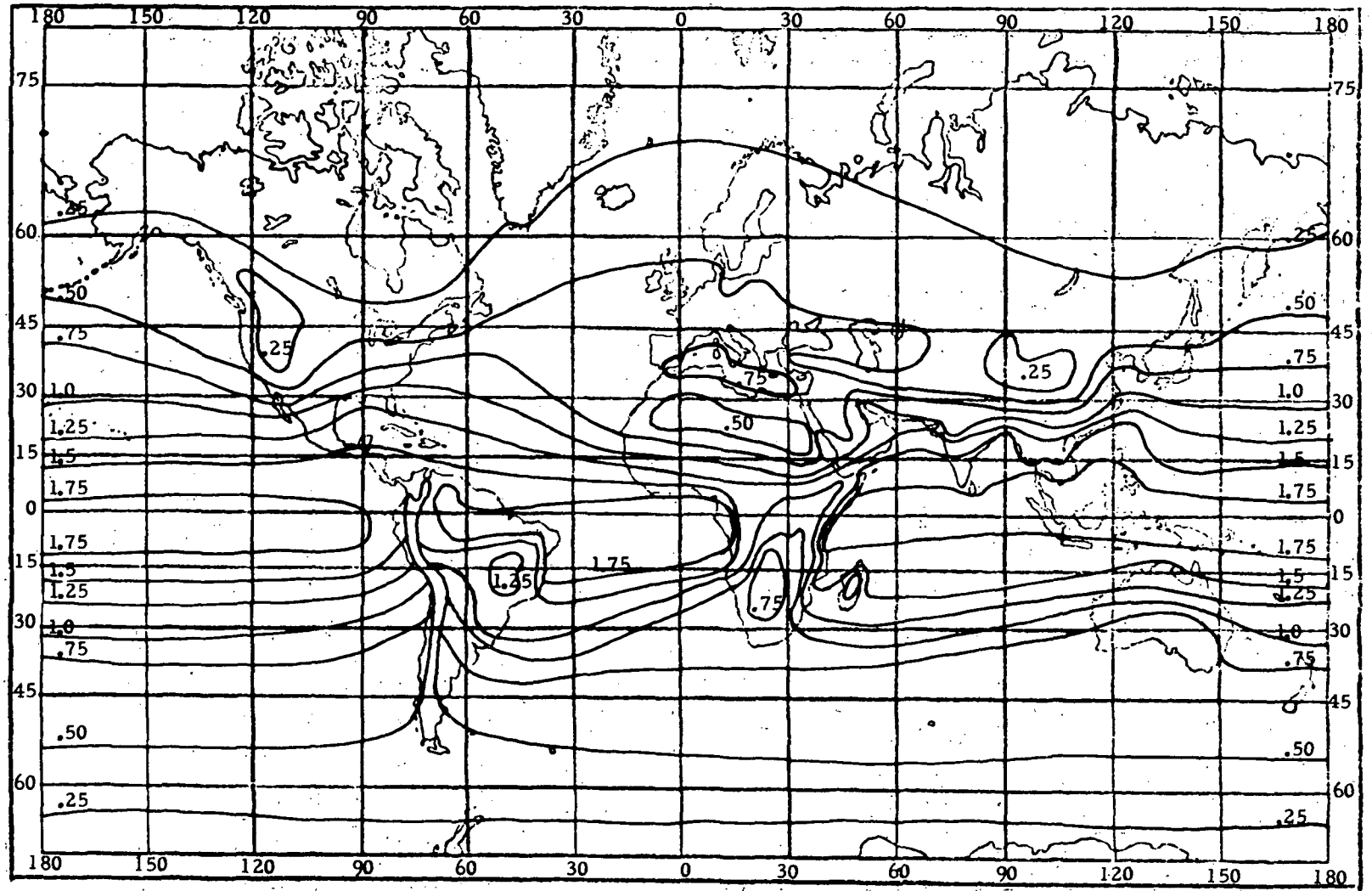

Figure 7.5.2 April Mean Precipitable Water (in inches) from Tuller - 1968

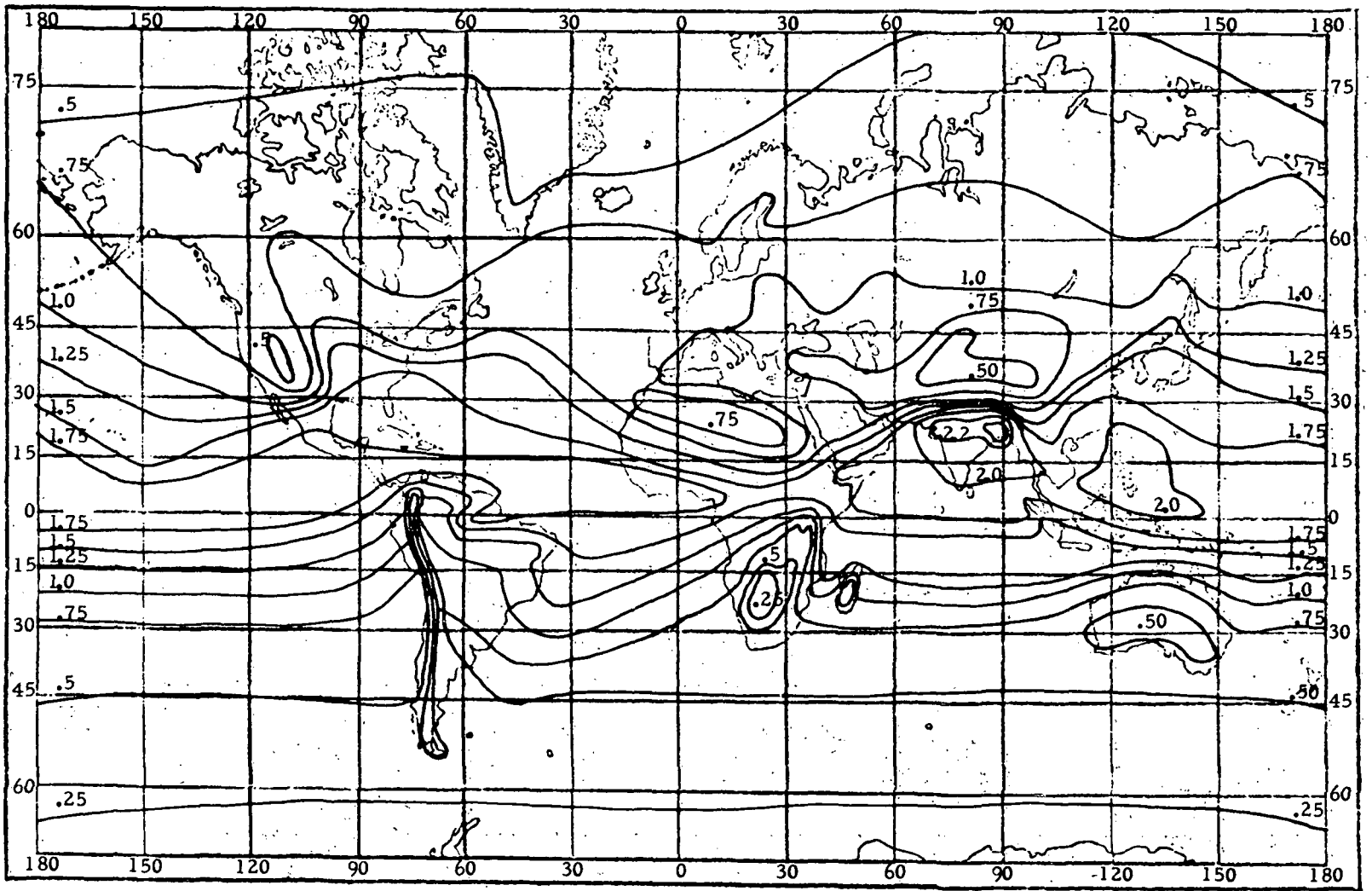

Figure 7.5.3 July Mean Precipitable Water (in inches) from Tuller - 1968

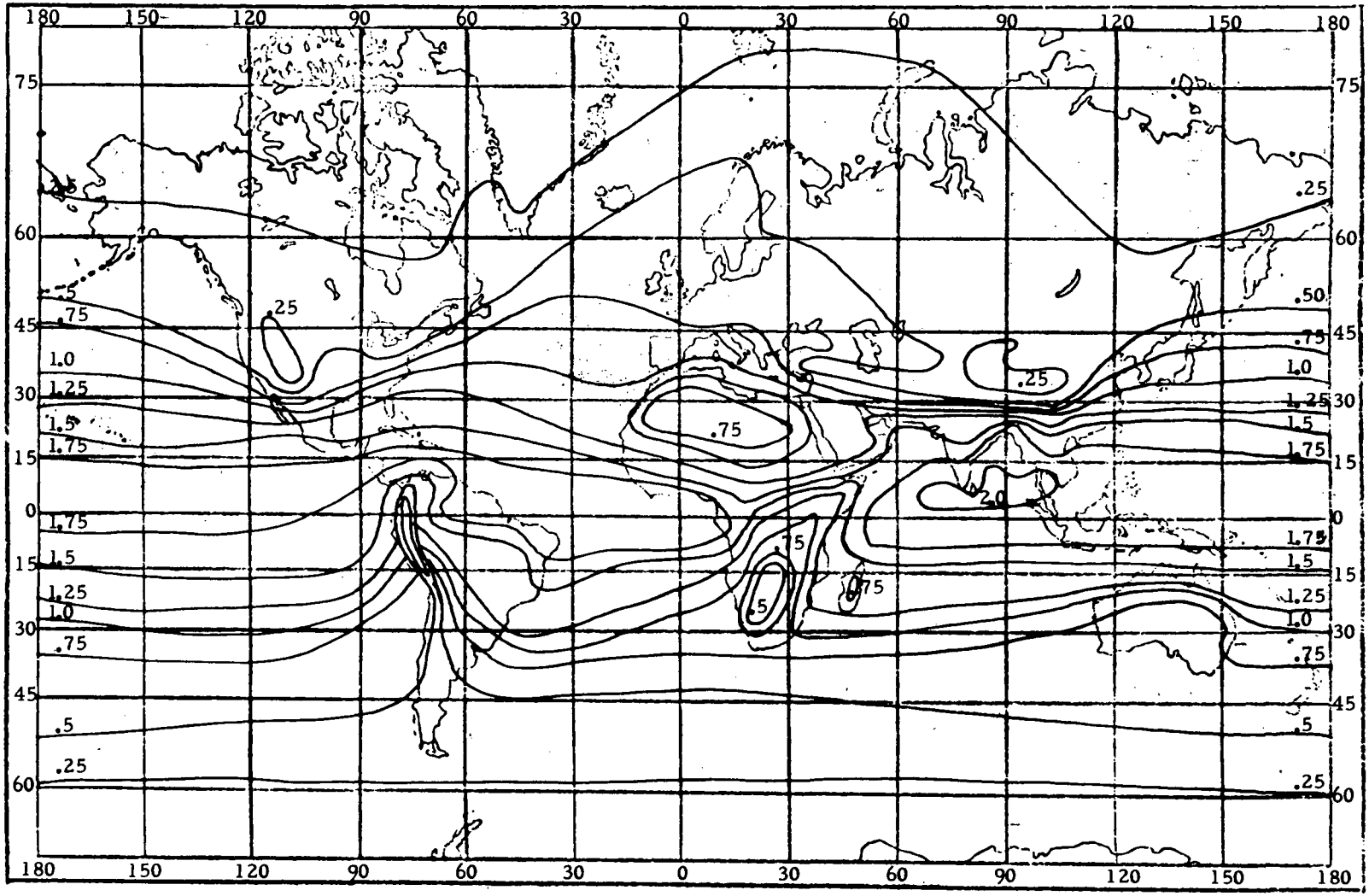

Figure 7.5.4 October Mean Precipitable Water (in inches) from Tuller - 1968

7.5.2.3 The Fundamental Band: - The results for the analysis for the fundamental (4.6 μ) band in Tables 7.5.16 through 7.5.21 (Cases P through T). The cases employ weighting functions obtained using CO model 1 as the base runs with 1.5 x CO density of model 1 (Case S), urban CO density model (Case T), very low CO density model (Case P), and the low-altitude sink model (Case R) for the target runs. As would be expected the best results are obtained for Cases P and R. However, it is to be noted that in all cases the temperature inversion model gives poor results with sinks not detected. This is an intolerable result. If CO densities for such critical conditions are in error by 26% (Case P) or by 71% (Case R) existing sinks will not be found. Cases P and R are thought to be as reasonable as any tests that could be made for this band and other tests would be expected to show similar results.

Case O uses the temperature inversion layer run as a part of the base set in determining the weighting functions. This is not a very practical case but it does improve the results as a function of temperature. There is, however, still an overlap in the CO low altitude sink and the CO standard model results which indicate that it could not be used to see a sink.

In all 4.6 μ cases, the source runs show up with large negative errors. In most all urban model runs, negative CO densities are calculated. These are meaningless and undoubtedly smaller sources would show up as sinks. This is an intolerable situation.

Certain other tests were made to help show the effect of atmospheric and earth-surface parameter variations. Results are shown in Table 7.5.21.

Significant effects are found, even for the runs, P and R, which use better sets of runs for determining weighting functions. A few degrees difference in the ground and the 0 km atmosphere temperatures cause a few percent difference in calculated CO. A reduction of surface emissivity to 0.7 causes drastic effects. Changing the temperature model of both the

entire atmosphere and the ground by 2^{o} produces no significant effect. This is as expected. However, a random variation with altitude of $\pm 2^{o}$ would produce large effects as seen in Section 7.1.4 with the single-line model. A change in the total pressure significantly changes the calculated CO since it reduces the atmospheric emission relative to the earthshine. The effects of these variations for the 2.3 μ band were shown in Section 7.1 to be small.

7.5.2.4 Summary: - The following summarizes the results for the two bands based on the calculations with the multi-line model. They are similar to those obtained with the single-line model.

The conclusions for the two wavelengths studied may be summarized on the basis of the following considerations.

Optical Thickness:

4.6: For much of the range, the absorption curve is not linear. The higher optical thicknesses may be so high that there is little sensitivity in that range.

2.3: The optical thickness is suitable for the range of concentrations of interest. The only limit is the upper limit of the limb experiment but it will be suitable for a sink at any reasonable expected altitude.

Interpretation:

4.6: Very difficult because of the need for accurate atmospheric temperature data as a function of altitude, ground temperature, and ground emissivity at 4.6 μ.

2.3 Data directly presented in terms of CO density.

Sensitivity to Low Altitude Sink:

4.6 Sensitivity to low altitude CO is very low and errors introduced are likely to be larger than the CO decrease effect being sought.

2.3: Sensitivity at low altitude same as the similar effect at high altitude. Sinks of less than 10% CO density decrease can be detected.

Temperature Inversion Layer:

4.6: Drastic effects on calculated CO densities prohibit detection of significant sinks.

2.3: No appreciable effect.

Line Strengths:

4.6: Strong.

2.3: About 1% of 4.6 lines. This is strong enough.

Atmospheric Emission:

4.6: Considerable emission in this band causes much variation from straight absorption model and leads to difficulty in interpretation as mentioned.

2.3: Emission negligible.

Night Use:

4.6: Possible.

2.3: Not likely to be possible, at least with acceptable sensitivity.

Mapping Experiment:

4.6: Emission effects disastrous.

2.3: Interferents cause problems but these are overcome by technique used.

Limb Experiment:

4.6: Atmosphere optically thick at lower altitudes of interest.

2.3: Sensitivity limits altitude but altitude range reasonable.

8. CONCLUSIONS

The correlation interferometric techniques has been shown by analysis to be capable of measuring atmospheric trace species accurately. Specifically it has been shown to measure atmosphere amounts of carbon monoxide with an accuracy of better than 10%. Thus the technique should be capable of picking out CO sinks which are only 10% or less lower in CO column density using measurements which are made by determining the absorption in a part of the first overtone band of CO in the 2.3 μ region of the spectrum. It has been determined that the use of this band is preferable to the use of the fundamental band in the 4.6 μ region. The latter is unsuitable because of the effect of atmospheric parameters including the atmospheric temperature profile (and the associated atmospheric emission) (see Tables 7.1.4 and 7.1.5), the ground temperature (see Tables 7.1.6 and 7.1.7), the ground emissivity at the wave lengths being used (see Table 7.1.8), atmospheric pressure and atmospheric path length. For that band, atmospheric emission causes an enhancement of the radiation which is a function of temperature and must be taken into account. If at some altitude the atmospheric temperature is greater than the ground temperature the effect of absorption below is minimized. Effectively, the instrument can not see well below an atmospheric temperature peak. Then the absorption does not follow the CO profile at low altitudes but rather there is less absorption near the ground even for CO profiles when there is more CO in that region (see Figures 7.1.6 and 7.1.7). These difficulties arise for any species with all spectral techniques which are primarily involved with radiation of wavelengths greater than about 3.5 μ. This is because of the predominance of earthshine over reflected solar radiation at these wavelengths (see Figure 3.2.1). The overtone band is not affected significantly by variaties in the parameters noted above and absorption in this band follows closely the atmospheric CO profile for any reasonable atmo-

spheric model. Atmospheric scintillations have little effect at either wavelength region.

Spectral interferents can be overcome by the correlation interferometry technique. The chief spectral interferants in the 2.3 μ spectral region are water and methane. By using the interferogram directly, carbon monoxide can be accurately measured in the presence of atmospheric amounts of these gases which would prevent accurate measurement of CO by ordinary spectral methods. In order to accomplish the interferometric measurement it is necessary to calibrate the instrument over the entire range of density of interferents for which it will be used and to do so with variation of important atmospheric parameters over which it will be used. Thus the calibration must cover the range of methane of about 2 to 5 atmosphere cm. since this is the range that is expected to be encountered and to cover the range of about 0.2 to 3 precipitable cm. of water since variations from dry to wet atmospheres include this range. Further, since the population of the rotational water levels are appreciably affected by temperature, variations corresponding to changes in atmospheric temperature profiles must be included in the calibration, thus necessitating calibration for conditions of a cold dry, a hot dry, a cold wet, and a hot wet atmosphere as well as conditions in between these.

The calibration determines the weighting function which multiplies the section of the interferogram in such a way as to minimize the effect of spectral interferents and maximize the effect of the gas to be measured (see Chapters 5 and 6). The choice of conditions used to determine the weighting functions is critical. The use of a wide range of conditions and interpolation between these gives much better results than use of a narrow range with extrapolation. In practice under flight conditions, it may be best to use a weighting function derived from a wide range of conditions to obtain an approximate measure of CO density and conditions and then use a weighting function derived from a narrower range of density and conditions to obtain a more accurate CO density measurement.

The feasibility analysis thus shows the correlation interferometry technique to be capable of the measurement from a remote platform of carbon monoxide in the atmosphere over the desired range of density. The measurement can be made in the mapping mode (observing sunlight reflected by the earth) and the limb mode (observing direct sunlight through the earth's limb). It can further be stated that the technique is applicable to a variety of other gases present in trace amounts in the atmosphere.

APPENDIX A

LISTING OF PROGRAM SPECTRA

Page Intentionally Left Blank

```
                      SEGZERO(SEG0,SPECTRA)
                      SEGMENT(SEG1,VOIGT,K,K1,K2,K3)
                      SEGMENT(SEG2,HEIGHT,INTERP)
                      SEGMENT(SEG3,LINER)
                      SEGMENT(SEG4,COEFFS)
                      SEGMENT(SEG5,SPECT)
                      SEGMENT(SEG6,TRANF,FLTRS,FRXFM)
                      SEGMENT(SEG7,SPPLOT)
                      FORTRAN IV PROGRAM SPECTRA (INPUT, OUTPUT, PUNCH,
                     1                            TAPE5=INPUT, TAPE6=OUTPUT, -
                     2                            TAPE7=PUNCH, TAPE2)
                C           PROJECT COPE
                C           ATMOSPHERIC ABSORPTION MODEL PROGRAM
                C     COMPUTES MULTI-LINE TRANSMISSION SPECTRUM THROUGH ATMOSPHERE
                C     SOLVES RADIATIVE TRANSFER EQUATION AND INTEGRATES OVER ALTITUDES
                C
                C     WRITTEN BY G. LIFBLING, GENERAL ELECTRIC CO., JAN 1971
                C
                C
                C     INPUTS ARE LINE POSITIONS AND STRENGTH
                C     OUTPUT IS TRANSMITTED SPECTRUM PRINTED ON LINE PRINTER AND
                C        ALSO WRITTEN ON DISC FOR PLOTTING, IF DESIRED
                C
                C     THIS IS MAIN CALLING PROGRAM
                C     ALL COMPUTATIONS DONE IN LINKED SUBROUTINES TO CONSERVE STORAGE
   000003             DOUBLE PRECISION CFREQ
   000003             COMMON  CFREQ(150)
   000003             COMMON  ABSB(150, 98), A(27,25), B(25,25), C(25,25),
                     1       PATH( 98), ATEMP( 98), CONC(3, 98), ALOK( 98), DOPP(3,98),
                     2                  STEQ(150), SPEQ(150), STRONG(150), ENGY(160),
                     3       TITLE(18), AQ(3), BQ(3), CQ(3), ALBEDO, GTEMP, GEMIS
   000003             COMMON  FSTART, FSTOP
   000003             COMMON  LTYPE(150), NTYPE(3), NLINE, NSPEC, IN, IOUT, ICASE
   000003             DIMENSION S1(2), S2(2), S3(2), S4(2), S5(2), S6(2), S7(2)
   000003             DATA  S1/4HSEG1,0/,  S2/4HSEG2,0/,  S3/4HSEG3,0/,  S4/4HSEG4,0/,
                     1      S5/4HSEG5,0/,  S6/4HSEG6,0/,  S7/4HSEG7,0/
   000003             DATA  IFILE/4HSEGS/
   000003             IN = 5
   000004             IOUT = 6
                C
                C     READ NUMBER OF SPECTRA TO BE CALCULATED
   000005             READ (IN, 1010) NSPEC
```

```
000013          MSPECC = 1
                C
000014      110 READ (IN, 1030) TITLE
                C
                C     GO TO SUBROUTINE TO SET UP ARRAY OF VOIGT PROFILES
000022          CALL SEGMENT (IFILE, 3, S1, 0, 0)
000026          CALL VOIGT
                C
                C
                C     GO TO SUBROUTINE TO READ ATMOSPHERIC MODEL DATA AND DESIRED
                C     GEOMETRY AND CALCULATE TABLES OF ALTITUDES, TEMPERATURES AND
                C     SPECIES CONCENTRATIONS FOR DESIRED PATH
                C
                C     SUBROUTINE ALSO CALCULATES DOPPLER AND LORENTZ LINEWIDTH
                C     FACTORS FOR EACH ALTITUDE AND SPECIES
000027          CALL SEGMENT (IFILE, 3, S2, 0, 0)
000033          CALL HEIGHT
                C
                C     GO TO SUBROUTINE TO READ IN LINES, SORT, AND SET UP
                C     LIMITS FOR LINE OVERLAPPING
000034          CALL SEGMENT (IFILE, 3, S3, 0, 0)
000040          CALL LINER
                C
                C     GO TO SUBROUTINE TO CALCULATE ABSORPTION AND EMISSION COEFFICIENTS
                C     FOR EACH LINE AT EACH ALTITUDE
                C     ABSORPTION COEFFICIENT CORRECTED FOR SPONTANEOUS EMISSION
000041          CALL SEGMENT (IFILE, 3, S4, 0, 0)
000045          CALL COEFFS
                C
                C     AT LAST READY TO COMPUTE SPECTRUM
000046          CALL SEGMENT (IFILE, 3, S5, 0, 0)
000052          CALL SPECT
                C
                C     RETURN FROM SPECTRUM CALCULATION
                C     COMPUTE FOURIER TRANSFORM OF SPECTRUM
000053          CALL SEGMENT (IFILE, 3, S6, 0, 0)
000057          CALL TRANF
                C
                C     PLOT SPECTRUM AND TRANSFORM
000060          CALL SEGMENT (IFILE, 3, S7, 0, 0)
000064          CALL SPPLOT (MSPECC, MSPEC)
                C
                C     ARE ANY MORE SPECTRA TO BE CALCULATED
```

```
000066          IF (MSPECC .GE. MSPEC) GO TO 150
000071          MSPECC = MSPECC + 1
000072          GO TO 110
                C
000073    150   CONTINUE
000073          STOP
000075    1010  FORMAT (I2)
000075    1030  FORMAT (18A4)
000075          END
```

```
                      SUBROUTINE VOIGT
                C           SUBROUTINE TO SET UP TABLES OF VOIGT PROFILES FOR USE IN
                C           COMPUTING TRANSMISSION SPECTRA
                C     COMPUTES PROFILES FOR TABULATED VALUES OF X AND Y
                C     THEN FITS PARABOLA TO THREE CONSECUTIVE POINTS IN X,
                C     PROFILE TABLE CONTAINS PARABOLA COEFFICIENTS, NOT ACTUAL PROFILES
     000002           DOUBLE PRECISION CFREQ
     000002           COMMON  CFREQ(150)
     000002           COMMON  ABSB(150, 98), A(27,25), B(25,25), C(25,25),
                     1        PATH( 98), ATEMP( 98), CONC(3, 98), ALOR( 98), DOPP(3,98),
                     2                  STFQ(150), SPFQ(150), STRONG(150), ENGY(160),
                     3        TITLE(18), AQ(3), BQ(3), CQ(3), ALBEDO, GTEMP, GEMIS
     000002           COMMON  FSTART, FSTOP
     000002           COMMON  LTYPE(150), NTYPE(3), NLINE, NSPEC, IN, IOUT, ICASE
                C
                C     TABLES OF X AND Y COEFFICIENTS
     000002           DIMENSION X(27), Y(25), PHI(27,25)
     000002           EQUIVALENCE (PHI(1,1), A(1,1))
     000002           REAL K, K1, K2, K3
     000002           DATA  X / 0.00, 0.25, 0.50, 0.75, 1.00, 1.25, 1.50, 1.75, 2.00,
                     1          2.50, 3.00, 3.50, 4.00, 5.00, 6.00, 8.00, 10.00, 15.00,
                     2          20.00, 30.00, 50.00, 100.00, 500.00, 1000.00,
                     3          5000.00,  7500.00, 10000.00 /
     000002           DATA  Y / 0.00, 0.25, 0.50, 0.75, 1.00, 1.50, 2.00, 2.50, 3.00,
                     1          3.50, 4.00, 4.50, 5.00, 6.00, 7.00, 8.00, 9.00, 10.00,
                     2          12.00, 14.00, 16.00, 18.00, 20.00, 22.00, 24.00 /
     000002           CONST = SQRT( ALOG(2.0) / 3.141596)
                C
                C     LOOP FOR EVALUATING PROFILES
                C     K IS VOIGT PROFILE FUNCTION
     000010           DO 150 IY = 1,25
     000011           DO 150  IX = 1,27
     000012           XX = X(IX)
     000014           YY = Y(IY)
     000016   150     PHI(IX, IY) =  CONST * K(XX, YY)
                C
                C     ALL PROFILES CALCULATED
                C     NOW FIT PARABOLA TO GROUPS OF THREE X VALUES
     000031           DO 200  IY = 1,25
     000033           DO 200  IX = 1,25
     000034           YONE = PHI(IX, IY)
     000040           YTWO = PHI(IX+1, IY)
```

```
000043          YTHR = PHI(IX+2, IY)
000046          XONE = X(IX)
000047          XTWO = X(IX+1)
000051          XTHR = X(IX+2)
000052          XOSQ = XONE ** 2
000054          XTWS = XTWO **2
000055          XTHS = XTHR ** 2
          C     HAVE THREE LINEAR SIMULTANEOUS EQUATIONS IN THREE UNKNOWNS
          C     UNKNOWNS ARE PARABOLA COEFFICIENTS
          C     SOLVE USING DETERMINANTS
000057          DETN = XOSQ * XTWO + XONE * XTHS + XTWS * XTHR
                1      - XTHS * XTWO - XTHR * XOSQ - XTWS * XONE
000067          A(IX, IY) =  ( YONE * XTWO + XONE * YTHR + YTWO * XTHR
                1              -YTHR * XTWO - XTHR * YONE - YTWO * XONE) / DETN
000104          B(IX, IY) =  ( XOSQ * YTWO + YONE * XTHS + XTWS * YTHR
                1              -XTHS * YTWO - YTHR * XOSQ - XTWS * YONE) / DETN
000121   200    C(IX, IY) =  ( XOSQ * XTWO * YTHR + XONE * YTWO * XTHS
                1             + YONE * XTWS * XTHR - XTHS * XTWO * YONE
                2             - XTHR * YTWO * XOSQ - YTHR * XTWS * XONE) / DETN
000146          RETURN
000147          END
```

```
                      FUNCTION K(X,Y)
                C           THIS FUNCTION IS THE REAL PART OF THE COMPLEX PROBABILITY
                C           FUNCTION OR THE VOIGHT SPECTRUM LINE PROFILE
     000005           REAL K,K1,K2,K3
     000005           IF (Y.LT.1.0.AND.X.LT.4.0.OR.Y.LT.1.8/(X+1.0)) GO TO 300
     000023           IF (Y.LT.2.5.AND.X.LT.4.0) GO TO 200
     000033       100 K = K3(X,Y)
     000036           RETURN
     000037       200 K = K2(X,Y)
     000042           RETURN
     000043       300 K = K1(X,Y)
     000046           RETURN
     000047           END
```

```
                      FUNCTION K1(X,Y)
CCCCC5                REAL K1
CCCCC5                DOUBLE PRECISION C(34),COEF,BNC1,BNC2,BN,X1,F
                C     ENTER HUMMERS CHEBYSHEV COEFFICIENTS C(I)
CCCCC5                DATA C/  0.1999999999972224D+00,  -0.184CCCCCCC0299980+00,
                     1          0.1558399999965025D+00,  -0.1216640000043988D+00,
                     2          0.CB77081599940391D+CC,  -0.0585141248086907D+00,
                     3          0.0362157301623914D+00,  -0.0208497654398036D+00,
                     4          0.0111960116346270D+CC,  -0.5623189616710900D-02,
                     5          0.2648763417226500D-02,  -0.1173267075770400D-02,
                     6          0.4899519978C880CCD-03,  -0.1933630801528000D-03,
                     7          0.7228774467880000C-04,  -0.2565551249790000D-04,
                     8          0.8662C736841CCCCCD-C5,  -0.2787637971900000D-05,
                     9          0.8566873627000000C-06,  -0.2518433784000000D-06,
                     1          0.7C936022100000000-07,  -0.1917322570000000D-07,
                     2          0.4980125600000000-08,  -0.1244773400000000D-08,
                     3          0.2997777CCCCCCCCCD-09,  -0.6964500000000000D-10,
                     4          0.1562620CCCCCCCCCD-1C,  -0.3389700000000000D-11,
                     5          0.7116CCCCCCCCCCCCD-12,  -0.1447000000000000D-12,
                     6          0.285D-13,  -C.550D-14,   0.100D-14,  -0.200D-15/
CCCCC5                Y2 = Y**2
CCCCC5                IF ((X**2-Y2).GT.70.0) GO TO 2
CCCCC2                U1 = EXP(-X**2+Y2)*COS(2.*X*Y)
CCCC26                GO TO 5
CCCC27              2 U1 = C.0
CCCC30              5 IF (X.GT.5.0) GO TO 1000
                C     FROM HERE TO STATEMENT 30 WE CALCULATE DAWSONS FUNCTION
                C     CLENSHAWS ALGORITHM AS GIVEN BY HUMMER
CCCC34                BNC1 = 0.000
CCCC36                BNC2 = C.000
CCCC41                X1 = X/5.000
CCCC53                COEF = 4.000*X1**2-2.000
CCCC71                DO 20 I = 1,34
CCCC73                II = 35-I
CCCC74                BN = COEF*BNC1-BNC2+C(II)
CCC114                BNC2 = BNC1
CCC116             20 BNC1 = BN
CCC123             30 F = X1*(BN-BNC2)
CC0140             4C DNC1 = 1.0-2.0*X*SNGL(F)
CCC147           1100 DNC2 = SNGL(F)
CCC152                GO TO 1200
CCC154           1000  AX = C.0
```

```
000155          BX = 0.0
000155          CX = 0.0
000156          IF (X .GE. 1000.0)  GO TO 1005
000161          AX = 29.53125 / X**10
000163          BX = 162.4218 / X**12
000167          CX = 1055.7421 / X**14
000174    1005  DN01 = -(.5/X**2+.75/X**4+1.875/X**6+6.5625/X**8
                1        +AX + BX + CX )
000215          DN02 = (1.-DN01)/(2.*X)
000221    1200  FUNCT = Y*DN01
000222          IF (Y.LE.1.0E-08) GO TO 2500
000225          Q = 1.0
000226          YN = Y
000230          DO 2000 I = 2,50
000231          DN = (X*DN01+DN02)*(-2.)/FLOAT(I)
000237          DN02 = DN01
000237          DN01 = DN
000240          IF (MOD(I,2)) 2000,2000,1500
000245    1500  Q = -Q
000246          YN = YN*Y2
000250          G = DN*YN
000251          FUNCT = FUNCT+Q*G
000254          IF (ABS(G/FUNCT).LE.1.0E-08) GO TO 2500
000260    2000  CONTINUE
000262    2500  K1 = U1-1.12837917*FUNCT
000265          RETURN
000266          END
```

```
                FUNCTION K2(X,Y)
000005          REAL K2
000005          DIMENSION W(10), T(10)
000005          DATA W/4.62243670E-1,2.86675505E-1,1.09017206E-1,2.48105209E-2,
               1        3.24377334E-3,2.28338636E-4,7.80255648E-6,1.08606937E-7,
               2        4.39934099E-10,2.22939365E-13/
000005          DATA T/0.245340708,0.737473729,1.23407622,1.73853771,2.25497400,
               1        2.78880605,3.34785457,3.94476404,4.60368245,5.38748089/
000005          Y2 = Y * Y
000005          G = 0.0
000007          DO 100 I = 1,10
000010          R = T(I)-X
000012          S = T(I)+X
000013      100 G = G+(4.*T(I)**2-2.)*(R*ATAN(R/Y)+S*ATAN(S/Y)-.5*Y*(ALOG(Y2+R**2)
               1+ALOG(Y2+S**2)))*W(I)
000057          K2 = 0.31830988E6*G
000061          RETURN
000062          END
```

```
                      FUNCTION K3(X,Y)
000005                REAL K3
000005                DIMENSION W(10), T(10)
000005                DATA W/4.62243670E-1,2.86675505E-1,1.09017206E-1,2.48105209E-2,
                     1        3.24377334E-3,2.28338636E-4,7.80255648E-6,1.08606937E-7,
                     2        4.39934099E-10,2.22939365E-13/
000005                DATA T/0.24534070,0.737473729,1.23407622,1.73853771,2.25497400,
                     1        2.78880606,3.34785457,3.94476404,4.60368245,5.38748089/
000005                Y2 = Y * Y
000005                G = 0.0
000007                DO 100 I = 1,10
000010           100  G = G+(1.0E0/((X-T(I))**2+Y2)+1.0E0/((X+T(I))**2+Y2))*W(I)
000024                K3 = 0.31830988*Y*G
000026                RETURN
000027                END
```

```
                SUBROUTINE HEIGHT
          C     READS IN SPECIES AND MODEL ATMOSPHERE DATA AND GEOMETRY CASE
          C     COMPUTES TABLES OF PATH LENGTHS, CONCENTRATIONS,TEMPERATURES
          C     ALSO COMPUTES FACTORS FOR LORENTZ AND DOPPLER LINEWIDTHS
000002          DOUBLE PRECISION CFREQ
000002          COMMON  CFREQ(150)
000002          COMMON  ABSB(150, 98), A(27,25), B(25,25), C(25,25),
                1       PATH( 98), ATEMP( 98), CONC(3, 98), ALOR( 98), DOPP(3,98),
                2                  STFQ(150), SPFQ(150), STRONG(150), ENGY(160),
                3       TITLE(18), AQ(3), BQ(3), CQ(3), ALBEDO, GTEMP, GEMIS
000002          COMMON  FSTART, FSTOP
000002          COMMON  LTYPE(150), NTYPE(3), NLINE, NSPEC, IN, IOUT, ICASE
000002          DIMENSION FMASS(3), ALTAB(50), TEMTAB(50),  CONTAB(3,50),
                1         HINC(50), HTAB(100), SNAME(3), PRESTB(50), PRESS(98)
000002          DATA  REARTH, PI,     CLIGHT,  ALOSCH,     GAS,       FLOREN /
                1     6371.1, 3.1416, 3.0E+10, 2.6875E+19, 8.3144E+7, 0.06   /
000002          DATA  FLIMB/4HLIMB/ ,  SUN/4HSUNL/
          C
          C     READ THREE DIFFERENT SPECIES
          C     READ IN SPECIES NAME AND MOLECULAR WEIGHT
          C     READ NUMBER OF LINES OF THIS SPECIES TO BE INCLUDED
          C     ALSO READ COEFFICIENTS OF PARABOLA DESCRIBING PARTITION FUNCTION
000002          NSEC = 0
000003          NSPEC = 0
000004          DO 120  I = 1,3
000005          READ (IN, 1100) SNAME(I), FMASS(I), NTYPE(I), AQ(I), BQ(I), CQ(I)
          C     IS CARD BLANK
000024          IF (FMASS(I)) 140, 140, 120
000026    120   NSPEC = NSPEC + 1
          C
          C     READ GEOMETRY CASE AND APPROPIATE PARAMETERS
000032    140   READ (IN, 1250) WORD, NMOD, TEMP1, TEMP2, ALBEDO
          C
          C     READ MODEL ATMOSPHERE CHARACTERISTICS
          C     MODEL MUST GO FROM 0 TO 100 KM ALTITUDE
          C     ALTITUDE SCALE
000050          READ(IN, 1260) (ALTAB(I), I = 1, NMOD)
          C     TEMPERATURES
000063          READ(IN, 1260) (TEMTAB(I), I = 1, NMOD)
          C     PRESSURES
000076          READ(IN, 1300) (PRESTB(I), I = 1, NMOD)
          C     SPECIES CONCENTRATIONS
```

```
000111          DO 150  I = 1, NSPEC
000113    150   REAC (IN, 1300) (CONTAB(I,J), J = 1, NMOD)
              C
              C     WRITE TITLES
000131          WRITE (IOUT, 1360)  TITLE
000136          WRITE (IOUT, 1370) (SNAME(I), I = 1,NSPEC)
              C
              C     DETERMINE GEOMETRY CASE
              C     CASE 1. LOOKING AT BLACKBODY RADIATION FROM GROUND (4.6 MICRONS)
              C          2. LIMB TRANSMISSION (2.3 OR 4.6 MICRONS)
              C          3. DOUBLE PASS  SUN - GROUND - SATELLITE (2.3 MICRONS)
              C          4. SAME AS 3 BUT INCIDENT AND EXIT ANGLES EQUAL
000151          NALT = 49
000152          ICASE = 1
000153          IF (WORD .EQ. FLIMB) ICASE = 2
000156          IF (WORD .EQ. SUN  ) ICASE = 3
000161          GO TO (240, 170, 240, 240), ICASE
              C
              C     LIMB CASE
000171    170   GRAZE = TEMP1
              C     PATHLENGTH INCREMENT IS 1/48 OF TOTAL PATH THROUGH ATMOSPHERE
              C     ATMOSPHERE IS DEFINED TO STOP AT 100KM ALTITUDE
000173          TPATH= SQRT((REARTH + 100.0)**2 - (REARTH + GRAZE)**2)
              C     ASSUME PATH IS SYMETRICAL AND CALCULATE HALF
000203          PINC =TPATH/ 24.0
              C     FIRST POINT IN PATH IS AT 100KM
000205          PATH(1) = 0.0
000206          HTAB(1) = 100.0
000207          ATEMP(1) = TEMTAB(NMOD)
000211          PRESS(1) = PRESTB(NMOD)
000213          DO 180 I = 1, NSPEC
000214    180   CONC(I,1) = CONTAB(I,NMOD)
000223          DO 200  IP = 2, 25
000225          PATH(IP) = PATH(IP-1) + PINC
              C     COMPUTE ALTITUDE AT NEW PATH POINT
000230          TPATH = TPATH - PINC
000231          PALT = SQRT( TPATH**2 + (REARTH + GRAZE)**2)  - REARTH
000240          HTAB(IP) = PALT
              C     GO TO INTERPOLATION ROUTINE TO GET TEMPERATURE AND
              C     SPECIES CONCENTRATIONS AT GIVEN ALTITUDE
000242    200   CALL INTERP(PALT, NMOD, ALTAB, TEMTAB, PRESTB, CONTAB, NSPEC,
                 1            ATEMP, PRESS, CONC, IP)
              C     DO SECOND HALF OF PATH - MIRROR IMAGE
```

```
000257          DO 210  IP = 26, 49
000261    210   PATH(IP) = PATH(IP-1) + PINC
000265          DO 220  IP = 1, 25
000267          IPR = 50 - IP
000271          HTAB(IPR) = HTAB(IP)
000273          ATEMP(IPR) = ATEMP(IP)
000274          PRESS(IPR) = PRESS(IP)
000276          DO 220  I = 1,NSPEC
000277    220   CONC(I,IPR) = CONC(I,IP)
          C     FINISHED LIMB CASE - GO TO LINEWIDTH CALCULATIONS
000311          GO TO 360
          C
          C     EARTHSHINE AND DOUBLE PASS CASES
          C     COMPUTATIONS IDENTICAL EXCEPT DOUBLE PASS CASE REQUIRES
          C     SECOND CALCULATION AT EXIT ANGLE
          C     SKIP SECOND CALCULATION IF INCIDENT AND EXIT ANGLES EQUAL
          C
000312    240   ANGLE = TEMP1
000314          IF (ICASE .EQ. 3  .AND.  TEMP1 .EQ. TEMP2)  ICASE = 4
000325          N1 = 2
000326          N2 = 49
000327          N3 = 1
000330          IPASS = 1
          C     SET UP TABLE OF NOMINAL INCREMENTS
          C     ASSUME TOP  ALTITUDE OF 96KM
000331    245   I = 1
000332          DO 250 J = 1,3
000334          DO 250 K = 1,16
000335          HINC(I) = J
000340    250   I = I + 1
000344          HTOT = 96.0
          C     DETERMINE PATH LENGTH FROM GROUND TO 96KM FOR GIVEN ANGLE
          C     USING LAW OF COSINES GET QUADRATIC EQUATION
000346          AP = 1.0
000347          BP = -2.0 * REARTH * COS((180.0 - ANGLE) * (PI /180.0))
000357          CP = REARTH **2 - (HTOT + REARTH)**2
000362          PTOT =(- BP + SQRT(BP**2 - 4.0 * AP * CP)) / (2.0 * AP)
          C     INCREASE ALTITUDE INCREMENTS BY RATIO OF ACTUAL PATHLENGTH TO
          C     VERTICAL PATH LENGTH
000374          DO 270  I = 1,48
000375    270   HINC(I) = HINC(I) * PTOT / HTOT
          C     CALCULATE PATH PARAMETERS
          C     FIRST POINT IN PATH IS AT GROUND
```

```
000402          PATH(N3)= 0.0
000403          HTAE(N3) = 0.0
000404          ATEMP(N3)= TEMTAB(1)
000406          PRESS(N3) = PRESTB(1)
000407          DO 290 I = 1,NSPEC
000411    290   CONC(I,N3) = CONTAB(I,1)
000420          DO 310  I = 2, 49
000422          IP = I + NSEC
000424          PATH(IP) = PATH(IP - 1) + HINC(I - 1)
                C     CALCULATE HEIGHT AT EACH POINT IN PATH
                C     USE LAW OF COSINES
000427          PALT = SQRT(REARTH**2 + PATH(IP)**2 - 2.0 * REARTH * PATH(IP) *
               1             COS((180.0 - ANGLE) *(PI/180.0))) - REARTH
000450          HTAB(IP) = PALT
000452    310   CALL INTERP(PALT, NMOD, ALTAB, TEMTAB, PRESTB, CONTAB, NSPEC,
               1             ATEMP, PRESS, CONC, IP)
                C
                C     IF DOUBLE PASS GEOMETRY REPEAT FOR SECOND PASS
000467          GO TO (315, 350, 320, 350), ICASE
                C     GROUND TEMPERATURE AND EMISSIVITY PARAMETERS FOR CASE 1
000477    315   GTEMP = TEMP2
000501          IF (GTEMP .EQ. 0.0)  GTEMP = 288.2
000503          GEMIS = ALBEDO
000505          IF (GEMIS .EQ. 0.0)  GEMIS = 1.0
000507          GO TO 350
000510    320   GO TO (330, 350), IPASS
000516    330   IPASS = 2
000517          NALT = 98
000520          ANGLE = TEMP2
000522          N3 = 50
000523          NSEC = 49
000524          GO TO 245
000524    350   CONTINUE
                C
                C     COMPUTE TABLES TO BE USED IN CALCULATING DOPPLER AND
                C     LORENTZ LINEWIDTHS
000524    360   CONST1 = SQRT(2.0 * GAS * ALOG(2.0)) / CLIGHT
000534          CONST2 = SQRT(273.0)
000536          CONST3 = SQRT(ALOG(2.0))
000542          PRSTD = 1000.0
000543          DO 400  J = 1, NALT
000545          SRTEMP = SQRT(ATEMP(J))
000550          DO 380  I = 1, NSPEC
```

```
000551          TEMP = SQRT(FMASS(I))
000554    380   DOPP(I,J) = CONST1 * SRTEMP   /(TEMP * CONST3)
000564    400   ALOR(  J) = FLOREN * (PRESS(J)/PRSTD) * (CONST2/SRTEMP)
          C
          C     WRITE OPTICAL PATH PARAMETERS
000573          DO 450  J = 1,NALT
000574    450   WRITE (IOUT, 1350)  J, PATH(J), HTAB(J), ATEMP(J), PRESS(J),
                1                     (CONC(I,J), I = 1,NSPEC)
000624          GO TO (470, 490, 510, 530),  ICASE
000634    470   WRITE (IOUT, 1400)  GTEMP, GEMIS, ANGLE
000646          GO TO 550
000647    490   WRITE (IOUT, 1420)  GRAZE
000655          GO TO 550
000656    510   WRITE (IOUT, 1440)  TEMP1, TEMP2, ALBEDO
000670          GO TO 550
000671    530   WRITE (IOUT, 1460)  TEMP1, TEMP2, ALBEDO
000703    550   RETURN
          C
000704    1100  FORMAT (    A4, 5X, F10.8, I3, 7X, 3F10.8)
000704    1250  FORMAT (A4, 5X, I2, 8X, 3F10.8)
000704    1260  FORMAT ( 12F6.2)
000704    1300  FORMAT ( 6E10.2)
000704    1350  FORMAT  (3X, I2, 6X, 0PF7.2, 12X, F6.2, 11X, F6.2, 9X,
                1         0PE10.3, 6X, 0PE10.4, 5X, 0PE10.4, 5X, 0PE10.4)
000704    1360  FORMAT  (1H1, 30X, 18A4)
000704    1370  FORMAT  (1H0, 8X, 13HPATH DISTANCE, 7X, 8HALTITUDE, 8X,
                1          11HTEMPERATURE, 8X, 8HPRESSURE, 8X,
                2          37HSPECIES CONCENTRATIONS - PARTICLES/CC, /
                3          13X, 2HKM, 17X, 2HKM, 14X, 5HDEG K, 13X, 4HMBAR,
                4          9X, A4, 11X, A4, 11X, A4 /)
000704    1400  FORMAT  (// 45H GEOMETRY CASE 1 - GROUND BLACKBODY RADIATION /
                1             20H GROUND TEMPERATURE , F6.2, 6H DEG K /
                2             20H GROUND EMISSIVITY  , F5.3, /
                3             22H ZENITH VIEWING ANGLE , F6.3, 4H DEG )
000704    1420  FORMAT  (// 36H GEOMETRY CASE 2 - LIMB TRANSMISSION /
                1             18H GRAZING ALTITUDE , F7.3, 3H KM )
000704    1440  FORMAT  (// 37H GEOMETRY CASE 3 - REFLECTED SUNLIGHT /
                1             34H INCIDENT RADIATION ZENITH ANGLE  , F6.3, 4H DEG /
                3             34H REFLECTED RADIATION ZENITH ANGLE , F6.3, 4H DEG /
                4              8H ALBEDO , F5.3  )
000704    1460  FORMAT  (// 37H GEOMETRY CASE 4 - REFLECTED SUNLIGHT /,
                1             37H INCIDENT AND REFLECTED ANGLES EQUAL  /,
                2             34H INCIDENT RADIATION ZENITH ANGLE  , F6.3, 4H DEG /
```

```
                2           34H REFLECTED RADIATION ZENITH ANGLE , F6.3, 4H DEG /
                3            8H ALBEDO , F5.3  )
  C00704         END
```

```
      SUBROUTINE INTERP (PALT, NMOD, ALTAB, TEMTAB, PRESTB, CONTAB,
     1                   NSPEC, ATEMP, PRESS, CONC, IP)
C          SUBROUTINE TO DO INTERPOLATIONS OF MODEL ATMOSPHERE DATA TO
C          GET PARAMETERS ALONG PATH
C
000016     DIMENSION  ALTAB(50), TEMTAB(50), CONTAB(3,50), CONC(3,98),
     1            ATEMP(98), PRESTB(50), PRESS(98)
C
C     INTERPOLATE TO GET TEMPERATURE AND SPECIES CONCENTRATIONS
000016     DO 200  IK = 1, NMOD
000017     IF (PALT .GE. ALTAB(IK))  GO TO 200
C     LINEAR TEMPERATURE INTERPOLATION
000022     ATEMP(IP) =  ((PALT - ALTAB(IK-1))  * (TEMTAB(IK) - TEMTAB(IK-1)))
     1              /(ALTAB(IK) - ALTAB(IK-1)) + TEMTAB(IK-1)
C
C     LOGARITHMIC INTERPOLATION OF PRESSURE
000037     PRESS(IP) = (PALT - ALTAB(IK-1)) *
     1            (ALOG10(PRESTB(IK)) - ALOG10(PRESTB(IK-1)))
     2            / (ALTAB(IK) - ALTAB(IK-1))
     3            + ALOG10(PRESTB(IK-1))
000103     PRESS(IP) = 10.0 ** PRESS(IP)
C
C     LOGARITHMIC INTERPOLATION OF SPECIES CONCENTRATIONS
000110     DO 150  IS= 1, NSPEC
000112     IF (CONTAB(IS,IK) .NE. 0.0 .AND. CONTAB(IS,IK-1) .NE. 0.0)
     1    GO TO 140
000124     CONC(IS,IP) = 0.0
000130     GO TO 150
000130 140 CONC(IS, IP)  =  ( PALT - ALTAB(IK-1)) *
     1                 (ALOG10(CONTAB(IS, IK))- ALOG10(CONTAB(IS,IK-1)))
     2                 / (ALTAB(IK) - ALTAB(IK-1)) +
     3                   ALOG10(CONTAB(IS, IK-1))
000200     CONC(IS, IP) = 10.0 ** CONC(IS, IP)
000207 150 CONTINUE
000212     GO TO 250
000212 200 CONTINUE
000215 250 RETURN
000216     END
```

```
                      SUBROUTINE LINER
                C           RCUTINE TO READ IN SPECTRAL LINES, SORT AND SET UP
                C           LIMITS FOR LINE CVERLAPPING
 000002                DOUBLE PRECISICN CFREQ
 000002                COMMCN  CFREQ(150)
 CCCC02                COMMCN  ABSB(150, 98), A(27,25), B(25,25), C(25,25),
                     1         PATH( 98), ATEMP( 98), CONC(3, 98), ALOR( 98), DOPP(3,98),
                     2                   STFQ(150), SPFQ(150), STRONG(150), ENGY(160),
                     3         TITLE(18), AQ(3), BQ(3), CQ(3), ALBEDO, GTEMP, GEMIS
 000002                COMMCN  FSTART, FSTOP
 000002                COMMCN  LTYPE(150), NTYPE(3), NLINE, NSPEC, IN, IOUT, ICASE
                C
 000002                DIMENSICN  IXST(150), STRT(150), ENGT(150), LTYPT(150)
 000002                DIMENSICN FNAMT(150), FNAME(150)
 CCCC02                DOUBLE PRECISICN DTEMP
 CCCC02                PERCNT = 1.0
                C
                C     READ IN SPECIFIED NUMBER OF LINES FOR EACH SPECIES
                C     ASSIGN SPECIES ID NUMBER TO EACH LINE AND COUNT LINES
 CCCCC4                NLINE = 0
 CCCCC5                DO 150  IT = 1,NSPEC
 CCCCC6                NL = NTYPE(IT)
 CCCCIC          140   NSTAR = NLINE + 1
 CCCCI2                NLINE = NLINE + NL
 CCCCI3                DO 145  I = NSTAR, NLINE
 CCCCI5                READ (IN, 1200)  FNAMT(I), TEMP, STRT(I), ENGT(I)
 CCCC3C          145   CFREQ(I) = TEMP
 CCCC35                DO 150  I = NSTAR, NLINE
 CCCC37          150   LTYPT(I) = IT
 CCCC45          170   CONTINUE
                C
                C     SET UP DUMMY INDEX TABLE SHOWING ORIGINAL LINE SEQUENCE
 CC0045                DO 205  I = 1, NLINE
 CCCC47          205   IXST(I) = I
                C
                C     SET UP TABLE OF FREQUENCY BANDS TO BE CONSIDERED FOR EACH LINE
                C     FIRST ARRANGE ALL LINES IN INCREASING ORDER OF CENTER FREQUENCY
 CC0052                N2 = NLINE
 CC0053                N1 = NLINE - 1
 CCCC55                DO 210  J = 1, N1
 CCCC56                N2 = N2 - 1
 CCCC60                DO 210  I = 1, N2
```

```
000061          IF (CFREQ(I+1) .GT. CFREC(I)) GO TO 210
000066          DTEMP = CFREC(I)
000070          CFREQ(I) = CFREC(I+1)
000074          CFREC(I+1) = DTEMP
                C     SWAP INDEX NUMBERS
000100          NTEMP = IXST(I)
000102          IXST(I) = IXST(I+1)
000103          IXST(I+1) = NTEMP
000105    210   CONTINUE
                C
                C     HAVE SORTED CENTER FREQUENCIES AND INDEX NUMBER
                C     NOW SORT REST OF INDIVIDUAL LINE PARAMETERS
000112          DO 220  J = 1, NLINE
000114          I = IXST(J)
                C
                C     LINE STRENGTHS
000116          STRONG(J) = STRT(I)
                C
                C     ENERGY VALUES
000120          ENGY(J) = ENGT(I)
                C
                C     LINE TYPE
000121          LTYPE(J) = LTYPT(I)
                C
                C     LINE NAME
000123          FNAME(J) = FNAMT(I)
000124    220   CONTINUE
                C
                C     NOW FIND WEAKEST LINE
000126          TEMP = STRONG(1)
000130          DO 240  J = 2,NLINE
000131          IF (STRONG(J) .GT. TEMP) GO TO 240
000135          TEMP = STRONG(J)
000136    240   CONTINUE
                C     THRESHOLD STRENGTH DEFINED AS PERCENTAGE OF WEAKEST LINE
                C     DESIRED PERCENTAGE IS INPUT DATA
000141          THRESH = PERCNT * TEMP / 100.0
                C     CALCULATE FREQUENCY AT WHICH EACH LINE REACHES THRESHOLD
                C     ASSUME NOMINAL LORENTZ HALF-HALFWIDTH OF 0.06 CM-1
000143          WIDTH = 0.06
000145          TEMP = WIDTH / THRESH
000146          DO  260  J = 1, NLINE
000150          DELF = SQRT(STRONG(J) * TEMP  - WIDTH**2)
```

```
000156          IF (DELF .GT.  5.0) DELF =  5.0
000161          STFQ(J) = CFREQ(J) - DELF
000170   260    SPFQ(J) = CFREQ(J) + DELF
               C
               C     HAVE NOW DEFINED FREQUENCY BAND OVER WHICH EACH LINE MUST
               C     BE CONSIDERED
000201          WRITE (IOUT, 1210)  TITLE
000206          DO 280  J = 1, NLINE
000210          TEMP = CFREQ(J)
000213   280    WRITE (IOUT, 1220)  J, FNAME(J), TEMP, STFQ(J), SPFQ(J),
              1                          STRENG(J), ENGY(J)
000237          RETURN
000240   1200   FORMAT  (A6, 3X, F10.3, E10.4, F10.3)
000240   1210   FORMAT  (1H1, 30X, 18A4, //, 17X, 4HLINE, 8X, 11HLINE CENTER,
              1          6X, 19HLINE INCLUSION BAND, 11X, 13HLINE STRENGTH, 10X,
              2          18HLOWER STATE ENERGY / 29X, 11HWAVENUMBERS, 6X,
              3          5HSTART, 9X, 4HSTOP, 14X, 10HCM-2 ATM-1, 14X,
              4          11HWAVENUMBERS / )
000240   1220   FORMAT  (5X, I3, 7X, A6,10X, F8.3, 6X, F8.3, 5X, F8.3, 10X,
              1          F11.8, 16X, F9.4)
000240          END
```

```
                SUBROUTINE COEFFS
C                    SUBROUTINE TO COMPUTE FACTORS USED IN ABSORPTION AND
C                    EMISSION COEFFICIENTS
C
C       INPUTS ARE
C       ENERGY OF EACH TRANSITION IN WAVENUMBERS
C       LINE STRENGTHS AT STP IN  CM**-2 * ATM**-1
C       SPECIES NUMBER DENSITIES AND TEMPERATURES AS FUNCTION
C       OF ALTITUDE  -  DERIVED IN SUBROUTINE HEIGHT
C       RATIO OF PARTITION FUNCTIONS AT T AND 300K
C       PARTITION FUNCTION IS INPUT AS PARABOLIC COEFFICIENTS
C
000002          DOUBLE PRECISION CFREQ
000002          COMMON  CFREQ(150)
000002          COMMON  ABSB(150, 98), A(27,25), B(25,25), C(25,25),
               1        PATH( 98), ATEMP( 98), CONC(3, 98), ALOR( 98), DOPP(3,98),
               2                  STFQ(150), SPFQ(150), STRONG(150), ENGY(160),
               3        TITLE(18), AQ(3), BQ(3), CQ(3), ALBEDO, GTEMP, GEMIS
000002          COMMON  FSTART, FSTOP
000002          COMMON  LTYPE(150), NTYPE(3), NLINE, NSPEC, IN, IOUT, ICASE
000002          DIMENSION EMIS(150, 49), QZERO(3)
000002          EQUIVALENCE (ABSB(1, 50), EMIS(1, 1))
000002          DATA    AN,          CTWO,   TZERO /
               1        2.6875E+19, 1.4388, 300.0 /
C         2 * C**2 * H
000002          CH = 2.0 * 2.99791E+10**2 * 6.6252E-34 * 1.0E+07
C
000006          NALT = 49
000007          IF (ICASE .EQ. 3) NALT = 98
C
C       CALCULATE PARTITION FUNCTIONS FOR EACH SPECIES AT 300 DEG
000012          DO 150  I = 1,NSPEC
000014   150    QZERO(I) = AQ(I) * TZERO**2 + BQ(I) * TZERO + CQ(I)
C
000024          DO 200  I = 1, NLINE
000025          IT = LTYPE(I)
000027          TEXP = -CTWO * CFREQ(I) / TZERO
000044          GC1 = 1.0 - EXP(TEXP)
000047          F3 = CFREQ(I) ** 3
C
000054          DO 200  J = 1, NALT
000055          TEMP = ATEMP(J)
```

```
      C     RATIO OF PARTITION FUNCTIONS  Q(300) / Q(T)
000057      QRAT = QZERO(IT) / (AQ(IT) * TEMP**2 + BQ(IT) * TEMP + CQ(IT))
      C
000065      GC2 = (CONC(IT, J) / AN) * EXP(ENGY(I) * CTWO *
     1                                (1.0/TZERO - 1.0/TEMP))
000102      TEXP = -CTWO * CFREQ(I) / TEMP
000120      GC3 = EXP(TEXP)
000122      ABSB(I,J) = GC2 *((1.0 - GC3) / GC1)* STRONG(I) * QRAT
      C     SKIP EMISSION TERM IF GEOMETRY CASE 3 OR 4
000132      GO TO (180, 180, 200, 200),  ICASE
000142  180 EMIS(I,J) = GC2 * (GC3 / GC1)* CH * STRONG(I) * F3 * QRAT
000153  200 CONTINUE
000160      RETURN
000161      END
```

```
                      SUBROUTINE SPECT
                C           SUBROUTINE TO COMPUTE SPECTRA
                C           USES TABULATED ABSORPTION AND EMISSION COEFFICIENTS,
                C           VOIGT PROFILES AND ALTITUDES
 000002                 DOUBLE PRECISION CFREQ
 000002                 COMMON  CFREQ(150)
 000002                 COMMON  ABSB(150, 98), A(27,25), B(25,25), C(25,25),
                       1        PATH( 98), ATEMP( 98), CONC(3, 98), ALOR( 98), DOPP(3,98),
                       2                  STFQ(150), SPFQ(150), STRONG(150), ENGY(160),
                       3        TITLE(18), AQ(3), BQ(3), CQ(3), ALBEDO, GTEMP, GEMIS
 000002                 COMMON  FSTART, FSTOP
 000002                 COMMON  LTYPE(150), NTYPE(3), NLINE, NSPEC, IN, IOUT, ICASE
 000002                 DOUBLE PRECISION FREQ(101),  FREQD, DELF, DTEMP
 000002                 DIMENSION   AITEN(101), DIFF(2), XX(25), YY(25), SINGF(101)
 000002                 DIMENSION  EMISC(50), ABSBC(50), LTAB(50)
 000002                 DIMENSION  ABINT(50), EMH(50)
 000002                 DIMENSION  YIN1(23), YIN2(23), YIN3(23)
 000002                 DIMENSION EMIS(150, 49)
 000002                 EQUIVALENCE (ABSB(1, 50), EMIS(1, 1))
 000002                 DATA XX / 0.00, 0.25, 0.50, 0.75, 1.00, 1.25, 1.50, 1.75, 2.00,
                       1          2.50, 3.00, 3.50, 4.00, 5.00, 6.00, 8.00, 10.00, 15.00,
                       2          20.00, 30.00, 50.00, 100.00, 500.00, 1000.00, 5000.00/
 000002                 DATA YY / 0.00, 0.25, 0.50, 0.75, 1.00, 1.50, 2.00, 2.50, 3.00,
                       1          3.50, 4.00, 4.50, 5.00, 6.00, 7.00, 8.00, 9.00, 10.00,
                       2          12.00, 14.00, 16.00, 18.00, 20.00, 22.00, 24.00 /
                C
 000002                 ITAPE = 2
 000003                 REWIND ITAPE
                C       READ LIMITS OF SPECTRUM TO BE COMPUTED
 000005                 READ (IN, 1570) FSTART, FSTOP
 000015                 NALT = 49
 000016                 NSEC = 0
 000017                 TLN2 = ALOG10(2.0)
 000022                 ALN2 = SQRT(ALOG(2.0))
 000026                 IF (ICASE .LE. 2)  ALBEDO = 1.0
                C
                C
                C       SET UP FACTORS TO BE USED IN VOIGT FUNCTION INTERPOLATION
 000032                 DO 140  I = 1,23
 000034                 YIN1(I) = 1.0 / ((YY(I) - YY(I+1)) * (YY(I) - YY(I+2)))
 000041                 YIN2(I) = 1.0 / ((YY(I) - YY(I+1)) * (YY(I+1) - YY(I+2)))
 000046    140          YIN3(I) = 1.0 / ((YY(I) - YY(I+2)) * (YY(I+1) - YY(I+2)))
```

```
            C
            C     CONSTANTS FOR IZERO COMPUTATION
            C     I(BLACKBODY) = 2* H*C**2 * WAVENO**3 (EXP(H*C*WAVENO/K*T) -1)**-1
            C     IF GEOMETRY CASE 1, T = 288.2K UNLESS SPECIFIED OTHERWISE
            C     IF CASE 2 OR 3, T = 5800K, BUT BLACKBODY IS PER CM**2 OF SOLAR
            C     SURFACE.  THEREFORE MUST MULTIPLY BY SOLAR SURFACE AREA AND
            C     DIVIDE BY DISTANCE TO SUN SQUARED
            C     AREA = 6.087E22 CM**2
            C     DISTANCE = 1.49599E13 CM
  000055          GO TO (142, 144, 144, 144),  ICASE
            C     GROUND SOURCE TEMPERATURE
  000065    142   T = GTEMP
            C     2 * H * C**2 * GROUND EMISSIVITY
  000067          BBCON = 1.19089OE-12 * GEMIS
  000071          GO TO 150
            C     SOLAR SOURCE TEMPERATURE
  000071    144   T = 5800.0
            C     2 * H * C**2 * AREA OF SUN / DISTANCE TO SUN**2
  000073          BBCON = 3.120376E-16
            C
            C     FOR EACH FREQUENCY POINT FIRST DETERMINE PERMISSABLE INCREMENT
  000074    150   NLAST = 1
  000075          FREQ(2) = FSTART
  000077          NFREQ = 0
            C     CALCULATE SPECTRUM IN 100 POINT GROUPS
  000100          WRITE (IOUT,1550) TITLE
  000106    280   DO 580  NPT = 2,101
  000110          IF (NFREQ  .EQ. 0)  GO TO 355
            C     DETERMINE DISTANCE TO NEAREST LINE
  000111          DIFF(1) = 100.0
  000112          DIFF(2) = 100.0
  000113          DO 330 I = NLAST, NLINE
            C     NEAREST LINE AT LOWER FREQUENCY
  000115          TEMP = FREQ(NPT-1) - CFREQ(I)
  000124          ATEMP = ABS(TEMP)
  000126          IF (ATEMP .LT. 0.001)  GO TO 320
  000130          IF (TEMP) 310 , 320, 300
  000131    300   DIFF(1) = TEMP
  000133          GO TO 330
            C     NEAREST LINE AT HIGHER FREQUENCY
  000133    310   DIFF(2) = ATEMP
  000135          JLN = I
  000136          GO TO 335
```

```
      C     IF EXACTLY AT LINE CENTER USE SMALLEST FREQUENCY INCREMENT
000137  320   DELF = 1.0D-03
000142        GO TO 350
000142  330   CONTINUE
000145        GO TO 340
000145  335   IF (JLN .GT. 1)  NLAST = JLN - 1
      C
      C     NOW HAVE DISTANCES TO NEAREST LINES AT LOWER AND HIGHER FREQUENCY
      C     CALCULATE APPROPRIATE INCREMENT FOR SMALLER OF TWO DISTANCES
      C     CRITERION IS FIRST INCREMENT IS 0.001 CM**-1
      C     AT EVERY SECOND POINT INCREMENT DOUBLES
000151  340   TEMP = DIFF(1)
000153        IF (DIFF(1) .GT. DIFF(2)) TEMP = DIFF(2)
000156        IF (TEMP .LT. 1.0)  GO TO 345
000161        DELF = 5.12D-01
000163        GO TO 350
      C     EXPRESSED ANALYTICALLY, DELF = 2**(N-1)
      C     WHERE 2**N = DIFF + 0.002
      C        I.E.  N =  LOG(DIFF + 0.002) / LOG 2
000164  345   N = ALOG10(TEMP     * 1000.0 + 2.0) / TLN2
000174        DTEMP = 2 ** (N-1)
000202        DELF = DTEMP / 1.0D+03
      C     NEXT FREQUENCY POINT
000215  350   FREQ(NPT) = FREQ(NPT-1) + DELF
000225  355   FREQC = FREQ(NPT)
000230        SINGF(NPT) = FREQC
000232        FREQD = FREQ(NPT)
      C
000234        NFREQ = NFREQ + 1
000236        NPTS = NPT
000237        NINC = 0
      C
      C     COMPUTE BLACK BODY SOURCE INTENSITY (IZERO) FOR NEW FREQUENCY
      C     APPROPRIATE CONSTANTS SET UP EARLIER
000240        AIZERO = (BBCON * FREQC**3) / (EXP(1.43868 * FREQC /T) -1.0)
      C
      C     AT NEW FREQUENCY MUST DETERMINE WHICH LINES ARE TO BE INCLUDED
      C     SCAN LIST  OF STARTING FREQUENCIES
000250        DO 360  I = 1,NLINE
000252        IF (FREQC .LT. STFQ(I))  GO TO 360
000255        IF (FREQC .GT. SPFQ(I))  GO TO 360
      C     LINE MUST BE INCLUDED
      C     PUT INDEX NUMBER OF LINE IN TABLE
```

```
000260          NINC = NINC + 1
000261          LTAB(NINC) = I
000263    360   CONTINUE
000266          IF (NINC) 365, 365, 370
000267    365   AITEN(NPT) = AIZERO * ALBEDO
000272          GO TO 580
                C
                C     HAVE LIST OF LINES TO BE INCLUDED AT THIS FREQUENCY
                C     MUST NOW COMPUTE ABSORPTION AND EMISSION COEFFICIENTS FOR
                C     EACH LINE AND ADD TOGETHER
                C     MUST DO FOR EACH ALTITUDE STEP
                C
                C     SET UP LOGIC FOR THREE DIFFERENT GEOMETRIES
                C        1. LOOKING AT BLACKBODY RADIATION FROM GROUND (4.6 MICRONS)
                C        2. LIMB TRANSMISSION (2.3 OR 4.6 MICRONS)
                C        3. DOUBLE PASS  SUN - GROUND - SATELLITE  (2.3 MICRONS)
                C        4. SAME AS 3 BUT INCIDENT AND EXIT ANGLES EQUAL
                C     CASES 1 AND 2 HANDLED IDENTICALLY, EXCEPT FOR ADJUSTMENT OF IZERO
                C     FOR CASE 3 COMPUTE INTENSITY AT GROUND FROM FIRST PASS
                C     USE INTENSITY AS NEW IZERO FOR SECOND PASS
                C     FOR CASE 4 JUST DOUBLE ABSORPTION CALCULATED IF FIRST PASS
000272    370   GO TO (400, 400, 390, 390), ICASE
                C
000302    390   IPASS = 1
000303          NSEC = 0
000304    400   DO 490 IH = 1, NALT
                C     FOR EACH ALTITUDE MUST INCLUDE ALL LINES
000306          IHN = IH + NSEC
000310          ABSLM = 0.0
000311          EMSUM = 0.0
000312          ALORN = ALOR(IHN)
000314          DO 480 ILT= 1, NINC
000315          IL = LTAB(ILT)
                C
                C     SKIP CALCULATION IF SPECIES HAS ZERO CONCENTRATION
                C     E.G. H2O AT HIGH ALTITUDES
000317          ABCOEF  = ABSB(IL,IHN)
000323          IF (ABCOEF .EQ. 0.0)  GO TO 480
                C
                C     CALCULATE DOPPLER, LORENTZ WIDTHS, X,  Y  FOR EACH LINE
000324          IT = LTYPE(IL)
000325          DOPW = DOPP(IT, IHN) * CFREQ(IL)
000334          TEMP = FREQD - CFREQ(IL)
```

```
000343          X = ABS(TEMP) / DOPW
000346          Y = ALORN / DOPW
000347          DOPW = 1.0/(DOPW * ALN2)
                C
                C     GIVEN X AND Y COORDINATES, GET VOIGT FUNCTION
                C     FIND X AND Y IN TABLES OF STANDARD VALUES
000351          IX = 25
000352          DO 420 I = 2,25
000354          IF (X .GE. XX(I)) GO TO 420
000357          IX = I - 1
000361          GO TO 430
000361    420   CONTINUE
000363    430   IY = 23
000364          DO 435 I = 2,23
000366          IF (Y .GE. YY(I))  GO TO 435
000371          IY = I - 1
000373          GO TO 440
000373    435   CONTINUE
                C     COMPUTE THREE VOIGT PROFILES FOR THREE CONSECUTIVE Y VALUES
000375    440   VONE = X * (X * A(IX, IY) + B(IX, IY)) + C(IX, IY)
000407          IZ = IY + 1
000411          VTWO = X * (X * A(IX, IZ) + B(IX, IZ)) + C(IX, IZ)
000423          IZ = IZ + 1
000425          VTHR = X * (X * A(IX, IZ) + B(IX, IZ)) + C(IX, IZ)
                C     NOW DO THREE POINT LAGRANGE INTERPOLATION
000437          T1 = Y - YY(IY)
000442          T2 = Y - YY(IY+1)
000443          T3 = Y - YY(IY+2)
000445          VPROF =  T2 * T3 * YIN1(IY) * VONE - T1 * T3 * YIN2(IY) * VTWO
               1       + T1 * T2 * YIN3(IY) * VTHR
                C
                C     HAVE VOIGT  FUNCTION, COMPUTE ABSORPTION AND EMISSION COEFFICIENTS
                C     SKIP EMISSION IF CASE 3 OR 4
000456          VPROF = VPROF * DOPW
000460          GO TO (460, 460, 470, 470),  ICASE
000470    460   EMSUM = EMSUM + EMIS(IL,IH) * VPROF
000476    470   ABSUM = ABSUM + ABCOEF * VPROF
000501          IF (NFREQ .NE. 29)  GO TO 480


000533    480   CONTINUE
000536          EMISC(IH) = EMSUM
000540    490   ABSBC(IH) = ABSUM
```

```
C
C     ABSORPTION AND EMISSION COEFFICIENTS COMPUTED FOR ALL CONTRIBUTING
C     LINES AT ALL ALTITUDES
C     NOW INTEGRATE OVER ALTITUDE USING SIMPSON'S RULE
C
C     INTEGRATE ABSORPTION OVER TWO INCREMENTS
000544      N2 = NALT - 2
C     IF THIS IS CASE 3 OR 4 DO ALTERNATE INTEGRATION EXCLUDING EMISSION
000546      GO TO (500, 500, 555, 555),  ICASE
000556  500 DO 510  I = 1,N2,2
000560  510 ABINT(I) = (ABSBC(I) + 4.0*ABSBC(I+1) + ABSBC(I+2)) *
           1                ((PATH(I+1) - PATH(I)) * 0.3333E+5)
000572      ABINT(NALT) = 0.0
C
C     CALCULATE EMISSION AT EACH ALTITUDE, AS DIMINISHED BY ABSORPTION
000574      TEMP = 0.0
000575      DO 530  I = 1,N2,2
000576      IREV = N2 - I + 1
000601      TEMP = TEMP + ABINT(IREV)
000603  530 EMH(IREV) = EMISC(IREV) * EXP(-TEMP)
000613      EMH(NALT) = EMISC(NALT)
C
C     NOW INTEGRATE EMISSION OVER ALTITUDE
000615      N2 = NALT - 4
000617      TEMP2 = 0.0
000617      DO 550  I = 1,N2,4
000621  550 TEMP2 = TEMP2 + (EMH(I) + 4.0 * EMH(I+2) + EMH(I+4)) *
           1                ((PATH(I+1) - PATH(I)) * 0.66667E+5)
000635  552 AITEN(NPT) = AIZERO * EXP(-TEMP) + 1.0E-7 * TEMP2
000645      GO TO 580
C
C     ALTERNATE INTEGRATION OF ABSORPTION FOR GEOMETRY CASE 3 OR 4
000645  555 TEMP = 0.0
000646      DO 557  I = 1,N2, 2
000650      IHN = I + NSEC
000652  557 TEMP = TEMP + (ABSBC(I) + 4.0*ABSBC(I+1) + ABSBC(I+2)) *
           1             ((PATH(IHN+1) - PATH(IHN)) * 0.33333E+5)
000666      AITEN(NPT) = AIZERO * EXP(-TEMP)
000674      IF (ICASE .NE. 4)  GO TO 560
000676      AITEN(NPT) = AITEN(NPT) * ALBEDO * EXP(-TEMP)
000705      GO TO 580
C
C     READ FOR SECOND PASS
```

```
000705    560   GO TO (565, 580), IPASS
000713    565   IPASS = 2
000714          NSEC = 49
000715          AIZERO = AITEN(NPT) * AL8ECO
000720          GO TO 400
          C
          C     STOP IF END FREQUENCY IS REACHED
000720    580   IF (FREQC .GT. FSTOP) GO TO 600
          C
          C     END OF LOOP FOR 100 POINTS
          C     WRITE POINTS AND DO NEXT 100 UNLESS END OF SPECTRUM WAS REACHED
000726    600   WRITE (IOUT, 1500)  (SINGF(NPT), AITEN(NPT), NPT = 2, NPTS)
000743          WRITE(ITAPE) (NPTS, ((FREQ(I), AITEN(I)), I = 2,NPTS))
000761          FREQ(1) = FREQ(101)
000764          IF (FREQC .LT. FSTOP)  GO TO 620
000766          WRITE (IOUT, 1560) NFREQ
000774          END FILE ITAPE
000776          REWIND ITAPE
001000          RETURN
          C     START NEW PAGE EVERY 200 POINTS
001001    620   IF (NFREQ .NE. 200*(NFREQ/200))  GO TO 280
001006          WRITE (IOUT, 1550) TITLE
001014          GO TO 280
001015    1500  FORMAT  (5 (1X, F10.4, 2X, E11.4, 2X))
001015    1550  FORMAT  (1H1,5X 18A4 ,5X 16HFREQ(CM**-1) VS
                1          27HINTENSITY(W/CM**2 - CM**-1) , /
                2          5 (26H  FREQUENCY    INTENSITY  ))
001015    1560  FORMAT  (// 28H THIS SPECTRUM CONSISTED OF , I4, 7H POINTS )
001015    1570  FORMAT  (2F9.3)
001C15          END
```

```
                SUBROUTINE TRANF
      C         SUBROUTINE TO CONVERT SPECTRUM CALCULATED ABOVE ON VARIABLE
      C         WAVENUMBER SCALE TO UNIFORM SCALE AND TAKE FOURIER TRANSFORM
      C         OF RESULTANT SPECTRUM
      C     ALSO MULTIPLIES SPECTRUM BY INPUT FILTER BANDPASS DATA
      C
      C
000002          DOUBLE PRECISION CFREQ
000002          COMMON  CFREQ(150)
000002          COMMON  ABSB(150, 98), A(27,25), B(25,25), C(25,25),
               1        PATH( 98), ATEMP( 98), CONC(3, 98), ALOR( 98), DOPP(3,98),
               2                  STFQ(150), SPFQ(150), STRONG(150), ENGY(160),
               3        TITLE(18), AQ(3), BQ(3), CQ(3), ALBEDO, GTEMP, GEMIS
000002          COMMON  FSTART, FSTOP
000002          COMMON  LTYPE(150), NTYPE(3), NLINE, NSPEC, IN, IOUT, ICASE
      C
000002          DIMENSION  FILTER(4100),  SPCTRM(4100), ZERO(4100), ARRAY(18),
               1           FWAVE(50), FRESP(50), SPECT(101), SFREQ(4100),
               2           DINT(2050), BINT(2050), PINT(2050),
               3           ALINE(101), BLINE(101)
000002          DOUBLE PRECISION AFREQ(4100), FREQ(101), DELF, DTEMP,
               1                 FWAVE, CENTER, FLAST, DELF2
      C
000002          EQUIVALENCE (AFREQ(1), ABSB(1,1)),(FILTER(1), ABSB(1,56)),
               1           (SPCTRM(1), ABSB(1,84))
000002          EQUIVALENCE (AFREQ(1), ZERO(1))
000002          EQUIVALENCE (FILTER(1), SFREQ(1))
000002          EQUIVALENCE (FILTER(1), BINT(1)), (FILTER(2051), PINT(1))
000002          EQUIVALENCE (AFREQ(2051), DINT(1))
      C
000002          DATA  ENDF/4HEND /, FNONE/4HNONE/, PUNCH/4HPUNC/, PFON/4HPOWE/,
               1      GAUSS/4HGAUS/, FLOR/4HLORE/, CAL/4HCALC/
000002          ITAPE = 2
      C
      C         READ PLOT LIMIT DATA CARD
000003          READ (IN, 2000) N2POW,FLEFT, FRIGHT, FREF, YBOT, YTOP, PWORD
000025          READ (IN, 2010) DSCALE, DSTART, DSTOP
      C         SET DEFAULT OPTIONS
      C         NUMBER OF POINTS (POWER OF 2, MAX 2**12 = 4096)
000037          IF (N2POW .EQ. 0) N2POW = 12
000041          NPOINT = 2 ** N2POW
000045          FNPT = NPOINT
```

```
      C     INTERFERCMETER PLOT SCALE
000047        IF (DSCALE .EQ. 0.0) DSCALE = 0.1
000051        IF (DSTOP .EQ. 0.0) DSTOP = 1.4
      C     SET SPECTRAL LIMITS TO LIMITS COMPUTED ABOVE OR PLOTTING LIMITS
      C        WHICHEVER IS SMALLER
000053        IF (FLEFT  .EQ. 0.0)  FLEFT = FSTART
000055        SSTART = FSTART
000057        IF (FLEFT .GT. FSTART) SSTART = FLEFT
000062        IF (FRIGHT .EQ. 0.0) FRIGHT = FSTOP
000064        SSTOP = FSTOP
000066        IF (FRIGHT .LT. FSTOP) SSTOP  = FRIGHT
      C
      C     FREQUENCY SCALE INCREMENT
000071        DELF = (SSTOP - SSTART) / FNPT
000075        DELF2 = DELF / 2.0
000107        SDELF2 = DELF2
      C     SET UP FREQUENCY ARRAY
000111        AFREQ(1) = SSTART
000113        DO 150  I = 2,NPOINT
000115  150   AFREQ(I) = AFREQ(I-1) + DELF
      C
      C     RESTORE FILTER ARRAY
000127        DO 155  I = 1,NPOINT
      C     READ FILTER FUNCTION DATA
000131  155   FILTER(I) = 1.0
000135  160   READ (IN, 2020) WORD1, WORD2,  TEMP,   WIDTH, PEAK, NFPOW
000155        CENTER = TEMP
000157        IF (WORD1 .EQ. ENDF)  GO TO 251
      C     DETERMINE FILTER TYPE
000161        IF (WORD2 .EQ. FNONE) GO TO 160
000163  180   IF (WORD2 .EQ. GAUSS) ITYPE = 1
000166        IF (WORD2 .EQ. FLOR ) ITYPE = 2
000171        IF (WORD2 .EQ. CAL  ) ITYPE = 3
000174        IF (WORD2 .EQ. PFCN ) ITYPE = 4
      C
      C     IF FILTER CAL CURVE IS GIVEN, READ IN POINTS  (MAXIMUM OF 50)
000177  247   IF (ITYPE .NE. 3) GO TO 250
000201        NCAL = CENTER
000204        READ (IN, 2140) (FWAVE(I), FRESP(I), I = 1,NCAL)
      C     SET UP FILTER ARRAY
000221  250   CALL FLTRS (FILTER, AFREQ, ITYPE, CENTER, WIDTH, PEAK,
     1                  NCAL, FWAVE, FRESP, NPOINT, NFPOW)
      C     ONE FILTER FUNCTION COMPLETED - CHECK FOR MORE FILTERS
```

```
000234          GO TO 160
000235    251   CONTINUE
          C
          C
          C     READ SPECTRUM FROM TAPE AND INTERPOLATE TO PUT ON
          C     UNIFORM WAVENUMBER SCALE
          C     SET UP LOOP FOR UNIFORM FREQUENCY SCALE
          C
000235    253   NBLOCK = 101
000236          NBPT   = 200
000237          IPASS = 1
          C
000240          DO 312  IS = 2, NPOINT
          C     IS NEW BLOCK OF DATA NEEDED FROM TAPE
000242    255   IF (NBPT .LE. NBLOCK)   GO TO 268
          C     NEW BLOCK IS NEEDED
          C     FIRST TRANSFER LAST POINT OF OLD BLOCK TO FIRST POINT OF NEW
          C     SKIP IF THIS IS FIRST BLOCK
000245          IF (IPASS .EQ. 1) GO TO 258
000247          FREQ(1)= FREQ(101)
000251          SPECT(1) = SPECT(101)
          C
          C     BEFORE READING NEW BLOCK INTEGRATE REMAINDER OF OLD BLOCK
000253          SEGONE = (ALINE(NLAST) / 2.0) * (FREQ(NLAST)**2 - FLAST**2)
                1        +  BLINE(NLAST) * (FREQ(NLAST) - FLAST)
000320          IF (NLAST .GE. NBLOCK) GO TO 258
000322          NLAST1 = NLAST + 1
000324          DO 257 I = NLAST1, NBLOCK
000325    257   SEGONE = SEGONE + (ALINE(I) / 2.0) * (FREQ(I)**2 - FREQ(I-1)**2)
                1                 +  BLINE(I) * (FREQ(I) - FREQ(I-1))
000377    258   NLAST = 1
          C
000400          NBPT = 2
          C
          C     READ IN NEW BLOCK OF 100 POINTS
000401          READ (ITAPE) (NBLOCK, ((FREQ(I), SPECT(I)), I = 2,NBLOCK))
          C
          C     IF THIS IS FIRST BLOCK OF SPECTRUM SET FIRST TWO POINTS EQUAL
000417          IF (IPASS .NE. 1)  GO TO 260
000421          FREQ(1) = FREQ(2) - 0.001
000427          SPECT(1) = SPECT(2)
000431          IPASS = 2
000432          NLAST = 2
```

```
000433          FLAST = AFREQ(1)
000435          SEGONE = 0.0
                C
                C     FIT STRAIGHT LINE TO EACH SPECTRAL INTERVAL
                C     TO BE USED LATER FOR SPECTRAL INTEGRATION
000436    260   DO 262  IL = 2, NBLOCK
000440          ALINE(IL) = (SPECT(IL-1) - SPECT(IL)) / (FREQ(IL-1) - FREQ(IL))
000465    262   BLINE(IL) = SPECT(IL) - ALINE(IL) * FREQ(IL)
                C
                C     NOW FIND CURRENT FREQUENCY POINT IN DATA BLOCK
000500    268   IF (AFREQ(IS) - FREQ(NBPT))  270, 270, 285
                C
                C     IF THIS POINT AND LAST POINT ARE IN SAME INTERVAL COMPUTE
                C     INTEGRAL OVER APPROPRIATE SEGMENT OF INTEGRAL
000511    270   IF (NBPT .NE. NLAST) GO TO 272
000513          SPCTRM(IS) = (ALINE(NBPT) / 2.0) * (AFREQ(IS) **2 - FLAST**2)
               1            +   BLINE(NBPT) * (AFREQ(IS) - FLAST)
000560          FLAST = AFREQ(IS)
000564          GO TO 310
                C
                C
                C     IF THIS POINT AND LAST POINT ARE IN CONSECUTIVE INTERVALS
                C     INTEGRATE AND ADD APPROPRIATE INTERVAL SEGMENTS
000564    272   IF (NLAST .EQ. 1)  GO TO 273
000566          SEGONE =  (ALINE(NLAST) /2.0) * (FREQ(NLAST)**2 - FLAST**2)
               1            +  BLINE(NLAST) * (FREQ(NLAST) - FLAST)
                C
000633    273   SEGTWO = (ALINE(NBPT) / 2.0) * (AFREQ(IS) **2 - FREQ(NBPT-1)**2)
               1        +  BLINE(NBPT) * (AFREQ(IS) - FREQ(NBPT-1))
                C
000701          IF (NBPT .NE. (NLAST+1)) GO TO 274
000704          SPCTRM(IS) = SEGONE + SEGTWO
000707          FLAST = AFREQ(IS)
000712          NLAST = NBPT
000713          GO TO 310
                C
                C
                C     IF POINTS INCLUDE SEVERAL INTERVALS INTEGRATE INTERVALS IN BETWEEN
000714    274   NBPT1 = NBPT - 1
000716          NLAST1 = NLAST + 1
000720          SINTG = 0.0
000721          DO 276  I = NLAST1, NBPT1
000723    276   SINTG = (ALINE(I) / 2.0) * (FREQ(I) **2 - FREQ(I-1) **2)
```

```
                     1      +  BLINE(I) * (FREQ(I) - FREQ(I-1)) + SINTG
000775               SPCTRM(IS) = SINTG + SEGONE + SEGTWO
001001               NLAST = NBPT
001003               FLAST = AFREQ(IS)
001006               GO TO 310
               C
               C     FREQUENCY GREATER THAN BLOCK DATA FREQUENCY
               C     TRY NEXT POINT IN BLOCK
001007     285       NBPT = NBPT + 1
001011               GO TO 255
               C
001011     310       SPCTRM(IS) = SPCTRM(IS) * (FILTER(IS) + FILTER(IS-1)) / 2.0
001016     312       CONTINUE
001020               SPCTRM(1) = SPCTRM(2)
               C
               C     FINISHED SPECTRUM
               C
               C     WRITE SPECTRUM ON SCRATCH TAPE FOR FUTURE PLOTTING
               C
               C     CONVERT FREQUENCIES TO SINGLE PRECISION FOR PLOTTING
001021               DO 315 I = 1, NPOINT
001023     315       SFREQ(I) = AFREQ(I) - DELF2
               C
001034               REWIND ITAPE
001036               WRITE(ITAPE) (NPOINT, FLEFT, FRIGHT, YBOT, YTOP)
001053               WRITE(ITAPE) ((SFREQ(I), SPCTRM(I)), I = 1,NPOINT)
               C
               C     FOURIER TRANSFORMATION AND PLOTTING SECTIONS
               C     MODELLED AFTER BARRINGER PROGRAM
               C
001067     330       DO 335  I = 1,NPOINT
001071     335       ZERO(I) = 0.0
001075               CALL FRXFM (SPCTRM, ZERO, N2POW)
001077               G = 0.0
001100               DG = (FREF - SSTART - SDELF2)/ (SSTOP - SSTART)
001106               ZPD = SQRT (SPCTRM(1) * SPCTRM(1) + ZERO(1) * ZERO(1))
001113               RAT = EXP (1.0 / FNPT)
001117               DEC = 1.0 / RAT
001120               DECCN = DEC
001121               DINC = 1.0 / (SSTOP - SSTART)
001124               NINT = 0
               C
001125     350       DO 380  NPD = 1, NPOINT
```

```
001127          BI   = SPCTRM(NPD) * SPCTRM(NPD) + ZERO(NPD) * ZERO(NPD)
001133          DECON = DECON * RAT
001134          BI   = SQRT(BI) / ZPD * 7.0 * DECON
                C
001142          PHAS = ATAN2 (ZERO(NPD), SPCTRM(NPD)) / 6.2831853
001146          G = G + DG
001150          PHAS = G - PHAS
001151          PHAS = PHAS - AINT(PHAS)
001153          IF (PHAS .GT. 0.5) PHAS = PHAS - 1.0
                C
001160          XNPD = NPD
001162          XX = XNPD * DINC
001164          IF (XX .LT. DSTART)  GO TO 380
001166          IF (XX .GT. DSTOP )  GO TO 405
001172          NINT = NINT + 1
001173          DINT(NINT) = XX
001175          BINT(NINT) = BI
001176          PINT(NINT) = PHAS
001200    380   CONTINUE
                C     WRITE INTERFEROGRAM ON SCRATCH TAPE FOR PLOTTING
001203    405   WRITE(ITAPE) (DSTART, DSTOP, DSCALE, NINT)
001216          WRITE(ITAPE) ((DINT(I), BINT(I), PINT(I)), I = 1,NINT)
001234          REWIND ITAPE
                C
                C     PUNCH INTERFEROGRAM ON CARDS IF DESIRED
001236          IF (PWORD .NE. PUNCH)  GO TO 430
001240          IPUN = 7
001241          NPUN = 100
001242          FNPUN = NPUN
001244          DPSTOP = DSTART + FNPUN * DINC
001247          WRITE (IPUN, 2200)  TITLE
001254          WRITE (IPUN, 2210)  NPUN, DSTART, DPSTOP, DINC
001270          NPUN2 = NPUN / 2
001272          DO 420  I = 1, NPUN2
001273          I2 = I * 2
001274    420   WRITE (IPUN, 2220)  SPCTRM(I2-1), ZERO(I2-1),
               1                    SPCTRM(I2), ZERO(I2), TITLE(1), I
001317    430   CONTINUE
                C
                C
001317          RETURN
                C
                C     FORMATS
```

```
001320    2C00  FORMAT  (I2, 7X, 3F10.4, 2E10.3, 5X, A4)
001320    2010  FORMAT  (F9.4, 2F10.4)
001320    2C20  FORMAT  (A4, 5X, A4, 6X, 3F10.4, I2)
001320    2140  FORMAT (F9.3, 5F10.3)
001320    2200  FORMAT  (18A4)
001320    2210  FORMAT  (I4, 15H POINTS, DELAY , F7.3, 7H CM TO , F7.3,
                1          5H CM, , F7.3, 9H CM/POINT )
0C1320    2220  FORMAT  (4X, 2(2X, OPE13.6, 2X, OPE13.6, 2X), 4X, A4, I4)
0C1320          END
```

```
                      SUBROUTINE FLTRS (FILTER, AFREQ, ITYPE, CENTER, WIDTH, PEAK,
                     1                  NCAL, FWAVE, FRESP, NPOINT, NFPOW)
                C
                C
                C     SUBROUTINE TO COMPUTE FILTER FUNCTIONS GIVEN EITHER
                C     GAUSSIAN OR LORENTZIAN CHARACTERISTICS OR CALIBRATION CURVE
                C
 000016               DOUBLE PRECISION  AFREQ, FWAVE, CENTER
 000016               DIMENSION  FILTER(4100),  AFREQ(4100),  FWAVE(50), FRESP(50)
                C     CHECK FILTER TYPE
 000016               GO TO (200, 300, 400, 350), ITYPE
                C
                C     GAUSSIAN FILTER
 000025   200         DO 220  I = 1, NPOINT
 000027               BEX =  ( AFREQ(I) - CENTER ) / WIDTH
 000051   220         FILTER(I) = FILTER(I) *  EXP( -(BEX * BEX))  * PEAK
 000065               RETURN
                C
                C     LORENTIAN FILTER
 000066   300         DO 320  I = 1, NPOINT
 000070               BEX =   ( AFREQ(I) - CENTER)
 000077   320         FILTER(I) = FILTER(I) * (WIDTH / (WIDTH + BEX * BEX)) * PEAK
 000106               RETURN
                C
                C     POWER FUNCTION FILTER
 000107   350         WIDTH1 = WIDTH - 1.0
 000111               DO 370  I = 1, NPOINT
 000113               DELF = DABS(AFREQ(I) - CENTER)
 000130               IF (DELF .LT. WIDTH1)  GO TO 355
 000133               FILTER(I) = 0.0
 000135               GO TO 370
 000135   355         FILTER(I) = PEAK * (1.0 - (DELF/WIDTH)**2) ** NFPOW
 000145   370         CONTINUE
 000150               RETURN
                C
                C     CALIBRATION CURVE GIVEN - MUST CONVERT TO SAME FREQUENCY
                C     SCALE AS SPECTRUM
 000151   400         DO 500  IF = 1, NPOINT
                C     FREQUENCY ARRAY POINTS BELOW FIRST OR ABOVE LAST CALIBRATION
                C     POINT ARE SET TO ZERO
 000153               IF (AFREQ(IF) .GE. FWAVE(1)) GO TO 410
 000157               FILTER(IF) = 0.0
```

```
000161          GO TO 500
000161   410    IF (AFREQ(IF) .LE. FWAVE(NCAL)) GO TO 420
000167          FILTER(IF) = 0.0
000171          GO TO 500
                C
                C     USE LINEAR INTERPOLATION FOR ALL OTHER POINTS
000171   420    NF = 2
000172   430    IF (AFREQ(IF) .LE. FWAVE(NF))  GO TO 450
000200          NF = NF + 1
000201          GO TO 430
000202   450    FILTER(IF) = FILTER(IF) * ( FRESP(NF) - ( (FWAVE(NF) - AFREQ(IF))
               1                 * ( FRESP(NF) - FRESP(NF-1))
               2                 / ( FWAVE(NF) - FWAVE(NF-1))))
000266   500    CONTINUE
000271          RETURN
000272          END
```

```
      SUBROUTINE FRXFM(X,Y,N2POW)
C                SUBROUNTINE FRXFM
C            COMPUTES FOURIER TRANSFORM OF SPECTRUM
C
C
C                  FRXFM
C                  *****
C
C     FINITE DISCRETE FOURIER TRANSFORM
C     IT REPLACES THE VECTOR Z=X+IY BY ITS FOURIER TRANSFORM
C     THE LENGTH OF THE VECTOR IS NTHPOW=2**N2POW
C     THE FINITE DISCRETE FOURIER TRANSFORM IS THE PRODUCT WITH
C     THE MATRIX WHOSE I,J ELEMENT IS W**(I*J), WHERE
C     W=CEXP(2.*PI*I/NTHPOW), THE NTHPOW PRINCIPLE ROOT OF UNITY
C     I,J=0..NTHPOW-1
C     NOTE ZERO SUBSCRIPTS HERE REFER TO FORTRAN SUBSCRIPTS=1 IN THE
C     CODE. I.E. THE FORTRAN SUBCRIPTS RUN FROM 1 TO NTHPOW.
C     DEVELOPED BY B. LANGDON AND G. SANDE FROM THE APPROACH OF
C     J.W. TUKEY AND J. COOLEY.
C     PRINCETON UNIVERSITY, NOVEMBER 1965.
C
000006      REAL X(2), Y(2), I, I1, I2, I3, I4
000006      INTEGER PASS, SEQLOC, L(13)
000006      EQUIVALENCE (NTHPOW,IJ), (J,JI), (N4POW,J5), (PASS,J6),
           1    (NXTLTH,J7), (LENGTH,J8), (SEQLOC,J9), (SCALE,J10),
           2    (ARG,J11), (C1,J12), (C2,L1), (C3,L2), (S1,L3),
           3    (S2,L4), (S3,L5), (R1,L6), (R2,L7), (R3,L8), (R4,L9),
           4    (I1,L10), (I2,L11), (I3,L12), (I4,L13), (R,I)
000006      EQUIVALENCE (L13,L(1)),(L12,L(2)),(L11,L(3)),(L10,L(4)),
           1    (L9,L(5)),(L8,L(6)),(L7,L(7)),(L6,L(8)),(L5,L(9)),
           2    (L4,L(10)),(L3,L(11)),(L2,L(12)),(L1,L(13))
000006        INVERT=1
000007        IF(N2POW.LT.0)INVERT=-1
000011        IF(N2POW.LT.0)N2POW=-N2POW
000013      NTHPOW=2**N2POW
000017      N4POW=N2POW/2
000021      IF(N4POW.EQ.0) GO TO 3
C     RADIX 4 PASSES, IF ANY.
000022      DO 2 PASS=1,N4POW
000023      NXTLTH=2**(N2POW-2*PASS)
000031      LENGTH=4*NXTLTH
000033      SCALE=6.283185307/FLOAT(LENGTH)
000035      DO 2 J=1,NXTLTH
```

```
000036          ARG=FLOAT(J-1)*SCALE
000041          C1=COS(ARG)
000044          S1=SIN(ARG)
000046          C2=C1*C1-S1*S1
000050          S2=C1*S1+C1*S1
000052          C3=C1*C2-S1*S2
000055          S3=C2*S1+S2*C1
000060          DO 2 SECLOC=LENGTH,NTHPOW,LENGTH
000064          J1=SECLOC-LENGTH+J
000067          J2=J1+NXTLTH
000071          J3=J2+NXTLTH
000072          J4=J3+NXTLTH
000073          R1=X(J1)+X(J3)
000075          R2=X(J1)-X(J3)
000101          R3=X(J2)+X(J4)
000105          R4=X(J2)-X(J4)
000110          I1=Y(J1)+Y(J3)
000114          I2=Y(J1)-Y(J3)
000117          I3=Y(J2)+Y(J4)
000123          I4=Y(J2)-Y(J4)
000126          X(J1)=R1+R3
000132          Y(J1)=I1+I3
000134          IF(J.EQ.1) GO TO 1
000136          X(J3)=C1*(R2-I4)-S1*(I2+R4)
000146          Y(J3)=S1*(R2-I4)+C1*(I2+R4)
000156          X(J2)=C2*(R1-R3)-S2*(I1-I3)
000166          Y(J2)=S2*(R1-R3)+C2*(I1-I3)
000176          X(J4)=C3*(R2+I4)-S3*(I2-R4)
000206          Y(J4)=S3*(R2+I4)+C3*(I2-R4)
000216          GO TO 2
000217        1 X(J3)=R2-I4
000223          Y(J3)=I2+R4
000225          X(J2)=R1-R3
000231          Y(J2)=I1-I3
000233          X(J4)=R2+I4
000237          Y(J4)=I2-R4
000241        2 CONTINUE
              C   END OF RADIX 4
000251        3 IF(N2POW.EQ.2*N4POW) GO TO 5
              C   RADIX 2 PASS, IF ANY.
000253          DO 4 J=1,NTHPOW,2
000255          R=X(J)+X(J+1)
000260          X(J+1)=X(J)-X(J+1)
```

```
000263          X(J)=R
000264          I=Y(J)+Y(J+1)
000267          Y(J+1)=Y(J)-Y(J+1)
000271        4 Y(J)=I
              C   SET UP PARAMETERS FOR SORT
000276        5 DO 6 J=1,13
000300          L(J)=1
000302        6 IF(J.LE.N2POW) L(J)=2**(N2POW+1-J)
              C   NOTE EQUIVALENCE OF LI AND L(14-I)
              C   BINARY SORT
000314          IJ=1
000315          DO 7 J1=1,L1
000317          DO 7 J2=J1,L2,L1
000320          DO 7 J3=J2,L3,L2
000321          DO 7 J4=J3,L4,L3
000322          DO 7 J5=J4,L5,L4
000323          DO 7 J6=J5,L6,L5
000324          DO 7 J7=J6,L7,L6
000325          DO 7 J8=J7,L8,L7
000326          DO 7 J9=J8,L9,L8
000327          DO 7 J10=J9,L10,L9
000330          DO 7 J11=J10,L11,L10
000331          DO 7 J12=J11,L12,L11
000332          DO 7 JI=J12,L13,L12
000333          IF(IJ.GE.JI) GO TO 7
000335          R=X(IJ)
000336          X(IJ)=X(JI)
000341          X(JI)=R
000343          I=Y(IJ)
000345          Y(IJ)=Y(JI)
000350          Y(JI)=I
000352        7 IJ=IJ+1
000414            IF(INVERT.GT.0)RETURN
000416            IJ=1
000417          JI = L13 + 1
000421          DO 8  J2 = L12, L13
000423          JI = JI - 1
000425            IJ=IJ+1
000426            R=X(IJ)
000430            X(IJ)=X(JI)
000433            X(JI)=R
000435            I=Y(IJ)
000437            Y(IJ)=Y(JI)
```

```
000442   8       Y(JI)=I
000447           RETURN
000450           END
```

```
                      SUBROUTINE SPPLOT (MSPECC, MSPEC)
                C
                C     SUBROUTINE TO PLOT SPECTRA AND FOURIER TRANSFORMS
                C
000005                DOUBLE PRECISION CFREQ
000005                COMMON  CFREQ(150)
000005                COMMON  ABSB(150, 98), A(27,25), B(25,25), C(25,25),
                     1        PATH( 98), ATEMP( 98), CONC(3, 98), ALOR( 98), DOPP(3,98),
                     2                  STFQ(150), SPFQ(150), STRONG(150), ENGY(160),
                     3        TITLE(18), AQ(3), BQ(3), CQ(3), ALBEDO, GTEMP, GEMIS
000005                COMMON  FSTART, FSTOP
000005                COMMON  LTYPE(150), NTYPE(3), NLINE, NSPEC, IN, IOUT, ICASE
                C
000005                DIMENSION SFREQ(4100), SPCTRM(4100), SMULT(3),
                     1          DINT(2050), PINT(2050), BINT(2050)
000005                EQUIVALENCE  (ABSB(1,1), DINT(1)), (ABSB(1,15), PINT(1)),
                     1             (ABSB(1,29), BINT(1)),
                     2             (ABSB(1,57), SFREQ(1)), (ABSB(1,85), SPCTRM(1))
000005                DATA SMULT / 1.0, 10.0, 10.0/
000005                ITAPE = 2
                C
                C     INITIALIZE PLOTTER IF THIS IS FIRST SPECTRUM
000006                IF (MSPECC .EQ. 1)  CALL CALCOMP
                C
                C     SPECTRUM PLOTTING SECTION
                C
                C     READ SPECTRUM FROM SCRATCH TAPE
000013                READ (ITAPE) (NPOINT, FLEFT, FRIGHT, YBOT, YTOP)
000030                READ (ITAPE) ((SFREQ(I), SPCTRM(I)), I = 1,NPOINT)
                C
000044                CALL CALPLT (0.0, 0.5, -3)
                C
                C     WRITE TITLE
                C     USE LOOP SINCE TITLE STORED ONLY 4 CHARACTERS / WORD
000047                TX= 1.0
000051                TY   = 5.0
000052                HGT  = 0.14
000054                ONE  = 1.0
000055                ZERO = 0.0
000056                DO 150 I=1,18
000061                CALL NOTATE ( TX, TY, HGT, TITLE(I), ZERO, 4 )
000066                TX = TX + 0.48
```

```
000070      150 CONTINUE
000074          CALL CALPLT (11.0, 1.0, -3)
            C
            C     PLOT SPECTRUM OF SEMI-LOG GRID
            C
            C     DRAW GRID
            C     NUMBER OF CYCLES
000076          NCYC = ALOG10 (YTOP/YBOT)
000104          CYC = NCYC
            C     INCHES / CYCLE - ASSUME 8 INCH AXIS
000105          CINCH = 8.0 / CYC
            C     X AXIS LENGTH - ASSUME 10 WAVENUMBERS / INCH
000107          XLN = (FRIGHT - FLEFT) / 10.0
000112          CALL LOGRID (XLN, CINCH, -1, NCYC, 0.0, 1.0, 1.0, 10.0)
            C
            C     LABEL X AXIS
000121          DV   = 10.0
000123          TMIN = 2.0
000124          CALL AXES ( ZERO, ZERO, ZERO, XLN, FLEFT, DV, ONE, TMIN,
                1                 18HFREQUENCY - CM**-1 , HGT, -18 )
            C
            C     LABEL Y AXIS
000137          NCYC = NCYC + 1
000141          YEXP = ALOG10 (YBOT)
000143          YLBOT = YEXP
000144          DO 200  I = 1, NCYC
000147          FI = I - 1
000151          DELY = FI * CINCH
000153          YTEN = DELY - 0.1
000155          TX   = -0.70
000156          MONE = -1
000157          CALL NUMBER ( TX, YTEN, HGT, DV,   ZERO, MONE )
000163          TX   = -0.46
000165          CALL NUMBER ( TX, DELY, HGT, YEXP, ZERO, MONE )
000171  200     YEXP = YEXP + 1.0
000177          TY   = 1.8
000201          ANG = 90.0
000202          CALL NOTATE ( MONE, TY, HGT,
                1                 37HSPECTRAL INTENSITY - W/(CM**2-CM**-1) , ANG, 37 )
            C
            C     PLOT POINTS
000206          DO 220  I = 1, NPOINT
000211          DTEMP = (SFREQ(I) - FLEFT) / 10.0
```

```
000214          IF (SPCTRM(I) .LT. YBOT)  SPCTRM(I) = YBOT
000220          BTEMP = (ALOG10(SPCTRM(I)) - YLBOT) * CINCH
000226          IND = 2
000227          IF (I .EQ. 1)  IND = 3
000233    220   CALL CALPLT ( DTEMP, BTEMP, IND)
              C
              C     ADVANCE PAPER
000242          DTEMP = DTEMP + 2.0
000244          CALL CALPLT (DTEMP, 0.0, -3)
              C
              C
              C     FOURIER TRANSFORM PLOTTING SECTION
              C     PLOTS TRANSFORM ON X1, X10, X100 SCALES
              C     ALSO PLOTS PHASES
              C
              C
              C     READ INTERFEROGRAM FROM SCRATCH TAPE
000247          READ (ITAPE) (DSTART, DSTOP, DSCALE, NPT)
000262          READ (ITAPE) ((DINT(I), BINT(I), PINT(I)), I = 1,NPT)
000300          REWIND ITAPE
              C
              C
              C     PLOT IFGM
              C
000302          CALL CALPLT ( 0.0, 1.0, -3)
              C     DRAW X AXIS
000305          XLN = (DSTOP - DSTART) / DSCALE
              C     INCHES / POINT
000310          PINC = 1.0 / ((FSTOP - FSTART) * DSCALE)
000314          CALL AXES ( ZERO, ZERO, ZERO, XLN, DSTART, DSCALE, ONE, TMIN,
                1                10HDELAY - CM , HGT, -10 )
              C
              C     PLOT IFGM ON X1, X10 AND X100 SCALES
              C
000326          DO 320  IS = 1,3
000331          CALL CALPLT ( 0.0, 0.0, 3)
000333          DO 300  IP = 1, NPT
000336          BTEMP = BINT(IP) * SMULT(IS)
000341          IF (BTEMP .GT. 8.0)  BTEMP = 8.0
000344          FIP = IP - 1
000347          DTEMP = PINC * FIP
000350    300   CALL CALPLT ( DTEMP, BTEMP, 2)
000357    320   CONTINUE
```

```
C
C     PLOT PHASES
C
000361      CALL CALPLT ( DTEMP, -1.2, 3)
000364      CALL CALPLT ( 0.0, -1.2, -2)
000367      OLD = PINT(1)
000371      DO 340  IP = 1, NPT
000374      TPINT = PINT(IP)
000376      FIP = IP - 1
000400      DTEMP = FIP * PINC
000402      IND = 2
000403      DIF = OLD - TPINT
000405      IF (ABS(DIF) .GT. 0.5)  IND = 3
000411      CALL CALPLT ( DTEMP, TPINT, IND)
000414  340 OLD = TPINT
C
C     ADVANCE PAPER
000422      DTEMP = DTEMP + 2.0
000424      CALL CALPLT ( DTEMP, -1.3, -3)
C     TERMINATE PLOTTER IF THIS IS LAST SPECTRUM
000426      IF (MSPECC .EQ. MSPEC) CALL CALPLT (0.0, 0.0, 999)
000435      RETURN
000436      END
```

APPENDIX B

LISTING OF CORRELATION FUNCTION PROGRAM

Page Intentionally Left Blank

```
      FORTRAN IV PROGRAM WEIGHT (INPUT, OUTPUT, TAPE5=INPUT,                    100000
     1                           TAPE10, TAPE11, TAPE6=OUTPUT)                  200000
CWAIT       MAIN WEIGHTING FUNCTION PROGRAM                                    300000
C             PROGRAM TO SIMULATE MEASUREMENT OF INTERFEROGRAMS.                400000
C                                                                               500000
C       THIS VERSION FOR USE ON CDC SYSTEM AT LANGLEY                           600000
C       PROGRAM CREATES NEW WEIGHTING FUNCTION FROM IFGMS STORED                700000
C       ON RANDOM ACCESS DISK                                                   800000
C       THE FUNCTION IS APPLIED TO TEST IFGMS TO GIVE MEASUREMENTS              900000
CC                                                                              1000000
000003       DIMENSION H(2,64), WW(2,14,64), W(1792), WT(14), SNEEZE(4),        1100000
     1           ARA(196), NITAB(14), NFRG(14), NSCAN(14), FNAME(18,14),        1200000
     2           WTI(2,14,64), LIST(250), SPCON(3), SPTAB(14)                   1300000
000003       DIMENSION IX(1502), TBLOCK(64)                                     1400000
000003       DIMENSION  FGMR(64), IDAT(64)                                      1500000
000003         EQUIVALENCE(WW(1,1,1),W(1))                                      1600000
000003       EQUIVALENCE  (NFG, TBLOCK(24)), (NSC, TBLOCK(26)),                 1700000
     2                  (SPCON(1), TBLOCK(27))                                 1800000
000003       EQUIVALENCE (NREC, IDAT(1))                                        1900000
000003       INTEGER DISK                                                       2000000
000003       DATA ILIST, H2O, CH4 / 4HLIST, 3HH2O, 3HCH4/                       2100000
C                                                                               2200000
000003       DATA IN, IOUT, DISK, NA, NWD, NOM, NTG, WT                         2300000
     1     /5,    6,   10,  2,  64,   1,   2, 14*1.0/                         2400000
C      TRANSFER SEQUENTIAL FILE TO RANDOM ACCESS                                2500000
000003       CALL OPENMS (DISK, IX, 1502, 0)                                    2600000
000006       REWIND 11                                                          2700000
000010       READ (11)  IDAT                                                    2800000
000015       REWIND 11                                                          2900000
000017       NMAX = 3 * NREC + 1                                                3000000
000022       DO 120  NR = 1, NMAX                                               3100000
000023       READ (11)  IDAT                                                    3200000
000030  120  CALL WRITMS (DISK, IDAT, NWD, NR)                                  3300000
000036       REWIND 11                                                          3400000
C      READ FIRST, LAST INDICES, NOM, TARGET IFGM NOS., OTHER IFGM NOS.         3500000
000040  130  READ (5, 5070)  N1, N2, (NITAB(I), I = 1, 14)                      3600000
000056       IF (N1 .EQ. 0)  GO TO 600                                          3700000
000057       N = N2 - N1 + 1                                                    3800000
000062       FNP = N                                                            3900000
C      COUNT IFGMS                                                              4000000
000063       NSG = 2                                                            4100000
000064       DO 150  I = 3, 14                                                  4200000
```

```
000066   150   IF (NITAB(I) .NE. 0)  NSG = NSG + 1                                4300000
               C     SPECIFY SPECIES, OBSERVATION TIME, FREQ INTERVAL, NOISES     4400000
000073         READ (IN, 5120)   SPEC, TIME, DNU, (SNEEZE(L), L = 1,4)            4500000
000113         IS = 1                                                             4600000
000114         IF (SPEC .EQ. H2O)  IS = 2                                         4700000
000117         IF (SPEC .EQ. CH4)  IS = 3                                         4800000
               C                                                                  4900000
000122         DO 200  I = 1, NSG                                                 5000000
               C     READ TITLE                                                   5200000
000124         NR = 3 * NITAB(I) - 1                                              5100000
000127         CALL READMS (DISK, TBLOCK, NWD, NR)                                5300000
000132         DO 160  J = 1, 18                                                  5400000
000134   160   FNAME(J,I) = TBLOCK(J)                                             5500000
000143         SPTAB(I) = SPCON(IS)                                               5600000
000145         NFRG(I) = NFG                                                      5700000
000147         NSCAN(I) = NSC                                                     5800000
               C     READ REST OF IFGM                                            5900000
000150         NR = NR + 1                                                        6000000
000152         CALL READMS (DISK, FGMR   , NWD, NR)                               6100000
000155         DO 180  J = 1, NWD                                                 6200000
000157   180   WTI(1, I, J) = FGMR  (J)                                           6300000
000167         NR = NR + 1                                                        6400000
000171         CALL READMS (DISK, FGMR   , NWD, NR)                               6500000
000174         DO 200  J = 1, NWD                                                 6600000
000176   200   WTI(2, I, J) = FGMR  (J)                                           6700000
000211         CALL WSHIFT (WTI, W, NSG, NA, N1, N, N2, NFRG, NSCAN)              6800000
000221         SPUNIT = SPTAB(NTG) - SPTAB(NOM)                                   6900000
000224         SPSTD = SPTAB(NCM)                                                 7000000
               C                                                                  7100000
000226         W00 = 10.0                                                         7200000
               C       FORM DIFFERENCE INTERFEROGRAMS                           7300000
               C                                                                  7400000
000227         CALL DIFF(W,2,NSG,N,NOM)                                           7500000
000233         DT = TIME / FNP                                                    7600000
               C       SPECIFY NOISE SEVERITIES                                 7700000
               C                                                                  7800000
               C       ENTRIES ARE                                              7900000
               C             SQRT(DET. AREA)/(D* X P   )                        8000000
               C                              NU                                8100000
               C                                                                8200000
               C             FRANC ( DEFINED BY ((H-HO)/H) =FR/SQRT(T)          8300000
               C                                          T                     8400000
               C                                                                8500000
```

```
C              F      (MEAN OPTICAL DEPTH OF UNACCOUNTED INTERFERENTS)                  8600000
C                                                                                       8700000
C              F0     (PROCESSING ERROR)                                                8800000
C                                                                                       8900000
C                                                                                       9000000
000235         IF (DNU .EQ. 0.0)  DNU = 0.1592356                                       9100000
000237         SNEEZE(1) = SNEEZE(1) * SNEEZE(1) / (6.28 * DNU * DNU * DT)              9200000
000243         SNEEZE(2) = SNEEZE(2) * SNEEZE(2) / DT                                   9300000
000244         SNEEZE(3) = (SNEEZE(3) * W00 * 0.1) ** 2                                 9400000
000246         SNEEZE(4) = SNEEZE(4) * SNEEZE(4)                                        9500000
000247         CALL WHOP (W, H, N, NSG, NTG, WT, SNEEZE, SNEEZE, ARA, 2, SBYN)          9600000
000262         SBYN = SQRT(SBYN)                                                        9700000
000265         WRITE (IOUT, 6010)  SBYN, SPEC                                           9800000
000274         WRITE (IOUT, 6100)  N1, N2, TIME, DNU, (SNEEZE(I), I = 1,4)              9900000
000316         WRITE (IOUT, 6080)                                                      10000000
000322         DO 400  JJ = 1, NSG                                                     10100000
000324         CALL MESURE (W, H, 2, NSG, N, JJ, SUM)                                  10200000
000332         PCT = 0.0                                                               10300000
000333         SPTEST = SPSTD + SUM * SPUNIT                                           10400000
000336         IF (SPTAB(JJ))  380, 380, 390                                           10800001
000340   380   WRITE (IOUT, 6030) NITAB(JJ), (FNAME(IW,JJ), IW=1,17), SUM,             10800002
              1                   SPTEST, SPTAB(JJ)                                 10800003
000364         GO TO 400                                                               10800004
000365   390   PCT = (SPTEST - SPTAB(JJ)) * 100.0 / SPTAB(JJ)                          10800005
000371         WRITE (IOUT, 6020) NITAB(JJ), (FNAME(IW,JJ), IW=1,17), SUM,             10800006
              1                   SPTEST, SPTAB(JJ), PCT                            10800007
000417   400   CONTINUE                                                                10800008
C                                                                                      10900000
C      NOW READY TO ANALYZE IFGMS                                                      11000000
000422   410   CONTINUE                                                                11100000
000422         WRITE (ICUT, 6060)  SPEC                                                11200000
000430         WRITE (ICUT, 6080)                                                      11300000
C      READ LIST OR RANGE OF IFGMS TO BE TESTED                                        11400000
000434         READ (IN, 5200)  IWORD, (LIST(I), I = 1,14)                             11500000
000450         IF (IWORD .EQ. ILIST)  GO TO 500                                        11600000
000452         NLIST = LIST(2) - LIST(1) + 1                                           11700000
000455         DO 480  I = 2, NLIST                                                    11800000
000456   480   LIST(I) = LIST(I - 1) + 1                                               11900000
000462         GO TO 520                                                               12000000
000463   500   NLIST = 0                                                               12100000
000464         DO 510  I = 1, 14                                                       12200000
000466         IF (LIST(I) .EQ. 0)  GO TO 520                                          12300000
000467   510   NLIST = NLIST + 1                                                       12400000
```

```
000472   520   CONTINUE                                                        12500000
000472         DO 570  I = 1, NLIST                                            12600000
         C     READ IFGM                                                       12700000
000474         NR = 3 * LIST(I) - 1                                            12800000
000477         CALL READMS (DISK, TBLOCK, NWD, NR)                             12900000
000502         DO 530  J = 1, 18                                               13000000
000504   530   FNAME(J,1) = TBLOCK(J)                                          13100000
000511         SPACT = SPCON(IS)                                               13200000
000513         NFRG(1)  = NFG                                                  13300000
000514         NSCAN(1) = NSC                                                  13400000
000516         NR = NR + 1                                                     13500000
000517         CALL READMS (DISK, FGMR  , NWD, NR)                             13600000
000522         DO 535  J = 1, NWD                                              13700000
000524   535   WTI(1, 1, J) = FGMR(J)                                          13800000
000533         NR = NR + 1                                                     13900000
000535         CALL READMS (DISK, FGMR  , NWD, NR)                             14000000
000540         DO 540  J = 1, NWD                                              14100000
         C     SAVE DESIRED SEGMENT OF IFGM                                    14300000
000542   540   WTI(2, 1, J) = FGMR(J)                                          14200000
000551         CALL WSHIFT (WTI, W,  1, NA, N1, N, N2, NFRG, NSCAN)            14400000
000562         CALL MESURE (W, H, 2, 1, N, 1, SUM)                             14500000
000571         SPTEST = SPUNIT * SUM  + SPSTO                                  14600000
000574         IF (SPACT)  545, 545, 550                                       14700000
000576   545   WRITE (IOUT, 6030) LIST(I), (FNAME(IW,1), IW=1,17), SUM,       15100001
              1                   SPTEST, SPACT                               15100002
000620         GO TO 570                                                       15100003
000621   550   PCT = (SPTEST - SPACT) * 100.0 / SPACT                          15100004
000624   555   WRITE (IOUT, 6020) LIST(I), (FNAME(IW,1), IW=1,17), SUM,        15100005
              1                    SPTEST, SPACT, PCT                         15200000
000650   570   CONTINUE                                                        15300000
000653         GO TO 130                                                       15400000
         C                                                                     15500000
000653   600   STOP                                                            15600000
         C                                                                     15700000
         C     FORMATS                                                         15800000
         C                                                                     15900000
000655   5070  FORMAT (16I5)                                                   16000000
000655   5120  FORMAT ( A3, 7X, F10.3, 5F10.3)                                 16100000
000655   5200  FORMAT  ( A4, 6X, 14I5)                                         16200000
000655   6010  FORMAT ( 1H1, 31H S/N FOR WEIGHTING FUNCTIONS = ,  E9.2  //,    16300000
              1        * CHECK OF * A3 * IN BASE IFGMS * / )                  16400000
000655   6020  FORMAT ( /1X,I4,1X, 17A4, 2X, E10.3, 6X, F8.5, 7X, F8.5, 4X, F7.2)  16900001
000655   6030  FORMAT ( /1X,I4,1X,17A4,2X,E10.3,6X,F8.5,7X,F8.5,4X,7H  XXXXX)  16900002
```

```
000655   6060  FORMAT ( /// 1X A3, 21H BURDEN OF TEST IFGMS / )                                  16900003
000655   6080  FORMAT (75X, 41H  MEASURED        MEASURED        ACTUAL    ,                   16900004
               1             10H   PERCENT /                                                   16900005
               2         75X, 40H TEST UNITS       CM-ATM          CM-ATM ,                   16900006
               3              11H     ERROR )                                                  17000000
000655   6100  FORMAT ( / 22H POINTS INCLUDED FROM , I3, 4H TO , I3,                            17100000
               1         / 26H TOTAL OBSERVATION TIME - , F10.3, 8H SECONDS                    17200000
               2         / 26H DELAY INTERVAL / POINT - , F7.3,                                17300000
               3         / 15H NOISES - RA - ,   E10.3, / 10X, 5HRM - ,   E10.3,               17400000
               4         / 10X, 5HSA - ,   E10.3,       / 10X, 5HSM - ,   E10.3 )            17500000
000655         END                                                                             17600000
```

```
                SUBROUTINE WSHIFT(WT, WD,NSG, NA, N1, N, N2, NFRG, NSCAN)                17700000
      CWSHFT        SUBROUTINE WSHIFT                                                    17800000
      C             SUBROUTINE TO JUGGLE INPUT FROM ARRAYS                               17900000
      C             SAVES DESIRED PART AND PUTS FIRST POINT OF EACH IFGM AT END          18000000
      C                                                                                  18100000
000014                DIMENSION  WD(NA, NSG, N), WT(2, 14, 64), NFRG(14), NSCAN(14)      18200000
      C                                                                                  18300000
000014                DO 115 II = 1, NSG                                               18400000
000015                FRNG = NFRG(II)                                                  18500000
000020                SCAN = NSCAN(II)                                                 18600000
000022                TFAC = 1.0 / (FRNG * SCAN)                                       18700000
000025                DO 115 IR = 1, 2                                                 18800000
000026                NPT = 1                                                          18900000
000027                DO 110 IP = N1, N2                                               19000000
000031                WD(IR, II, NPT) = WT(IR, II, IP) * TFAC                          19100000
000047          110   NPT = NPT + 1                                                    19200000
000053          115   CONTINUE                                                         19300000
000057                RETURN                                                           19400000
000060                END                                                              19500000
```

```
                SUBROUTINE DIFF(W,NA,NB,N,JO)                                   19600000
      CDIFF         SUBROUTINE DIFF                                             19700000
      C             FORMS DIFFERENCE IFGMS                                      19800000
      C                                                                         19900000
000010          DIMENSION W(NA,NB,N)                                            20000000
000010          DO 10 J=1,NB                                                    20100000
000011          IF(J.EQ.JO)GO TO 10                                             20200000
000012          DO 20 K=1,N                                                     20300000
000014          DO 20 I=1,2                                                     20400000
000015    20    W(I,J,K)=W(I,J,K)-W(I,JO,K)                                     20500000
000040    10    CONTINUE                                                        20600000
000043          RETURN                                                          20700000
000044          END                                                             20800000
```

```
                SUBROUTINE MESURE(W,H,NA,NB,N,J,SUM)                    20900000
      CMEAS         SUBROUTINE MESURE                                   21000000
      C             PERFORMS IFGM MEASUREMENT                           21100000
      C                                                                 21200000
      C                                                                 21300000
000012                DIMENSION W(NA,NB,N),H(NA,N)                      21400000
000012                SUM=0.                                            21500000
000013                DO 10 K=1,N                                       21600000
000015                DO 10 I=1,NA                                      21700000
000016    10          SUM=SUM+W(I,J,K)*H(I,K)                           21800000
000040                RETURN                                            21900000
000041                END                                               22000000
```

```
      SUBROUTINE WHOP(W,H,NPTS,NSG,JO,Q,A,D,ARA,MODE,SBYN)                22100000
CWHOP      SUBROUTINE WHOP                                                22200000
C          COMPUTES WEIGHTING FUNCTIONS                                   22300000
C                                                                         22400000
C     THIS SUBROUTINE CALCULATES AN OPTIMIZED WEIGHTING FUNCTION H(K)     22500000
C     FOR THE MEASUREMENT OF THE STRENGTH OF A TARGET FUNCTION W(JO,K)    22600000
C     IN THE PRESENCE OF OTHER SIGNALS W(J,K)                             22700000
C     FOR A SPECIFIED DWELL AT EACH POINT D(K).                           22800000
C                                                                         22900000
C     THE FUNCTION IS THAT WHICH MINIMIZES A COMBINATION OF FOUR          23000000
C     TYPES OF NOISE, EACH OF RELATIVE IMPORTANCE A(L):                   23100000
C             L=1     RANDOM    ADDITIVE                                  23200000
C               2       (     MULTIPLICATIVE                            23300000
C               3     SYNCHRN.        ADDITIVE                          23400000
C               4       (     MULTIPLICATIVE                            23500000
C                                                                         23600000
C     NSG     NUMBER OF SIGNAL COMPONANTS TO BE CONSIDERED                23700000
C     NPT     NUMBER OF OBSERVATION POINTS                                23800000
C     MODE    2 IF OBSERVATIONS ARE COMPLEX, 1 OTHERWISE                  23900000
C     J       SIGNAL COMPONANT INDEX                                      24000000
C     K       OBSERVATION PNT.   (                                        24100000
C     I       REAL - IMAG.       (                                        24200000
C     L       NOISE FACTOR       (                                        24300000
C     JO      INDEX OF TARGET COMPONANT                                   24400000
C                                                                         24500000
C     W(I,J,K)        STRENGTH OF J*TH COMPONANT AT K*TH POINT            24600000
C     Q(J)    OVERALL RELATIVE STRENGTH OF COMPONANT                      24700000
C     A(L)    RELATIVE IMPORTANCE OF L*TH NOISE FACTOR                    24800000
C     D(K)    DURATION OF OBSERVATION AT K*TH POINT                       24900000
C     H(I,K)  WEIGHTING FUNCTION                                          25000000
C     SBYN    SQUARE OF SIG/NOISE RATIO.                                  25100000
C                                                                         25200000
C     ARA(NSG,NSG) IS CORRELATION MATRIX (SET UP BY PROGRAM)              25300000
C                                                                         25400000
C     OUTPUTS ARE H + SBYN. EVERYTHING ELSE (EXCEPT ARA) IS INPUT         25500000
C                                                                         25600000
C                                                                         25700000
C     ************************************************************      25800000
C                                                                         25900000
C     METHOD                                                            26000000
C     ******                                                            26100000
C                                                                         26200000
```

```
C       (THE INDEX I IS SUPPRESSED FOR THIS EXPLANATION)                        26300000
C                                                                               26400000
C       THE  ALGORITHM IS SET UP TO GIVE                                        26500000
C                                                                               26600000
C               M(J)=SUM H(K)*D(K)*W(J,K)=DELTA(J,J0)                           26700000
C                    K                                                          26800000
C                                                                               26900000
C       THE NOISE MINIMIZED IS                                                  27000000
C                                                                               27100000
C               NOISE=SUM (H(K)**2 * G(K))                                      27200000
C                     K                                                         27300000
C       WHERE                                                                   27400000
C               G(K)=(A(1)+A(2)*R)*D + (A(3)+A(4)*R)*D*D                        27500000
C               R(K)=SUM(Q(J)*W(J,K))**2                                        27600000
C                    J                                                          27700000
C                                                                               27800000
C       THE SOLUTION IS                                                         27900000
C               H(K)=SUM (ARA(J,J0)*W(J,K))/ROOT(G)                             28000000
C                    J                                                          28100000
C                                                                               28200000
C       WHERE ARA(J,J1) IS THE INVERSE OF THE CORRELATION MATRIX                28300000
C               WHICH HAS ELEMENTS                                              28400000
C                                                                               28500000
C               SUM W(J,K)*W(J1,K)/G                                            28600000
C                K                                                              28700000
C                                                                               28800000
C       THE SQUARE OF THE S/N RATIO IS ARA(J0,J0)                               28900000
C                                                                               29000000
C       ***************************************************************         29100000
C                                                                               29200000
000016        DIMENSION W(MODE, NSG, NPTS), Q(NSG), D(NPTS), H(MODE, NPTS),     29300000
             1          ARA(NSG, NSG), A(4)                                     29400000
C                                                                               29500000
C     DEFINE 1/G, STORE IN H                                                    29600000
C                                                                               29700000
000016        DKI = 1.0                                                         29800000
000017          DO 10 K=1,NPTS                                                  29900000
000021          DO 20 I=1,MODE                                                  30000000
000022          R=0.                                                            30100000
000023          DO 30 J=1,NSG                                                   30200000
000025    30    IF(J.NE.J0)R=R+(Q(J)*W(I,J,K))**2                               30300000
000045    20    H(I,K) = 1.0 / ((A(1) + A(2) * R) * DKI + A(3) + A(4) * R)      30400000
000065    10    CONTINUE                                                        30500000
```

```
      C                                                                 30600000
      C       SET UP MATRIX                                             30700000
      C                                                                 30800000
000067          DO 60 J=1,NSG                                           30900000
000070          DO 40 J1=J,NSG                                          31000000
000071          SUM=0.                                                  31100000
000072          DO 50 K=1,NPTS                                          31200000
000074          DO 50 I=1,MODE                                          31300000
000075    50    SUM=SUM+W(I,J,K)*W(I,J1,K)*H(I,K)                       31400000
000132          ARA(J,J1)=SUM                                           31500000
000137    40    ARA(J1,J)=SUM                                           31600000
000145    60    CONTINUE                                                31700000
      C                                                                 31800000
      C       INVERT MATRIX                                             31900000
      C                                                                 32000000
000147          CALL MINV(ARA,NSG,R)                                    32100000
000151          IF(R.EQ.0.)GO TO 999                                    32200000
000156          SBYN=1./ARA(J0,J0)                                      32300000
      C                                                                 32400000
      C                                                                 32500000
      C       CALCULATE H                                               32600000
      C                                                                 32700000
000163          DO 80 K=1,NPTS                                          32800000
000165          DO 80 I=1,MODE                                          32900000
000166          SUM=0.                                                  33000000
000167          DO 90 J=1,NSG                                           33100000
000171    90    SUM=SUM+ARA(J,J0)*W(I,J,K)                              33200000
000215    80    H(I,K) = SUM * H(I,K) * DKI                             33300000
000227          RETURN                                                  33400000
      C                                                                 33500000
      C                                                                 33600000
000230    999   WRITE (6, 6010)                                         33700000
000234    6010  FORMAT ( // 33H THE **$(=**)$ MATRIX IS SINGULAR /)     33800000
000234          STOP 2                                                  33900000
000236          END                                                     34000000
```

```
                SUBROUTINE MINV(A,N,D)                                          34100000
      CMINV         SUBROUTINE MINV                                           34200000
      C             PERFORMS MATRIX INVERSION                                 34300000
      C                                                                       34400000
000006          DIMENSION A(1),L(20),M(20)                                    34500000
000006          D=1.0                                                         34600000
000007          NK=-N                                                         34700000
000010          DO80K=1,N                                                     34800000
000011          NK=NK+N                                                       34900000
000012          L(K)=K                                                        35000000
000013          M(K)=K                                                        35100000
000014          KK=NK+K                                                       35200000
000015          BIGA=A(KK)                                                    35300000
000020          DO20J=K,N                                                     35400000
000021          IZ=N*(J-1)                                                    35500000
000024          DO20I=K,N                                                     35600000
000026          IJ=IZ+I                                                       35700000
000030    10    IF(ABS(BIGA)-ABS(A(IJ)))15,20,20                              35800000
000035    15    BIGA=A(IJ)                                                    35900000
000037          L(K)=I                                                        36000000
000041          M(K)=J                                                        36100000
000043    20    CONTINUE                                                      36200000
000050          J=L(K)                                                        36300000
000051          IF(J-K)35,35,25                                               36400000
000053    25    KI=K-N                                                        36500000
000055          DO30I=1,N                                                     36600000
000056          KI=KI+N                                                       36700000
000057          HOLD=-A(KI)                                                   36800000
000061          JI=KI-K+J                                                     36900000
000063          A(KI)=A(JI)                                                   37000000
000066    30    A(JI)=HOLD                                                    37100000
000073    35    I=M(K)                                                        37200000
000075          IF(I-K)45,45,38                                               37300000
000077    38    JP=N*(I-1)                                                    37400000
000102          DO40J=1,N                                                     37500000
000104          JK=NK+J                                                       37600000
000105          JI=JP+J                                                       37700000
000107          HOLD=-A(JK)                                                   37800000
000111          A(JK)=A(JI)                                                   37900000
000114    40    A(JI)=HOLD                                                    38000000
000121    45    IF(BIGA)48,46,48                                              38100000
000122    46    D=0.0                                                         38200000
```

```
000123          RETURN                                                  38300000
000124   48     DO55I=1,N                                               38400000
000126          IF(I-K)50,55,50                                         38500000
000130   50     IK=NK+I                                                 38600000
000132          A(IK)=A(IK)/(-BIGA)                                     38700000
000135   55     CONTINUE                                                38800000
         C                REDUCTION                                    38900000
000140          DO65I=1,N                                               39000000
000141          IK=NK+I                                                 39100000
000142          IJ=I-N                                                  39200000
000144          DO65J=1,N                                               39300000
000145          IJ=IJ+N                                                 39400000
000146          IF((I-K)*(K-J))62,65,62                                 39500000
000153   62     KJ=IJ-I+K                                               39600000
000155          A(IJ)=A(IK)*A(KJ)+A(IJ)                                 39700000
000163   65     CONTINUE                                                39800000
000170          KJ=K-N                                                  39900000
000171          DO75J=1,N                                               40000000
000173          KJ=KJ+N                                                 40100000
000174          IF(J-K)70,75,70                                         40200000
000176   70     A(KJ)=A(KJ)/BIGA                                        40300000
000201   75     CONTINUE                                                40400000
000204          A(KK)=1.0/BIGA                                          40500000
000207   80     CONTINUE                                                40600000
         C                FINAL INTERCHANGE                            40700000
000211          K=N                                                     40800000
000211   100    K=K-1                                                   40900000
000213          IF(K)150,150,105                                        41000000
000214   105    I=L(K)                                                  41100000
000216          IF(I-K)120,120,108                                      41200000
000220   108    JQ=N*(K-1)                                              41300000
000223          JR=N*(I-1)                                              41400000
000227          DO110J=1,N                                              41500000
000230          JK=JQ+J                                                 41600000
000231          HOLD=A(JK)                                              41700000
000233          JI=JR+J                                                 41800000
000235          A(JK)=-A(JI)                                            41900000
000240   110    A(JI)=HOLD                                              42000000
000244   120    J=M(K)                                                  42100000
000246          IF(J-K)100,100,125                                      42200000
000250   125    KI=K-N                                                  42300000
000252          DO130I=1,N                                              42400000
000253          KI=KI+N                                                 42500000
```

```
000254          HOLD=A(KI)                                      42600000
000256          JI=KI-K+J                                       42700000
000260          A(KI)=-A(JI)                                    42800000
000263    130   A(JI)=HOLD                                      42900000
000270          GOTO100                                         43000000
000270    150   RETURN                                          43100000
000271          END                                             43200000
```

REFERENCES

Abel, P. G., Ellis, P. J., Houghton, J. T., Peckham, G., Rogers, C. D., Smith, S. D., and Williamson, E. J., Proc. Roy. Soc., London, A320, 35 (1970) a.

Abel, P. G., Houghton, J. T., Matley, J. B., and Williamson, E. J., Proc. Roy. Soc., London A320, 57 (1970) b.

AFCRL: U. S. Standard Atmosphere, 1966 Supplement, Air Force Cambridge Research Laboratory (1966).

Anding, D., Univ. of Michigan Infrared and Optical Sensor Laboratory, NAVSO. P-24499-1, "Band Model Methods for Computing Atmospheric Slant-Path Molecular Absorption," Feb. 1967.

Armstrong, B. H., J. Quant. Spect. and Rad. Transfer, 7, 61 (1967).

Benedict, W. S., Herman, R., Moore, G. E., and Silverman, S., Ap. J. 135, 277 (1962).

Bortner, M. H., Dick, R., Goldstein, H. W., Grenda, R. N., and Levy, G. M., "A Breadboard Correlation Interferometer for Development of the Carbon Monoxide Pollution Experiment,", NASA CR 112212, March 1973.

Bortner, M. H., Grenda, R. N., and Zomber, G. L., General Electric Co., SSL, 1971. Unpublished work.

Bortner, M. H., and Kummler, R. H., "The Chemical Kinetics and the Composition of the Earth's Atmosphere," General Electric Co. Report GE-9500-ECS-SR-1, July 1968.

Bortner, M. H., and Kummler, R. H., 1971. Unpublished work.

Bortner, M. H., Kummler, R. H., and Jaffe, L. S., "A Review of Carbon Monoxide Sources, Sinks, and Concentrations in the Earth's Atmosphere," NASA CR-2081, June 1972.

Bowen, T. R., "Blackbody Radiation Tables," U. S. Army Missile Command Report TN-AMSMI-RNR-1-63, May 1963.

Cadle, R., and Powers, J., Tellus 18, 176 (1966).

Chandrasekhar, S., Radiative Transfer, Dover Publ., N. Y., 1960.

CIRA: COSPAR International Reference Atmosphere 1965, North-Holland Publishing Co., Amsterdam, 1965.

Cooley, J. W., and Turkey, J. W., Math. of Computation 19, 297 (1965).

Fried, D. L., and Cloud, J. D., JOSA 56, 1667, 1966.

Fried, D. L., JOSA 57, 1967, a.

Fried, D. L., JOSA 57, 1967, b.

Fried, D. L., and Seidman, J. B., JOSA 57, 181, 1967.

Gentlemen, W. M., and Sande, G., "Fast Fourier Transforms for Fun and Profit," Proc. 1966 Fall Joint Computer Conf., pp 563-578, 1966.

Grenda, R. N., Bortner, M. H., LeBel, P. J., Davies, J. H., and Dick, R., "Carbon Monoxide Pollution Experiment (I). A Solution to the Carbon Monoxide Sink Anomaly," AIAA Paper No. 71-1120, Joint Conf. on Sensing of Environmental Pollutants, Palo Alto, 1971.

Houghton, J. T., and Smith, S. D., Proc. Roy. Soc., London, A320, 23 (1970).

JANAF Thermochemical Tables, Thermal Research Laboratory, Dow Chemical Co., Midland, Mich.

Keneshea, T. J., Zimmerman, S. P., and George, J. D., "The Latitudinal Variation of Major and Minor Neutral Species in the Upper Atmosphere," 14th COSPAR Meeting, Seattle, 1971.

Kostkowski, H. J., and Bass, A. M., J. Quant. Spect. and Rad. Transfer 1, 177 (1961).

Kulander, J. L., "Non-Equilibrium Radiation," General Electric Co. Report, GE 71SDR64SD41, June 1964.

Ludwig, C. B., priv. comm., 1970.

Mertz, L., Transformation in Optics, p. 63, Wiley, N. Y. (1965).

Penner, S. S., Quantitative Molecular Spectroscopy and Gas Emissivities, p. 20, Addison-Wesley, Reading, Mass., 1959.

Plyler, E. K., Benedict, W. S., and Silverman, S., J. Chem. Phys. 20, 175 (1952).

Tatarskii, V. I., Wave Propagation in a Turbulent Medium, Translated by R. A. Silverman, McGraw-Hill, N. Y., 1961.

Thekaekara, M. P., "Solar Electromagnetic Radiation", NASA SP-8805, Rev. 1971.

Tuller, S. E., Monthly Weather Rev. 96, 785 (1968).

Vachon, D. N., 1971. Unpublished work.

*U.S. GOVERNMENT PRINTING OFFICE: 1973-739-153/42

NATIONAL AERONAUTICS AND SPACE ADMINISTRATION
WASHINGTON, D.C. 20546

OFFICIAL BUSINESS
PENALTY FOR PRIVATE USE $300

SPECIAL FOURTH-CLASS RATE BOOK

POSTAGE AND FEES PAID
NATIONAL AERONAUTICS AND SPACE ADMINISTRATION
451

U.S.MAIL

POSTMASTER: If Undeliverable (Section 158 Postal Manual) Do Not Return

"The aeronautical and space activities of the United States shall be conducted so as to contribute . . . to the expansion of human knowledge of phenomena in the atmosphere and space. The Administration shall provide for the widest practicable and appropriate dissemination of information concerning its activities and the results thereof."

—NATIONAL AERONAUTICS AND SPACE ACT OF 1958

NASA SCIENTIFIC AND TECHNICAL PUBLICATIONS

TECHNICAL REPORTS: Scientific and technical information considered important, complete, and a lasting contribution to existing knowledge.

TECHNICAL NOTES: Information less broad in scope but nevertheless of importance as a contribution to existing knowledge.

TECHNICAL MEMORANDUMS: Information receiving limited distribution because of preliminary data, security classification, or other reasons. Also includes conference proceedings with either limited or unlimited distribution.

CONTRACTOR REPORTS: Scientific and technical information generated under a NASA contract or grant and considered an important contribution to existing knowledge.

TECHNICAL TRANSLATIONS: Information published in a foreign language considered to merit NASA distribution in English.

SPECIAL PUBLICATIONS: Information derived from or of value to NASA activities. Publications include final reports of major projects, monographs, data compilations, handbooks, sourcebooks, and special bibliographies.

TECHNOLOGY UTILIZATION PUBLICATIONS: Information on technology used by NASA that may be of particular interest in commercial and other non-aerospace applications. Publications include Tech Briefs, Technology Utilization Reports and Technology Surveys.

Details on the availability of these publications may be obtained from:

SCIENTIFIC AND TECHNICAL INFORMATION OFFICE

NATIONAL AERONAUTICS AND SPACE ADMINISTRATION

Washington, D.C. 20546